Rhenium-osmium geochronology and geochemistry of ancient lacustrine sedimentary and petroleum systems

VIVIEN MARY CUMMING

Rhenium-osmium geochronology and geochemistry of ancient lacustrine sedimentary and petroleum systems

Vivien Mary Cumming

A thesis submitted in partial fulfilment of the requirements for the degree of Doctor of Philosophy at Durham University

Department of Earth Sciences, Durham University

2012

Abstract

The Re-Os geochronometer is a valuable tool able to provide precise depositional ages of marine organic-rich sedimentary rocks as well as the generation age of hydrocarbons. In addition, Os isotopes afford vital insights into seawater Os fluctuations and provide the ability to fingerprinting hydrocarbons to their source. This thesis presents new research on extending the Re-Os geochronometer to lacustrine sedimentary and petroleum systems, which provide exceptionally high-resolution records of continental geological processes as well as significant hydrocarbons sources.

Lacustrine organic-rich sedimentary rocks possess similar Re and Os abundances to those found in marine successions. New Re-Os depositional dates from the Eocene Green River Formation are in agreement with Ar-Ar and U-Pb ages of intercalated tuff horizons. As also documented in marine systems, precision is controlled by the variation in initial $^{187}Os/^{188}Os$ and the range of $^{187}Re/^{188}Os$ ratios, which are controlled by depositional setting and type of organic matter. The Os isotope composition of lake water at the time of deposition suggests the lake was dominated by inputs from continental runoff, giving insights into continental weathering.

The Green River Formation is the source rock for the Green River petroleum system in the Uinta Basin. Three types of hydrocarbons are derived from this petroleum system; oils, tar sands and gilsonite. Re-Os geochronology of these different hydrocarbon phases broadly agrees with previous generation models. Hydrous pyrolysis experiments yield similar Re and Os transfer systematics to the natural system observed and importantly reinforce that Os isotope compositions are directly transferred from source to hydrocarbon, providing a powerful correlation tool.

Lacustrine units are also important records of Earth's climate system. New geochemical and Re-Os data from the late Mesoproterozoic Nonesuch Formation yield a Re-Os depositional age of 1078 ± 24 Ma, while Os isotope compositions strongly support existing evidence for a lacustrine setting. Fe-S-C systematics suggest that the Nonesuch Formation was deposited from an anoxic Fe-rich water column.

Declaration

I declare that this thesis, which I submit for the degree of Doctor of Philosophy at Durham University, is my own work and not substantially the same as any which has previously been submitted at this or any other university.

Vivien M. Cumming
Durham University
December 2012

Acknowledgements

Before I thank the people that have helped me get through my PhD, I must acknowledge the sources of funding that have made this research possible. Lundin petroleum has generously funded my PhD for 3.5 years, made possible by Daniel Stoddart. In addition, during the course of my PhD I have received several grants that have allowed me to travel to conferences and go on much-needed fieldwork. The funding bodies include the AAPG Grants-in-Aid scheme, the Rocky Mountain Association of Geologists, the Geochemical Society and the GSA international section.

Firstly, I would like to thank my main supervisor Dave Selby, for initially getting this project funded, offering it to me, and of course for supervising me. Dave has been a fantastic supervisor; he has always allowed me to follow my interests, even when they have gone wildly off topic. Thanks to Dave, I have been able to present my work at numerous international conferences, even one in Australia. Thanks especially for sending work back so quickly (an unusual trait for a supervisor) and for always trying (sometimes in vain) to make sure I stay positive.

Importantly, thank you to my other supervisors and the main contributors to this work. Paul Lillis at the USGS, you have been very supportive throughout this project, even with my constant email hassle and thanks for a great time in the field. Mike Lewan, thank you for letting me into your lab, it was great fun, and your wit will never get old. Simon Poulton, thank you for giving me the run of your lab and the choice of samples from all corners of the world. Your encouragement has really helped me get through this PhD. Daniel Stoddart from Lundin petroleum, though you have mostly been in the background, when I have shown you my data, you have been very positive and your admiration for my work has always been emboldening.

During this PhD I have benefited hugely from all the people in the different labs I've worked in. The lab team at the USGS have provided much needed organic geochemical analyses and so I must thank Augusta Warden, Tammy Hannah, Zachary Lowry, Mark Dreier and Robert Dias. All those in Simon Poulton's lab at Newcastle, thanks for

letting me get in the way, and particularly Christian, Romain, Katy and Suha for helping me out when needed. And of course everyone in the labs at Durham; Chris Ottley, Geoff Nowell and Chris Dale for the much needed mass spec support; Sarah, Jo, Ali, Alice, Chris, Alan, Alex for fun times and eclectic music in the Re-Os lab. I mention as well the people that have helped get this thesis finished with their proof reading skills; Iona, Sarah, Alex and Alan; Iona especially for her impeccable grammar.

I must thank all my friends for their unending support. To all those in Scotland, London and Cornwall thank you for keeping me sane! My many weekend visits and holidays to escape Durham have kept me going. Thanks especially to Bryony, Sarah, Alice, Tom, Jennie, Lucy, Annie, Lindsay, Mark, Lyndsey, Duncan, Harry, Beth, Matt and Georgie. Thank you to everyone in Durham for the amazing nights out, lots of hockey fun and procrastination chats; particularly Fiona, Andy, Kat, Simon, Sarah, Iona, Sam, BJ, Sian and Amy. Ben, thank you for being a very easy going housemate, putting up with the rants and just generally being a good friend. Thank you to Alan for his unfailing support and encouragement through thick and thin.

Most importantly I must thank my family; my parents and sisters (Lily and Jussie), and also Celia and Meredith. Thank you all for your constant encouragement, support and love, I couldn't have done it without you.

Finally I leave with a quote from a very inspiring book that has helped to remind me why I am doing what I am doing. 'The Age of the Earth' by Arthur Holmes (1913):

> *'To bring together all the scattered pages of earth history in chronological order is by no means an easy task. The stratified rocks have accumulated layer upon layer and wherever a continuous succession of beds can be seen it is obvious that the lowest must be the oldest and those at the top the youngest. But the succession is by no means everywhere clear….'*

Contents

List of Figures

List of Tables

Chapter 1

Introduction

Chapter 1: Introduction

The aims of the research presented in this thesis focus on enhancing the capabilities of the rhenium-osmium (Re-Os) geochronometer in geological applications. This introduction provides a brief summary of the history and major advances of Re-Os geochronology, describing the different uses of the tool and current gaps in our knowledge. I will also briefly outline the contents of the four chapters that comprise the remainder of this thesis.

1.1 The history of the Re-Os geochronometer

The Re-Os geochronometer is based on the β^- decay of ^{187}Re to ^{187}Os which has a half-life of 41.6 Ga (Smoliar et al., 1996). The long-lived nature of the decay of ^{187}Re was originally discovered by Naldrett and Libby (1948), and led to development of the Re-Os geochronometer in the following decades. This work involved various attempts at determining the half-life of ^{187}Re, initially by direct counting of Re decay (Naldrett and Libby, 1948), and then by calculation from chemical measurements of Re and Os present in molybdenite (Herr et al., 1954; Hirt et al., 1963) or iron meteorites (Luck and Allegre, 1983). Attempts by Lindner et al. (1989) provided a more precise and accurate measurement (half-life = 4.23 ± 0.13 x $10^{10}y^{-1}$), which was based on chemical measurements of the number of daughter atoms of ^{187}Os produced over a certain time period. The uncertainty on the calculated decay constant of ^{187}Re ($\lambda^{187}Re$) continued to restrict Re-Os geochronology as the uncertainty in this measurement is one of the principal factors in limiting the accuracy of age determinations from radioactive isotope systems (Begemann et al., 2001). A pivotal study by Smoliar et al. (1996) on iron meteorites reported the most precise decay constant to date of 1.666 ± 0.0017 x $10^{-11}y^{-1}$. Various studies then proceeded to attempt to confirm the accuracy of $\lambda^{187}Re$. One example combined Re-Os molybdenite geochronology of magmatic ore deposits with U-Pb zircon geochronology of the related magmatic bodies and repeated this on deposits from Archean to Cretaceous age (Selby et al., 2007a) yielding a $\lambda^{187}Re$ value that was identical within uncertainty to that reported by Smoliar et al. (1996). Cross-

calibration of Re-Os organic-rich sedimentary rock geochronology with U-Pb zircon geochronology at the Devonian-Mississippian boundary also agreed with the Smoliar et al. (1996) λ^{187}Re value. Thus Re-Os geochronology data calculated using the λ^{187}Re value of 1.666 ± 0.0017 x $10^{-11}y^{-1}$ is now considered reliable.

1.1.1 Applications to the Earth sciences

The chalcophilic, siderophilic and organophilic properties of Re and Os mean that the Re-Os geochronometer has a multitude of geological uses beyond the capabilities of other geochronometers and it has driven major advancements in our understanding of the Earth sciences. Early applications of the Re-Os system determined crystallisation ages of early solar system asteroids and the formation of iron meteorites, work made feasible in part due to the long half-life of ^{187}Re (e.g. Luck et al., 1980; Luck and Allègre, 1983; Walker and Morgan, 1989; Horan et al., 1992; Morgan et al., 1992; Shen et al., 1996; Smoliar et al., 1996). The Re-Os system has also played a critical role in dating and understanding sulphide ore genesis and related tectonic events, mantle evolution, crustal growth and diamond formation (e.g. Herr et al., 1964; Luck and Allègre, 1982; Morgan, 1986; Walker et al., 1989; Herzberg, 1993; Walker et al., 1994; Pearson et al., 1995; Foster et al., 1996; Suzuki et al., 1996; Markey et al., 1998; Pearson et al., 1998; Raith and Stein, 2000; Selby et al., 2002). More recent work has developed the use of Re-Os geochronology for providing depositional ages for marine organic-rich sedimentary rocks with concurrent assessment of the oceanic Os isotope composition (e.g. Ravizza and Turekian, 1989; Cohen et al., 1999; Creaser et al., 2002; Selby and Creaser, 2003; Hannah et al., 2004; Kendall et al., 2004, 2009a; Finlay et al., 2010a; Rooney et al., 2010). Finally, the most recent developments have revolved around the finding that hydrocarbons contain Re and Os with the chronometer being used to date hydrocarbon generation and Os isotopes being used to fingerprint oil to its source (Selby and Creaser, 2005a; Selby et al., 2005, 2007b; Finlay et al., 2011, 2012; Rooney et al., 2012). An area that has only been partially investigated using Re-Os geochronology is the dating of lacustrine organic-rich sedimentary rocks (Creaser et al., 2008; Poirier and Hillaire-Marcel, 2009, 2011), and

the use of Re-Os hydrocarbon generation geochronology and Os isotope fingerprinting has never been assessed in a lacustrine petroleum system. This thesis focuses on providing a full assessment of Re-Os geochronology and geochemistry of lacustrine organic-rich sedimentary rocks and petroleum systems in order to bring these applications in line with other Re-Os research. In order to introduce this topic I will outline and discuss some of the milestones in the field of Re-Os organic-rich sedimentary rock geochronology and petroleum system analysis.

1.1.2 Mass spectrometry and analytical techniques

Advancement of the Re-Os geochronometer and application to geological problems has been consistently hampered by the difficulty in precisely analysing the low abundances of these metals (nanogram and sub-nanogram). Conventional thermal ionisation mass-spectrometry (TIMS) cannot surmount this issue owing to the high ionisation potential of these elements (8.7 eV). Re-Os mass spectrometry techniques have evolved in several stages, each making previous studies partially obsolete. Initial development involved electron bombardment mass spectrometry, followed by secondary ionization mass spectrometry (Allègre and Luck, 1980), resonance ionization mass spectrometry (Walker and Fassett, 1986), accelerated mass spectrometry (Fehn et al., 1986) and inductively coupled plasma mass spectrometry (Russ et al., 1987). All of these techniques suffered from low sensitivity and precision. The most significant advancement in Re-Os isotope mass spectrometry was the successful development of negative thermal ionisation mass spectrometry (NTIMS; Creaser et al., 1991; Völkening et al., 1991; Walczyk et al., 1991), which provided analytical precision better than ± 2‰. The NTIMS method involves loading Re and Os as salts onto Ni and Pt filaments respectively and then coating the sample with an electron emitter such as $Ba(NO_3)_2$ which results in ionization efficiencies of up to 10 to 20 % for both elements. The improvement in sensitivity and precision resulting from the application of NTIMS for measuring Re and Os isotopes means that this is now the most common method used, particularly for geochronological studies that require the greatest precision.

The analytical techniques for the application of Re-Os geochronology have developed slowly. Achieving full mixing and equilibration of samples with enriched Re and Os isotope spikes has been a limitation on progression. Spike and sample equilibration is especially critical in Re-Os geochemistry due to the numerous oxidation states and species possible for each element (Shirey and Walker, 1998). Studies have utilized either acid or fusion digestion as the means of dissolving phases and equilibrating spikes with samples. Pioneering work by Ravizza and Turekian (1989) on Re-Os geochronology of marine organic-rich sedimentary rocks utilised the nickel sulphide fire assay technique, measured the isotope ratios using an ion microprobe and plotted an isochron using a York regression (York, 1966). This method is now obsolete but this study provided an important building block for the advancement of marine organic-rich sedimentary rock geochronology. The Carius tube digestion method (inverse aqua regia at 200 - 260°C; Shirey and Walker, 1995) resolved issues such as digesting phases resistant to low temperature (<150°C) alkaline or acid digestion and achieving complete spike equilibration (Walker, 1988; Birck et al., 1997; Shirey and Walker, 1998). The first precise study on organic-rich sedimentary rocks (Cohen et al., 1999) used the Carius tube method and also benefited from the more accurate value for λ^{187}Re provided by Smoliar et al. (1996), the new NTIMS analytical techniques (Creaser et al., 1991; Völkening et al., 1991; Walczyk et al., 1991) and improved chemical separation and purification protocols for Os (Cohen and Waters, 1996; Birck et al., 1997). The inverse aqua regia whole-rock digestion method, however, was found to liberate non-hydrogenous Re and Os from detrital minerals contained within organic-rich sedimentary rocks. These detrital components negatively impact the precision and accuracy of Re-Os ages as they are responsible for much of the geological scatter about the line of an isochron (Ravizza et al., 1991; Ravizza and Esser, 1993; Cohen et al., 1999; Peucker-Ehrenbrink and Hannigan, 2000; Creaser et al., 2002). To limit the release of detrital Re and Os from organic-rich sedimentary rock matrices, a new whole-rock digestion protocol using a Cr^{VI}–H_2SO_4 solution was developed (Selby and Creaser, 2003). This technique also utilised Carius tubes but has the benefit of incorporating hydrogenous Re and Os. Once sample digestion and

equilibration are achieved, Os is separated from the rock matrix via solvent extraction and Re is separated using anion exchange chromatography (Cohen and Waters, 1996; Birck et al., 1997; Shirey and Walker, 1998 and references therein).

An aspect of Re-Os organic-rich sedimentary rock geochronology that deserves to be mentioned is the protocol for sampling appropriate material. It is necessary to target samples that have not been significantly affected by post-depositional processes such as weathering (Peucker-Ehrenbrink and Hannigan, 2000), metamorphism (above greenschist grade; Kendall et al., 2004) and hydrothermal fluid flow (Kendall et al., 2009b; Rooney et al., 2011), in order to minimise any post-depositional mobilisation of Re and Os within the samples (Kendall et al., 2009a). In addition, however, optimal sampling strategies need to be determined in order to avoid the generation of erroneous and/or imprecise Re-Os dates. The production of a precise Re-Os isochron requires that the samples begin with similar $^{187}Os/^{188}Os$ ratios but have varied $^{187}Re/^{188}Os$ ratios (Cohen et al., 1999). In order to achieve this, a thin stratigraphic sampling interval is needed to obtain homogenous $^{187}Os/^{188}Os$ ratios. A review of sampling protocols used in various studies suggests intervals ranging from a few centimetres to several metres can be used to produce precise ages, with at least 20 grams of powdered sample required to achieve sample homogeneity (Kendall et al., 2009a). If Re and Os are distributed heterogeneously in a sample due to incomplete powder homogenization this could result in irreproducible sample aliquots and therefore produce inaccurate variation within an isochron. The sampling and analytical procedures described here are used throughout this study and are also outlined in Selby and Creaser (2003) and Selby (2007).

1.2 Re-Os geochronology and systematics of organic-rich sedimentary rocks

The fundamental conditions required for Re-Os geochronology of marine organic-rich sedimentary rocks are that Re and Os are organophilic and also arguably redox-sensitive. Simply, this allows uptake of Re and Os into organic matter during

deposition of sedimentary rocks permitting depositional age geochronology and providing vital information on the Os isotope composition of seawater at the time of deposition (Ravizza et al., 1991; Ravizza and Turekian, 1992; Colodner et al., 1993; Selby and Creaser, 2005b; Crusius et al., 1996; Levasseur et al., 1998; Kendall et al., 2009a; Selby et al., 2009).

1.2.1 Re and Os uptake into organic-rich sedimentary rocks

Currently there is only a partial understanding of Re and Os uptake into organic-rich sedimentary rocks. It occurs at or below the sediment-water interface under sub-oxic to anoxic or euxinic conditions (Koide, 1991; Colodner et al., 1993; Crusius et al., 1996; Cohen et al., 1999; Morford and Emerson, 1999). These early works, and subsequent experimental studies, provide evidence that Re and Os behave differently in the water column and that uptake mechanisms are not the same for both elements (Sundby et al., 2004; Yamashita et al., 2007; Morford et al., 2009). Rhenium is transported to the oceans by rivers and removed from seawater by reductive capture (soluble $Re^{VII}O_4^-$ is reduced to insoluble Re^{IV}) under low Eh conditions (Colodner et al., 1993; Yamashita et al., 2007). The rate of removal is controlled by precipitation kinetics and has been shown to be unaffected by changes in sediment accumulation rate and sulphide concentration (Crusius and Thompson, 2000; Sundby et al., 2004). The dominant source of present-day seawater Os (~70 - 80%) is derived from weathering of the upper continental crust (McDaniel et al., 2004), with the remainder from cosmic dust (Peucker-Ehrenbrink, 1996) and hydrothermal alteration of oceanic crust and peridotites (~20 - 30%; Ravizza et al., 1996; Sharma et al., 2000, 2007; Cave et al., 2003; McDaniel et al., 2004). Reduction of dissolved Os species (Os [IV]) occurs over a range of Eh and pH conditions and this process is relatively fast compared to Re reduction and may occur below the depth of Re enrichment (Poirier, 2006; Yamashita et al., 2007). Removal from seawater into organic-rich sedimentary rocks is directly associated with organic matter (Levasseur et al., 1998), and occurs first as Os (IV) and is then further reduced to Os (III) by organic complexation (Yamashita et al., 2007; Kendall et al., 2009a).

Rhenium and Os concentrations in marine organic-rich sedimentary rocks range from average upper-crustal abundances (0.2 - 1 ng/g Re and 30 - 50 pg/g Os; Esser and Turekian, 1993; Peucker-Ehrenbrink and Jahn, 2001; Hattori et al., 2003; Sun et al., 2003) to several hundred ng/g of Re and several ng/g of Os (e.g. Cohen et al., 1999). The high $^{187}Re/^{188}Os$ ratios of organic-rich sedimentary rocks derived from seawater (the present day seawater $^{187}Re/^{188}Os$ ratio is ~3200 to 5300) means that only moderate enrichments in Re are required to generate radiogenic present day $^{187}Os/^{188}Os$ ratios for ancient organic-rich sedimentary rocks (Kendall et al., 2009). Yamashita et al. (2007) note that Re is more readily incorporated into organic-rich sedimentary rocks under highly reducing conditions leading to high $^{187}Re/^{188}Os$ ratios. The variable mechanisms of uptake of Re and Os may be what causes Re-Os fractionation, but specific controls on fractionation are poorly constrained. It has been shown in marine systems that there is no correlation of redox conditions with $^{187}Re/^{188}Os$ values of organic-rich sedimentary rocks (Selby et al., 2009), and that Re-Os abundances do not always correlate to total organic carbon (TOC) despite the majority of these metals being held within the kerogen (Rooney et al., 2010, 2012). Other factors such as sedimentation rate, recharge of Re and Os in the water column and post-depositional processes have a combined and complex effect on the Re and Os uptake and fractionation. This is in agreement with our understanding of the enrichment of other metals such as V and Ni in organic-rich sedimentary rocks (Lewan and Maynard, 1982; Crusius and Thomson, 2000; Turgeon et al., 2007; Kendall et al., 2009a). It has also been suggested that there is potentially an unknown method of biological uptake of Re over Os (Morford et al., 2009; Georgiev et al., 2011), however, there is little data on the biotic enrichment of Re and Os and these elements are usually considered to be unrelated to the biological cycle (Crusius et al., 1996). Work in restricted basins indicate that organic matter sedimentation draws down dissolved Re and Os thus shortening residence time and causing lower abundances and rapid $^{187}Os/^{188}Os$ variations (McArthur et al., 2008). McArthur et al. (2008) concluded their inability to produce precise Re-Os ages of Lower Toarcian black shales of the Cleveland Basin was due to the effect of water mass restriction, which they suggest is more

severely restricted than the modern Black Sea. The Black Sea sediments have also been analysed for Re-Os isotopic compositions and heterogeneous $^{187}Os/^{188}Os$ values were found and suggested to be problematic for Re-Os geochronology of restricted basins (Ravizza et al., 1991). In addition, it has been suggested that Re and Os display no correlation to TOC in terrestrial basins and that organic-rich sedimentary rocks deposited in terrestrial basins will possess low $^{187}Re/^{188}Os$ values (<200; Baioumy et al., 2011). These limited studies on restricted and terrestrial basins suggest that Re-Os uptake and fractionation in these systems could hamper Re-Os geochronology.

1.2.2 Re-Os geochronology of marine organic-rich sedimentary rocks

The main assumptions associated with the Re-Os marine organic-rich sedimentary rock geochronometer are that Re and Os in these marine deposits are hydrogenous in origin (derived from seawater); there is rapid immobilisation of Re and Os after deposition thus Re-Os dates reflect the age of deposition and not a younger diagenetic age; all samples analysed have a consistent initial $^{187}Os/^{188}Os$ isotope composition (Os_i) derived from seawater at the time of deposition; and the samples have remained in a closed system with little or no post-depositional mobilisation of Re and Os (Kendall et al., 2009 and references therein).

Pioneering work by Ravizza and Turekian (1989) provided a Re-Os depositional age for Devonian/Mississippian organic-rich sedimentary rocks, indistinguishable from the accepted age of this timescale boundary. Despite the large uncertainty produced (~14%) this work highlighted the fact that Re-Os geochronology can provide depositional ages of sedimentary successions as well as the Os isotope composition of seawater throughout geological time. With the advent of new methodologies a more accurate study on Jurassic organic-rich sedimentary rocks yielded depositional ages that were identical, within uncertainty (~3 - 7%), to the interpolated stratigraphic ages (Cohen et al., 1999). This study also provided estimates of the Os_i of the Jurassic oceans, allowing inferences to be made on the balances between continental weathering and hydrothermal and volcanic activity during the Jurassic.

Subsequent studies began to assess more complex sedimentary systems including the Exshaw Formation, a source rock of the Western Canadian Sedimentary Basin (Creaser et al., 2002). Re-Os geochronology was evaluated on immature, mature and overmature hydrocarbon source rocks (organic-rich sedimentary rocks). The ages produced showed no significant variation and were in agreement with known ages of the Exshaw Formation. Importantly, Creaser et al. (2002) demonstrated that hydrocarbon maturation and migration does not adversely affect Re-Os systematics in organic-rich sedimentary rocks. An artificial maturation study of organic-rich sedimentary rocks verified the finding that Re-Os systematics are not affected by hydrocarbon maturation since only an insignificant portion of Re and Os are transferred to hydrocarbons (Rooney et al., 2012). Additional work on the Exshaw Formation at the Devonian-Mississippian boundary provided accurate and precise age data in excellent agreement with the interpolated age from U-Pb zircon geochronology (Selby and Creaser, 2005b). Organic-rich sedimentary horizons often span geological boundaries and lack horizons suitable for U-Pb or Ar-Ar geochronology, therefore this study highlighted the potential for the Re-Os geochronometer to resolve issues associated with calibration of the geological timescale. Further studies have made this more apparent, e.g. a Re-Os age for the Oxfordian-Kimmeridgian boundary was ~45% more precise than the established age derived from correlation of ammonite zones and the M-sequence polarity scale (Selby, 2007). Rhenium-osmium data for the Aptian/Albian and Cenomanian/Turonian stage boundaries yielded accurate, but imprecise, isochron ages (Selby et al., 2009). The lack of precision is attributed to the limited spread in $^{187}Re/^{188}Os$ ratios, highlighting the need for variation in $^{187}Re/^{188}Os$ ratios but no variation in initial $^{187}Os/^{188}Os$ to produce precise Re-Os dates. This study, however, provided important Os_i data that can be correlated with geological processes such as increased volcanism associated with large igneous provinces that occurred during the Cretaceous. A study by Turgeon et al. (2007) on four TOC-rich shale intervals spanning the Frasnian-Famennian boundary reported two precise ages and two imprecise ages which are again attributed to a lack of spread in $^{187}Re/^{188}Os$ ratios. They suggest this lack of spread is due to exhaustion of the Re reservoir due to increasing

anoxia leading up to the Frasnian-Famennian boundary; however, this has never been corroborated. The Os_i from the Frasnian-Famennian boundary study also provide important insights into continental weathering during this time period and the mechanisms of the Late Devonian mass extinction.

Most early Re-Os studies focused on organic-rich sedimentary rocks with TOC of >10% due to an apparent association of Re and Os with TOC (Ravizza and Turekian, 1989; Cohen et al., 1999; Creaser et al., 2002). Kendall et al. (2004) used low TOC (<1%) shales of the Old Fort Point Formation, Australia, and produced precise and accurate Neoproterozoic ages. These shales had also experienced chlorite-grade metamorphism and so the results from this study indicated that low TOC samples and low-grade metamorphism do not have a detrimental effect on Re-Os geochronology. This was further corroborated by Rooney et al. (2011) who demonstrated that Re-Os geochronology can be successful on rocks of the Dalradian Supergroup of Scotland with low TOC that have undergone anhydrous metamorphism. This study also demonstrated the first successful application of the chronometer to rocks with Re and Os abundances below average upper continental crustal levels (<1 ng/g Re and < 50 pg/g Os; Rooney et al., 2011). These studies suggest that TOC of at least ~0.5% is required for Re-Os enrichment necessary for geochronology (Kendall et al., 2004; Rooney et al., 2011). Other Proterozoic studies have demonstrated the importance of the Re-Os geochronometer in deducing depositional ages of rocks that were previously poorly dated. Re-Os geochronology of the Lapa Formation of the Vazante Group, Brazil, provided an age of 1100 ± 77 Ma for a unit previously thought to be ~700 Ma based on chemostratigraphic correlation (Azmy et al., 2008). Rooney et al. (2010) reported similar ages of ~1100 Ma for the Atar Group of the Taoudeni basin, Mauritania, which was previously considered to be Mid-Tonian based on Rb-Sr illite and glauconite geochronology. These two studies also provided equivalent estimates of the Os isotope composition of Late Mesoprotrozoic seawater (~0.3; Azmy et al., 2008; Rooney et al., 2010). Work by Kendall et al. (2009b) reported accurate and precise Re-Os geochronology for the Roper Group, Australia. The Re-Os data was coupled with Mo isotope data and used to evaluate changes in redox chemistry of the

Roper basin and the global ocean redox chemistry during the Mesoproterozoic, indicating the significance of Re-Os geochronology in multi-disciplinary studies. These studies highlight the importance of Re-Os geochronology for producing accurate depositional ages, coupled with Os isotopes that can be used to elucidate numerous geological processes.

1.2.3 The marine osmium isotope record

As Re and Os in marine organic-rich sedimentary rocks are dominantly hydrogenous, the initial $^{187}Os/^{188}Os$ composition reflects that of seawater at the time of deposition (Ravizza and Turekian, 1992; Cohen et al., 1999). The geochronological studies described in the previous section illustrate that the application of Re-Os geochronology to marine organic-rich sedimentary rocks can be an important tool in reconstructing marine Os evolution. In addition, particularly over the last 20 years, many studies have focused on Os isotope stratigraphy rather than Re-Os geochronology in order to build up the marine Os curve through time (Peucker-Ehrenbrink and Ravizza, 2000, 2012 and references therein). These studies have highlighted that understanding the global ocean Os isotope record and its perturbations is vital for increasing our knowledge of global ocean chemistry and continental weathering. The Cenozoic has received considerable attention with works showing that the global ocean became progressively more radiogenic with respect to Os ($^{187}Os/^{188}Os$ composition increased progressively from 0.56 at 50 Ma to 1.06 today; Peucker-Ehrenbrink and Ravizza, 2000; Kato et al., 2011). The causes of this change remain debated. The Sr record has seen a similar increase to more radiogenic values today which have been related to increases in continental weathering due, principally, to the uplift of the Himalayas (Raymo and Ruddiman, 1992; Richter et al., 1992); however Himalayan uplift may not have had such a profound influence on the Os record (Sharma et al., 1999). The Sr record is buffered by carbonate weathering and has a residence time of 1 to 4 Myrs, meaning that smaller scale perturbations are not recorded (Peucker-Ehrenbrink and Blum, 1998). In contrast, the residence time of Os in the oceans is ≤10,000 years and so the Os record provides a much more detailed

picture of continental weathering (Peucker-Ehrenbrink and Ravizza, 2000). The $^{187}Os/^{188}Os$ composition of seawater today records a balance of radiogenic and unradiogenic inputs. It is marked by perturbations to more unradiogenic values due to meteorite impacts and flood basalt events as well as hydrothermal alteration of oceanic crust ($^{187}Os/^{188}Os$ = ~0.12; Peucker-Ehrenbrink and Ravizza, 2000; Schmitz et al., 2004). The most abundant flux to the ocean is continental runoff with several studies producing estimates for present day $^{187}Os/^{188}Os$ composition of upper continental crust ($^{187}Os/^{188}Os$ = ~1.2 – 1.3; Esser and Turekian, 1993; $^{187}Os/^{188}Os$ = ~1.05; Peucker-Ehrenbrink and Jahn, 2001) and runoff ($^{187}Os/^{188}Os$ = ~1.54; Levasseur et al., 1999). In addition, radiogenic Os is supplied to the ocean during weathering of organic-rich sedimentary rocks and Precambrian crust ($^{187}Os/^{188}Os$ ≤13.6; Peucker-Ehrenbrink and Blum, 1998). Unravelling the relative changes in the influences on the marine Os isotope record remains a challenge, but with increasing numbers of studies more and more problems are being resolved.

1.2.4 Re-Os geochronology of lacustrine organic-rich sedimentary rocks

The first study on lacustrine organic-rich sedimentary rocks analysed source rocks from the Brazilian marginal basins (Creaser et al., 2008). The Re contents for these lacustrine shales are lower than marine shales at equivalent values of TOC, and they show a more restricted range in $^{187}Re/^{188}Os$ ratios making determination of precise ages challenging. This was overcome by multiple sampling of identical horizons throughout the basin to obtain meaningful ages. The initial $^{187}Os/^{188}Os$ values were between 1.3 and 1.5 showing a distinctly terrestrial input. Unfortunately, this data is only published in abstract format and so further analysis and comparison of the data is not possible.

Re-Os geochronology and Os isotope studies of sediments from the Lomonosov Ridge in the Arctic Ocean records an Eocene ‘lake stage’ before the onset of marine conditions (Poirier and Hillaire-Marcel, 2009, 2011). These provide the only published studies of organic-rich sedimentary rocks that may be lacustrine in origin. Rhenium and Os abundances are tightly controlled by TOC with the ‘lake stage’ sediments having the

highest TOC (~2 wt.%) and Re and Os abundances of ~12 ng/g and ~100 pg/g, respectively (deduced from figure 1 of Poirier and Hillaire-Marcel, 2011). The Re-Os geochronology from the boundary between lacustrine and marine deposition has an age of 36.64 ± 0.74 Ma, but this is only a three point isochron which cannot be considered significant as a three point regression will grossly underestimate the uncertainty on the age (Ludwig, 2008). It is considered to be a lacustrine deposit due to the initial $^{187}Os/^{188}Os$ of 1.2 (seawater is ~0.4 at this time). The most interesting aspect of this study is the $^{187}Os/^{188}Os$ curve produced. During the Arctic Ocean 'lake stage', $^{187}Os/^{188}Os$ values are radiogenic (0.9 to 1.3), but with the inception of marine conditions the values reduce to ~0.4 and then follow the increasing trend of marine Os isotope evolution up to ~1 at the present day (Poirier and Hillaire-Marcel, 2009, 2011). The authors suggest that the influx of radiogenic Os resulting from the opening of the Fram Strait and connection of the Arctic 'lake' with the global ocean may have caused the increase to more radiogenic values in the marine Os isotope curve up to the present day. Though this study does not produce geochronology that is robust or definitely lacustrine, it does provide interesting insights into Os evolution.

1.3 Re-Os geochronology and systematics of petroleum systems

1.3.1 Re-Os hydrocarbon generation geochronology

Rhenium and Os are present in natural hydrocarbons (Barre et al., 1995; Woodland et al., 2001; Selby and Creaser, 2005a; Selby et al., 2007b) and bitumens (Selby et al., 2005). An early study provided an accurate age (112 ± 5.3 Ma) for the timing of hydrocarbon generation in the Western Canadian Sedimentary Basin suggesting that Re-Os geochronology of hydrocarbons records the age of oil generation (Selby and Creaser, 2005a). In addition, the Re-Os isotopic data yielded vital information about the source rock of these hydrocarbons. Petroleum exploration is often hampered by a lack of understanding of the spatial and temporal controls on hydrocarbon formation. Traditionally, dating the timing of hydrocarbon generation involves basin modelling using estimated parameters (e.g. Ruble et al., 2001).

Therefore knowing the absolute age of petroleum generation provides vital constraints for elucidating petroleum maturation and migration. Another study provided evidence of the accuracy of the Re-Os hydrocarbon geochronometer by dating bitumen from the Polaris Mississippi-Valley-type deposit, Canada, giving an age of 374.9 ± 9 Ma in agreement with a paleomagnetic date and an Rb-Sr sphalerite age of mineralisation (Selby et al., 2005). This suggests that the migration of fluids associated with sulphide mineralisation was contemporaneous with hydrocarbon generation. These studies indicated that the Re-Os geochronometer has great potential for understanding petroleum system processes.

These initial studies provided strong evidence that the Re-Os hydrocarbon geochronometer could be a valuable tool for petroleum exploration but little was known about the systematics of Re and Os in hydrocarbons. Selby et al. (2007b) assessed the Re and Os isotopic compositions and abundances in twelve oils from various petroleum systems throughout the world. The results indicated that the majority of Re (>90%) and Os (>83%) are held in the asphaltene fraction of oil and it was postulated that they could be located within metalloporphyrins as Ni and V are located in these compounds or heteroatomic ligands due to their abundance in asphaltene (Selby et al., 2007b). In addition, asphaltenes were separated from oils during this study using *n*-heptane and the isotopic compositions in the extracted asphaltenes were the same as the whole oil. This study advanced the analytical application of this tool since separation of asphaltene for Re-Os analysis allows much higher abundances to be analysed producing more precise results.

A subsequent Re-Os study provided further evidence that Re-Os geochronology of hydrocarbons records the age of oil generation rather than migration or emplacement ages and also that it is unaffected by biodegradation. The study on the UK Atlantic margin oil fields provided a Re-Os generation age of 68 ± 13 Ma which agrees with basin models and also with an Ar-Ar age of K-feldpars that contain oil fluid inclusions (Finlay et al., 2011). Furthermore it provided evidence for Os isotope

compositions being a useful tool for oil to source fingerprinting supporting the hypothesis of Selby et al. (2007b).

1.3.2 Oil to source fingerprinting using Os isotopes

Oil to source fingerprinting is most commonly carried out by using carbon isotopes and/or biomarkers, however these methods can be hampered by biodegradation as they rely on the light fractions of oil that are removed by biodegradation (Peters et al., 1999, 2005). Rhenium and Os are found within the heavy asphaltene fraction of oil and Os isotopes have been shown to be a potential oil to source correlation tool (Selby and Creaser, 2005a; Selby et al., 2005, 2007b; Finlay et al., 2011). It has been suggested that the initial $^{187}Os/^{188}Os$ (Os_i) of oil is inherited from the source rock $^{187}Os/^{188}Os$ at the time of oil generation (Os_g; Finlay et al., 2010b, 2011, 2012). Finlay et al. (2011) found that the UK Atlantic margin oils have similar Os_i to the Os_g of the known source rock, the Kimmeridge Clay Formation. A further study also showed that the Western Canadian oil sands are sourced predominantly from the Gordondale Formation, with only minor amounts from the previously postulated Exshaw Formation (Finlay et al., 2012). In addition, this study used Pt/Pd ratios for correlation as they have similar properties to Re and Os. The Pt/Pd ratios validated the Os results for the UK Atlantic margin oils and the Western Canadian oil sands (Finlay et al., 2012). A study on North Sea oils showed that there are two populations of oils in terms of Os, one is related to the source rock, but the other is more unradiogenic (0.17 – 0.48) and from oils related to the basin bounding faults (Finlay et al., 2010b). These Os compositions were hypothesised to be associated with mantle fluids that had contaminated the oils during faulting. This study demonstrated the importance of Os in understanding crustal-scale fluid dynamics and oil migration pathways.

The reliability of Os as an oil to source fingerprinting tool was further corroborated by a Re-Os study of the Permian Phosphoria and Jurassic Staffin Formations using hydrous pyrolysis experiments (Rooney et al., 2012). This involved artificial maturation of the source rocks and then Re-Os analysis of the original rocks and the products derived from the hydrous pyrolysis experiments in order to assess

transfer of Re and Os from source to oil. Unfortunately the experiments found no measurable Re or Os in the oils produced since the kinetic parameters needed for transfer were not attained in the artificial high temperature and pressure experiments. However bitumen formation (a precursor to oil) allowed the Re-Os isotopic systematics to be assessed and it was found that hydrocarbon generation does not affect Re-Os systematics in source rocks or in generated hydrocarbons. In particular, the $^{187}Os/^{188}Os$ compositions in bitumens were found to be the same as their source rock in both units studied, providing strong evidence that Os isotopes can be used as powerful oil-source correlation tools.

The studies described in section 1.3 have all utilised marine petroleum systems with hydrocarbons sourced from Type II, II-S and III kerogens (Selby and Creaser, 2005a; Selby et al., 2005, 2007b, Finlay et al., 2010b, 2011, 2012; Rooney et al., 2012). With an increasing need to understand more diverse and complicated petroleum systems due to the demand for oil, there is a need to assess the use of Re-Os hydrocarbon geochronology and Os isotope fingerprinting in variable petroleum systems.

1.4 Thesis rationale

This thesis is presented in the format of scientific papers with three main research chapters representing the work carried out, which have been written as distinct papers. The rationale behind each chapter is presented below. As the chapters have been written separately as scientific papers there is minor repetition, particularly in the methodology section of each chapter.

The aim of the research carried out for this thesis involved widening the capabilities of the Re-Os geochronometer in organic-rich sedimentary rocks and hydrocarbons. Previous studies have utilised the Re-Os geochronometer with great success in marine organic-rich sedimentary rocks increasing our understanding of complex sedimentary basins and improving time scale calibration (Cohen et al., 1999; Selby and Creaser, 2005b; Kendall et al., 2009a; Yang et al., 2009; Rooney et al., 2010).

Organic-rich sedimentary rocks also provide source rocks for petroleum systems and it was discovered that Re and Os are transferred to oil and thus the Re-Os geochronometer can be used to date the timing of oil generation (Selby and Creaser 2005a; Selby et al., 2005; Finlay et al., 2011). In addition Os isotopes can be used as an oil to source fingerprinting tool (Selby et al., 2007b; Finlay et al., 2012; Rooney et al., 2012). All of these wide-ranging capabilities, however, have only been carried out on marine sedimentary and petroleum systems. The continental archive provided by lacustrine sedimentary rocks is of crucial importance to understanding geological and climatic processes. Minor changes and variations in these processes have a significant effect on sediment and water balance in lakes, which results in much higher resolution records than globally averaged marine records (Pietras and Carroll, 2006). However, lacustrine rock records are often hampered by the lack of biostratigraphic constraints that are present in the marine record. The application of the Re-Os geochronometer to lacustrine organic-rich sedimentary rocks has, until now, only been partially evaluated (Creaser et al., 2008, Poirier and Hillaire-Marcel, 2009, 2011). Furthermore, lacustrine organic-rich sedimentary rocks are becoming increasingly important hydrocarbon source rocks with a decline in the major reserves associated with large marine source rock intervals. Understanding lacustrine plays would be greatly aided by a tool that can date and fingerprint oil. The focus of this thesis is to test the Re-Os geochronometer in lacustrine sedimentary and petroleum systems in order to assess whether the tool is useful beyond marine systems.

The lacustrine Green River Formation, USA, is the world's best-documented lacustrine organic-rich sedimentary rock deposit and represents a classic model of lacustrine sediment deposition (Smith et al., 2008). The Green River Formation was deposited in three main tectono-sedimentary basins (Uinta, Piceance and Greater Green River), occupied by two large lakes covering an area of 65,000 km^2 (Dyni, 2006). The basins formed east of the thin-skinned Sevier orogenic belt and are separated by Laramide basement-cored uplifts, the geometry of which is controlled by Precambrian and late Palaeozoic structures (Johnson, 2002). The extensive Green River lake system was associated with warm temperate to subtropical climate of the early to middle

Eocene (Smith et al., 2008). Lake level fluctuations allowed for deposition of thick packages of organic-rich carbonaceous shales interbedded with fluvial clastic deposits (Keighley et al., 2003; Pietras and Carroll, 2006). At the maximum extent of these lakes they became progressively more saline with a stratified anoxic bottom layer developing which was conducive to the preservation of organic-rich sedimentary rocks and the sequestration of Re-Os (Boyer, 1982; Colodner et al., 1993; Crusius et al., 1996; Carroll and Bohacs, 2001). The Green River Formation is also interbedded with tuffs, which have been utilised for Ar-Ar and U-Pb geochronology (Smith et al., 2003, 2006, 2008, 2010). These provide a detailed chronology ideal for assessing the accuracy of the Re-Os geochronometer and this succession also provides an ideal opportunity for assessing Re-Os systematics in lacustrine systems and Os isotopes as a continental weathering proxy.

Furthermore, the Green River Formation represents a substantial source rock and is a characteristic model for lacustrine source rock deposition and hydrocarbon generation from these types of source rock facies (Type I lacustrine kerogen; Ruble et al., 2001). The Green River petroleum system of the Uinta Basin in northwest Utah receives considerable attention as it has generated >500 million bbl oil and has >12 billion bbl oil inferred in tar sand deposits, along with oil shales containing an estimated 1 trillion bbl recoverable oil and solid bitumen deposits (Fouch et al., 1994; Ruble et al., 2001; Dyni, 2006). These variable hydrocarbon types make it an ideal petroleum system for testing Re-Os hydrocarbon geochronology and Os isotope fingerprinting on new hydrocarbon types sourced from a Type I lacustrine kerogen. Our understanding of the systematics of Re and Os in hydrocarbons at present is limited; we do not fully understand how the elements are transferred and how the isotopes fractionate. The Green River petroleum system provides an extensive suite of samples from which to assess the behaviour of Re and Os in a natural system. In addition, hydrous pyrolysis experiments on the same source rocks allow artificial maturation of the source rock to be compared to the natural system in order to gain further insights into Re-Os systematics and fractionation.

Following on from the Green River study, a more 'elusive' lacustrine system was chosen for assessment of Re-Os geochronology. The Nonesuch Formation was deposited in the 1100 Ma intracratonic Mid-Continent Rift System of central North America (Ojakangas et al., 2001). Geophysical evidence coupled with exposures in the Lake Superior region show that the Mid-Continent Rift System was one of the world's largest continental rifts reaching >2000 km in length. Extension was <100 km due to rift failure as a result of the onset of the Grenvillian orogeny to the east (Ojakangas et al., 2001). In the Lake Superior region up to 30 km of volcanic and sedimentary rift-fill sequences make up the Keweenawan Supergroup, one of the few comprehensive records of early rifting processes. The Keweenawan Supergroup consists of 20 km of predominantly flood basalts that are overlain by post-rift fluvial and alluvial red beds of the Oronto and Bayfield Groups. The Oronto Group consists of fluvial and alluvial volcaniclastics with one exception: the Nonesuch Formation, a ~200 m thick lens of organic-rich grey to black siltstones and shales. Geochronology of the Keweenawan Supergroup is based upon U-Pb zircon ages of rift-related volcanics. The overlying post-rift sediments, however, are poorly constrained temporally. Depositional characteristics of the Nonesuch Formation and paleogeographic reconstructions strongly suggest that it was deposited in a restricted lacustrine setting (Elmore et al., 1989; Ojakangas et al., 2001). In contrast, a marine embayment/estuarine environment has been suggested due to the presence of biomarkers similar to those found in Phanerozoic marine-sourced oils and evidence from sulphur isotopes (Pratt et al., 1991; Hieshima and Pratt, 1991). The Nonesuch Formation provides the ability to test the Re-Os geochronometer in a Precambrian lacustrine system and assess whether Os isotopes can be used to deduce depositional conditions. Iron speciation techniques are also employed to assess the redox conditions of the lake water column. Along with Os this provides a pioneering assessment of water column conditions in a Mesoproterozoic lake.

The Re-Os geochronology results are presented in this thesis as isochrons. Error propagation of uncertainties includes sample-weighing, spike calibration, blank abundances, isotope compositions and reproducibility of standard Re and Os isotope

values and are presented with 2σ uncertainties. The Re-Os isotope data, 2σ calculated uncertainties for $^{187}Os/^{188}Os$ and $^{187}Re/^{188}Os$ ratios and the associated error correlation function (rho) are regressed to generate an isochron using Isoplot V. 4.15 with the $\lambda^{187}Re$ of 1.666 x 10^{-11} a^{-1} (Ludwig, 1980; Smoliar et al., 1996; Ludwig, 2008). The $^{187}Os/^{188}Os$ intercept records the initial Os isotope composition at the time of deposition or oil generation (Ravizza et al., 1989; Selby and Creaser, 2003; Selby and Creaser 2005a). By incorporating these errors and uncertainties I have compensated for sources of analytical scatter and the data produced should only reflect any geological scatter. In order to generate an isochron representing meaningful data, the mean square of weighted deviations (MSWD) is generally required to be <3, and thus higher values require explanation. Additionally, the Isoplot V. 4.15 program of Ludwig, (2008) generates isochrons with varying degrees of assigned errors (Model 1, 2 or 3). The Model 1 age represents a fit of the data to a line with the assigned analytical errors representing the only reason that the data-points scatter from a straight line. Model 2 ages are generated by assigning equal weights and zero error-correlations to each point. This avoids weighting the points according to analytical errors when it is clear that some other cause of scatter is involved. A Model 3 age assumes that the scatter on the isochron is due to a combination of the assigned errors plus an unknown error e.g., geological error due to variations in initial isotope ratios (Ludwig, 2008).

1.4.1 Chapter Two: Re-Os geochronology of the Green River Formation

The focus of this chapter is to establish Re-Os geochronology as a tool to date lacustrine organic-rich sedimentary rocks in the same way as marine organic-rich sedimentary rocks are dated using Re-Os. In order to do this Re-Os geochronology of the Green River Formation is compared to Ar-Ar and U-Pb ages of interbedded tuffs to assess the accuracy of Re-Os data. In addition, Rock-Eval pyrolysis was carried out on the samples to assess their organic properties and maturity and whether this has any control on Re-Os systematics. This chapter presents Re-Os geochronology of the Green River Formation, Re-Os systematics in lacustrine systems in relation to organic geochemical properties, and the use of Os isotopes to understand paleocontinental

processes. Samples for this study were collected from the US Geological Survey core research centre by the author. All sample preparation, laboratory work, data collection and evaluation for the Re-Os geochronology study were carried out by the author. Determination of TOC contents and Rock-Eval pyrolysis was carried out by Weatherford laboratory, Houston, USA. The chapter was written by the author with Dr David Selby (supervisor – Durham University) and Dr Paull G. Lillis (supervisor – US Geological Survey) providing editorial comments and suggestions. A version of this chapter has been published in *Earth and Planetary Science Letters*, co-authored by David Selby and Paul G. Lillis (see Appendix A).

1.4.2 Chapter Three: Re-Os geochronology and Os isotope fingerprinting of the Green River petroleum system

This chapter details Re-Os geochronology for the Green River petroleum system hydrocarbons in the Uinta Basin, including oils, tars sands and gilsonite. Osmium isotope fingerprinting is then used to trace the hydrocarbons to their source, the Green River Formation. In addition to Re-Os analysis, hydrous pyrolysis experiments are carried out on the Green River Formation. This technique involves artificial maturation of a source rock and provides oil and bitumen samples, which are then analysed for their Re and Os abundances and isotopic compositions. This allows the transfer and fractionation behaviour of Re and Os to be assessed. Oil samples for this study were provided by Dr Paul G. Lillis at the US Geological Survey. Tar sand and gilsonite samples were collected in the field by the author and Dr Paul G. Lillis with some gilsonite samples provided by Dr Tim Ruble of Weatherford laboratories, Houston. Source rock samples from core were collected from the US Geological Survey core research centre by the author. Source rock samples used for the hydrous pyrolysis experiments were collected in the field by Dr Tim Ruble and Dr Michael D. Lewan of the US Geological Survey. All sample preparation, laboratory work, data collection and evaluation for Re-Os geochronology and Os isotope fingerprinting were carried out by the author. The hydrous pyrolysis experiments were carried out by the author with Dr Michael D. Lewan at the US Geological Survey, Denver, USA, who also supervised the

bitumen Soxhlet extractions. This chapter was written by the author with Drs Selby, Lillis and Lewan providing editorial comments and suggestions. A version of this chapter will be submitted for publication to *Geochimica et Cosmochimica Acta*, co-authored by David Selby, Michael D. Lewan and Paul G. Lillis.

1.4.3 Chapter Four: Re-Os geochronology and Fe speciation of the Nonesuch Formation

This chapter involves dating the late Mesoproterozoic lacustrine Nonesuch Formation, in order to assess Re-Os geochronology in more complex lacustrine systems. The depositional setting is assessed using Os isotopes to provide an appraisal for this technique. Iron speciation is also employed to assess the water column redox conditions of the lake during deposition of the Nonesuch Formation. This is carried out because the redox nature of lakes at this time is unknown and has not been previously assessed. All outcrop samples were collected in the field by the author and Dr Alan D. Rooney of Harvard University. Core samples were collected by Prof. Simon W. Poulton of Leeds University from the Michigan Core Repository. All sample preparation, laboratory work, data collection and evaluation for Re-Os geochronology and Fe speciation was carried out by the author. Iron speciation was undertaken at Newcastle University supervised by Prof. Simon W. Poulton. This chapter was written by the author with Drs Selby, Poulton and Rooney providing editorial comments and suggestions. A version of this chapter is in press at *Geology*, co-authored by, Simon W. Poulton, Alan D. Rooney and David Selby.

1.4.4 Chapter Five: Conclusions and future work

The final chapter provides a summary of the work outlined in each chapter and the overall conclusions. Furthermore, this chapter provides suggestions of possible future work that would build on the findings of the research carried out for this thesis.

1.5 References

Allègre, C. L. and Luck, J. M., 1980. Osmium isotopes as petrogenetic and geological tracers. Earth and Planetary Sciences Letters 48, 148-154.

Azmy, K., Kendall, B., Creaser, R. A., Heaman, L., and de Oliveira, T. F., 2008. Global correlation of the Vazante Group, Sao Francisco Basin, Brazil: Re-Os and U-Pb radiometric age constraints. Precambrian Research 164, 160-172.

Barre, A. B., Prinzhofer, A., Allegre, C.J., 1995. Osmium isotopes in the organic matter of crude oil and asphaltenes. Terra Abstracts 7, 199.

Baioumy, H.M., Eglinton, L.B., Peucker-Ehrenbrink, B., 2011. Rhenium-osmium isotope and platinum group element systematics of marine vs. non-marine organic-rich sediments and coals from Egypt. Chemical Geology 285, 70-81.

Boyer, B.W., 1982. Green River laminites: does the playa-lake model really invalidate the stratified-lake model? Geology 10, 321-324.

Begemann, F., Ludwig, K. R., Lugmair, G. W., Min, K., Nyquist, L. E., Patchett, P. J., Renne, P. R., Shih, C.-Y., Villa, I. M., and Walker, R. J., 2001. Call for an improved set of decay constants for geochronological use. Geochimica et Cosmochimica Acta 65, 111-121.

Birck, J. L., RoyBarman, M., and Capmas, F., 1997. Re-Os measurements at the femtomole level in natural samples. Geostandards Newsletter 20, 19-27.

Carroll, A.R., Bohacs, K.M., 2001. Lake-type controls on petroleum source rock potential in nonmarine basins. AAPG Bulletin 85, 1033-1053.

Cave, R. R., Ravizza, G. E., German, C. R., Thomson, J., Nesbitt, R. W., 2003. Deposition of osmium and other platinum-group elements beneath the ultramafic-hosted Rainbow hydrothermal plume. Earth and Planetary Science Letters 210, 65-79.

Cohen, A. S., Waters, F. G., 1996. Separation of osmium from geological materials by solvent extraction for analysis by TIMS. Analytical Chimica Acta 332, 269-275.

Cohen, A. S., Coe, A. L., Bartlett, J. M., and Hawkesworth, C. J., 1999. Precise Re-Os ages of organic-rich mudrocks and the Os isotope composition of Jurassic seawater. Earth and Planetary Science Letters 167, 159-173.

Colodner, D., Sachs, J., Ravizza, G.,Turekian, K.K., Edmond, J., Boyle, E., 1993. The geochemical cycles of rhenium: a reconnaissance. Earth and Planetary Science Letters 117, 205-221.

Creaser, R. A., Papanastassiou, D. A., and Wasserburg, G. J., 1991. Negative thermal ion mass spectrometry of osmium, rhenium and iridium. Geochimica et Cosmochimica et Acta 55, 397-401.

Creaser, R. A., Sannigrahi, P., Chacko, T., and Selby, D., 2002. Further evaluation of the Re-Os geochronometer in organic-rich sedimentary rocks: A test of hydrocarbon maturation effects in the Exshaw Formation, Western Canada Sedimentary Basin. Geochimica et Cosmochimica Acta 66, 3441-3452.

Creaser, R., Szatmari, P., Milani, E.J., 2008. Extending Re-Os shale geochronology to lacustrine depositional systems: a case study from the major hydrocarbon source rocks of the Brazilian Mesozoic marginal basins. In: proceedings of the 33rd International Geological Congress, Oslo (abstract).

Crusius, J., Calvert, S., Pedersen, T., Sage, D., 1996. Rhenium and molybdenum enrichments in sediments as indicators of oxic, suboxic and sulfidic conditions of deposition. Earth and Planetary Science Letters 145, 65-78.

Crusius, J. and Thomson, J., 2000. Comparative behavior of authigenic Re, U, and Mo during reoxidation and subsequent long-term burial in marine sediments. Geochimica et Cosmochimica 64, 2233-2242.

Dyni, J.R., 2006. Geology and resources of some world oil-shale deposits. U.S. Geological Survey Scientific Investigations Report 2005–5294.

Elmore, D. R., Milavec, G. J., Imbus, S. W., and Engel, M. H., 1989, The Precambrian nonesuch formation of the North American mid-continent rift, sedimentology and organic geochemical aspects of lacustrine deposition: Precambrian Research, v. 43, no. 3, p. 191-213.

Fehn, U., Teng, R., Elmore, D., and Kubik, P. W., 1986. Isotope Composition of Osmium in Terrestrial Samples Determined by Accelerator Mass-Spectrometry. Nature 323, 707-710.

Finlay, A.J., Selby, D., Gröcke, D.R., 2010a. Tracking the Hirnantian glaciation using Os isotopes. Earth and Planetary Science Letters 293, 339-348.

Finlay, A. J., Selby, D., Osborne, M.J., Finucane, D., 2010b. Fault-charged mantle-fluid contamination of United Kingdom North Sea oils: Insights from Re-Os isotopes. Geology 38, 979-982.

Finlay, A. J., Selby, D., Osborne, M.J., 2011. Re-Os geochronology and fingerprinting of United Kingdom Atlantic margin oil: Temporal implications for regional petroleum systems. Geology 39, 475-478.

Finlay, A. J., Selby, D., Osborne, M.J., 2012. Petroleum source rock identification of United Kingdom Atlantic Margin oil fields and the Western Canadian Oil Sands using Platinum, Palladium, Osmium and Rhenium: Implications for global petroleum systems. Earth and Planetary Science Letters 313–314, 95-104.

Foster, J. G., Lambert, D. D., Frick, L. R., and Maas, R., 1996. Re-Os isotope evidence for genesis of Archaean nickel ores from uncontaminated komatiites. Nature 382, 703-706.

Fouch, T. D., Nuccio, V., Anders, D.E., Rice, D.D., Pitman, J.K., Mast, R.F., 1994. Green River (!) petroleum system, Uinta Basin, Utah, USA. AAPG Memoirs 60, 399-421.

Georgiev, S., Stein, H.J., Hannah, J.L., Bingen, B., Weiss, H.M., Piasecki, S., 2011. Hot acidic late Permian seas stifle life in record time. Earth and Planetary Science Letters 310, 389-400.

Hannah, J. L., Bekker, A., Stein, H.J., Markey, R.J., Holland, H.D., 2004. Primitive Os and 2316 Ma age for marine shale: implications for Paleoproterozoic glacial events and the rise of atmospheric oxygen. Earth and Planetary Science Letters 225, 43-52.

Hattori, Y., Suzuki, K., Honda, M., Shimizu, H., 2003. Re-Os isotope systematics of the Taklimakan Desert sands, moraines and river sediments around the Taklimakan Desert, and of Tibetan soils. Geochimica et Cosmochimica Acta 67, 1203-1213.

Herr, W., Hintenberger, H., and Voshage, H., 1954. Half-life of rhenium. Physics Review 95, 1691.

Herr, W., Wolfle, R., Eberhardt, P., and Kopp, E., 1964. Development and recent applications of the Re/Os dating method. Radioactive Dating and Methods of Low-Level Counting: International Atomic Energy Agency, 499-508.

Herzberg, C. T., 1993. Lithosphere Peridotites of the Kaapvaal Craton. Earth and Planetary Science Letters 120, 13-29.

Hieshima, G. B., and Pratt, L. M., 1991, Sulfur/carbon ratios and extractable organic matter of the middle proterozoic nonesuch formation, north american midcontinent rift: Precambrian Research, v. 54, no. 1, p. 65-79.

Hirt, B., Tilton, G. R., Herr, W., and Hoffmeister, W., 1963. The half-life of ^{187}Re. In: Geiss, J. and Goldberg, E. Eds.), Earth Science and Meteoritics. North Holland, Amsterdam.

Horan, M. F., Morgan, J. W., Walker, R. J., and Grossman, J. N., 1992. Rhenium-Osmium Isotope Constraints on the Age of Iron-Meteorites. Science 255, 1118-1121.

Johnson, S.Y., 1992. Phanerozoic evolution of sedimentary basins in the Uinta-Piceance Basin region, northwestern Colorado and northeastern Utah. U.S. Geological Survey Bulletin 1787-FF.

Kato, Y., Fujinaga, K., Suzuki, K., 2011. Marine Os isotopic fluctuations in the early Eocene greenhouse interval as recorded by metalliferous umbers from a Tertiary ophiolite in Japan. Gondwana Research 20, 594-607.

Keighley, D., Flint, S., Howell, J., Moscariello, A., 2003. Sequence stratigraphy in lacustrine basins: a model for part of the Green River Formation (Eocene), southwest Uinta Basin, Utah, U.S.A. Journal of Sedimentary Research 73, 987-1006.

Kendall, B., Creaser, R. A., and Selby, D., 2009a. ^{187}Re-^{187}Os geochronology of Precambrian organic-rich sedimentary rocks. Geological Society, London, Special Publications 326, 85-107.

Kendall, B., Creaser, R. A., Gordon, G. W., and Anbar, A. D., 2009b. Re-Os and Mo isotope systematics of black shales from the Middle Proterozoic Velkerri and Wollogorang Formations, McArthur Basin, northern Australia. Geochimica et Cosmochimica Acta 73, 2534-2558.

Kendall, B. S., Creaser, R. A., Ross, G. M., and Selby, D., 2004. Constraints on the timing of Marinoan 'Snowball Earth' glaciation by ^{187}Re – ^{187}Os dating of a Neoproterozoic post-glacial black shale in Western Canada. Earth and Planetary Science Letters 222, 729-740.

Koide, M., Goldberg, E.D., Niemeyer, S., Gerlach, D., Hodge, V., Bertine, K.K., Padova, A., 1991. Osmium in marine sediments. Geochimica et Cosmochimica Acta 55, 1641-1648.

Levasseur, S., Birck, J.-L., Allègre, C.J., 1998. Direct measurement of femtomoles of osmium and the ^{187}Os/^{186}Os ratio in seawater. Science 282, 272-274.

Levasseur, S., Birck, J.L., Allègre, C.J., 1999. The osmium riverine flux and the oceanic mass balance of osmium. Earth and Planetary Science Letters 174, 7-23.

Lewan, M. D. and Maynard, J. B., 1982. Factors controlling enrichment of vanadium and nickel in the bitumen of organic sedimentary rocks. Geochimica et Cosmochimica Acta 46, 2547-2560.

Lindner, M., Leich, D. A., Russ, G. P., Bazan, J. M., and Borg, R. J., 1989. Direct determination of the half-life of ^{187}Re. Geochimica et Cosmochimica Acta 53, 1597-1606.

Luck, J.M., Birck, J.L., Allegre, C.J., 1980. ^{187}Re-^{187}Os systematics in meteorites: early chronology of the solar system and age of the galaxy. Nature 283, 256-259.

Luck, J.M., and Allègre, C.J., 1982. The study of molybdenites through the ^{187}Re-^{187}Os chronometer. Earth and Planetary Science Letters 61, 291-296.

Luck, J.M., Allegre, C.J., 1983. ^{187}Re-^{187}Os systematics in meteorites and cosmochemical consequences. Nature 302, 130-132.

Ludwig, K.R., 1980. Calculation of uncertainties of U-Pb isotope data. Earth and Planetary Science Letters 46, 212-220.

Ludwig, K., 2008. Isoplot, version 4.0: a geochronological toolkit for microsoft Excel. Berkeley Geochronology Center Special Publication No. 4.

Markey, R., Stein, H., and Morgan, J., 1998. Highly precise Re-Os dating for molybdenite using alkaline fusion and NTIMS. Talanta 45, 935-946.

McArthur, J.M., Algeo, T.J., van de Schootbrugge, B., Li, Q., Howarth, R.J., 2008. Basinal restriction, black shales, Re-Os dating, and the Early Toarcian (Jurassic) oceanic anoxic event. Paleoceanography 23(4), PA4217.

McDaniel, D. K., Walker, R. J., Hemming, S.R., Horan, M.F., Becker, H., Grauch, R.I., 2004. Sources of osmium to the modern oceans: new evidence from the ^{190}Pt-^{186}Os system. Geochimica et Cosmochimica Acta 68, 1243-1252.

Morford, J.L. and Emerson, S., 1999. The geochemistry of redox sensitive trace metals in sediments. Geochimica et Cosmochimica Acta 63, 1735-1750.

Morford, J.L., Martin, W.R., Francois, R., Carney, C.M., 2009. A model for uranium, rhenium, and molybdenum diagenesis in marine sediments based on results from coastal locations. Geochimica et Cosmochimica Acta 73, 2938-2960.

Morgan, J. W., 1986. Ultramafic Xenoliths - Clues to Earths Late Accretionary History. Journal of Geophysical Research-Solid Earth and Planets 91, 2375-2387.

Morgan, J. W., Walker, R. J., and Grossman, J. N., 1992. Rhenium-Osmium Isotope Systematics in Meteorites .1. Magmatic Iron Meteorite Group-Iiab and Group-Iiiab. Earth and Planetary Science Letters 108, 191-202.

Naldrett, S. N. and Libby, W. F., 1948. Natural radioactivity of rhenium. Physics Review 73, 487-493.

Ojakangas, R. W., Morey, G. B., and Green, J. C., 2001, The Mesoproterozoic Midcontinent Rift System, Lake Superior Region, USA: Sedimentary Geology, v. 141-142, p. 421-442.

Pearson, D. G., Carlson, R. W., Shirey, S. B., Boyd, F. R., and Nixon, P. H., 1995. Stabilization of Archean Lithospheric Mantle - a Re-Os Isotope Study of Peridotite Xenoliths from the Kaapvaal Craton. Earth and Planetary Science Letters 134, 341-357.

Pearson, D. G., Shirey, S. B., Harris, J. W., and Carlson, R. W., 1998. Sulphide inclusions in diamonds from the Koffiefontein kimberlite, S Africa: constraints on diamond ages and mantle Re-Os systematics. Earth and Planetary Science Letters 160, 311-326.

Peters, K.E., Fraser, T.H., Amris, W. Rustanto, B., Hermanto, E. 1999. Geochemistry of crude oils from eastern Indonesia. AAPG Bulletin 83, 1927-1924.

Peters, K. E., Walters, C.C., Moldowan, J. M. 2005. The Biomarker Guide Volume 1: Biomarkers and Isotopes in the Environment and Human History (Cambridge University Press. 2005).

Peucker-Ehrenbrink, B., 1996. Accretion of extraterrestrial matter during the last 80 million years and its effect on the marine osmium isotope record. Geochimica et Cosmochimica Acta 60, 3187-3196.

Peucker-Ehrenbrink, B., Blum, J. D., 1998. Re-Os isotope systematics and weathering of Precambrian crustal rocks: implications for the marine osmium isotope record. Geochimica et Cosmochimica Acta 62, 3193-3203.

Peucker-Ehrenbrink, B., Ravizza, G., 2000. The marine osmium isotope record. Terra Nova 12, 205-219.

Peucker-Ehrenbrink, B. and Hannigan, R. E., 2000. Effects of black shale weathering on the mobility of rhenium and platinum group elements. Geology 28, 475-478.

Peucker-Ehrenbrink, B. and Jahn, B., 2001. Rhenium-osmium isotope systematics and platinum group element concentrations: Loess and the upper continental crust, Geochem. Geophys. Geosyst. 2, 1061 - 1083.

Peucker-Ehrenbrink, B., Ravizza, G., 2012. Osmium isotope stratigraphy, in: Gradstein, F. M., Ogg, J. G., Schmitz, M., Ogg, G. 2012, The Geological Timescale, 1. Elsevier, Oxford, 145 – 166.

Pietras, J.T., Carroll, A.R., 2006. High-resolution stratigraphy of an underfilled lake basin: Wilkins Peak Member, Eocene Green River Formation, Wyoming, U.S.A. Journal of Sedimentary Research 76, 1197-1214.

Poirier, A., 2006. Re–Os and Pb isotope systematics in reduced fjord sediments from Saanich Inlet (Western Canada). Earth and Planetary Science Letters 249, 119-131.

Poirier, A., Hillaire-Marcel, C., 2009. Os-isotope insights into major environmental changes of the Arctic Ocean during the Cenozoic. Geophysical Research Letters 36. L11602.

Poirier, A., Hillaire-Marcel, C., 2011. Improved Os-isotope stratigraphy of the Arctic Ocean. Geophysical Research Letters 38. L14607.

Pratt, L. M., Summons, R. E., and Hieshima, G. B., 1991, Sterane and triterpane biomarkers in the Precambrian Nonesuch Formation, North American Midcontinent Rift: Geochimica et Cosmochimica Acta, v. 55, no. 3, p. 911-916.

Raith, J. G. and Stein, H. J., 2000. Re-Os dating and sulfur isotope composition of molybdenite from W-Mo deposits in western Namaqualand, South Africa: implications for ore genesis and low-P high-grade metamorphism. Mineralium Deposita 35, 741-753.

Ravizza, G. and Turekian, K. K., 1989. Application of the ^{187}Re-^{187}Os system to black shale geochronometry. Geochimica et Cosmochimica Acta 53, 3257-3262.

Ravizza, G. and Turekian, K.K., 1992. The Osmium isotopic composition of organic-rich marine sediments. Earth and Planetary Science Letters 110, 1-6.

Ravizza, G. and Esser, B. K., 1993. A possible link between the seawater osmium isotope record and weathering of ancient sedimentary organic matter. Chemical Geology 107, 255-258.

Ravizza, G., Turekian, G. G., and Hay, B. J., 1991. The geochemistry of rhenium and osmium in recent sediments from the Black Sea. Geochimica et Cosmochimica Acta 55, 3741-3752.

Ravizza, G., Martin, C.E., German, C.R., Thompson, G., 1996. Os isotopes as tracers in seafloor hydrothermal systems: metalliferous deposits from the TAG hydrothermal area, 26°N Mid-Atlantic Ridge. Earth and Planetary Science Letters 138, 105-119.

Raymo, M.E., Ruddiman, W.F., 1992. Tectonic forcing of late Cenozoic climate. Nature 359, 117-122.

Richter, F.M., Rowley, D.B., Depaolo, D.J., 1992. Sr isotope evolution of seawater - the role of tectonics. Earth and Planetary Science Letters 109, 11-23.

Rooney, A.D., Selby, D., Houzay, J.-P., Renne, P.R., 2010. Re-Os geochronology of a Mesoproterozoic sedimentary succession, Taoudeni basin, Mauritania: implications for basin-wide correlations and Re-Os organic-rich sediments systematics. Earth and Planetary Science Letters 289, 486-496.

Rooney, A. D., Chew, D. M., Selby, D., 2011. Re-Os geochronology of the Neoproterozoic-Cambrian Dalradian Supergroup of Scotland and Ireland: implications for Neoproterozoic stratigraphy, glaciations and Re-Os systematics. Precambrian Research 185, 202-214.

Rooney, A.D., Selby, D., Lewan, M.D., Lillis, P.G., Houzay, J.-P., 2012. Evaluating Re–Os systematics in organic-rich sedimentary rocks in response to petroleum generation using hydrous pyrolysis experiments. Geochimica et Cosmochimica Acta 77, 275-291.

Ruble, T.E., Lewan, M.D., Philp, R.P., 2001. New insights on the Green River Petroleum System in the Uinta Basin from hydrous pyrolysis experiments. AAPG Bulletin 85, 1333-1371.

Russ, G. P. and Bazan, J. M., 1987. Osmium Isotope Ratio Measurements by Inductively Coupled Plasma Source-Mass Spectrometry. Analytical Chemistry 59, 984-989.

Schmitz, B., Peucker-Ehrenbrink, B., Heilmann-Clausen, C., Åberg, G., Asaro, F., Lee, C.A., 2004. Basaltic explosive volcanism, but no comet impact, at the Paleocene-Eocene boundary: high-resolution chemical and isotopic records from Egypt, Spain and Denmark. Earth and Planetary Science Letters 225, 1-17.

Selby, D., Creaser, R.A., Hart, C.J.R., Rombach, C.S., Thompson, J.F.H., Smith, M.T., Bakke, A.A., Goldfarb, R.J., 2002. Absolute timing of sulfide and gold mineralization: A comparison of Re-Os molybdenite and Ar-Ar mica methods from the Tintina Gold Belt, Alaska. Geology 30, 791-794.

Selby, D. and Creaser, R. A., 2003. Re-Os geochronology of organic rich sediments: an evaluation of organic matter analysis methods. Chemical Geology 200, 225-240.

Selby, D. and Creaser, R. A., 2005a. Direct radiometric dating of hydrocarbon deposits using rhenium-osmium isotopes. Science 308, 1293-1295.

Selby, D. and Creaser, R. A., 2005b. Direct radiometric dating of the Devonian-Mississippian time-scale boundary using the Re-Os black shale geochronometer. Geology 33, 545-548.

Selby, D., Creaser, R. A., Dewing, K., and Fowler, M., 2005. Evaluation of bitumen as a Re-187-Os-187 geochronometer for hydrocarbon maturation and migration: A test case from the Polaris MVT deposit, Canada. Earth and Planetary Science Letters 235, 1-15.

Selby, D., Creaser, R. A., Stein, H. J., Markey, R. J., and Hannah, J. L., 2007a. Assessment of the Re-187 decay constant by cross calibration of Re-Os molybdenite and U-Pb zircon chronometers in magmatic ore systems. Geochimica et Cosmochimica Acta 71, 1999-2013.

Selby, D., Creaser, R. A., and Fowler, M. G., 2007b. Re-Os elemental and isotope systematics in crude oils. Geochimica et Cosmochimica Acta 71, 378-386.

Selby, D., 2007. Direct Rhenium-Osmium age of the Oxfordian-Kimmeridgian boundary, Staffin bay, Isle of Skye, U.K., and the Late Jurassic time scale. Norwegian Journal of Geology 87, 9.

Selby, D., Mutterlose, J., and Condon, D.J., 2009. U-Pb and Re-Os geochronology of the Aptian/Albian and Cenomanian/Turonian stage boundaries: Implications for timescale calibration, osmium isotope seawater composition and Re-Os systematics in organic-rich sediments. Chemical Geology 265, 394-409.

Sharma, M., Wasserburg, G.J., Hofmann, A.W., Chakrapani, G.J., 1999. Himalayan uplift and osmium isotopes in oceans and rivers - its relation to global tectonics and climate. Geochimica et Cosmochimica Acta 63, 4005-4012.

Sharma, M., Wasserburg, G.J., Hofmann, A.W., Butterfield, D.A., 2000. Osmium isotopes in hydrothermal fluids from the Juan de Fuca Ridge. Earth and Planetary Science Letters 179, 139-152.

Sharma, M., Rosenberg, E.J., Butterfield, D.A., 2007. Search for the proverbial mantle osmium sources to the oceans: Hydrothermal alteration of mid-ocean ridge basalt. Geochimica et Cosmochimica Acta 71, 4655-4667.

Shen, J. J., Papanastassiou, D. A., and Wasserburg, G. J., 1996. Precise Re-Os determinations and systematics of iron meteorites. Geochimica et Cosmochimica Acta 60, 2887-2900.

Shirey, S. B. and Walker, R. J., 1995. Carius tube digestion for low-blank rhenium-osmium analysis. Anal Chem 67, 2136-2141.

Shirey, S. B. and Walker, R. J., 1998. The Re-Os isotope system in cosmochemistry and high temperature geochemistry. Annual Reviews Earth and Planetary Science Letters 26, 423-500.

Smith, M.E., Singer, B., Carroll, A., 2003. $^{40}Ar/^{39}Ar$ geochronology of the Eocene Green River Formation, Wyoming. Geological Society of America Bulletin 115, 549-565.

Smith, M.E., Singer, B.S., Carroll, A.R., Fournelle, J.H., 2006. High-resolution calibration of Eocene strata: $^{40}Ar/^{39}Ar$ geochronology of biotite in the Green River Formation. Geology 34, 393-396.

Smith, M.E., Carroll, A.R., Singer, B.S., 2008. Synoptic reconstruction of a major ancient lake system: Eocene Green River Formation, western United States. Geological Society of America Bulletin 120, 54-84.

Smith, M.E., Chamberlain, K.R., Singer, B.S., Carroll, A.R., 2010. Eocene clocks agree: Coeval $^{40}Ar/^{39}Ar$, U-Pb, and astronomical ages from the Green River Formation. Geology 38, 527-530.

Smoliar, M. I., Walker, R. J., and Morgan, J. W., 1996. Re-Os isotope constraints on the age of Group IIA, IIIA, IVA, and IVB iron meteorites. Science 271, 1099-1102.

Sun, W., Bennett, V.C., Eggins S, M., Kamenetsky, V.S., Arculus R.J., 2003. Enhanced mantle to crust rhenium transfer in undegassed arc magmas. Nature 422, 294–297.

Sundby, B., Martinez, P., Gobeil, C., 2004. Comparative geochemistry of cadmium, rhenium, uranium, and molybdenum in continental margin sediments. Geochimica et Cosmochimica Acta 68, 2485-2493.

Suzuki, K., Shimizu, H., and Masuda, A., 1996. Re-Os dating of molybdenites from ore deposits in Japan: Implications for the closure temperature of the Re-Os system for molybdenite and the cooling history of molybdenum ore deposits. Geochimica et Cosmochimica Acta 60, 3151-3159.

Turgeon, S. C., Creaser, R. A., and Algeo, T. J., 2007. Re-Os depositional ages and seawater Os estimates for the Frasnian-Famennian boundary: Implications for weathering rates, land plant evolution, and extinction mechanisms. Earth and Planetary Science Letters 261, 649-661.

Völkening, J., Walczyk, T., and G. Heumann, K., 1991. Osmium isotope ratio determinations by negative thermal ionization mass spectrometry. International Journal of Mass Spectrometry and Ion Processes 105, 147-159.

Walczyk, T., Hebeda, E., Heumann, K.G., 1991. Osmium isotope ratio measurements by negative thermal ionization mass spectrometry (NTI-MS). Fresenius Journal of Analytical Chemistry 341, 537-541.

Walker, R. J., 1988. Low-blank chemical separation of rhenium and osmium from gram quantities of silicate rock for measurement by resonance ionization mass spectrometry. Anal Chem 60, 1231-1234.

Walker, R. J. and Fassett, J. D., 1986. Isotope measurement of subnanogram quantities of rhenium and osmium by resonance ionization mass spectrometry. Anal Chem 58, 2923-2927.

Walker, R. J. and Morgan, J. W., 1989. Rhenium-Osmium Isotope Systematics of Carbonaceous Chondrites. Science 243, 519-522.

Walker, R. J., Morgan, J. W., Horan, M. F., Czamanske, G. K., Krogstad, E. J., Fedorenko, V. A., and Kunilov, V. E., 1994. Re-Os Isotope Evidence for an Enriched-Mantle Source for the Norilsk-Type, Ore-Bearing Intrusions, Siberia. Geochimica et Cosmochimica Acta 58, 4179-4197.

Woodland, S., Ottley, C., Pearson, D.G., Swarbrick, R.E., 2001. Microwave digestion of oils for analysis of platinum group and rare earth elements by ICP-MS. Special Publications of the Royal Society of Chemistry 267, 17-24.

Yamashita, Y., Takahashi, Y., Haba, H., Enomoto, S., Shimizu, H., 2007. Comparison of reductive accumulation of Re and Os in seawater-sediment systems. Geochimica et Cosmochimica Acta 71, 3458-3475.

Yang, G., Hannah, J. L., Zimmerman, A., Stein, H. J., and Bekker, A., 2009. Re-Os depositional age for Archean carbonaceous slates from the southwestern Superior Province: Challenges and insights. Earth and Planetary Science Letters 280, 83-92.

York, D., 1966. Least-Squares Fitting of a Straight Line. Canadian Journal of Physics 44, 1079-1086.

Chapter 2

Re-Os geochronology of the lacustrine Green River Formation

Re-Os geochronology of the lacustrine Green River Formation: Insights into direct depositional dating of lacustrine successions, Re-Os systematics and paleocontinental weathering

A version of this chapter has been published in *Earth and Planetary Science Letters*, **359 - 360,** 194 - 205, 2012; co-authored by David Selby of Durham University and Paul G. Lillis of the U.S. Geological Survey, Denver. See Appendix A.

2.1 Introduction

Lake systems are common to the continental landscape throughout the world and frequently record deposition over millions of years (e.g., Carroll et al., 1992; Olsen, 1997). Lacustrine sediments provide a valuable archive of continental geological processes, responding to tectonic, climatic and magmatic influences. These lacustrine records are of a much higher resolution than globally averaged marine records (Pietras and Carroll, 2006), and are therefore essential for correlating geological and climatic phenomena across continents and furthermore the globe. The importance of lacustrine deposits is exemplified by the numerous studies providing vital insights into processes such as continental tectonics and magmatism, paleoclimatic fluctuations, geomagnetic timescales, Milankovitch cycles, terrestrial biotic evolution and economic resources (e.g., Lambiase, 1990; Carroll and Bohacs, 1999; Katz, 2001; Machlus et al., 2004; Meyers, 2008; Hao et al., 2011). Sedimentation in lake settings can range from fluvial to highly organic-rich profundal deposits documenting a complex amalgamation of continental and atmospheric processes. A more complete understanding of the relationship of lacustrine sediments to global geological systems requires accurate and precise geochronological frameworks. Age control in lacustrine settings is often hampered by the lack of biostratigraphic constraints common to the marine record. In the absence of tuff horizons for U-Pb and Ar-Ar geochronology, or sufficient and documented mammalian biostratigraphy, direct dating of lacustrine sedimentary stratigraphy is challenging.

The Re-Os geochronometer is a widely-used tool for determining precise and accurate depositional ages of marine organic-rich sedimentary rocks (e.g., Cohen et al., 1999; Selby and Creaser, 2005; Kendall et al., 2009a; Xu et al., 2009; Georgiev et al., 2011). These and additional studies have demonstrated that Re-Os systematics are not adversely affected by processes such as hydrocarbon maturation and greenschist-grade metamorphism (e.g., Creaser et al., 2002; Kendall et al., 2004; Yang et al., 2009; Rooney et al., 2010, 2012). However, application of the Re-Os geochronometer to lacustrine strata has only been partially evaluated (Creaser et al., 2008; Poirier and

Hillaire-Marcel, 2011). Here I present a comprehensive study of one of the world's best documented lacustrine systems, the Green River Formation, to assess whether Re-Os geochronology can be used as a tool to directly date the deposition of lacustrine organic-rich sedimentary rocks.

Previous studies suggest the uptake of Re and Os in marine organic-rich sedimentary rocks relies on the capture of hydrogenous Re and Os at or below the sediment/water interface under oxygen limited conditions (Ravizza et al., 1991; Ravizza and Turekian, 1992; Colodner et al., 1993; Crusius et al., 1996; Cohen et al., 1999), with the majority of Re and Os bound in organic matter (Cohen et al., 1999; Selby and Creaser, 2003; Georgiev et al., 2011; Rooney et al., 2012). This implies that organic-rich sedimentary rocks deposited in the reducing bottom waters of a stratified lake should be predisposed to Re and Os uptake, and thus viable for Re-Os geochronology, provided there is sufficient runoff containing dissolved Re and Os. As interpreted for the marine realm, the initial $^{187}Os/^{188}Os$ (Os_i) composition of lacustrine organic-rich sedimentary rocks should reflect the $^{187}Os/^{188}Os$ composition of lake water at the time of deposition (Ravizza and Turekian, 1989, 1992; Cohen et al., 1999). The $^{187}Os/^{188}Os$ composition of seawater records a balance of radiogenic (~1.40) continental inputs derived chiefly from runoff with minor contributions from aeolian dust, and unradiogenic (~0.12) inputs derived from cosmic dust and hydrothermal alteration of oceanic crust (Peucker-Ehrenbrink and Ravizza, 2000). Assuming that runoff from the surrounding continental crust is the predominant source of Os into a lake, the $^{187}Os/^{188}Os$ composition of lake water will reflect the composition of regional continental runoff at the time of deposition. Os isotopes therefore provide an insight into regional geological processes and allow chemostratigraphic correlation making Re-Os geochronology beneficial beyond direct depositional age dating.

Here I evaluate and discuss lacustrine Re-Os geochronology and Os isotope compositions of the Green River Formation in the Uinta Basin, Utah, USA. The Green River Formation succession represents a classic model of lacustrine sediment deposition and is primarily comprised of organic-rich carbonaceous siltstones,

mudstones and marly oil shales (Tuttle and Goldhaber, 1993; Keighley et al., 2003; Smith et al., 2008a). Interbedded tuff horizon Ar-Ar and U-Pb dates provide an extensive geochronological framework, which has been tied to mammalian biostratigraphy, paleomagnetic and astronomical ages (Smith et al., 2003, 2006, 2008a, 2010). This temporal framework makes the Green River Formation an ideal natural laboratory for testing the applicability of the Re-Os geochronometer to lacustrine deposits.

2.2 Geological setting

2.2.1 Geology of the Green River Formation basins

The Green River Formation was deposited in three main continental basins (Fig. 2.1: Uinta, Piceance and Greater Green River), in Colorado, Wyoming and Utah (Dyni, 2006). The basins formed east of the thin-skinned Sevier orogenic belt, and are separated by Laramide basement-cored uplifts associated with Precambrian and late Palaeozoic structures (Johnson, 1992). The extensive Green River lake system (65,000 km^2) was associated with temperate to subtropical climate of the early to middle Eocene (Smith et al., 2008a), which resulted in exceptionally high continental denudation rates (175 ± 30 m/Myr; Smith et al., 2008b). Sedimentary facies within the Green River Formation can be divided into fluvio-lacustrine, fluctuating profundal and evaporative facies (Carroll and Bohacs, 1999, 2001; Fig. 2.2). Deposition occurred in freshwater to hypersaline lakes with lake-level fluctuations resulting in thick packages of organic-rich carbonaceous shales interbedded with fluvial clastic deposits (Keighley et al., 2003; Pietras and Carroll, 2006). The final stages of Green River Formation deposition occurred at the end of the Laramide orogeny when the basins were infilled from the north by volcanics from the Absaroka volcanic field (Johnson, 1992). The Uinta Basin was the final basin to be infilled and therefore had the longest-lived lake containing the thickest section of Green River Formation (>3 km). Organic-rich units from the Uinta Basin were sampled for this study as they record the complete history of the Green River Formation.

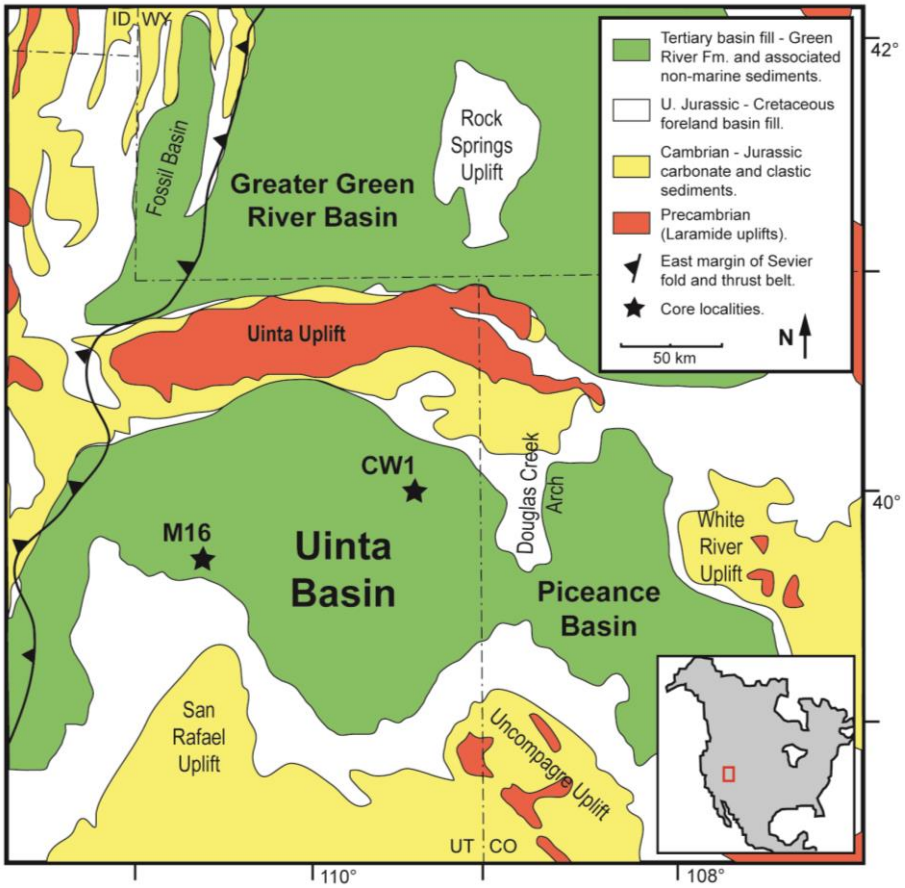

Figure 2.1: Location map displaying the main basins containing the Green River Formation, surrounding geology and the location of the sampled Marsing 16 (M16; 39° 57' 1.4904" N, 111° 1' 37.527" W) and Coyote Wash 1 (CW1; 40° 1' 22.224" N, 109° 18' 38.4834" W) cores in the Uinta Basin (adapted from Smith et al., 2008a). The CW1 core is located in the central depocentre of an asymmetric basin structure (See Fig. 2.2, inset A), while the M16 core is proximal to the lake margin. Inset map of North America shows the study area.

2.2.2 Uinta Basin stratigraphy

Lacustrine deposition in the Uinta Basin began in the early Eocene following eastward retreat of the Late Cretaceous seaway (Ryder et al., 1976). Initial deposition began with the Colton Formation (coarse grained clastic beds and red mudstones), which was deposited in a fluvial setting. As lake-levels rose the depositional setting evolved into fluvio-lacustrine deposition of sandstones interbedded with the base of the Green River Formation and at the lake edges (Fig. 2.2). Stratigraphically above the Colton Formation the Douglas Creek Member of the Green River Formation was deposited in response to rising lake-levels (Bradley, 1931; Tuttle and Goldhaber, 1993). The Douglas Creek Member is a siliciclastic-dominated interval with fluvial sandstones and siltstones deposited at the edges of the basin and oil shales deposited in the central depocentres, considered correlative to the green shale and black shale facies of the Green River Formation in other parts of the basin (Remy, 1992; Ruble et al., 2001). This depositional model has been attributed to fluctuating profundal facies deposition (Carroll and Bohacs, 2001). Following deposition of this interval an increase in salinity is attributed to the development of a more arid climate between 49 and 50 Ma (Ryder et al., 1976; Tuttle and Goldhaber, 1993). Increased aridity resulted in evaporitic deposition of saline minerals interbedded with dolomitic marlstones, mudstones, sandstones and oil shales of the carbonate dominated Parachute Creek Member, stratigraphically above the Douglas Creek Member (Fig. 2.2). The basal section of the Parachute Creek Member (~49 Ma) records a rise in lake-levels to their maximum extent that resulted in the deposition of oil shales interbedded with mudstones, marlstones and siltstones. This section, the Mahogany Zone, is the most organic-rich horizon of the Green River Formation (total organic carbon [TOC] up to 30 wt.%; Bradley, 1931; Tuttle and Goldhaber, 1993; Smith et al., 2008a). Deposition in the Uinta Basin continued until ~44 Ma with conditions becoming progressively more evaporitic (Smith et al., 2008a). Above the Parachute Creek Member red-brown shale and fluvial coarse-grained clastics make up interbeds of the Uinta Formation of the Green River Formation (Keighley et al., 2003).

2.2.3 Previous geochronology

The current geochronological framework for the Green River Formation is based on Ar-Ar ages of interbedded tuffs concentrated in the Greater Green River and Uinta Basins (Smith et al., 2003, 2006, 2008a). More recently, the Ar-Ar ages have been recalibrated to Fish Canyon Sanidine (KO_8) and accurately correlated to U-Pb zircon ages from the tuff beds and astronomical ages preserved within cyclical sediments (Kuiper et al., 2008; Smith et al., 2010). Uinta Basin deposition began ~52 Ma, but the oldest dated tuff is the Curly tuff at 49.32 ± 0.30 Ma lying just below the Mahogany Zone (Fig. 2.2). This makes correlation of the older stratigraphy in the Uinta Basin more difficult, especially as there is a lack of surface exposure (Smith et al., 2008a). Lacustrine deposition ended just after deposition of the Strawberry tuff dated at 44.27 ± 0.93 Ma (Fig. 2.2). Geochronology in the Uinta Basin allows cross-correlation of Re-Os and Ar-Ar ages in order to assess the accuracy of Re-Os lacustrine organic-rich sedimentary rock geochronology.

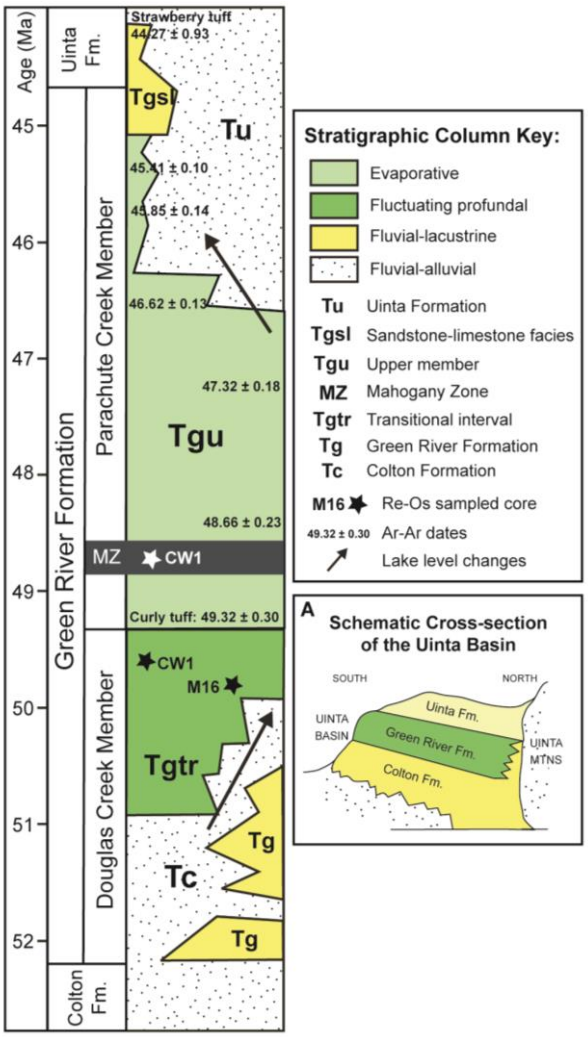

Figure 2.2: Generalised chronostratigraphy displaying the main members of the Green River Formation and the location of sampled units. Age constraints labelled on the stratigraphic column are based on Ar-Ar dates of interbedded tuffs. Lacustrine facies associations of each unit are illustrated in the right hand panel of the stratigraphic column; these are adapted from lithostratigraphy of Smith et al. (2008a). This lithostratigraphy illustrates the complex nature of spatial and temporal variation of units within the Uinta Basin. Nomenclature of Smith et al. (2008a) is included in the key in order to aid comparison with Ar-Ar ages. Inset A is a simplified cross-section of the Uinta Basin at the present day that illustrates the asymmetric nature of the basin and that the erosional remnant now outcrops within the southern limb of a gentle syncline, dipping <5° to the North. The southern margin of the basin has mostly been eroded, with the most continuous exposure in the northeast corner of the basin where up to ~4 km of sediment was deposited. With a lack of surface exposure this asymmetric nature makes correlation of units challenging.

2.3 Sampling and analytical methodology

2.3.1 Sampling

The Green River Formation samples were collected from two exploration drill cores (Coyote Wash 1[CW1; 40° 1' 22.224" N, 109° 18' 38.4834" W] and Marsing 16 [M16; 39° 57' 1.4904" N, 111° 1' 37.527" W]) from the Uinta Basin, which are held at the USGS Core Research Centre in Denver, Colorado. The Mahogany Zone and the Douglas Creek Member were sampled as these are the most organic-rich intervals of Green River Formation in the Uinta Basin (3.5 – 28.1 wt.% TOC: Table 2.1). The sampled stratigraphy comprises grey-black carbonaceous mudstones and oil shales of the profundal dominated intervals. Samples weighing 40 to 70 g were collected at 5 to 10 cm intervals stratigraphically. Each sample represents approximately a 1 to 2 cm vertical interval of stratigraphy. All sampled core sections are absent of alteration and veining.

In the CW1 core located in the central depocentre two intervals were sampled; the Mahogany Zone at depths between 682.5 and 685.4 m and the Douglas Creek Member at depths between 1026.0 and 1028.0 m. The Mahogany Zone is made up of quartz, calcite, dolomite, sodium feldspar, dawsonite and pyrite (Tuttle, 1991). The Douglas Creek Member is comprised of quartz, calcite, dolomite, aragonite, sodium feldspar, illite and minor other clays (Tuttle, 1991). In the M16 core at the southwest edge of the basin the equivalent of the Douglas Creek Member was sampled at depths between 323.8 and 325.4 m. This lies ~60 m above intertonguing fluvial sandstones of the Colton Formation. The three sampled units are named Mahogany Zone (CW1), Douglas Creek Member (CW1) and Douglas Creek Member (M16) throughout the chapter.

2.3.2 Re-Os analysis

In preparation for Re-Os analysis, all fresh core samples were polished removing all cutting and drilling marks to eliminate any contamination. The samples were air dried at 60°C for ~12 hours, broken into chips with no metal contact, and then

crushed to a fine powder (~30 μm) in a zirconium mill. Samples of 40 - 70 g were used to ensure that Re-Os abundances were homogenised in the powdered samples (Kendall et al., 2009). The Re-Os isotope analysis was performed at Durham University's TOTAL laboratory for source rock geochronology and geochemistry at the Northern Centre for Isotopic and Elemental Tracing. For sample digestion a Cr^{VI}–H_2SO_4 solution was used to preferentially liberate hydrogenous Re and Os, limiting the incorporation of detrital Re and Os (Kendall et al., 2004; Selby and Creaser, 2003).

Sample powder weighing 0.2 - 0.4 g, a tracer (spike) solution of ^{190}Os and ^{185}Re and the Cr^{VI}–H_2SO_4 solution were digested in a sealed carius tube for 48 hours at 220°C (Selby and Creaser, 2003; Kendall et al., 2004). The Re and Os were purified using the solvent extraction ($CHCl_3$), micro-distillation and anion chromatography methods, followed by negative thermal ionisation mass spectrometry as outlined by Selby and Creaser (2003) and Selby (2007). The Re and Os fractions were loaded onto Ni and Pt filaments, respectively (Selby, 2007). Isotopic measurements were performed using a ThermoElectron TRITON mass spectrometer via static Faraday collection for Re and ion-counting using a secondary electron multiplier in peak-hopping mode for Os. Total procedural blanks during this study were 14.6 ± 0.16 pg and 0.05 ± 0.01 pg (1σ S.D., n = 3) for Re and Os, respectively, with an average $^{187}Os/^{188}Os$ value of 0.61 ± 0.03 (n = 3).

Uncertainties for $^{187}Re/^{188}Os$ and $^{187}Os/^{188}Os$ were determined by full error propagation of uncertainties in Re and Os mass spectrometer measurements, blank abundances and isotopic compositions, spike calibrations and reproducibility of standard Re and Os isotopic values. The Re–Os isotopic data including the 2σ calculated uncertainties for $^{187}Re/^{188}Os$ and $^{187}Os/^{188}Os$ and the associated error correlation function (rho) were regressed to yield a Re–Os date using *Isoplot V*. 4.0 and the $\lambda^{187}Re$ of $1.666 \times 10^{-11}a^{-1}$ (Ludwig, 1980, 2008; Smoliar et al., 1996). The age uncertainty including the uncertainty of 0.35% in $\lambda^{187}Re$ only affects the third decimal place (Selby, 2007; Smoliar et al., 1996).

Two in-house Re and Os solution standards were analysed to monitor the long-term reproducibility of mass spectrometer measurements. The Re solution standard

yields an average $^{185}Re/^{187}Re$ ratio of 0.598071 ± 0.001510 (1 S.D., n = 67), which is in excellent agreement with the value reported for the AB-1 standard (Finlay et al., 2010; Rooney et al., 2010 and references therein). The Os isotope reference solution (DROsS) gave an $^{187}Os/^{188}Os$ ratio of 0.160892 ± 0.000559 (1 S.D., n = 67), which is in agreement with previous studies (Finlay et al., 2010; Rooney et al., 2010 and references therein).

2.3.3 TOC and Rock-Eval Analysis

Total organic carbon (TOC) values for the Green River Formation samples were determined commercially using a LECO C200 Carbon Analyser at Weatherford labs, Houston, USA. A known weight (~0.1 g) of powdered and carbonate free (prior removal using HCl) rock sample was combusted in oxygen at a temperature of about 1200°C. The carbon dioxide produced was passed, via traps for water, sulphur dioxide and halogens, into the infrared detector previously calibrated on standard samples.

Rock-Eval pyrolysis was also performed at Weatherford labs, Houston, USA to assess thermal maturity and organic matter characteristics of the samples using a Rock-Eval II instrument. Ground samples were heated in an inert environment to measure the yield of three groups of compounds (S1, S2, and S3), measured as three peaks on a program in mg hydrocarbons per gram of rock (S1 and S2) and mg carbon dioxide per gram of rock (S3). Sample heating at 300°C for 3 minutes produces the S1 peak by vaporizing the free (unbound) hydrocarbons. High S1 values indicate either large amounts of kerogen-derived bitumen or the presence of migrated hydrocarbons. The oven then increases in temperature by 25°C/minute to 600°C, and the S2 and S3 peaks are measured from the pyrolytic degradation of the kerogen in the sample. The S2 peak is proportional to the amount of hydrogen-rich kerogen in the rock, and the S3 peak measures the carbon dioxide released (to 390^{O}C) providing an assessment of the oxygen content of the kerogen. The temperature at which the S2 peak reaches a maximum, "T_{max}", is a measure of the source rock maturity (T_{max} accuracy is ±1 - 3°C; Peters, 1986).

2.4 Results

2.4.1 TOC and Rock-Eval

The TOC and Rock-Eval pyrolysis results for all samples are presented in Table 2.1. The Douglas Creek Member (M16) has the lowest TOC of the 3 sections (3.5 to 9.7 wt.%), with the Douglas Creek Member (CW1) possessing highly variable TOC (2.6 to 24.7 wt.%), with 9 of the 12 samples yielding TOC <10 wt.%. In comparison, the Mahogany Zone (CW1) possesses TOC values between 9.3 and 28.1 wt.%, with 9 of 11 samples analysed yielding TOC >10 wt.%. Rock-Eval pyrolysis is used to assess the type and maturity of organic matter in the samples. The T_{max} (assessment of maturity using the temperature at maximum generation of remaining hydrocarbons after free oil is removed) values for all the samples are similar and range between 432 and 448°C signifying moderate maturity. The type of organic matter in the samples is assessed using the hydrogen and oxygen indexes (HI versus OI), as screening proxies to the van Krevelen atomic H/C versus O/C diagram (Espitalie et al., 1977; Peters, 1986; Fig. 2.3). The HI and OI data illustrate that all samples are Type I kerogen, consistent with previous Green River Formation studies (Katz, 1995; Tissot et al., 1978).

2.4.2 Re-Os geochronology

The Re and Os abundances for the Douglas Creek Member (M16) are 21.0 - 62.4 ng/g and 178 - 490 pg/g, respectively (Table 2.1). This is a substantial enrichment in comparison to estimates for average continental crust (0.2 - 1 ng/g Re and 30 - 50 pg/g Os; Esser and Turekian, 1993; Peucker-Ehrenbrink and Jahn, 2001; Hattori et al., 2003; Sun et al., 2003). These abundances generally co-vary and are comparable to abundances in marine organic-rich sedimentary rocks (e.g., Cohen et al., 1999; Selby and Creaser, 2005; Kendall et al., 2009a; Xu et al., 2009). The $^{187}Re/^{188}Os$ and $^{187}Os/^{188}Os$ ratios for the Douglas Creek Member (M16) range from 328.6 to 1015.2 and 1.82 to 2.35, respectively. Linear regression of the Re-Os data yields a Model 3 age of 48.4 ± 2.7 Ma (2σ, *n* = 13, Mean Squared of Weighted Deviation [MSWD] = 6.8, Os_i = 1.54 ± 0.03; Fig. 2.4A; all ages include $\lambda^{187}Re$ uncertainty). Douglas Creek Member

samples (CW1) are also enriched in Re and Os with abundances of 10.5 - 83.5 ng/g and 114 - 412 pg/g, respectively (Table 2.1). The $^{187}Re/^{188}Os$ ratios range from 326.9 to 1830.5, with $^{187}Os/^{188}Os$ ratios between 1.57 and 2.89. Linear regression of the Re-Os data yield a Model 3 age of 49.8 ± 4.8 Ma (2σ, *n* = 13, MSWD = 39, Os_i = 1.41 ± 0.06; Fig. 2.4D). Samples from the Mahogany Zone (CW1) also display enriched Re and Os abundances ranging from 11.8 to 39.5 ng/g and 198 to 815 pg/g, respectively (Table 2.1). The $^{187}Re/^{188}Os$ values have a limited range from 296 to 451 but exhibit a positive correlation to the $^{187}Os/^{188}Os$ values ranging from 1.72 to 1.83. Regression of this Re-Os data yield a Model 1 age of 47.8 ± 9.9 Ma (2σ, *n* = 13, MSWD = 0.43, Os_i of 1.48 ± 0.06; Fig. 2.4F).

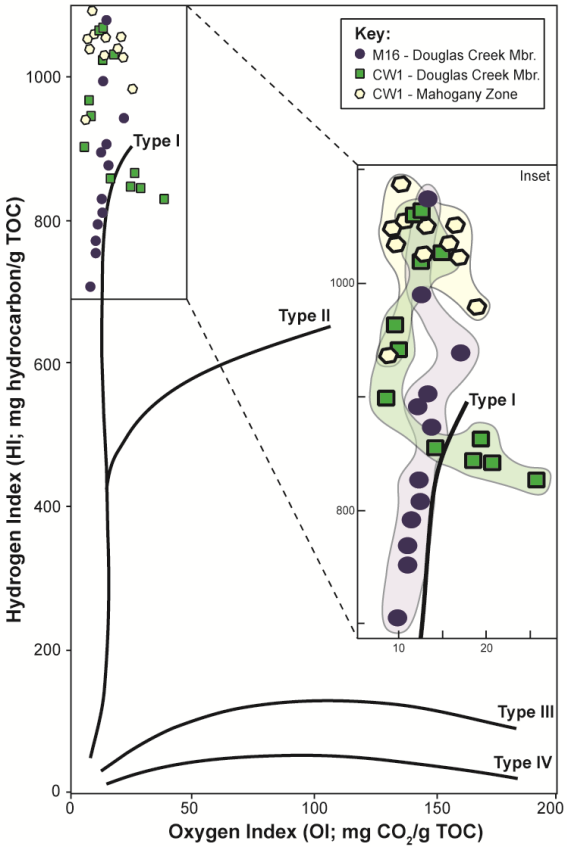

Figure 2.3: Graph of hydrogen index versus oxygen index (HI/OI) as a proxy to an atomic H/C versus atomic O/C van Krevelen diagram (Espitalie et al., 1977; Peters, 1986). Lines for kerogen Types I to IV are annotated on the graph (taken from Hunt, 1996). All the samples are plotted illustrating that they are all Type I kerogen. The enlarged inset shows the area where samples are plotted with each of the sampled units outlined in order to demonstrate the variation.

Table 2.1: Re-Os isotope data, total organic carbon (TOC) content and Rock-Eval data for the Green River Formation samples

Sample	Depth (m)	Re (ng/g)	±	Os (pg/g)	±	^{192}Os (pg/g)	±	^{187}Re/^{188}Os	±	^{187}Os/^{188}Os	±	rho [a]	Os_i [b]	TOC (wt.%)	Tmax (°C) [c]	S1 [d]	S2 [e]	S3 [f]	HI [g]	OI [h]
Douglas Creek Member, Marsing 16 core (39° 57' 1.4904" N, 111° 1' 37.527" W)																				
M16-27†	323.8	22.6	0.1	341.3	2.3	115.3	0.9	390.2	3.3	1.831	0.018	0.722	1.52	5.96	435	2.33	59.28	0.81	994	13.6
M16-26†	323.9	23.6	0.1	333.5	2.6	112.3	1.0	418.3	4.1	1.861	0.022	0.718	1.52	6.47	437	2.17	51.46	0.74	796	11.4
M16-25†	324.0	42.6	0.1	490.0	2.8	163.4	0.9	518.6	3.3	1.950	0.013	0.680	1.53	9.71	437	2.89	68.68	0.86	707	8.9
M16-24†	324.0	27.8	0.1	393.8	3.0	132.7	1.2	417.4	4.0	1.854	0.022	0.704	1.52	7.09	440	2.85	54.60	0.78	770	11.0
M16-23†	324.5	54.9	0.2	341.6	1.9	109.5	0.6	997.4	6.5	2.336	0.014	0.819	1.53	8.20	435	1.99	61.77	0.93	753	11.3
M16-22†	324.6	56.0	0.2	343.1	2.1	109.8	0.7	1015.2	7.1	2.352	0.016	0.790	1.53	-	-	-	-	-	-	-
M16-21†	324.6	62.4	0.2	392.8	2.5	126.0	0.8	984.8	6.9	2.326	0.017	0.735	1.53	5.42	438	1.91	44.93	0.69	829	12.7
M16-20†	324.7	40.1	0.1	351.6	1.5	115.7	0.4	690.2	3.2	2.079	0.008	0.599	1.52	5.53	441	2.10	49.53	0.73	896	13.2
M16-19†	324.7	24.5	0.1	263.1	1.4	87.5	0.4	556.4	3.4	1.982	0.013	0.665	1.53	3.53	437	1.64	33.23	0.78	942	22.1
M16-18*	324.9	29.2	0.1	273.4	1.5	90.0	0.4	645.0	3.8	2.078	0.013	0.651	1.56	6.39	448	2.23	68.53	0.89	1073	13.9
M16-16*	325.1	21.0	0.1	178.2	1.2	58.2	0.4	716.3	5.5	2.145	0.019	0.725	1.57	5.71	443	13.44	51.69	0.81	906	14.2
M16-15*	325.3	22.9	0.1	297.1	1.6	99.4	0.5	458.1	2.7	1.923	0.012	0.648	1.55	5.23	442	1.56	42.36	0.73	811	14.0
M16-14*	325.4	16.8	0.1	300.2	1.8	101.5	0.6	328.6	2.2	1.819	0.014	0.654	1.55	4.87	445	1.23	42.67	0.75	877	15.4
Douglas Creek Member, Coyote Wash 1 core (40° 1' 22.224" N, 109° 18' 38.4834" W)																				
CW1-40§	1026.0	23.4	0.1	307.8	1.7	104.6	0.6	445.0	2.9	1.774	0.012	0.682	1.40	6.01	441	2.13	52.15	1.59	867	26.4
CW1-41§	1026.1	14.6	0.1	258.5	1.9	89.0	0.8	326.9	3.2	1.654	0.020	0.699	1.38	7.55	444	1.72	63.99	1.90	848	25.2
CW1-42§	1026.2	10.5	0.0	184.0	1.5	63.3	0.7	330.0	3.6	1.657	0.022	0.732	1.38	6.83	442	2.35	57.89	1.95	847	28.5
CW1-44	1026.5	14.2	0.1	245.4	1.8	85.2	0.8	331.7	3.3	1.573	0.020	0.702	1.30	7.07	442	1.50	73.03	1.24	1032	17.5
CW1-45	1026.6	30.3	0.1	256.7	1.5	84.9	0.5	711.0	4.7	2.028	0.014	0.728	1.44	9.98	439	5.24	106.70	1.28	1069	12.8
CW1-46	1026.8	34.9	0.1	303.2	1.6	100.2	0.5	692.4	4.2	2.036	0.013	0.695	1.46	7.44	438	3.06	76.44	1.06	1027	14.2
CW1-48§	1027.0	15.3	0.1	145.4	1.3	48.6	0.6	627.6	7.4	1.921	0.027	0.756	1.40	2.67	434	2.62	22.24	1.03	832	38.5
CW1-49§	1027.2	83.5	0.3	298.9	1.8	90.7	0.5	1830.5	11.1	2.889	0.018	0.712	1.37	7.85	441	2.74	83.74	0.92	1066	11.7
CW1-50§	1027.4	46.6	0.2	412.1	3.8	137.3	1.5	675.1	7.6	1.963	0.032	0.635	1.40	15.46	440	4.48	146.19	1.20	946	7.8
CW1-51	1027.5	11.5	0.0	114.3	1.1	38.2	0.5	600.3	8.2	1.936	0.030	0.807	1.44	4.97	436	1.22	42.69	0.86	859	17.3
CW1-53	1027.7	17.7	0.1	180.5	1.4	60.2	0.6	584.4	5.9	1.960	0.023	0.751	1.47	-	-	-	-	-	-	-
CW1-54§	1027.8	39.1	0.1	346.0	1.9	115.3	0.6	674.9	4.1	1.956	0.013	0.645	1.40	24.70	438	8.12	222.95	1.51	903	6.1
CW1-55	1028.0	33.8	0.1	385.3	2.1	129.5	0.7	519.5	3.1	1.879	0.012	0.635	1.45	16.92	437	5.05	163.78	1.30	968	7.7
Mahogany Zone, Coyote Wash 1 core (40° 1' 22.224" N, 109° 18' 38.4834" W)																				
CW1-05	682.5	15.2	0.1	294.0	2.3	100.5	1.0	301.1	3.2	1.716	0.022	0.719	1.48	11.28	439	6.45	117.31	2.13	1040	18.9
CW1-06	682.7	28.0	0.1	486.0	2.9	165.7	1.0	336.0	2.4	1.746	0.014	0.673	1.48	22.78	443	11.69	237.11	1.92	1041	8.4
CW1-07	682.8	25.5	0.1	464.1	2.8	158.5	1.0	320.2	2.3	1.730	0.014	0.673	1.48	22.59	445	9.55	248.16	2.10	1099	9.3
CW1-09	683.2	26.7	0.1	362.6	4.5	122.6	2.2	433.0	7.8	1.822	0.048	0.668	1.48	25.82	436	11.95	272.55	1.81	1055	7.0
CW1-10	683.4	20.8	0.1	383.2	3.0	130.8	1.2	316.4	3.2	1.735	0.022	0.698	1.48	14.47	437	7.47	149.11	2.04	1031	14.1
CW1-12	683.6	15.5	0.1	264.2	2.8	89.9	1.4	344.1	5.3	1.765	0.036	0.721	1.49	9.69	434	6.65	95.36	2.48	985	25.6
CW1-13	683.7	15.6	0.1	295.3	2.4	100.8	1.0	307.1	3.4	1.737	0.023	0.717	1.49	9.39	434	6.84	96.77	2.01	1031	21.4
CW1-14	683.9	16.7	0.1	326.8	3.3	111.8	1.6	297.9	4.5	1.717	0.034	0.710	1.48	-	-	-	-	-	-	-
CW1-15	684.3	11.8	0.0	198.4	2.2	67.5	1.1	349.0	5.8	1.768	0.037	0.742	1.49	10.30	439	6.29	108.94	2.20	1058	21.4
CW1-16	684.5	14.6	0.1	286.2	2.3	97.7	1.0	296.6	3.3	1.730	0.024	0.717	1.49	11.35	441	5.70	119.94	1.68	1057	14.8
CW1-20	684.9	32.7	0.1	426.9	5.3	144.1	2.7	451.2	8.5	1.837	0.048	0.684	1.48	28.15	436	13.85	265.66	1.80	944	6.4
CW1-22	685.2	39.2	0.1	559.9	4.4	189.4	1.6	411.3	3.8	1.816	0.023	0.612	1.49	21.14	432	10.45	223.98	2.01	1060	9.5
CW1-23	685.4	20.1	0.1	366.4	3.2	125.0	1.4	320.1	3.7	1.737	0.026	0.704	1.48	-	-	-	-	-	-	-

[a] Rho is the associated error correlation at 2σ (Ludwig, 1980)

[b] Os_i is the initial $^{187}Os/^{188}Os$ isotope ratio calculated at 48.4, 49.8 and 47.8 Ma for each unit, respectively

[c] Tmax = temperature at maximum evolution of S2 hydrocarbons

[d] S1 = free oil content (mg hydrocarbons/g of rock)

[e] S2 = remaining hydrocarbon potential (mg hydrocarbons/g of rock)

[f] S3 = organic carbon dioxide (mg CO_2/g of rock)

[g] HI = Hydrogen Index (mg hydrocarbon/g C_{org})

[h] OI = Oxygen Index (mg CO_2/g C_{org})

All uncertainties are stated as 2 σ

* Re-Os Age = 50.1 ± 2.6 Ma

† Re-Os Age = 49.2 ± 1.0 Ma

§ Re-Os Age = 48.7 ± 0.6 Ma

2.5 Discussion

2.5.1 Re-Os lacustrine organic-rich sedimentary rock geochronology

Regression of all Re-Os data from the individually sampled sections of the CW1 and M16 cores yield ages that agree, within uncertainty, with the Green River Formation Ar-Ar and U-Pb dates (see section 2.5.2). However, Model 3 ages and large MSWD values strongly suggest that any scatter about the isochron is controlled by geological factors, rather than purely analytical uncertainties (Ludwig, 2008). Precise Re-Os geochronology requires samples with similar Os_i, and a spread in $^{187}Re/^{188}Os$ ratios of at least a few hundred units (Cohen et al., 1999; Selby and Creaser, 2005; Kendall et al., 2009a). To assess whether samples have similar Os_i, the isotopic compositions of each sample are back-calculated using $\lambda^{187}Re$ ($1.666 \times 10^{-11}a^{-1}$; Smoliar et al., 1996) and the age determined from the respective isochron (Table 2.1).

Regression of the Douglas Creek Member (M16) yields a Model 3 age of 48.4 ± 2.7 Ma, (MSWD = 6.8; Fig. 2.4A). The calculated Os_i at 48.4 Ma for all the samples varies from 1.52 to 1.57, with stratigraphically lower samples having higher Os_i values of 1.55 – 1.57 (n = 4) and the remaining stratigraphically higher samples possessing Os_i values of 1.52 – 1.53 (n = 9). Separate regression of the Re-Os data based on the Os_i values (1.55 – 1.57 and 1.52 – 1.53; Table 2.1), yield Model 1 ages of 50.1 ± 2.6 Ma (2σ, n = 4, MSWD = 0.43, Os_i = 1.54 ± 0.02; Fig. 2.4C) and 49.2 ± 1.0 Ma (2σ, n = 9, MSWD = 0.99, Os_i = 1.52 ± 0.01; Fig. 2.4B), respectively. Both of these ages are identical within uncertainty, with the 49.2 ± 1.0 Ma date providing the most precise depositional age for the Douglas Creek Member. The Model 1 ages and lower MSWD values suggest that stratigraphic changes in Os_i values is the principal control on the degree of scatter associated with the isochron of all M16 samples. The precise and accurate ages for these subsets strongly discounts any post-depositional disturbance to the Re-Os system. The stratigraphic variation in Os_i suggests a change in Os inputs or alteration of the balance and/or flux of Os inputs into the lake over time. In the case of the M16 samples, the 1 m of stratigraphy sampled could represent approximately 2.5 – 10 Ka (Smith et al., 2008a).

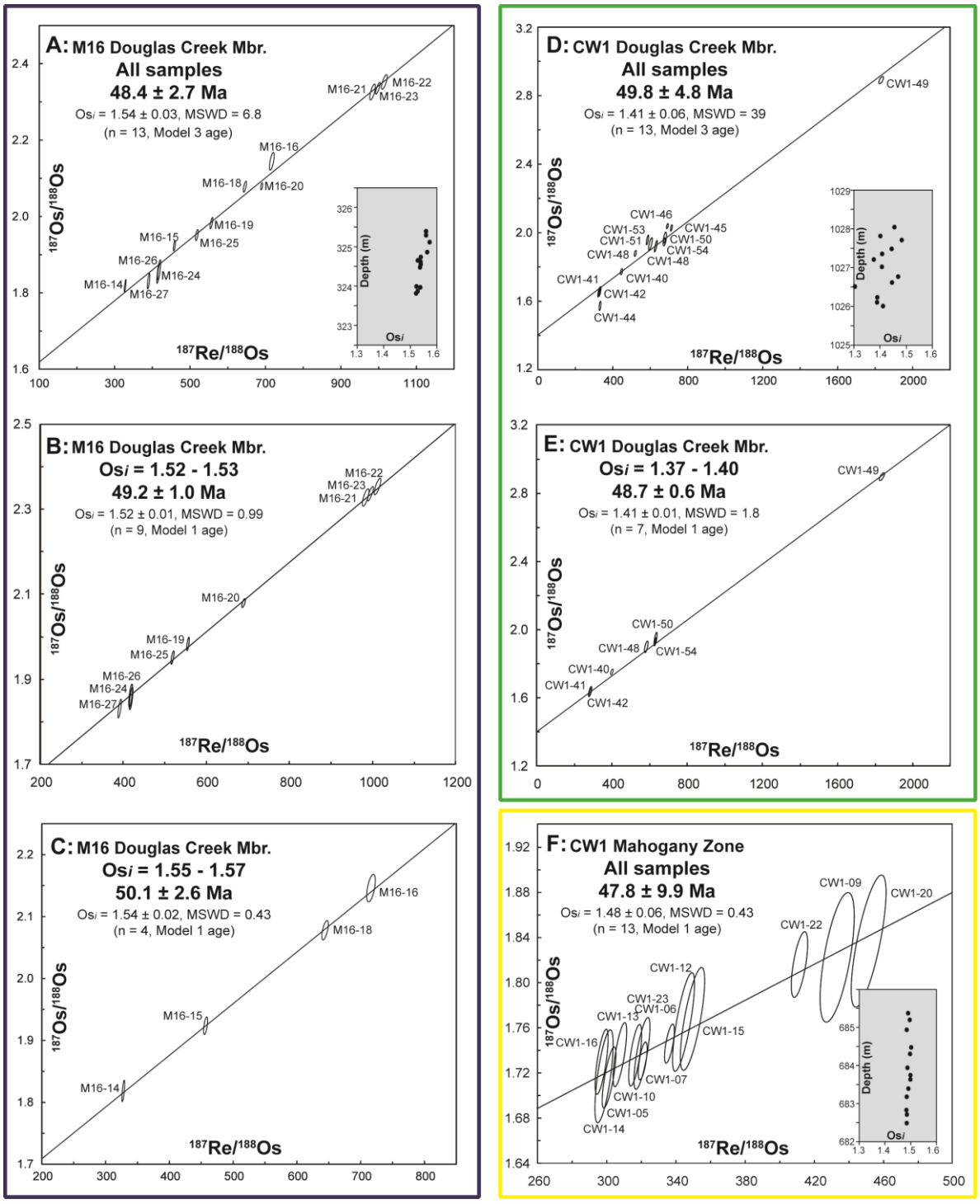

Figure 2.4: Re-Os isochron diagrams for the Douglas Creek Member in the Marsing 16 core (A, B and C) and the Coyote Wash 1 core (D and E), and for the Mahogany Zone (F). Isochrons A, D and F represent regression of all the samples for each horizon and isochrons B, C and E represent regression of samples with similar initial $^{187}Os/^{188}Os$ (see text for discussion). Isochron E provides a precise depositional age for the Douglas Creek Member (CW1); however, although it

agrees within uncertainty of the other ages, it has questionable validity due to the nature of the Os_i variation (see text for discussion). It can also be suggested that isochron E is pinned by sample CW1-49, but when the other 6 points are regressed they produce a Model 1 age of 51.0 ± 2.7 Ma (2σ, *n* = 6, MSWD = 1.5, Os_i = 1.39 ± 0.02) which is within uncertainty of the seven point Re-Os seen in isochron E. The inset graphs show the Os_i versus depth of the samples for each horizon. The scales are the same for each graph so the variation in sampling depth and Os_i is visible. The sampled horizon for the Douglas Creek Member in the M16 core is 1.6 m, in the CW1 core it is 2 m and in the Mahogany Zone in the CW1 core it is 2.9 m.

The Douglas Creek Member (CW1) yields a Model 3 age of 49.8 ± 4.8 Ma with an MSWD of 39 (Fig. 2.4D). The Os_i values calculated at 49.8 Ma vary substantially (1.30 – 1.47; Table 2.1). Unlike the Douglas Creek Member (M16), there is no stratigraphic relationship to Os_i in this core, suggesting that Os influx into the basin was very heterogeneous or that the Re-Os isotopic system has been disturbed during post-depositional processes. The isochronous nature of the samples and good agreement between the Re-Os data and Ar-Ar geochronology of the Green River Formation suggest limited or no disturbance to the Re-Os system. I suggest that the scatter about the linear regression relates to variations in the Os_i of these samples (Fig. 2.4D inset). Interestingly seven of the samples have similar Os_i (1.37 – 1.40) and regression of this Re-Os data yields a precise Model 1 age of 48.7 ± 0.6 Ma (2σ, *n* = 7, MSWD = 1.8, Os_i = 1.41 ± 0.01; Table 2.1; Fig. 2.4E).

The Mahogany Zone (CW1) Re-Os data yield a Model 1 age of 47.8 ± 9.9 Ma, MSWD 0.43 (Fig. 2.4F). The Os_i values calculated at 47.8 Ma are very similar (1.48 – 1.49; Table 2.1) and $^{187}Re/^{188}Os$ and $^{187}Os/^{188}Os$ values display limited spread through this core (150 and 0.1 units, respectively). These ranges are much smaller than the Douglas Creek Member (M16 and CW1) sections which have ranges in $^{187}Re/^{188}Os$ values >650 and >1500 units, respectively and ranges in $^{187}Os/^{188}Os$ values >0.5 and >1.3 units, respectively. The lower MSWD is due to the very small range in $^{187}Os/^{188}Os$, which exaggerates the measured uncertainty thereby permitting an isochron fit. The

larger uncertainty in the age for the Mahogany Zone CW1 can be attributed to the small ranges in $^{187}Os/^{188}Os$ and $^{187}Re/^{188}Os$. In an attempt to increase the variation in $^{187}Re/^{188}Os$ values, the sampled interval was increased from 2 m to 3 m (see Fig. 2.4), however $^{187}Re/^{188}Os$ and $^{187}Os/^{188}Os$ values remained extremely similar. The small spread cannot be attributed to sampling or analytical problems as the same protocols were used for all units and previous studies on marine sequences (e.g. Selby and Creaser, 2005; Kendall et al., 2009a; Rooney et al., 2012).

A limited spread in $^{187}Re/^{188}Os$ of organic-rich sedimentary rocks has also been seen for marine units. For example, over the Frasnian-Famennian (F-F) boundary $^{187}Re/^{188}Os$ values range only ~20 units, with the Re-Os data yielding an imprecise date of 476 ± 140 Ma (Turgeon et al., 2007). Three other units surrounding the F-F boundary produced more precise ages with $^{187}Re/^{188}Os$ values spanning 200 – 400 units. The low spread in $^{187}Re/^{188}Os$ was interpreted to be the result of Re drawdown due to increasing anoxia (Turgeon et al., 2007), with the dated interval at the F-F boundary recording the highest sea-level and most anoxic stage compared to the other dated intervals (Johnson et al., 1985; Ver Straeten et al., 2011). Likewise, it has also been suggested that in restricted basins organic matter sedimentation draws down dissolved Re and Os from the water column thus shortening residence time and causing rapid variations in Os_i values due to higher sensitivity to changes in Os inputs (McArthur et al., 2008). This may be the case for the Douglas Creek Member (CW1) unit where the largest variation in Os_i values is seen which is causing scatter about the isochron (Fig. 2.4D). However, large gradients in Os_i values are not observed in the Green River Formation and there is no significant change in Re and Os abundance through the sampled intervals suggesting that Re and Os drawdown does not occur. In similarity to the F-F boundary interval, the Mahogany Zone was deposited during the highest lake-levels and most anoxic period (Bradley, 1931; Tuttle and Goldhaber, 1993). I suggest that, rather than having intense Re or Os drawdown, the Mahogany Zone depositional environment (high lake-level, steady sedimentation and stable water column stratification; Tuttle and Goldhaber, 1993; Smith et al., 2008a) allowed for homogenous Re and Os uptake and thus minimal fractionation throughout the

sampled interval, which hampers the utility of the strata for precise Re-Os geochronology.

In addition, it has been suggested that organic-rich sedimentary rocks deposited in terrestrial basins will possess low $^{187}Re/^{188}Os$ values (<200; Baioumy et al., 2011). However, the $^{187}Re/^{188}Os$ data for all Green River Formation sections is >200, with two of the sections (Douglas Creek Member) that represent more restricted deposition yielding significant variation in $^{187}Re/^{188}Os$ ratios (328 – 1831), similar to marine organic-rich sedimentary rocks (Kendall et al., 2009a and references therein). As such, my findings contradict previous studies that suggest restricted and terrestrial deposits may not be viable for Re-Os geochronology (Baioumy et al., 2011; McArthur et al., 2008). I suggest that lacustrine deposits, like marine systems, vary enormously and basins should be assessed individually for Re-Os geochronology.

2.5.2 Comparison of Re-Os dates with Ar-Ar geochronology in the Uinta Basin

Although the Uinta Basin is an intensively studied lacustrine succession, correlation of the stratigraphy is hampered by informal and overlapping terminology, mainly due to a lack of surface exposure (Remy, 1992; Smith et al., 2008a). In this case Ar-Ar geochronology provides the ability to assess the accuracy of the Re-Os dates of the Green River Formation lacustrine organic-rich sedimentary rocks, although the Ar-Ar dates are more precise. The Curly tuff (Ar-Ar: 49.32 ± 0.30 Ma) is the oldest tuff dated in the Uinta Basin, lying ~50 m below the Mahogany Zone at the top of the Transitional interval (Smith et al., 2008a). This interval forms part of the lower Parachute Creek Member and the upper Douglas Creek Member (Fig. 2.2), defined as a time of fluctuating profundal deposition (Smith et al., 2008a). The Douglas Creek Member intervals sampled are ~300 m (CW1 core) and ~400 m (M16 core) below the Curly tuff (Tuttle and Goldhaber, 1993). With estimated sedimentation rates ranging from 100 to 400 mm/Kyr in the Green River basins (Smith et al., 2008a), 400 m of sediment could have been deposited in 1 to 4 Myr. This suggests that the Re-Os dates for the Douglas Creek Member and the Mahogany Zone (Fig. 2.4) are in agreement with the Ar-Ar date for the Curly tuff (Fig. 2.2). A larger sequence stratigraphic study of

the Uinta Basin would be needed to clarify this further. The oldest dated tuff in the adjacent Piceance Creek Basin is the Yellow tuff dated at 51.55 ± 0.52 Ma, which is stratigraphically equivalent to the lowest Douglas Creek Member and therefore should be and is older than the Re-Os dated sections. This agreement between the Ar-Ar and Re-Os geochronology demonstrates that the Re-Os system can be successfully applied to lacustrine organic-rich sedimentary rocks to provide much-needed direct depositional age constraints in lacustrine basins, especially in the absence of Ar-Ar and U-Pb tuff geochronology. The concordance between direct and indirect depositional age determinations emphasises the expediency of geochronological methods for correlating global phenomena.

2.5.3 Re-Os uptake and fractionation

The current understanding of the definitive controls of Re and Os uptake and fractionation in organic-rich sedimentary rocks is incomplete. Here I briefly summarise previous findings and reveal how this study contributes to solving the dilemma emphasising the complex nature of Re and Os systematics in organic-rich sedimentary rocks. Early studies suggested that sub-oxic to anoxic or euxinic conditions must exist for Re and Os uptake into organic-rich sedimentary rocks, which occurs at or below the sediment-water interface (Koide et al., 1991; Colodner et al., 1993; Crusius et al., 1996; Cohen et al., 1999; Morford and Emerson, 1999). These studies and further experimental works provided evidence that Re and Os behave differently in the water column, with distinct uptake mechanisms and unknown controls on fractionation (Levasseur et al., 1998; Sundby et al., 2004; Yamashita et al., 2007; Morford et al., 2009; Selby et al., 2009). Recent work has also questioned the notion that Re and Os are directly linked to TOC values, with correlations occasionally but not always apparent despite the majority of these metals being held within the kerogen (Cohen et al., 1999; Selby et al., 2009; Rooney et al., 2012). High TOC requires high primary productivity with preservation potential reliant on a calm, oxygen-poor water body, without scavenging benthic life (Demaison and Moore, 1980; Sageman et al., 2003), however, these factors may not solely regulate Re and Os uptake and fractionation.

Slow sedimentation has been proposed as one of the key factors in enhanced Re and Os uptake as seen for Ni and V enrichment in organic-rich sedimentary rocks (Lewan and Maynard, 1982; Crusius and Thomson, 2000; Selby et al., 2009; Rooney et al., 2012). However, slow sedimentation may adversely affect TOC preservation due to the longer residence time for oxidation (Ibach, 1982). Aside from the principal condition requiring Re and Os in the water column, other influences that have been proposed to control Re and Os enrichment and fractionation are salinity (Martin et al., 2001), post-deposition mobility of the elements (Crusius and Thomson, 2000; Kendall et al., 2009a), pH and temperature (Georgiev et al., 2011). Since Re and Os are bound within the kerogen of an organic-rich sedimentary rock (Rooney et al., 2012), but enrichment is affected by numerous processes beyond TOC preservation, a better appreciation of the organic matter chelating precursors of Re and Os is needed. In V and Ni studies it has been shown that the chelating precursor is not always preserved proportionally to organic matter (Lewan and Maynard, 1982) thus understanding the chelating precursor systematics of Re and Os will significantly advance the understanding of the Re-Os system.

My data have shown that Re-Os geochronology can be successfully applied to lacustrine organic-rich sedimentary rocks, and that element fractionation and abundances are similar to marine systems. However, the results are mixed with an accurate and precise isochron for the Douglas Creek Member (M16), but larger age uncertainties for the Mahogany Zone and Douglas Creek Member (CW1). I suggest that homogenous Re-Os fractionation is the cause of the larger uncertainty in the Mahogany Zone geochronology, although the reasons for this are currently ambiguous. In order to explain why these units behave differently in terms of Re-Os fractionation, TOC and Rock-Eval data are evaluated. These data yield insights into the Green River Formation organic matter and hence Re-Os uptake and fractionation in lacustrine settings.

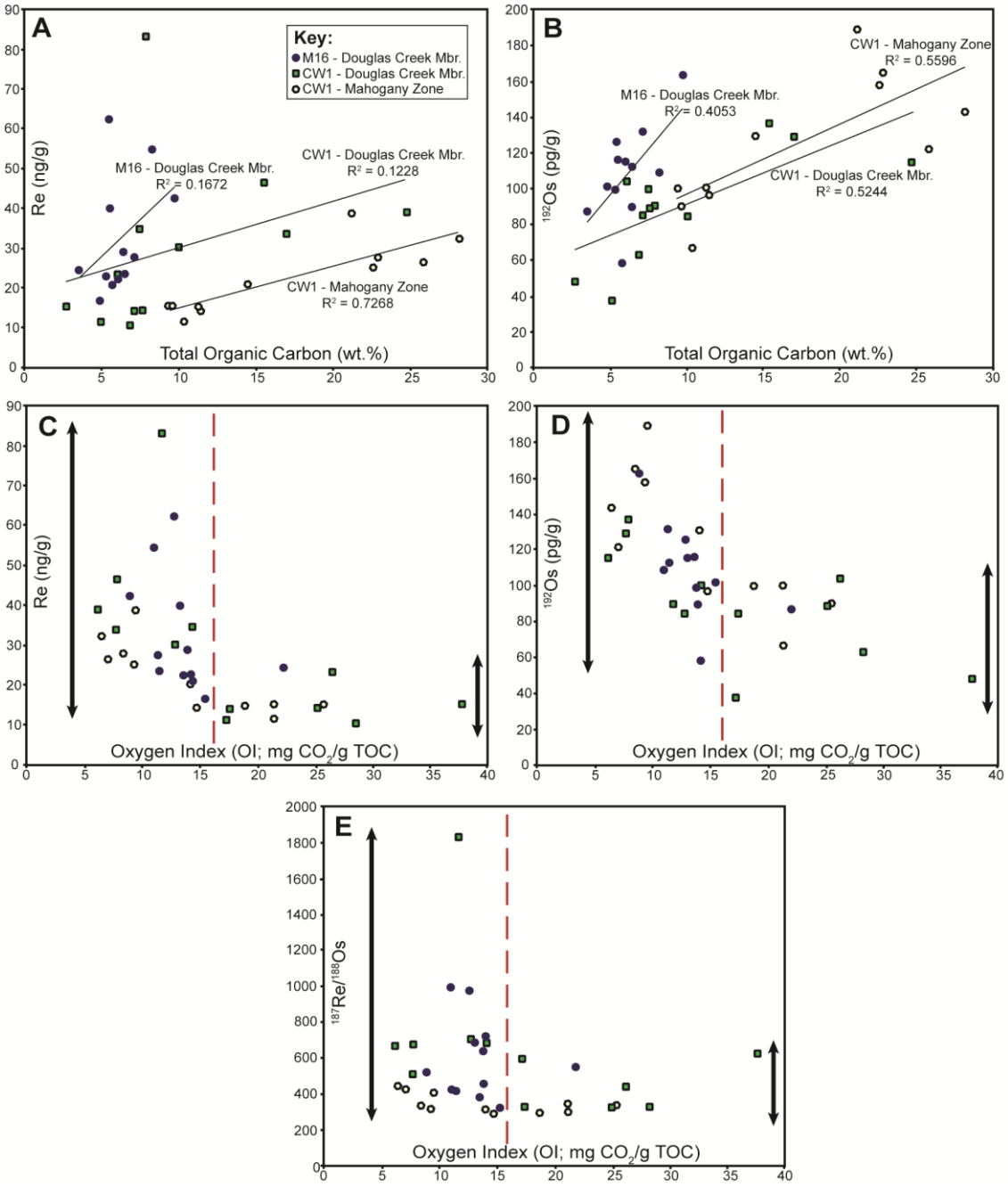

Figure 2.5: Graphs of total organic carbon (TOC) versus Re (A) and ^{192}Os (B) of all the studied Green River Formation units showing linear correlations. Common Os (^{192}Os) is plotted to remove the effect of radiogenic in-growth. The R^2 for each unit is annotated on the graphs. Oxygen index (OI) versus Re (C), ^{192}Os (D) and $^{187}Re/^{188}Os$ (E) of all the units are also plotted. The dashed line represents the threshold OI below which Re and Os concentrations are increased, and $^{187}Re/^{188}Os$ values are more variable (see text for discussion). The black bars represent the amount of variation in Re, Os and $^{187}Re/^{188}Os$ on each side of the dashed threshold line.

2.5.3.1 Insights from TOC and depositional conditions

In the three Green River Formation units a positive but weak linear correlation of Re and common Os (^{192}Os) to TOC exists (Figs. 2.5A and 2.5B), with the Mahogany Zone displaying the best correlation. Rhenium versus TOC in the Mahogany Zone displays a positive trend (R^2 of 0.73) yet the Douglas Creek Member shows no correlation (R^2 of 0.12 [CW1] and 0.17 [M16]). In terms of ^{192}Os versus TOC there is no strong correlation in any of the sections and they all have similar R^2 values (Mahogany Zone = 0.56; Douglas Creek Member CW1 = 0.52; Douglas Creek Member M16 = 0.41). Despite weak correlations, the sampled horizons display variable relationships to TOC. The Douglas Creek Member (M16) has negligible correlation of both Re and Os to TOC, but much higher slopes than the other two units. These findings suggest an uptake mechanism possibly unrelated to TOC dominated in this region of the lake/water column, in contrast to Re and Os uptake in the Mahogany Zone which has the best correlation with TOC. The Douglas Creek Member represents a proximal lake margin setting during a time of fluctuating lake-levels producing variation in the sedimentation rate and terrigenous input; possibly allowing variable Re-Os uptake and fractionation. In contrast, the Mahogany Zone was deposited in the distal lake centre when lake-levels were at their maximum and enhanced primary productivity and slow and steady sedimentation rates in a stratified water column produced an extremely organic-rich and homogenous section (Bradley, 1931; Boyer, 1982; Tuttle and Goldhaber, 1993; Smith et al., 2008a). The homogenous depositional system of the Mahogany Zone may have allowed greater association of Re and Os with organic matter allowing less ^{187}Re/^{188}Os fractionation making precise Re-Os geochronology challenging. The relationship to depositional conditions suggests that, contrary to the Mahogany Zone, in the Douglas Creek Member sections the organic chelating components responsible for Re and Os uptake are not being preserved uniformly or that there are variable chelating surfaces derived from different organic matter types.

Additional Green River Formation depositional factors to take into account are salinity, carbonate content and redox conditions. The Mahogany Zone is more saline

and carbonate-rich than the Douglas Creek Member (Tuttle and Goldhaber, 1993; Keighley et al., 2003), with increased salinity creating greater water column stability and higher pH (Tuttle and Goldhaber, 1993). Improved water column stability may have been a contributing factor to the uniform preservation and Re-Os fractionation of the Mahogany Zone, however, these parameters cannot be fully assessed as there is no study of my samples quantifying salinity or carbonate content. Redox conditions of the Green River Formation have not been directly studied although it has been suggested to be euxinic based on sulphur geochemistry (Tuttle and Goldhaber, 1993). During the late lake stage when the Mahogany Zone was deposited, $\delta^{34}S$ of sulphides (30 – 40 ‰) were higher than during deposition of the early stage Douglas Creek Member ($\delta^{34}S$: 5 – 15 ‰). In particular the Mahogany Zone values are unusual as they are much higher than those in marine, freshwater or modern saline lake systems, reflecting complex sulphur geochemistry (Tuttle and Goldhaber, 1993). Fundamentally, the $\delta^{34}S$ values are due to a constant supply of sulphate to the lake being progressively reduced by sulphate reducing bacteria causing a gradual enrichment of ^{34}S. Euxinic systems have been previously dated using Re-Os geochronology with success (e.g., Kendall et al., 2009b), however the influence on Re-Os fractionation of extensive sulphate reduction and an abundance of H_2S are unknown. I suspect that the resulting stable water column stratification, particularly evident during Mahogany Zone deposition, is likely to have contributed to the homogenous Re-Os fractionation observed in the Mahogany Zone. This gives further indication of the complex nature of the controls on Re and Os uptake and fractionation and suggests that the depositional system plays a large role in the Re-Os organic system.

2.5.3.2 Effects of organic matter type

The relationship of Re and Os to TOC and depositional setting highlights that organic matter type may play a key role in Re and Os uptake and fractionation and so hydrogen index (HI) and oxygen index (OI) values from Rock-Eval pyrolysis are used to assess organic matter type of the Green River Formation. A plot of HI/OI values indicates that all samples contain Type I kerogen, consistent with a lacustrine algal

source of organic matter, with minimal terrestrial organic matter input (Fig. 2.3). The variation in HI and OI values cannot easily be explained by changing maturity as all the samples have similar T_{max} values (Peters, 1986; Table 2.1). Generally both the Douglas Creek Member horizons display more variability in both HI and OI than the Mahogany Zone (See inset Fig. 2.3). This is consistent with previous observations that strata from the central lake (e.g. Mahogany Zone) contain predominantly alganite organic matter, whereas samples deposited nearer the lake margins or during fluctuating lake-levels (e.g. Douglas Creek Member) contain alganite but also some vitrinite (Castle, 1990). The predominance of alganite in the Mahogany Zone coupled with the lack of Re-Os fractionation may suggest that organic matter type is a controlling factor in Re-Os fractionation. It has previously been postulated that Re and Os are bound by different organic ligands causing variable $^{187}Re/^{188}Os$ in different organic fractions (Miller, 2004), and also that an unknown method of biological uptake of Re over Os may occur (Georgiev et al., 2011). The findings from this study suggest that variation in organic matter type (e.g. from terrestrial and algal sources) may enable variable $^{187}Re/^{188}Os$ (as is seen in the Douglas Creek Member sections), whereas homogenous algal organic matter may lead to homogenous $^{187}Re/^{188}Os$ (as is seen in the Mahogany Zone) through providing uniform chelating sites for both elements. These findings have strong implications for any future Re-Os geochronological study, however, further studies are required to fully quantify and assess the relationship of Re and Os with organic matter.

Oxygen index is a proxy measurement of oxygen content in kerogen, which can be derived from terrestrial organic matter or oxidation of organic matter (Peters, 1986). There is no correlation between OI and Re and Os abundance (Fig. 2.5C and 2.5D) but below an OI value of ~15 mg CO_2/g TOC, abundances of both Re and Os increase. This may suggest that Re and Os enrichment requires lower oxygen-bearing kerogen or lower oxygen conditions in which the kerogen was deposited. Vanadium and Ni have been found to be bound in tetrapyrroles, of which chlorophyll is the main precursor (Lewan and Maynard, 1982). Chlorophyll is sensitive to oxygen as it opens up the ring structure making it incapable of hosting metals and so sediments settling in an

oxygenated water column will have less chance to bind V and Ni in tetrapyrroles (Lewan and Maynard, 1982). The binding sites of Re and Os are unknown, but the relationship with OI illustrates the importance of deducing where these metals are held. If Re and Os are more enriched at low OI, this suggests that oxygen has a significant effect on the chelating precursors of Re and Os during deposition and also that the chelating precursors of Re and Os cannot be related to carboxyl complexes. The OI also seems to exert a minor control on $^{187}Re/^{188}Os$ fractionation below 15 mg CO_2/g TOC (Fig. 2.5E). This would support the findings of Yamashita et al. (2007) who note that Re is more readily incorporated into organic-rich sedimentary rocks under highly reducing conditions leading to high $^{187}Re/^{188}Os$. However, this study and previous studies concluded that specific controls on fractionation are poorly constrained. For organic matter of lacustrine sedimentary rocks, the non-linear relationship between OI and Re and Os potentially suggests that oxygen content in kerogen and/or organic matter type have a significant effect on chelation of Re and Os and hence Re-Os fractionation. If this proves to be the case in other studied sections, OI may provide a means of assessing whether a section may be viable for precise Re-Os geochronology providing an understanding of maturity and organic matter variation exists as these can affect OI values. However, as OI is a proxy for the atomic O/C ratio, future studies of atomic O/C versus Re-Os may shed further light on these findings and on the chelating precursors of Re and Os. Previous work has utilised OI as a proxy for weathering in order to assess Re-Os isochroneity, with non-isochronous samples possessing higher OI suggested to be caused by weathering (Georgiev et al., 2012). Disparity in OI can be caused by organic facies and maturity variations and therefore can only be a proxy for weathering in a weathering profile of identical strata. As such, ranges in OI should not be employed as a tool for estimating weathering intensity of differing strata.

2.5.4 Os isotope systematics

The Re-Os isotope data yield Os_i values of 1.54 ± 0.03, 1.41 ± 0.06 and 1.48 ± 0.06 (Fig. 2.4) for the Douglas Creek Member (M16), Douglas Creek Member (CW1),

and Mahogany Zone (CW1), respectively, suggesting a radiogenic terrestrial source of Os in the Uinta lake water column, derived primarily from continental runoff. The variation in Os_i between the three units may be explained by the proximity to different Os sources (e.g., radiogenic Precambrian crust or unradiogenic volcanic units) and the temporal variation in weathering into the Uinta Lake water column. Spatial and temporal variations related to drainage variation are also observed in Sr isotope studies from the Uinta and Greater Green River Basins (Rhodes et al., 2002; Davis et al., 2008). In the Uinta Basin Sr resolution through the Green River Formation is low, but $^{87}Sr/^{86}Sr$ is radiogenic (mean: 0.71183) and fluctuates (Davis et al., 2008) similarly to the Os_i from this study. In the Greater Green River Basin Sr exhibits fluctuations with more radiogenic $^{87}Sr/^{86}Sr$ (up to 0.71331) during lowstands due to more exposure of radiogenic crust leading to increased riverine input of radiogenic Sr (Rhodes et al., 2002). Although Sr and Os records are decoupled, it is suggested that this may also be a contributing factor to the change in Os_i seen in the separate samples used for Re-Os geochronology (see Fig. 2.4 insets and Table 2.1), although higher resolution Os isotope stratigraphy through the Green River Formation would be needed to confirm this. In light of the results from this study it is clear that the Os_i of lacustrine sediments, like Sr, can be a useful tool for deducing continental geological processes as it responds to changes in drainage from the surrounding geology, in turn controlled by regional climate, tectonics and magmatism. Oceanic Os has a shorter residence time (≤10,000 years) than Sr (1 to 4 Myrs), thus yielding much higher resolution perturbations in the geochemical record (Peucker-Ehrenbrink and Ravizza, 2000). However, the variable geological history of lakes means that each lake would need to be assessed individually to deduce Os and Sr residence time.

In addition to providing information about the regional geology and climate, the Os_i can also provide high-resolution data that are able to distinguish between marine and lacustrine deposition where other methods fail. The depositional setting of sedimentary basins is often ambiguous and can transition from lacustrine to marine to restricted marine with few clues to the precise nature and timing of these events. An Os isotope stratigraphic study of Lomonosov Ridge sediments from the Arctic Ocean

revealed a change from 'lake stage' deposition to oceanic conditions (Poirier and Hillaire-Marcel, 2011). In this case the Os_i is radiogenic (up to 1.3) during the 'lake stage' and with a change to oceanic conditions, the Os_i (~0.4) then matches the Cenozoic seawater $^{187}Os/^{188}Os$ curve. This allows for the exact transition in the stratigraphy to be determined. Poirier and Hillaire-Marcel's (2011) study coupled with data from this study suggest that if the $^{187}Os/^{188}Os$ of seawater at the time of sediment deposition is known (e.g., seawater during Green River Formation deposition = ~0.56; Kato et al., 2011), large deviations from this value would suggest that the sediments are not marine. Therefore Os_i stratigraphy could be especially helpful in basins where the depositional origin is uncertain or in marine basins that have undergone periods of restriction for unknown lengths of time.

Reconstructing the global ocean Os isotope record and understanding its fluctuations is a major challenge for the understanding of ocean chemistry (Peucker-Ehrenbrink and Ravizza, 2000, 2012). During the Cenozoic, the global ocean Os isotope composition became progressively more radiogenic (0.56 at 50 Ma to a modern day ratio of 1.06; Kato et al., 2011; Peucker-Ehrenbrink and Ravizza, 2000). The specific causes behind this change in Os isotope composition are unknown although similar changes in the Sr record have been related to increases in continental weathering due, principally, to the uplift of the Himalayas (Raymo and Ruddiman, 1992; Richter et al., 1992). However, these two records are decoupled as they vary in their influences and respective residence times and it has also been suggested that the Himalayas are not the dominant source of Os to the oceans during the Cenozoic (Sharma et al., 1999). An underlying problem is that, while we can reconstruct the past global ocean Os curve using marine sediments, we cannot accurately deduce the nature and changes in the sources of Os to the ocean and therefore cannot make accurate inferences as to what is causing the perturbations. Gaining further understanding of the sources of Os to the ocean in the past is vital to further elucidate these problems. The only reliable records of the geochemical composition of past continental runoff are lacustrine sediments as they are minimally affected by other potential inputs into the oceans (e.g. cosmic dust, mid-ocean ridge hydrothermal alteration). In this study the Os_i of the Green River

Formation (1.41 - 1.54) provides the $^{187}Os/^{188}Os$ composition of regional continental runoff into the Green River lakes, similar to estimates for present day $^{187}Os/^{188}Os$ composition of upper continental crust (1.40; Peucker-Ehrenbrink and Ravizza, 2000) and continental runoff (1.54; Levasseur et al., 1999). This similarity may suggest that the composition of continental runoff in the Eocene may have been comparable to the present day. While the Green River Formation Os_i cannot be used as a sole representation of continental runoff into the ocean, it can be noted that lacustrine basins do give an insight into past continental runoff regimes. Though this study cannot rule out an increase in radiogenic flux of Os from weathering as the cause of the increase in seawater $^{187}Os/^{188}Os$ over the last 50 Ma, it highlights that continental runoff may not have been the driving force for these changes due to the similarity of the Green River Formation Os composition with continental runoff today. Variations in the unradiogenic input to the oceans between 50 Ma and the present day should be more closely examined as a potential cause for seawater $^{187}Os/^{188}Os$ changes. Poirier and Hillaire-Marcel (2011) also find radiogenic $^{187}Os/^{188}Os$ (up to 1.3 at ~36 Ma) during the Arctic Ocean's 'lake stage' before it became fully connected with the global ocean, again suggesting that continental runoff may not have significantly varied over the last 50 Ma. Poirier and Hillaire-Marcel (2011) suggest that the opening of the Fram Strait at the end of the Arctic Ocean's 'lake stage' may have swamped the global ocean with radiogenic Os contributing to the Cenozoic seawater increase in $^{187}Os/^{188}Os$. These Os isotope studies of lacustrine systems provide valuable insights into continental Os inputs to the oceans and with further research could be used to reconstruct a picture of past global continental runoff and its influence on climate change.

2.6 Conclusions

The Re-Os systematics of three core intervals of the Green River Formation yield dates that are in agreement, within uncertainty, of U-Pb and Ar-Ar tuff geochronology. This demonstrates that the Re-Os geochronometer can be successfully applied to lacustrine carbonaceous organic-rich sedimentary rocks, providing a valuable tool for determining the direct depositional history of lacustrine systems and

furthermore, for understanding and correlating continental geological processes. The earliest Re-Os geochronology studies targeted marine black shales (Ravizza and Turekian, 1989; Cohen et al., 1999; Creaser et al., 2002), although the technique has since been shown to be effective on marine grey shales (Selby et al., 2009). The data presented here demonstrate that Re-Os geochronology can be applied to lacustrine organic-rich carbonates as well as marine black and grey shales. Recent work has also revealed that samples with TOC values as low as 0.5 wt.% can also be successfully utilized for Re-Os geochronology (Kendall et al., 2004; Rooney et al., 2011). These previous studies coupled with the data from this study suggest that, in general, any rock type deposited in conditions where organic matter is preserved and TOC is >0.5 % is viable for Re-Os geochronology and the tool is not just restricted to marine black shales, making this a far-reaching tool for lacustrine and marine depositional settings alike.

This study brings further to light the complexity of Re-Os systematics in organic-rich sedimentary rocks. The Re-Os dates for the Douglas Creek Member are controlled by the degree of variability of the initial $^{187}Os/^{188}Os$ composition within the sampled 2 m interval. For the Mahogany Zone the imprecise age relates to a small spread in $^{187}Re/^{188}Os$ values comparable to those seen in some marine systems (Turgeon et al., 2007). It is suggested that the controls on Re and Os fractionation within organic-rich sedimentary rocks are complex but in this case are related to depositional environment (proximal lake shore versus distal lake centre) and organic matter type (terrestrial versus algal). The relationship of Re and Os to OI highlights the importance of understanding the chelating precursors of Re and Os in organic matter, in order to further our knowledge of the Re-Os organic-rich sedimentary rock geochronometer.

In addition to geochronology, the initial $^{187}Os/^{188}Os$ composition of lacustrine organic-rich sedimentary rocks can be used to determine the geochemical signature of continental runoff into lake basins. This yields a potential tool to distinguish between marine and lacustrine sediments when seawater $^{187}Os/^{188}Os$ is well characterised (this

study; Poirier and Hillaire-Marcel, 2011). Furthermore, Os isotope stratigraphy of lacustrine successions can be applied to understanding regional climatic, tectonic and magmatic regimes and allows for chemostratigraphic correlations that combine direct depositional ages, giving much higher confidence in global correlations.

2.7 References

Baioumy, H.M., Eglinton, L.B., Peucker-Ehrenbrink, B., 2011. Rhenium-osmium isotope and platinum group element systematics of marine vs. non-marine organic-rich sediments and coals from Egypt. Chemical Geology 285, 70-81.

Boyer, B.W., 1982. Green River laminites: does the playa-lake model really invalidate the stratified-lake model? Geology 10, 321-324.

Bradley, W.H., 1931. Origin and microfossils of the oil shale of the Green River Formation of Colorado and Utah. U.S. Geological Survey, Prof. Paper,168

Carroll, A.R., Bohacs, K.M., 2001. Lake-type controls on petroleum source rock potential in nonmarine basins. AAPG Bulletin 85, 1033-1053.

Carroll, A.R., Bohacs, K.M., 1999. Stratigraphic classification of ancient lakes: balancing tectonic and climatic controls. Geology 27, 99-102.

Carroll, A.R., Brassell, S.C., Graham, S.A., 1992. Upper Permian lacustrine oil shales, southern Junggar Basin, Northwest China. AAPG Bulletin 76, 1874-1902.

Castle, J.W., 1990. Sedimentation in Eocene lake Uinta (Lower Green River Formation), northeastern Uinta basin, Utah, in: Katz, B.J., Lacustrine Basin Exploration: Case Studies and Modern Analogs. AAPG Memoir 50, AAPG Tulsa. 243-263.

Cohen, A.S., Coe, A.L., Bartlett, J.M., Hawkesworth, C.J., 1999. Precise Re-Os ages of organic-rich mudrocks and the Os isotope composition of Jurassic seawater. Earth and Planetary Science Letters 167, 159-173.

Colodner, D., Sachs, J., Ravizza, G., Turekian, K., Edmond, J., Boyle, E., 1993. The geochemical cycles of rhenium: a reconnaissance. Earth and Planetary Science Letters 117, 205-221.

Creaser, R., Szatmari, P., Milani, E.J., 2008. Extending Re-Os shale geochronology to lacustrine depositional systems: a case study from the major hydrocarbon source rocks of the Brazilian Mesozoic marginal basins. In: proceedings of the 33rd International Geological Congress, Oslo (abstract).

Creaser, R.A., Sannigrahi, P., Chacko, T., Selby, D., 2002. Further evaluation of the Re-Os geochronometer in organic-rich sedimentary rocks: a test of hydrocarbon maturation effects in the Exshaw Formation, Western Canada Sedimentary Basin. Geochimica et Cosmochimica Acta 66, 3441-3452.

Crusius, J., Calvert, S., Pedersen, T., Sage, D., 1996. Rhenium and molybdenum enrichments in sediments as indicators of oxic, suboxic and sulfidic conditions of deposition. Earth and Planetary Science Letters 145, 65-78.

Crusius, J., Thomson, J., 2000. Comparative behavior of authigenic Re, U, and Mo during reoxidation and subsequent long-term burial in marine sediments. Geochimica et Cosmochimica 64, 2233-2242.

Davis, S.J., Wiegand, B.A., Carroll, A.R., Chamberlain, C.P., 2008. The effect of drainage reorganization on paleoaltimetry studies: an example from the Paleogene Laramide foreland. Earth and Planetary Science Letters 275, 258-268.

Demaison, G.J., Moore, G.T., 1980. Anoxic environments and oil source bed genesis. Organic Geochemistry 2, 9-31.

Dyni, J.R., 2006. Geology and resources of some world oil-shale deposits. U.S. Geological Survey Scientific Investigations Report 2005–5294.

Espitalie, J., Laporte, J.L., Madec, M., Marquis, F., Leplat, P., Paulet, J., Boutefeu, A., 1977. Rapid method for source rocks characterization and for determination of petroleum potential and degree of evolution. Rev. Inst. Fr. Pet. 32, 23-42.

Esser, B.K., Turekian, K.K., 1993. The osmium isotopic composition of the continental-crust. Geochimica et Cosmochimica Acta 57, 3093-3104.

Finlay, A.J., Selby, D., Gröcke, D.R., 2010. Tracking the Hirnantian glaciation using Os isotopes. Earth and Planetary Science Letters 293, 339-348.

Georgiev, S., Stein, H.J., Hannah, J.L., Bingen, B., Weiss, H.M., Piasecki, S., 2011. Hot acidic late Permian seas stifle life in record time. Earth and Planetary Science Letters 310, 389-400.

Georgiev, S., Stein, H.J., Hannah, J.L., Weiss, H.M., Bingen, B., Xu, G., Rein, E., Hatlø, V., Løseth, H., Nali, M., Piasecki, S., 2012. Chemical signals for oxidative weathering predict Re–Os isochroneity in black shales, East Greenland. Chemical Geology 324-325, 108-121.

Hao, F., Zhou, X., Zhu, Y., Yang, Y., 2011. Lacustrine source rock deposition in response to co-evolution of environments and organisms controlled by tectonic subsidence and climate, Bohai Bay Basin, China. Organic Geochemistry 42, 323-339.

Hattori, Y., Suzuki, K., Honda, M., Shimizu, H., 2003. Re-Os isotope systematics of the Taklimakan Desert sands, moraines and river sediments around the Taklimakan Desert, and of Tibetan soils. Geochimica et Cosmochimica Acta 67, 1203-1213.

Hunt, J.M., 1996. Petroleum Geochemistry and Geology, 2nd ed. W.H. Freeman and Company, New York.

Ibach, L.E.J., 1982. Relationship between sedimentation-rate and total organic carbon content in ancient marine-sediments. AAPG Bull.Am. Assoc. Petr. Geol. 66, 170-188.

Johnson, J.G., Klapper, G., Sandberg, C.A., 1985. Devonian eustatic fluctuations in Euramerica. Geological Society of America Bulletin 96, 567-587.

Johnson, S.Y., 1992. Phanerozoic evolution of sedimentary basins in the Uinta-Piceance Basin region, northwestern Colorado and northeastern Utah. U.S. Geological Survey Bulletin 1787-FF.

Kato, Y., Fujinaga, K., Suzuki, K., 2011. Marine Os isotopic fluctuations in the early Eocene greenhouse interval as recorded by metalliferous umbers from a Tertiary ophiolite in Japan. Gondwana Research 20, 594-607.

Katz, B.J., 2001. Lacustrine basin hydrocarbon exploration - current thoughts. J. Paleolimn. 26, 161-179.

Katz, B.J., 1995. The Green River Shale: an Eocene Carbonate Lacustrine Source Rock, in: Katz, B.J. Petroleum Source Rocks. Springer-Verlag, Berlin, Heidelberg, 309-324.

Keighley, D., Flint, S., Howell, J., Moscariello, A., 2003. Sequence stratigraphy in lacustrine basins: a model for part of the Green River Formation (Eocene), southwest Uinta Basin, Utah, U.S.A. Journal of Sedimentary Research 73, 987-1006.

Kendall, B., Creaser, R.A., Selby, D., 2009a. ^{187}Re-^{187}Os geochronology of Precambrian organic-rich sedimentary rocks. Geological Society, London, Special Publications 326, 85-107.

Kendall, B., Creaser, R.A., Gordon, G.W., Anbar, A.D., 2009b. Re-Os and Mo isotope systematics of black shales from the Middle Proterozoic Velkerri and Wollogorang formations, McArthur Basin, northern Australia. Geochimica et Cosmochimica Acta 73, 2534-2558.

Kendall, B.S., Creaser, R.A., Ross, G.M., Selby, D., 2004. Constraints on the timing of Marinoan "Snowball Earth" glaciation by ^{187}Re -^{187}Os dating of a Neoproterozoic, post-glacial black shale in Western Canada. Earth and Planetary Science Letters 222, 729-740.

Koide, M., Goldberg, E.D., Niemeyer, S., Gerlach, D., Hodge, V., Bertine, K.K., Padova, A., 1991. Osmium in marine sediments. Geochimica et Cosmochimica Acta 55, 1641-1648.

Kuiper, K.F., Deino, A., Hilgen, F.J., Krijgsman, W., Renne, P.R., Wijbrans, J.R., 2008. Synchronizing rock clocks of Earth history. Science 320, 500-504.

Lambiase, J.J., 1990. A model for tectonic control of lacustrine stratigraphic sequences in continental rift basins, in: Katz, B.J., Lacustrine Basin Exploration: Case Studies and Modern Analogs. AAPG Memoir 50, AAPG Tulsa, 265-276.

Levasseur, S., Birck, J., Allegre, C.J., 1998. Direct measurement of femtomoles of osmium and the ^{187}Os/^{186}Os ratio in seawater. Science 282, 272-274.

Levasseur, S., Birck, J.L., Allègre, C.J., 1999. The osmium riverine flux and the oceanic mass balance of osmium. Earth and Planetary Science Letters 174, 7-23.

Lewan, M.D., Maynard, J.B., 1982. Factors controlling enrichment of vanadium and nickel in the bitumen of organic sedimentary rocks. Geochimica et Cosmochimica Acta 46, 2547-2560.

Ludwig, K., 2008. Isoplot, version 4.0: a geochronological toolkit for microsoft Excel. Berkeley Geochronology Center Special Publication No. 4.

Ludwig, K.R., 1980. Calculation of uncertainties of U-Pb isotope data. Earth and Planetary Science Letters 46, 212-220.

Machlus, M., Hemming, S.R., Olsen, P.E., Christie-Blick, N., 2004. Eocene calibration of geomagnetic polarity time scale reevaluated: evidence from the Green River Formation of Wyoming. Geology 32, 137-140.

Martin, C.E., Peucker-Ehrenbrink, B., Brunskill, G., Szymczak, R., 2001. Osmium isotope geochemistry of a tropical estuary. Geochimica et Cosmochimica Acta 65, 3193-3200.

McArthur, J.M., Algeo, T.J., van de Schootbrugge, B., Li, Q., Howarth, R.J., 2008. Basinal restriction, black shales, Re-Os dating, and the Early Toarcian (Jurassic) oceanic anoxic event. Paleoceanography 23(4), PA4217.

Meyers, S.R., 2008. Resolving Milankovitchian controversies: the Triassic Latemar Limestone and the Eocene Green River Formation. Geology 36, 319-322.

Miller, C.A., 2004. Re-Os dating of algal laminites: reduction-enrichment of metals in the sedimentary environment and evidence for new geoporphyrins. Masters Thesis, University of Saskatchewan, 124 - 128.

Morford, J.L., Emerson, S., 1999. The geochemistry of redox sensitive trace metals in sediments. Geochimica et Cosmochimica Acta 63, 1735-1750.

Morford, J.L., Martin, W.R., Francois, R., Carney, C.M., 2009. A model for uranium, rhenium, and molybdenum diagenesis in marine sediments based on results from coastal locations. Geochimica et Cosmochimica Acta 73, 2938-2960.

Olsen, P.E., 1997. Stratigraphic record of the early Mesozoic breakup of Pangea in the Laurasia-Gondwana rift system. Annu. Rev. Earth Planet. Sci. 25, 337-401.

Peters, K.E., 1986. Guidelines for evaluating petroleum source rock using programmed pyrolysis. AAPG Bulletin 70, 318-329.

Peucker-Ehrenbrink, B., Jahn, B., 2001. Rhenium-osmium isotope systematics and platinum group element concentrations: Loess and the upper continental crust. Geochem. Geophys. Geosyst. 2(10), 1061-1083.

Peucker-Ehrenbrink, B., Ravizza, G., 2012. Osmium isotope stratigraphy, in: Gradstein, F. M., Ogg, J. G., Schmitz, M., Ogg, G. 2012, The Geological Timescale, 1. Elsevier, Oxford, 145 – 166.

Peucker-Ehrenbrink, B., Ravizza, G., 2000. The marine osmium isotope record. Terr. Nova 12, 205-219.

Pietras, J.T., Carroll, A.R., 2006. High-resolution stratigraphy of an underfilled lake basin: Wilkins Peak Member, Eocene Green River Formation, Wyoming, U.S.A. Journal of Sedimentary Research 76, 1197-1214.

Poirier, A., Hillaire-Marcel, C., 2011. Improved Os-isotope stratigraphy of the Arctic Ocean. Geophys. Res. Lett. 38. L14607.

Ravizza, G., Turekian, K.K., 1992. The osmium isotopic composition of organic-rich marine sediments. Earth and Planetary Science Letters 110, 1-6.

Ravizza, G., Turekian, G.G., Hay, B.J., 1991. The geochemistry of rhenium and osmium in recent sediments from the Black Sea. Geochimica et Cosmochimica Acta 55, 3741-3752.

Ravizza, G., Turekian, K.K., 1989. Application of the ^{187}Re-^{187}Os system to black shale geochronometry. Geochimica et Cosmochimica Acta 53, 3257-3262.

Raymo, M.E., Ruddiman, W.F., 1992. Tectonic forcing of late Cenozoic climate. Nature 359, 117-122.

Remy, R.R., 1992. Stratigraphy of the Eocene part of the Green River Formation in the south-central part of the Uinta Basin, Utah. U.S. Geological Survey Bulletin 1787-BB.

Rhodes, M.K., Carroll, A.R., Pietras, J.T., Beard, B.L., Johnson, C.M., 2002. Strontium isotope record of paleohydrology and continental weathering, Eocene Green River Formation, Wyoming. Geology 30, 167-170.

Richter, F.M., Rowley, D.B., Depaolo, D.J., 1992. Sr isotope evolution of seawater - the role of tectonics. Earth and Planetary Science Letters 109, 11-23.

Rooney, A.D., Selby, D., Houzay, J.-P., Renne, P.R., 2010. Re-Os geochronology of a Mesoproterozoic sedimentary succession, Taoudeni basin, Mauritania: implications for basin-wide correlations and Re-Os organic-rich sediments systematics. Earth and Planetary Science Letters 289, 486-496.

Rooney, A. D., Chew, D. M., Selby, D., 2011. Re-Os geochronology of the Neoproterozoic-Cambrian Dalradian Supergroup of Scotland and Ireland: implications for Neoproterozoic stratigraphy, glaciations and Re-Os systematics. Precambrian Research 185, 202-214.

Rooney, A.D., Selby, D., Lewan, M.D., Lillis, P.G., Houzay, J.-P., 2012. Evaluating Re–Os systematics in organic-rich sedimentary rocks in response to petroleum generation using hydrous pyrolysis experiments. Geochimica et Cosmochimica Acta 77, 275-291.

Ruble, T.E., Lewan, M.D., Philp, R.P., 2001. New insights on the Green River Petroleum System in the Uinta Basin from hydrous pyrolysis experiments. AAPG Bulletin 85, 1333-1371.

Ryder, R.T., Fouch, T.D., Elison, J.H., 1976. Early Tertiary sedimentation in the western Unita Basin, Utah. Geological Society of America Bulletin 87, 496-512.

Sageman, B.B., Murphy, A.E., Werne, J.P., Ver Straeten, C.A., Hollander, D.J., Lyons, T.W., 2003. A tale of shales: the relative roles of production, decomposition, and dilution in the accumulation of organic-rich strata, middle–upper Devonian, Appalachian basin. Chemical Geology 195, 229-273.

Selby, D., 2007. Direct Rhenium-Osmium age of the Oxfordian-Kimmeridgian boundary, Staffin bay, Isle of Skye, U.K., and the late Jurassic time scale. Norwegian Journal of Geology 87, 291-300.

Selby, D., Creaser, R.A., 2003. Re-Os geochronology of organic rich sediments: an evaluation of organic matter analysis methods. Chemical Geology 200, 225-240.

Selby, D., Creaser, R.A., 2005. Direct radiometric dating of the Devonian-Mississippian time-scale boundary using the Re-Os black shale geochronometer. Geology 33, 545-548.

Selby, D., Creaser, R.A., Stein, H.J., Markey, R.J., Hannah, J.L., 2007. Assessment of the Re-187 decay constant by cross calibration of Re-Os molybdenite and U-Pb zircon chronometers in magmatic ore systems. Geochimica et Cosmochimica Acta 71, 1999-2013.

Selby, D., Mutterlose, J., Condon, D.J., 2009. U-Pb and Re-Os geochronology of the Aptian/Albian and Cenomanian/Turonian stage boundaries: implications for timescale calibration, osmium isotope seawater composition and Re-Os systematics in organic-rich sediments. Chemical Geology 265, 394-409.

Sharma, M., Wasserburg, G.J., Hofmann, A.W., Chakrapani, G.J., 1999. Himalayan uplift and osmium isotopes in oceans and rivers - its relation to global tectonics and climate. Geochimica et Cosmochimica Acta 63, 4005-4012.

Smith, M.E., Carroll, A.R., Singer, B.S., 2008a. Synoptic reconstruction of a major ancient lake system: Eocene Green River Formation, western United States. Geological Society of America Bulletin 120, 54-84.

Smith, M.E., Carroll, A.R., Mueller, E.R., 2008b. Elevated weathering rates in the Rocky Mountains during the Early Eocene Climatic Optimum. Nature Geoscience 1, 370-374.

Smith, M.E., Chamberlain, K.R., Singer, B.S., Carroll, A.R., 2010. Eocene clocks agree: Coeval $^{40}Ar/^{39}Ar$, U-Pb, and astronomical ages from the Green River Formation. Geology 38, 527-530.

Smith, M.E., Singer, B., Carroll, A., 2003. $^{40}Ar/^{39}Ar$ geochronology of the Eocene Green River Formation, Wyoming. Geological Society of America Bulletin 115, 549-565.

Smith, M.E., Singer, B.S., Carroll, A.R., Fournelle, J.H., 2006. High-resolution calibration of Eocene strata: $^{40}Ar/^{39}Ar$ geochronology of biotite in the Green River Formation. Geology 34, 393-396.

Smoliar, M.I., Walker, R.J., Morgan, J.W., 1996. Re-Os isotope constraints on the age of Group IIA, IIIA, IVA, and IVB iron meteorites. Science 271, 1099-1102.

Sun, W.D., Bennett, V.C., Eggins, S.M., Kamenetsky, V.S., Arculus, R.J., 2003. Enhanced mantle-to-crust rhenium transfer in undegassed arc magmas. Nature 422, 294-297.

Sundby, B., Martinez, P., Gobeil, C., 2004. Comparative geochemistry of cadmium, rhenium, uranium, and molybdenum in continental margin sediments. Geochimica et Cosmochimica Acta 68, 2485-2493.

Tissot, B., Deroo, G., Hood, A., 1978. Geochemical study of the Uinta Basin: formation of petroleum from the Green River Formation. Geochimica et Cosmochimica Acta 42, 1469-1485.

Turgeon, S.C., Creaser, R.A., Algeo, T.J., 2007. Re-Os depositional ages and seawater Os estimates for the Frasnian-Famennian boundary: implications for weathering rates, land plant evolution, and extinction mechanisms. Earth and Planetary Science Letters 261, 649-661.

Tuttle, M.L., 1991. Geochemical, Biogeochemical, and Sedimentalogical Studies of the Green River Formation, Wyoming, Utah and Colorado. U.S. Geological Survey Bulletin 1973-A-G.

Tuttle, M.L., Goldhaber, M.B., 1993. Sedimentary sulfur geochemistry of the Paleogene Green River Formation, western USA: implications for interpreting depositional and diagenetic processes in saline alkaline lakes. Geochimica et Cosmochimica Acta 57, 3023-3039.

Ver Straeten, C.A., Brett, C.E., Sageman, B.B., 2011. Mudrock sequence stratigraphy: a multi-proxy (sedimentological, paleobiological and geochemical) approach, Devonian Appalachian Basin. Palaeogeography, Palaeoclimatology, Palaeoecology 304, 54-73.

Xu, G.P., Hannah, J.L., Stein, H.J., Bingen, B., Yang, G., Zimmerman, A., Weitschat, W., Mork, A., Weiss, H.M., 2009. Re-Os geochronology of Arctic black shales to evaluate the Anisian-Ladinian boundary and global faunal correlations. Earth and Planetary Science Letters 288, 581-587.

Yamashita, Y., Takahashi, Y., Haba, H., Enomoto, S., Shimizu, H., 2007. Comparison of reductive accumulation of Re and Os in seawater-sediment systems. Geochimica et Cosmochimica Acta 71, 3458-3475.

Yang, G., Hannah, J.L., Zimmerman, A., Stein, H.J., Bekker, A., 2009. Re-Os depositional age for Archean carbonaceous slates from the southwestern Superior Province: challenges and insights. Earth and Planetary Science Letters 280, 83-92.

Chapter 3

Re-Os geochronology, Os isotope fingerprinting and hydrous pyrolysis of the Green River petroleum system in the Uinta Basin

Re-Os geochronology and Os isotope fingerprinting of petroleum sourced from a Type I lacustrine kerogen: Insights from the natural Green River petroleum system in the Uinta Basin and hydrous pyrolysis experiments

A version of this chapter has been submitted to *Geochimica et Cosmochimica Acta* co-authored by David Selby of Durham University, Paul G. Lillis and Michael D. Lewan both of the US Geological Survey.

3.1 Introduction

The majority of large oil discoveries are sourced from marine shales associated with major ocean anoxic events of the Jurassic and Cretaceous (Klemme and Ulmishek, 1991). Such large discoveries are becoming increasingly rare and thus there is a need to find smaller petroleum systems and more accurately trace oils to their source in order to improve migration pathway models and reserve calculations. A common problem for petroleum exploration surrounds understanding the spatial and temporal controls on hydrocarbon formation. Establishing the timing of hydrocarbon generation has, to-date, mainly been carried out through the use of basin modelling, often with poorly constrained parameters (e.g. Anders et al., 1992; Bredehoeft et al., 1994; Fouch et al., 1994). Therefore knowing the absolute age of petroleum generation provides vital information and controls on the understanding of a petroleum system.

The application of the rhenium-osmium (Re-Os) geochronometer to marine petroleum systems has permitted the determination of source rock depositional ages (e.g. Cohen et al., 1999; Creaser et al., 2002; Selby et al., 2005; Kendall et al., 2009; Xu et al., 2009; Rooney et al., 2010) and the timing of petroleum generation (Selby et al., 2005; Selby and Creaser, 2005a; Finlay et al., 2011). Furthermore, Os isotopes have been successfully used in marine basins to fingerprint oils to their source rocks (Finlay et al., 2012). Traditionally, oil-source rock correlation uses organic chemical analysis (e.g. biomarkers) of light hydrocarbon fractions, however common processes such as biodegradation preferentially remove light hydrocarbons from petroleum and therefore, even for moderately biodegraded oils, traditional oil to source fingerprinting techniques can be compromised. Hydrocarbon Re-Os geochronology and Os isotope fingerprinting, however, rely on the heavy fractions of oil (asphaltene; Selby et al., 2007). The Os isotope fingerprinting tool uses the initial $^{187}Os/^{188}Os$ composition (Os_i) of petroleum which reflects that of the source rock at the time of petroleum generation (Os_g) providing a novel inorganic oil-source fingerprinting technique (Selby et al., 2007; Finlay et al., 2011, 2012). As a result, inorganic geochemistry provides a

correlation tool where traditional organic methods can be hampered by biodegradation (Finlay et al., 2012).

Despite the promising success of Re-Os hydrocarbon geochronology and Os isotope fingerprinting in marine basins, there still remains little knowledge of the mechanism of Re and Os transfer from source rocks to oils (Selby et al., 2007; Rooney et al., 2012). A hydrous pyrolysis study of the Permian Phosphoria (Type II-S kerogen) and Jurassic Staffin Formations (Type III kerogen) involved artificial maturation of the source rocks in order to assess transfer of Re and Os from source rock to oil (Rooney et al., 2012). These experiments demonstrated that Re-Os systematics in the source rock are undisturbed during hydrocarbon maturation as previously suggested in the natural system (Creaser et al., 2002; Selby and Creaser, 2005a). However there was limited Re and Os in the oils produced since the kinetic parameters needed for transfer were not attained in these artificial experiments (Rooney et al., 2012). The bitumen produced contained Re and Os and it was found that during hydrocarbon generation the Os isotope composition of the source is transferred to the bitumen, providing strong evidence that Os isotopes can be used as an oil-source correlation tool, supporting the hypothesis derived from natural petroleum system studies (Selby and Creaser, 2005a; Selby et al., 2005, Selby et al., 2007; Finlay et al., 2012). However, given that the Re-Os hydrocarbon geochronology and Os isotope fingerprinting tools have only been assessed in natural marine petroleum systems sourced from Type II and Type II-S kerogens (Selby et al., 2005; Selby and Creaser, 2005a; Finlay et al., 2011, 2012), there is a need for further assessment and understanding of Re-Os systematics during hydrocarbon generation and in variable basin types in order to widen the applications of Re-Os hydrocarbon geochronology and Os isotope fingerprinting.

The Green River petroleum system in the Uinta Basin (Fig. 3.1) contains Type I lacustrine source rocks that have produced several different hydrocarbons (oil, tar sands and gilsonite) that are both biodegraded and non-biodegraded (Tissot et al., 1978; Anders et al., 1992; Fouch et al., 1994; Katz, 1995; Ruble et al., 2001). The Green River petroleum system therefore provides the ability to test whether Re-Os

geochronology and Os isotope fingerprinting can be applied to different hydrocarbon phases, biodegraded and non-biodegraded, and to a petroleum system derived from a Type I lacustrine kerogen. Herein I explore the capabilities of Re-Os geochronology and Os isotope fingerprinting on a Type I lacustrine kerogen and differing hydrocarbon phases to further establish the behaviour of these geochemical systems and widen their application to poorly constrained or non-traditional petroleum systems. In addition I use hydrous pyrolysis experiments to further elucidate the nature of Re and Os transfer to oil in particular with reference to Type I lacustrine kerogen. This data set allows valuable comparison of a natural system and an experimental approach on the same source rock in order to understand Re-Os systematics within petroleum systems.

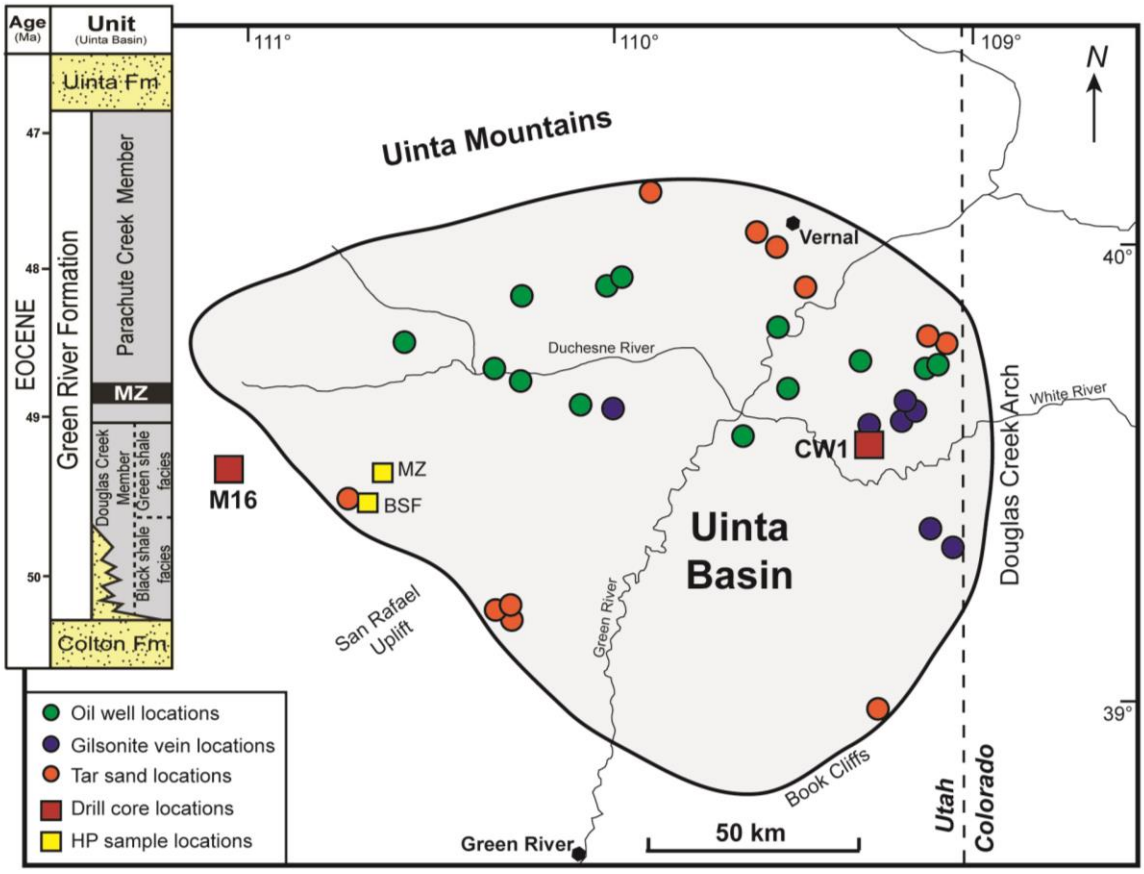

Figure 3.1: Map of the Uinta Basin illustrating the location of the sampled hydrocarbons and the source rocks sampled from two drill cores; Marsing 16 (M16; 39° 57' 1.4904" N, 111° 1' 37.527" W) and Coyote Wash 1 (CW1; 40° 1' 22.224" N, 109° 18' 38.4834" W). The CW1 core is located in the central depocentre of an asymmetric basin structure, while the M16 core is on the

flanks of this structure and has not seen significant burial. The outcrop samples used for the hydrous pyrolysis (HP) experiments are also shown, the Mahogany Zone (MZ; 930923-8; 39°53'12''N, 110°44'58''W) and black shale facies (BSF; 930922-1; 39°50'09''N, 110°47'05''W). Schematic stratigraphy of the Green River Formation is provided in the inset. This shows the intertonguing nature of the basal sandstones with the Douglas Creek Member. The Douglas Creek Member is split into the black shale and green shale facies after Ruble et al. (2001). Ages of the stratigraphy are based on chronostratigraphy of Smith et al. (2008).

3.2 Geological setting

The Green River petroleum system of the Uinta Basin in northwest Utah receives considerable attention as it has generated >500 million barrels of oil and has >12 billion barrels of oil inferred in tar sand deposits, along with oil shales containing an estimated 1 trillion barrels of recoverable oil and solid bitumen deposits (Fig. 3.1; Hunt, 1963; Anders et al., 1992; Fouch et al., 1994; Ruble et al., 2001; Dyni, 2006). The source rock for this petroleum system is the Eocene Green River Formation; a classic model for lacustrine source rock deposition and hydrocarbon generation from these types of source rock facies (Ruble et al., 2001). The unit exhibits variable organic enrichment (0.2 – 33.7 wt.%; Katz, 1995) and is the common reference type for a typical Type I kerogen (Vandenbroucke and Largeau, 2007).

The Green River Formation was deposited in three large continental basins named the Uinta, Piceance and Greater Green River Basins located in Colorado, Wyoming and Utah, USA. The basins formed east of the thin-skinned Sevier orogenic belt, and are separated by Laramide basement-cored uplifts, geometry of which is controlled by Precambrian and late Palaeozoic structures (Johnson, 1992). The depocentres were occupied by two large lakes associated with temperate to subtropical climate of the early to middle Eocene and covering an area of 65,000 km^2 (Dyni, 2006; Smith et al., 2008). The Green River Formation was deposited in freshwater to hypersaline lakes and lake level fluctuations allowed thick packages

(~3000 m) of organic-rich carbonaceous shales and oil shales interbedded with fluvial clastics to be deposited (Keighley et al., 2003; Pietras and Carroll, 2006). Sedimentary facies within the Green River Formation can be divided into fluvio-lacustrine, fluctuating profundal and evaporative facies (Carroll and Bohacs, 1999, 2001; Bohacs et al., 2000). The most important members of the Green River Formation in terms of source rocks are the Douglas Creek Member and Parachute Creek Member. The Douglas Creek Member was deposited initially as lake levels rose and represents fluctuating profundal deposition (Bradley, 1931; Tuttle and Goldhaber, 1993; Carroll and Bohacs, 2001). Here organic-rich units of the informally named black shale facies were deposited that are considered by some to be the only units to have generated oil (Remy, 1992; Katz, 1995; Ruble et al., 2001). The maximum extent of the lake occurred during deposition of the overlying Parachute Creek Member, at this time the most organic-rich oils shales (> 30 wt.% TOC) were deposited, named the Mahogany Zone (Bradley, 1931; Tuttle and Goldhaber, 1993; Smith et al., 2008). Despite the high TOC, this unit is considered not to be a significant source of petroleum due to insufficient burial thus it is a target for oil shale extraction (Ruble et al., 2001; Dyni, 2006). Due to a lack of detailed biostratigraphy in lacustrine records, the Green River Formation has been dated using predominantly Ar-Ar and U-Pb geochronology of interbedded tuffs as well as Re-Os dating of the source rock itself, with deposition constrained from ~52 to ~44 Ma (Smith et al., 2008, 2010; Cumming et al., 2012; Chapter 2).

The Green River Formation source rocks are deposited throughout the area, but are considered to have only been buried sufficiently for oil and gas generation in the northeast corner of the Uinta Basin (Tissot et al., 1978; Ruble et al., 2001). The thickness and nature of the lacustrine sedimentary facies means that the Green River Formation contains not only the source rock for this petroleum system, but also most of the reservoir and seal rocks (Fouch et al., 1994). The erosional remnant of the Uinta Basin outcrops within the southern limb of a gentle syncline, dipping <5° to the North (Keighley et al., 2003). Several oil fields (e.g. Altamont, Bluebell, Duchesne) are produced from lenticular lacustrine sandstone and carbonate reservoirs, with alluvial

deposits acting as seals stratigraphically trapping oil in down-dip reservoirs (Fouch et al., 1994). Migration distance for the oils is ≤100 km. The tar sands are surface expressions of oil that has migrated up structural dip through fluvio-lacustrine facies connected to the deeper oil fields. Most of the accumulations are associated with source rocks with vitrinite reflectance >0.5% R_m (0.5 - 0.7% R_m = moderately mature; Anders et al., 1992; Fouch et al., 1994). Early oil generation models suggest that generation began at the base of the Green River Formation around 40 Ma (only ~10 Myrs after deposition) at a depth of 3350 m, with peak oil generation in this lower region probably occurring during maximum burial (30-40 Ma; Fouch et al., 1994). Generation then reduced from 30 Ma to the present day and the zone of generation has risen stratigraphically through time. It is also suggested that the Mahogany Zone began hydrocarbon generation ~25 - 30 Ma and that this is probably still on-going (Fouch et al, 1994). Ruble et al. (2001) more recently proposed, using hydrous pyrolysis kinetic models, that hydrocarbon generation only began in the lower Green River Formation ~25 Ma and is on-going to the present day, without the Mahogany Zone going fully through the oil window meaning there is limited generation from this source.

Although this is a relatively simple petroleum system contained within one formation with a known source rock (the Green River Formation; Fouch et al., 1994), the source unit is over 3000 m thick in places and so the exact units generating oil are more ambiguous (Anders et al., 1992). Additionally, oil-source rock correlation in these settings is complicated as multifaceted lacustrine facies can obscure maturity relationships usually distinguished by biomarkers (Ruble et al., 2001). This therefore provides an ideal petroleum system to test the Re-Os hydrocarbon geochronometer and Os isotope oil source correlation tools on more diverse petroleum systems in order to widen their applicability.

3.3 Analytical methodology

3.3.1 Samples and sample preparation

3.3.1.1 Oils

Oils were obtained from the US Geological Survey oil library for Re-Os analysis. Well locations (Fig. 3.1) with well names, oil fields, reservoir formations and organic geochemical properties of each sample are given in Table 3.1. The sample set provides a representation of oils from across the entire Uinta Basin oil fields. Two oil types are recognised in the Uinta Basin, Green River A (GRA; the most common) and Green River B (GRB), which are defined based on organic geochemical parameters and are interpreted to have been sourced from the lower black shale facies of the Douglas Creek Member and the Mahogany Zone, respectively (Lillis et al., 2003). Source identification is based on the presence of beta carotane in the GRB oils, which is derived from the Mahogany source facies (Fig. 3.2).

The asphaltene fraction of the oil is utilised for the Re-Os analyses because it contains >90% of the Re and Os within an oil and possesses Re-Os isotopic compositions identical and more precise than whole oil analysis (Selby et al., 2007). Asphaltene was precipitated from the Green River oils using *n*–heptane (c.f. Selby et al., 2007). This process involved 1 gram of oil being thoroughly mixed in 40 ml of *n*–heptane in a 60 ml glass vial and then agitated for ~12 hrs. The contents of the vial were then centrifuged at 4000 rpm for 5 minutes to allow complete separation of the insoluble asphaltene and soluble maltene fractions. The asphaltene was dried on a hot plate at ~60˚C and then used for Re-Os analysis.

Table 3.1: Sample information for the oils, tar sands and gilsonites

Sample	Hydrocarbon	Field/deposit	Well name	Formation	Latitude	Longitude	β-carotane	Oil type	Asph (%)	Biodegradation
GR2268	Oil - USGS	Bluebell	Lamicq 2-6B1	Green River/Wasatch	40.335	-110.034	trace	GRA	4.78	no (0)
GR2266	Oil - USGS	Coyote Basin	Coyote Basin 21-7	Wasatch	40.143	-109.146	0	GRA	8.00	no (0)
GR2232	Oil - USGS	Coyote Basin	E. Red Wash 1-5	Green River	40.153	-109.126	0	GRA	7.37	no (0)
GR2239	Oil - USGS	Duchesne	Ute. Tribal 6-16 D	Green River	40.139	-110.344	trace	GRA	8.88	no (0)
GR2269	Oil - USGS	Horseshoe Bend	Federal 33-7 L	Green River	40.253	-109.566	+	GRA	7.24	no (0)
GR2264	Oil - USGS	Monument Butte	Federal 23-34B	Green River	40.072	-110.107	+	GRA	5.95	no (0)
GR2242	Oil - USGS	Natural Buttes	Natural Duck 4-21	Green River	40.026	-109.665	+	GRA	7.94	no (0)
GR2267	Oil - USGS	Wonsits Valley	WVU 133 & 71	Green River	40.118	-109.543	+	GRA	6.49	no (0)
GR2259	Oil - USGS	Altamont	Myrin Ranch 1-13 B4	Wasatch	40.312	-110.278	+	GRA	7.09	no (0)
GR2114	Oil - USGS	Sulphur Creek	Govt. 29-3	Wasatch	39.845	-108.414	++	GRA	9.77	no (0)
GRB-827	Oil - USGS	Bluebell	L L Pack 1-33A1	Green River	40.352	-110.004	++	GRB	18.50	no (0)
GRB-3885	Oil - USGS	Duchesne	Ute-Tribal 8	Green River	40.139	-110.348	++++	GRB	19.00	slightly (1)
GRB-1602	Oil - USGS	Duchesne	Willis Moon 1	Green River	40.130	-110.277	++++	GRB	14.06	slightly (1)
GRB-847	Oil - USGS	Blacktail Ridge	Ute Tribal 2/22-18	Green River	40.221	-110.607	++++	GRB	2.20	no (0)
GRB-824	Oil - USGS	Red Wash	Red Wash 120 23-28B	Green River	40.179	-109.334	++	GRB	1.65	no (0)
VC07-10	Gilsonite - USGS	Bonanaza vein	-	Uinta Formation	40.036	-109.229	-	GRB	-	-
VC05-10	Gilsonite - USGS	Cowboy vein	-	Uinta Formation	40.073	-109.220	-	GRB	-	-
VC06-10	Gilsonite - USGS	Rainbow vein	-	Upper Parachute Creek	39.822	-109.154	-	GRB	-	-
VC08-10	Gilsonite - USGS	Dragon mine	-	Lower Douglas Creek	39.775	-109.085	-	GRB	-	-
VC09-10	Gilsonite - USGS	CW1 core vein	-	Mahogany Zone	40.023	-109.311	-	GRB	-	-
VC44-10	Gilsonite - TR	Little Emma vein	-	-	-	-	-	GRB	-	-
VC45-10	Gilsonite - TR	Bonanza	-	-	-	-	-	GRB	-	-
VC46-10	Gilsonite - TR	Independant	-	-	-	-	-	GRB	-	-
VC47-10	Gilsonite - TR	Cowboy	-	-	-	-	-	GRB	-	-
VC12-10	Gilsonite - field	Cowboy/Bonanza	-	Uinta Formation	40.068	-109.201	++++	GRB	83.89	moderate (4)
VC16-10	Gilsonite - field	Pariette Bench	-	Uinta Formation	40.071	-110.028	++++	GRB	73.19	moderate (4)
VC34-10	Gilsonite - UCRC	Bonanza	-	-	-	-	-	GRB	-	-
VC03-10	Tar Sand - USGS	Asphalt Ridge	-	-	40.447	-109.616	0	GRA	-	heavy (5-6)
VC02-10	Tar Sand - USGS	Sunnyside	Amoco A-22	-	39.630	-110.310	0	GRA	-	heavy (5-6)
VC01-10	Tar Sand - USGS	Raven ridge	-	Upper Douglas Creek	40.206	-109.098	++	GRA	-	heavy (5-6)
VC04-10	Tar Sand - USGS	PR Springs	-	Upper Douglas Creek	39.439	-109.292	+	GRA	-	heavy (5-6)
VC35-10	Tar Sand - UCRC	PR Springs	PRS-3	Upper Douglas Creek	-	-	-	GRA	-	-
VC10-10	Tar Sand - field	White Rocks	-	Navajo Sandstone	40.569	-109.918	trace	GRA	15.85	heavy (5-6)
VC11-10	Tar Sand - field	Raven Ridge	-	Parachute Creek	40.225	-109.128	trace	GRA	26.80	heavy (5-6)
VC14-10	Tar Sand - field	Asphalt Ridge	-	Duschesne River	40.336	-109.485	trace	GRA	36.95	heavy (5-6)
VC15-10	Tar Sand - field	Asphalt Ridge	-	Duschesne River	40.416	-109.583	++	GRA	45.63	severe (7+)
VC20-10	Tar Sand - field	Sunnyside	-	Green River - lower	39.636	-110.348	trace	GRA	14.01	(6-7)
VC25-10	Tar Sand - field	Sunnyside	-	Green River - lower	39.636	-110.350	trace	GRA	27.22	(6-7)
VC32-10	Tar Sand - field	Sunnyside	-	Green River - lower	39.635	-110.347	trace	GRA	21.22	(6-7)
VC33-10	Tar Sand - field	Willow Creek	-	Green River - lower	39.844	-110.774	++	GRA	84.20	severe (7+)

(-) no data for these samples
USGS = U.S. Geological Survey
TR = donated by Tim Ruble
UCRC = Utah Core Research Centre

β-carotane estimates based on gas chromatograms of USGS
Oil type based on β-carotane (Lillis et al., 2003)
Asph = percentage asphaltene content derived from asphaltene extractions (oils) or USGS analysis
Biodegradation scale is zero to ten (Peters et al., 2005)

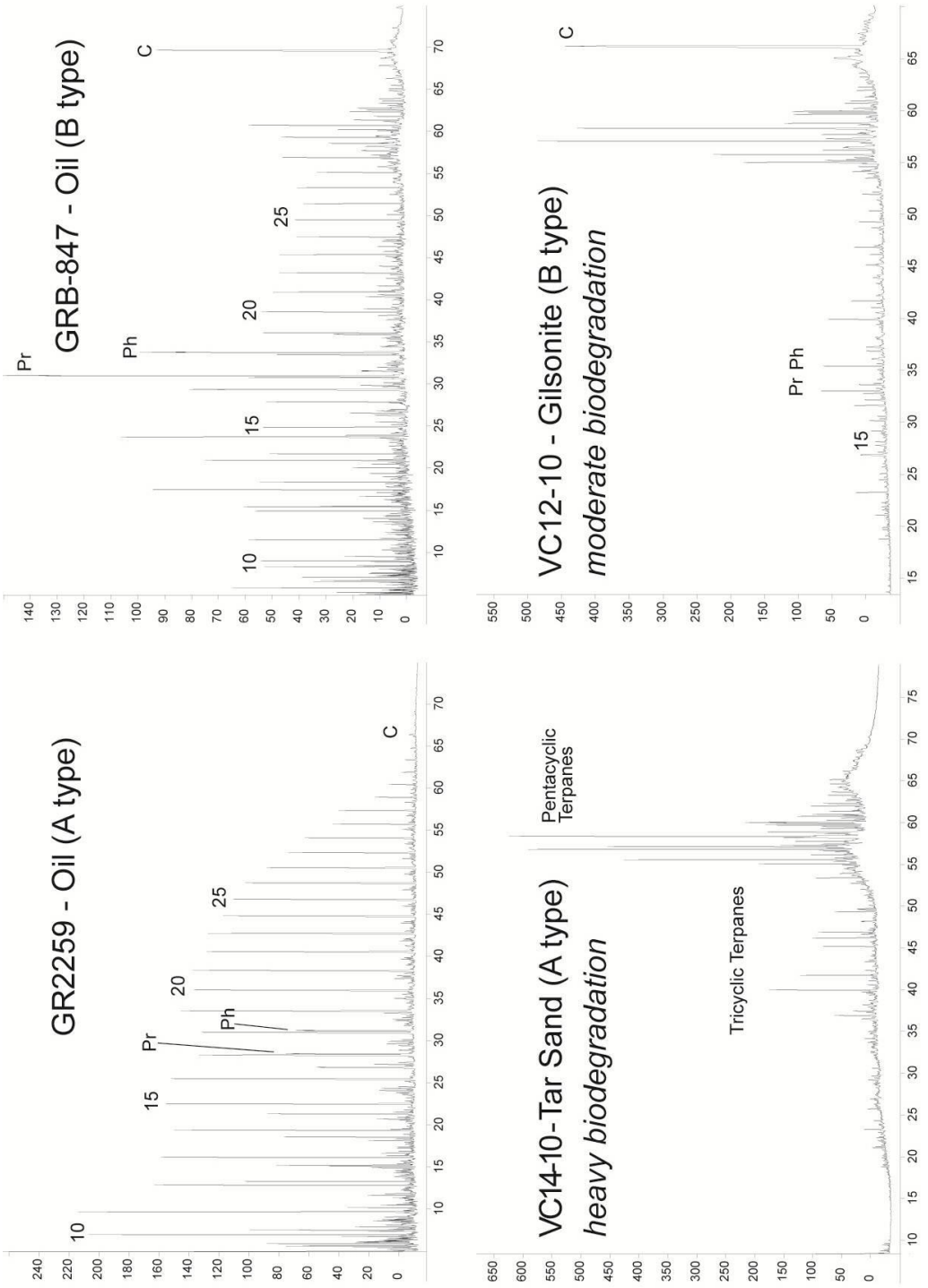

Figure 3.2: Gas chromatograms of the saturated hydrocarbon fraction of selected oils, tar sands, and gilsonite from the Uinta basin, Utah, showing nondegraded and biodegraded examples of GRA and GRB oil types (defined by Lillis et al., 2003). Pr is pristane, Ph is phytane, and C is β-carotane.

3.3.1.2 Tar sands

Tar sands were collected from outcrop throughout the Uinta Basin giving a wide representation of the instances of oil that has migrated up dip from deeper oil fields. Location and names of deposits are reported in Table 3.1 and Figure 3.1. Approximately ~500 g of tar sand was collected to ensure enough oil could be extracted from it for Re-Os analysis. The tar sands are heavily biodegraded oil accumulations the source of which is thought to be the same as the GRA oils (Fouch et al., 1994; Lillis et al., 2003; Ruble et al., 2001).

Oil is separated from the Green River tar sands using a method modified from Selby et al. (2005). Approximately 1 g of tar sand was washed in ~1/2 ml of $CHCl_3$ and then decanted into a 15 ml centrifuge tube, and repeated until the $CHCl_3$ remained clear. The $CHCl_3$ and oil solution was then centrifuged to separate any suspended sediment from the solution. Evaporation of the decanted $CHCl_3$ at ~ 60°C on a hot plate left the oil remaining. Tar sands are heavily biodegraded and are therefore naturally enriched in asphaltene (Evans et al., 1971), with the average for some of the Green River tar sands being ~34 wt.% (Table 3.1), rendering separation of asphaltenes for Re-Os analysis unnecessary (c.f. Selby and Creaser, 2005a).

3.3.1.3 Gilsonite

Gilsonite is a solid bitumen deposit of which there are several types in the Uinta Basin (ozocerite, albertite, tabbyite and wurtzilite; Ruble and Philp, 1991), with gilsonite being the most abundant (Verbeek and Grout, 1992). It crops out in northwest trending vertical fractures up to 5 m thick within the middle and upper Green River Formation (Cashion, 1967; Anders et al., 1992; Verbeek and Grout, 1992). The method of formation is not fully understood with suggestions of oil reservoirs penetrated by fractures allowing oil to migrate up the fractures and then solidify from inspissation or metamorphosis (Tetting, 1984). Other suggestions are that they are derived from early bitumen generation causing over-pressured source beds to initiate hydraulic fracturing (Verbeek and Grout, 1992). The fractures containing gilsonite

originate in the lacustrine facies of the Green River Formation, in particular the Mahogany Zone, this led to suggestions of the Mahogany Zone as the source where early maturity generation occurred and liquid hydrocarbons migrated into tensile fractures created during uplift (Hunt et al., 1954; Hunt, 1963) or where overpressure allowed hydraulic fracturing of the rock to produce the veins (Verbeek and Grout, 1992). The Mahogany Zone was further suggested as the source based on infra-red spectroscopy (Hunt et al., 1954) and carbon isotope and biomarker compositions (Ruble et al., 1994; Schoell et al., 1994).

Several gilsonite samples were collected from outcrops of different fracture systems throughout the Uinta Basin (Table 3.1, Fig. 3.1). Approximately 50 - 100 g samples were collected and then crushed with no metal contact for analysis. Gilsonite, although only moderately biodegraded (Fig. 3.2; Ruble et al., 1994), is naturally enriched in asphaltene (the average for two Green River samples is ~ 78.5 wt.%; Table 3.1) and so separation of asphaltene is unnecessary for Re-Os analysis.

3.3.1.4 Source rocks

Three Green River Formation source units from the Uinta Basin have previously been analysed for Re-Os isotopes, the data are presented in Table 3.2 (Cumming et al., 2012; Chapter 2). The units were sampled from two cores held at the US Geological Survey Core Research Centre; Coyote Wash 1 (CW1) in the central depocentre and Marsing 16 (M16) at the southwest edge of the Basin (Fig. 3.1). The Douglas Creek Member or black shale facies (TOC = 2.67 - 24.70 wt.%, Tmax = 434 - 448°C; Cumming et al., 2012; chapter 2) were sampled from both cores and the Mahogany Zone (TOC = 9.39 - 28.15 wt.%, Tmax = 432 - 445°C; Cumming et al., 2012; chapter 2) was sampled from the CW1 core. Additional analysis were performed to assess the spread of Os isotopic compositions across 30 – 50 m of each unit sampled, these analyses and sample depths can also be seen in Table 3.2. The Re-Os data from these units are used for correlation from oil to source rock. Sample preparation follows that outlined by

Cumming et al. (2012; chapter 2); all samples are cut, polished, dried and then crushed to a fine powder using no metal contact.

The source rocks used for the hydrous pyrolysis experiments are the Mahogany Zone (930923-8; 39°53’12’’N, 110°44’58’’W; Fig. 3.1) and black shale facies (930922-1; 39°50’09’’N, 110°47’05’’W; Fig. 3.1), details and locations of which are outlined in Ruble et al. (2001). These samples were selected as they have been previously characterised using hydrous pyrolysis experiments. The black shale facies represents the dominant source rock for the Green River hydrocarbons, whereas the Mahogany Zone is the most organic-rich unit within the Green River Formation with only minor generation (Ruble et al., 2001; Lillis et al., 2003).

Table 3.2: Re-Os isotope data for the three Green River Formation source rock units

Sample	Depth (m)	Re (ng/g)	±	Os (pg/g)	±	$^{187}Re/^{188}Os$	±	$^{187}Os/^{188}Os$	±	rho [a]	Os_g [b]	TOC (wt.%)
Douglas Creek Member, Marsing 16 core (39° 57' 1.4904" N, 111° 1' 37.527" W)												
M16-43	290.3	9.6	0.0	278.6	2.0	199.2	1.8	1.614	0.019	0.679	1.53	-
M16-37	304.2	23.0	0.1	223.4	1.3	619.6	3.9	2.054	0.014	0.714	1.80	-
M16-27*	323.8	22.6	0.1	341.3	2.3	390.2	3.3	1.831	0.018	0.722	1.67	5.96
M16-26*	323.9	23.6	0.1	333.5	2.6	418.3	4.1	1.861	0.022	0.718	1.69	6.47
M16-25*	324.0	42.6	0.1	490.0	2.8	518.6	3.3	1.950	0.013	0.680	1.73	9.71
M16-24*	324.0	27.8	0.1	393.8	3.0	417.4	4.0	1.854	0.022	0.704	1.68	7.09
M16-23*	324.5	54.9	0.2	341.6	1.9	997.4	6.5	2.336	0.014	0.819	1.92	8.20
M16-22*	324.6	56.0	0.2	343.1	2.1	1015.2	7.1	2.352	0.016	0.790	1.93	-
M16-21*	324.6	62.4	0.2	392.8	2.5	984.8	6.9	2.326	0.017	0.735	1.92	5.42
M16-20*	324.7	40.1	0.1	351.6	1.5	690.2	3.2	2.079	0.008	0.599	1.79	5.53
M16-19*	324.7	24.5	0.1	263.1	1.4	556.4	3.4	1.982	0.013	0.665	1.75	3.53
M16-18*	324.9	29.2	0.1	273.4	1.5	645.0	3.8	2.078	0.013	0.651	1.81	6.39
M16-16*	325.1	21.0	0.1	178.2	1.2	716.3	5.5	2.145	0.019	0.725	1.85	5.71
M16-15*	325.3	22.9	0.1	297.1	1.6	458.1	2.7	1.923	0.012	0.648	1.73	5.23
M16-14*	325.4	16.8	0.1	300.2	1.8	328.6	2.2	1.819	0.014	0.654	1.68	4.87
M16-06	334.2	13.9	0.0	234.9	1.5	348.0	2.7	1.848	0.017	0.694	1.70	-
M16-01	343.3	8.9	0.0	193.7	1.5	268.4	2.6	1.753	0.021	0.704	1.64	-
Douglas Creek Member, Coyote Wash 1 core (40° 1' 22.224" N, 109° 18' 38.4834" W)												
CW1-36	1021.7	14.4	0.4	186.1	1.5	453.0	13.6	1.798	0.023	0.266	1.61	-
CW1-40*	1026.0	23.4	0.1	307.8	1.7	445.0	2.9	1.774	0.012	0.682	1.59	6.01
CW1-41*	1026.1	14.6	0.1	258.5	1.9	326.9	3.2	1.654	0.020	0.699	1.52	7.55
CW1-42*	1026.2	10.5	0.0	184.0	1.5	330.0	3.6	1.657	0.022	0.732	1.52	6.83
CW1-44*	1026.5	14.2	0.1	245.4	1.8	331.7	3.3	1.573	0.020	0.702	1.43	7.07
CW1-45*	1026.6	30.3	0.1	256.7	1.5	711.0	4.7	2.028	0.014	0.728	1.73	9.98
CW1-46*	1026.8	34.9	0.1	303.2	1.6	692.4	4.2	2.036	0.013	0.695	1.75	7.44
CW1-48*	1027.0	15.3	0.1	145.4	1.3	627.6	7.4	1.921	0.027	0.756	1.66	2.67
CW1-49*	1027.2	83.5	0.3	298.9	1.8	1830.5	11.1	2.889	0.018	0.712	2.13	7.85
CW1-50*	1027.4	46.6	0.2	412.1	3.8	675.1	7.6	1.963	0.032	0.635	1.68	15.46
CW1-51*	1027.5	11.5	0.0	114.3	1.1	600.3	8.2	1.936	0.030	0.807	1.69	4.97
CW1-53*	1027.7	17.7	0.1	180.5	1.4	584.4	5.9	1.960	0.023	0.751	1.72	-
CW1-54*	1027.8	39.1	0.1	346.0	1.9	674.9	4.1	1.956	0.013	0.645	1.67	24.70
CW1-55*	1028.0	33.8	0.1	385.3	2.1	519.5	3.1	1.879	0.012	0.635	1.66	16.92
CW1-62	1042.9	40.6	1.1	469.8	2.1	502.6	14.3	1.716	0.008	0.108	1.51	-
CW1-69	1045.8	1.1	0.0	65.1	0.6	98.6	3.3	1.606	0.025	0.339	1.57	-
Mahogany Zone, Coyote Wash 1 core (40° 1' 22.224" N, 109° 18' 38.4834" W)												
CW1-01	672.4	20.2	0.1	346.7	2.0	340.6	2.3	1.766	0.014	0.678	1.62	-
CW1-05*	682.5	15.2	0.1	294.0	2.3	301.1	3.2	1.716	0.022	0.719	1.59	11.28
CW1-06*	682.7	28.0	0.1	486.0	2.9	336.0	2.4	1.746	0.014	0.673	1.61	22.78
CW1-07*	682.8	25.5	0.1	464.1	2.8	320.2	2.3	1.730	0.014	0.673	1.60	22.59
CW1-09*	683.2	26.7	0.1	362.6	4.5	433.0	7.8	1.822	0.048	0.668	1.64	25.82
CW1-10*	683.4	20.8	0.1	383.2	3.0	316.4	3.2	1.735	0.022	0.698	1.60	14.47
CW1-12*	683.6	15.5	0.1	264.2	2.8	344.1	5.3	1.765	0.036	0.721	1.62	9.69
CW1-13*	683.7	15.6	0.1	295.3	2.4	307.1	3.4	1.737	0.023	0.717	1.61	9.39
CW1-14*	683.9	16.7	0.1	326.8	3.3	297.9	4.5	1.717	0.034	0.710	1.59	-
CW1-15*	684.3	11.8	0.0	198.4	2.2	349.0	5.8	1.768	0.037	0.742	1.62	10.30
CW1-16*	684.5	14.6	0.1	286.2	2.3	296.6	3.3	1.730	0.024	0.717	1.61	11.35
CW1-20*	684.9	32.7	0.1	426.9	5.3	451.2	8.5	1.837	0.048	0.684	1.65	28.15
CW1-22*	685.2	39.2	0.1	559.9	4.4	411.3	3.8	1.816	0.023	0.612	1.64	21.14
CW1-23*	685.4	20.1	0.1	366.4	3.2	320.1	3.7	1.737	0.026	0.704	1.60	-
CW1-27	696.8	11.2	0.0	214.0	1.6	304.4	3.1	1.713	0.021	0.716	1.59	-
CW1-31	706.8	33.1	0.1	331.7	1.8	593.2	3.6	1.913	0.013	0.688	1.67	-

[a] Rho is the associated error correlation at 2σ (Ludwig, 1980)

[b] $Os_g = {}^{187}Os/{}^{188}Os$ isotope ratio calculated at the time of oil generation (25 Ma)

* Sample data taken from Cumming et al., 2012.

All uncertainties are stated as 2 σ

3.3.2 Re-Os analysis

Re-Os isotopic analyses were carried out at Durham University's TOTAL Laboratory for Source Rock Geochronology and Geochemistry at the Northern Centre for Isotopic and Elemental Tracing (NCIET) using protocols outlined by Selby and Creaser (2003) and Selby et al. (2007). A known weight (100-200 mg) of oil-asphaltene, tar sands oil or gilsonite was digested in a carius tube with a known amount of ^{190}Os and ^{185}Re tracer solution (spike) and inverse *aqua-regia* (3 ml ~11N HCl and 8 ml ~15.5N HNO_3) at 220°C for 48 hrs. Inverse *aqua-regia* allows complete sample digestion of the hydrocarbons and ensures sample-spike equilibration. For source rock analyses, 200-500 mg of sample material is digested in 8 ml of Cr^{VI}-H_2SO_4 solution (made from 0.25 g of CrO_3 per 1 ml of 4N H_2SO_4), replacing the inverse *aqua-regia* as the digesting medium as the Cr^{VI}-H_2SO_4 solution preferentially liberates Re and Os from the organic matter in the source rocks (Selby and Creaser, 2003; Kendall et al., 2004; Rooney et al., 2011). The Re and Os were purified from the inverse *aqua-regia* and Cr^{VI}-H_2SO_4 solutions using Re anion exchange chromatography (HCl-HNO_3) and Os solvent extraction ($CHCl_3$) then micro–distillation, respectively. The purified Re and Os were loaded onto Ni and Pt filaments, respectively, and analysed for their isotopic compositions and abundances using ID-NTIMS (Creaser et al., 1991; Völkening et al., 1991; Walczyk et al., 1991; Selby and Creaser, 2003).

Uncertainties for $^{187}Re/^{188}Os$ and $^{187}Os/^{188}Os$ ratios and elemental abundances are determined by full error propagation of uncertainties in Re and Os mass spectrometer measurements, blank abundances and isotopic compositions, spike calibrations and reproducibility of standard Re and Os isotopic values. Total procedural blanks during this study were 2.9 ± 0.06 pg Re and 0.11 ± 0.02 pg Os (1 SD, n = 4, *aqua-regia*), and 14.6 ± 0.16 pg Re and 0.05 ± 0.01 pg Os (1 SD, n = 3, Cr^{VI}-H_2SO_4 solution). The blank $^{187}Os/^{188}Os$ isotopic composition for *aqua-regia* are 0.26 ± 0.01 (1 SD, n = 4) and 0.61 ± 0.03 (1 SD, n = 3) for the Cr^{VI}-H_2SO_4 solution. Throughout the period of this study, the NCIET Re standard produced average $^{185}Re/^{187}Re$ values of 0.598071 ± 0.001510 (1 S.D. n = 67). The measured difference between the $^{185}Re/^{187}Re$ values and

the accepted $^{185}Re/^{187}Re$ value (0.5974; Gramlich et al., 1973) is used to correct for sample mass fractionation. The average $^{187}Os/^{188}Os$ ratio of the Durham Romil Osmium Standard (DROsS) is 0.160892 ± 0.000559 (1 S.D. *n* = 67). These Re and Os standard values are indistinguishable from those reported in previous studies (Nowell et al., 2008; Finlay et al., 2012; Rooney et al., 2012).

The $^{187}Re/^{188}Os$ and $^{187}Os/^{188}Os$ values, their 2σ uncertainty and the associated error correlation (rho) were regressed using Isoplot (V. 4.15; Ludwig, 1980; Ludwig 2009) and the ^{187}Re decay constant ($\lambda^{187}Re = 1.666 \times 10^{-11} a^{-1}$; Smoliar et al., 1996). Source rock and oil $^{187}Os/^{188}Os$ compositions at the time of oil generation (Os_g) are calculated using the age of 25 Ma for oil generation (Ruble et al., 2001) and $\lambda^{187}Re$ (Smoliar et al., 1996).

3.3.3 Hydrous Pyrolysis Methodology

Gravel-sized (0.5 to 2.0 cm) rock fragments of samples from an 18-cm thick bed of the Mahogany Zone (~200 g; 930923-8) and a 4-cm thick bed of the black shale facies (~450 g; 930922-1) were matured at peak bitumen and peak petroleum generation by isothermal hydrous pyrolysis (Lewan, 1985; Ruble et al., 2001). The hydrous pyrolysis experiments were conducted in Hastelloy C-276 reactors with carburised surfaces. The Mahogany Zone and black shale facies rock fragments were immersed in 400 and 350 ml distilled water, respectively, which is sufficient to maintain a liquid water phase in contact with the rock fragments at the experimental temperatures. The reactors were sealed and filled with ~6.9 MPa of He and leak-checked using a thermal conductivity leak detector. Temperatures were monitored with Type J thermocouples, which are calibrated against national standards, and remain within ± 0.5°C of the desired temperature. Four hydrous pyrolysis experiments were carried out at 330°C and 360°C for 72 h for each sample. These temperatures were selected as they represent peak bitumen generation and peak oil generation of the Green River source rock samples (Ruble et al., 2001). These temperatures also

provide the best conditions to gain sufficient quantities of oil and bitumen for precise Re and Os isotopic analysis, requiring ~200 mg of oil or bitumen.

Once the experiments had cooled to room temperature, pressure and temperature values were recorded and a sample of head-space gas was collected in an evacuated 30 cm^3 stainless-steel cylinder. Any expelled oil generated in the experiments was collected in three steps: 1) the expelled oil was collected from the surface of the water in the reactor with a Pasteur pipette; 2) the water and minor remaining expelled oil were decanted into a glass separatory funnel allowing the separated oil to concentrate at the funnel stopcock, where it was collected with the same Pasteur pipette; 3) the thin film of expelled oil on the reactor walls, separatory funnel, and Pasteur pipette were rinsed with benzene at room temperature, which was then filtered through a 0.45 µm PTFE filter and concentrated by evaporation of the benzene under a fume hood. The expelled oil collected with a Pasteur pipette as described above, is called 'free oil', whereas expelled oil rinsed from the equipment with benzene is called 'equipment rinse'. The equipment rinse only represents the C_{15+} fraction of the free oil because the benzene evaporation loses the lighter ends of the oil. The free oil represents the full C_{5+} range. The decanted water was filtered through a 0.45 µm cellulose-acetate/nitrate filter. Rock fragments were removed from the reactor and dried at room temperature (~20°C) in a HEPA fume hood until their weight was constant within 0.1 g after 4 or more hours. These pyrolysed rock fragments are called 'recovered rock'. For clarity the term 'original rock' rock refers to the rock sample that has not experienced hydrous pyrolysis.

The soluble organic matter within organic-rich rocks (bitumen) was extracted from both the original rock and recovered rock samples (~100 g) using a Soxhlet apparatus for 24 hours with $CHCl_3$. The refluxed solvent was filtered through a 0.45 µm polytetrafluoroethylene (PTFE) filter and the bitumen was concentrated by rotary vacuum evaporation. The bitumen only represents the C_{15+} fraction because evaporation removes lighter fractions. This does not pose a problem for Re-Os analysis as Re and Os are held in the heavier fractions of hydrocarbons (>90% in the asphaltene

fraction; Selby et al., 2007). The extracted original and recovered rock was allowed to dry at room temperature (~20°C) in a HEPA fume hood until their weight was constant (<1% change). These are termed 'extracted rock' for Re-Os analysis. For asphaltene separation from the free oil, the method outlined in section 3.3.1.1 was used.

In this study Re-Os analyses following the method outlined in section 3.3.2 were conducted on the original rock, recovered rock, extracted rock, bitumen, free oil, equipment rinse and asphaltenes (extracted from the free oil where possible). Re-Os analysis using the Cr^{VI}-H_2SO_4 digestion method was conducted on an aliquot (~200 to 500 mg) of the powdered rock fragments (~50 g) of the original rock, recovered rock and extracted rock samples. The rock fragments were powdered using no metal contact. A 200 mg aliquot of the bitumen, free oil, equipment rinse and asphaltenes were digested using inverse *aqua-regia* for Re-Os analysis.

3.4 Results

3.4.1 Re-Os abundances and geochronology of the Green River hydrocarbons

The asphaltene of the oils contain 0.35 - 15.83 ng/g Re and 18.20 - 196.72 pg/g Os (Table 3.3), which is low in comparison to some oil asphaltenes that can reach up to 264 ng/g Re and 1443 pg/g Os (Selby et al., 2007). Using approximate asphaltene contents established through this study (Table 3.1) the Green River oil Re and Os abundances can be calculated on a whole oil basis giving approximately 0.03 - 2.93 ng/g Re and 0.87 - 36.39 pg/g Os (Table 3.3). Re-Os isotopic data are presented in Table 3.3 with results of geochronology presented in Table 3.4. The oil samples have $^{187}Re/^{188}Os$ ratios ranging from 70.3 to 472.6 and $^{187}Os/^{188}Os$ ratios from 1.466 to 1.863, with one outlier (2.141, sample GRB-824A). When all the oil samples are regressed they yield a Model 3 age of 45 ± 31 Ma (*n* = 14, Mean Squared Weighted Deviation [MSWD] = 2.2; Table 3.4 - Isochron 1). This age does not include outlier sample GRB-824A which is suggested to be derived from a different source facies to the other samples (see discussion). The uncertainty in the oil geochronology is

hampered by the low precision in the $^{187}Os/^{188}Os$ ratios because of the very low Os abundances, the associated blank correction and propagation of all uncertainties.

The oils extracted from the tar sands contain 1.50 - 65.15 ng/g Re and 38.28 - 342.24 pg/g Os (Table 3.3). The tar sands are more enriched than the Green River oils, most probably because the tar sands are more enriched in asphaltene where Re and Os are known to be held (Selby et al., 2007). The tar sands have $^{187}Re/^{188}Os$ ratios ranging from 69.4 to 506.4 and $^{187}Os/^{188}Os$ ratios from 1.447 to 1.939. Geochronology of all the tar sands yields a Model 3 age of 4 ± 28 Ma (*n* = 12, MSWD = 29; Table 3.4 - Isochron 2). This does not include the outlying sample, VC03-10, which is thought to be contaminated by oil from another source (see discussion).

The gilsonite samples are the most consistently enriched of the Green River hydrocarbons in Re and Os, with 9.47 - 51.33 ng/g and 221.76 - 849.01 pg/g, respectively. The gilsonite $^{187}Re/^{188}Os$ and $^{187}Os/^{188}Os$ ratios show limited variation in comparison to the oil and tar sand samples, ranging from 247.1 to 403.9 and 1.693 to 1.849, respectively. All the gilsonite samples yield a Model 3 age of 45 ± 42 Ma (*n* = 12, MSWD = 42; Table 3.4 - Isochron 3). The large uncertainty is attributed to the limited variation in $^{187}Re/^{188}Os$ and $^{187}Os/^{188}Os$ ratios.

Table 3.3: Re-Os isotope data for the Green River petroleum system hydrocarbons

Sample	Re (ng/g)	±	Os (pg/g)	±	$^{187}Re/^{188}Os$	±	$^{187}Os/^{188}Os$	±	rho [a]	Os_i [b]	Os_i [c]
Re-Os data for the Green River oils.											
GR2242A	0.61	0.03	49.51	1.77	70.3	6.2	1.466	0.164	0.555	1.44	1.44
GR2264A	0.97	0.03	26.04	0.93	211.4	18.9	1.527	0.142	0.818	1.44	1.46
GR2269A	0.78	0.03	30.97	0.94	144.8	11.0	1.588	0.125	0.746	1.44	1.54
GR2232A	0.35	0.03	18.63	0.76	106.9	13.5	1.485	0.157	0.697	1.44	1.45
GR2266A	0.38	0.03	18.20	0.84	119.8	16.7	1.504	0.180	0.734	1.45	1.47
GR2267A	1.20	0.03	45.14	1.21	152.7	9.6	1.565	0.110	0.738	1.50	1.52
GR2239A	2.09	0.03	73.87	1.72	163.4	7.9	1.630	0.100	0.721	1.56	1.58
GRB-3885A	1.33	0.03	47.61	1.22	160.7	9.2	1.643	0.110	0.735	1.58	1.59
GRB-1602A	3.05	0.03	144.82	3.16	121.2	5.1	1.629	0.094	0.702	1.58	1.59
GR2268A	0.86	0.04	18.19	0.96	275.5	37.8	1.715	0.236	0.893	1.60	1.63
GRB-827A	15.83	0.06	196.72	4.34	472.6	19.5	1.807	0.104	0.711	1.61	1.66
GR2114A	3.36	0.03	62.07	1.51	316.8	15.7	1.774	0.112	0.757	1.64	1.67
GRB-847A	2.33	0.04	80.17	1.99	169.9	9.0	1.748	0.113	0.733	1.68	1.69
GR2259A	1.62	0.04	48.19	1.38	199.0	12.9	1.863	0.139	0.765	1.78	1.80
GRB-824A	1.75	0.07	60.69	2.16	175.4	15.7	2.141	0.198	0.786	2.07	2.09
Re-Os data for the Green River tar sands											
VC03-10	65.15	0.21	95.89	0.95	4021.7	65.8	1.878	0.031	0.940	0.20	0.60
VC25-10	17.75	0.06	151.08	1.36	674.1	9.2	1.590	0.026	0.776	1.31	1.38
VC15-10	5.49	0.16	342.24	4.33	90.6	3.3	1.447	0.042	0.412	1.41	1.42
VC32-10	11.24	0.33	143.11	1.37	452.7	14.6	1.627	0.029	0.359	1.44	1.48
VC02-10	10.16	0.04	116.78	1.43	506.4	10.5	1.724	0.043	0.793	1.51	1.56
VC04-10	9.29	0.04	95.86	1.48	567.0	15.9	1.766	0.061	0.794	1.53	1.59
VC20-10	4.44	0.13	94.02	1.42	272.8	10.9	1.649	0.056	0.533	1.54	1.56
VC14-10	11.92	0.05	183.30	1.83	379.1	5.9	1.733	0.032	0.786	1.57	1.61
VC01-10	5.50	0.04	97.38	1.54	329.1	9.7	1.723	0.061	0.789	1.59	1.62
VC35-10	6.43	0.04	129.95	1.85	287.5	7.1	1.706	0.054	0.740	1.59	1.61
VC33-10	1.50	0.04	124.25	1.84	69.4	2.5	1.622	0.054	0.576	1.59	1.60
VC11-10	4.24	0.13	167.09	2.32	149.4	5.6	1.824	0.055	0.449	1.76	1.78
VC10-10	4.28	0.03	87.28	1.36	292.1	8.2	1.939	0.066	0.772	1.82	1.85
Re-Os data for the Green River gilsonite											
VC12-10	21.48	0.62	359.33	2.71	347.0	10.5	1.693	0.021	0.227	1.55	1.58
VC47-10	24.32	0.09	431.97	2.80	327.0	2.7	1.702	0.016	0.696	1.57	1.60
VC16-10	9.47	0.04	221.76	2.00	247.1	3.3	1.670	0.027	0.730	1.57	1.59
VC05-10	26.84	0.09	399.95	2.83	391.3	3.5	1.737	0.019	0.694	1.57	1.61
VC46-10	28.71	0.10	490.41	3.21	341.4	2.7	1.740	0.017	0.670	1.60	1.63
VC45-10	25.07	0.09	426.70	2.74	342.8	2.7	1.744	0.016	0.686	1.60	1.64
VC44-10	34.46	0.12	499.20	3.18	403.9	3.0	1.769	0.016	0.670	1.60	1.64
VC08-10	22.10	0.08	343.99	2.73	376.0	3.9	1.771	0.023	0.716	1.61	1.65
VC07-10	24.95	0.09	412.87	2.89	353.7	3.1	1.773	0.019	0.696	1.63	1.66
VC06-10	33.29	0.11	500.91	4.28	389.8	4.3	1.793	0.026	0.682	1.63	1.67
VC34-10	33.42	0.96	538.62	3.21	364.1	10.7	1.797	0.014	0.155	1.64	1.68
VC09-10	51.33	0.17	849.01	4.26	356.8	1.9	1.849	0.011	0.598	1.70	1.74

[a] Rho is the associated error correlation at 2σ (Ludwig, 1980)

[b] $Os_i = {}^{187}Os/{}^{188}Os$ isotope ratio calculated at 25 Ma

[c] $Os_i = {}^{187}Os/{}^{188}Os$ isotope ratio calculated at 19 Ma

All uncertainties are stated as 2 σ

Table 3.4: Re-Os geochronology results

No.	Description	*n*	Ma	±	MSWD	Model	Os_i	±	Samples
1	Oils	14	45	31	2.2	3	1.50	0.12	GR2242A, GR2264A, GR2269A, GR2232A, GR2266A, GR2267A, GR2239A, GRB-3885A, GRB-1602A, GR2268A, GRB-827A, GR2114A, GRB-847A, GR2259A
2	Tar sands	12	4	28	29	3	1.67	0.18	VC25-10, VC15-10, VC32-10, VC02-10, VC04-10, VC20-10, VC14-10, VC01-10, VC35-10, VC33-10, VC11-10, VC10-10
3	Gilsonite	12	45	42	42	3	1.49	0.25	VC05-10, VC06-10, VC07-10, VC08-10, VC09-10, VC12-10, VC34-10, VC16-10, VC44-10, VC45-10, VC46-10, VC47-10
4	All samples	38	19	14	30	3	1.61	0.08	GR2242A, GR2264A, GR2269A, GR2232A, GR2266A, GR2267A, GR2239A, GRB-3885A, GRB-1602A, GR2268A, GRB-827A, GR2114A, GRB-847A, GR2259A, VC25-10, VC15-10, VC32-10, VC02-10, VC04-10, VC20-10, VC14-10, VC01-10, VC35-10, VC33-10, VC11-10, VC10-10, VC05-10, VC06-10, VC07-10, VC08-10, VC09-10, VC12-10, VC34-10, VC16-10, VC44-10, VC45-10, VC46-10, VC47-10
5	All samples without gilsonite	26	15	17	14	3	1.60	0.09	GR2242A, GR2264A, GR2269A, GR2232A, GR2266A, GR2267A, GR2239A, GRB-3885A, GRB-1602A, GR2268A, GRB-827A, GR2114A, GRB-847A, GR2259A, VC25-10, VC15-10, VC32-10, VC02-10, VC04-10, VC20-10, VC14-10, VC01-10, VC35-10, VC33-10, VC11-10, VC10-10
6	Os_i = 1.40 -1.55	12	33	12	6.6	3	1.45	0.07	GR2242A, GR2264A, GR2269A, GR2232A, GR2266A, GR2267A, VC15-10, VC32-10, VC02-10, VC04-10, VC20-10, VC12-10
7	Os_i = 1.55 - 1.70	21	29.9	9.5	4.7	3	1.57	0.06	GR2239A, GRB-3885A, GRB-1602A, GR2268A, GRB-827A, GR2114A, GRB-847A, GR2259A, VC14-10, VC01-10, VC35-10, VC33-10, VC05-10, VC06-10, VC07-10, VC08-10, VC34-10, VC16-10, VC44-10, VC45-10, VC46-10, VC47-10
8	Os_i = 1.40 -1.55 without gilsonite	11	32	11	2.9	3	1.44	0.07	GR2242A, GR2264A, GR2269A, GR2232A, GR2266A, GR2267A, VC15-10, VC32-10, VC02-10, VC04-10, VC20-10
9	Os_i = 1.55 - 1.70 without gilsonite	11	22.6	9.6	0.53	1	1.60	0.05	GR2239A, GRB-3885A, GRB-1602A, GR2268A, GRB-827A, GR2114A, GRB-847A, GR2259A, VC14-10, VC01-10, VC35-10, VC33-10
10	Non-biodegraded oils (Os_i = 1.40 -1.55)	6	29	78	0.44	1	1.47	0.19	GR2242A, GR2264A, GR2269A, GR2232A, GR2266A, GR2267A
11	Non-biodegraded oils (Os_i = 1.55 -1.70)	5	25	23	0.92	1	1.62	0.12	GR2239A, GR2268A, GRB-827A, GR2114A, GRB-847A
12	Tar sands (Os_i = 1.55 - 1.70)	7	15.6	7.5	1.15	1	1.62	0.05	VC02-10, VC04-10, VC20-10, VC14-10, VC01-10, VC35-10, VC33-10
13	GRA hydrocarbons	22	15	20	16	3	1.60	0.11	GR2242A, GR2264A, GR2269A, GR2232A, GR2266A, GR2267A, GR2239A, GR2268A,GR2114A, GR2259A, VC25-10, VC15-10, VC32-10, VC02-10, VC04-10, VC20-10, VC14-10, VC01-10, VC35-10, VC33-10, VC11-10, VC10-10
14	GRB hydrocarbons	16	31	19	30	3	1.58	0.11	GRB-3885A, GRB-1602A, GRB-827A, GRB-847A, VC05-10, VC06-10, VC07-10, VC08-10, VC09-10, VC12-10, VC34-10, VC16-10, VC44-10, VC45-10, VC46-10, VC47-10

n = number of samples

The outliers GRB-824A and VC03-10 described in the text are not included in this table

Os_i is calculated at 25 Ma (see text)

3.4.2 Hydrous Pyrolysis results

The total recovery for each of the individual hydrous pyrolysis experiments is over 98%, indicating reliable closed system pyrolysis (see Table 3.5). All the experiments generated bitumen, oil and gas, with the largest amount of oil generated during the 360˚C (peak oil) experiments, and the largest amount of bitumen generated at the 330°C (peak bitumen) experiments (Table 3.6). These results support the findings of Ruble et al. (2001) and provide sufficient organic material for Re-Os analysis.

Table 3.5: Hydrous Pyrolysis conditions and details of yields

Sample and temperature (°C)	Rock at start (g)	Water in reactor (g)	Recovered rock (g)	Water recovered (g)	Generated Gas (g)	Expelled Oil (g)	Total Recovery (%)
M 930923-8, 330°C/72 hr	200.3	400.0	185.0	399.1	4.00	4.21	98.67
M 930923-8, 360°C/72 hr	200.0	400.6	168.1	399.5	7.10	18.08	98.70
BS 930922-1, 330°C/72 hr	450.1	350.5	435.7	344.0	4.50	4.02	98.45
BS 930922-1, 360°C/72 hr	450.4	350.2	421.8	348.8	6.90	14.03	98.87

Table 3.6: Organic phases recovered from the hydrous pyrolysis experiments

Sample and temperature (°C)	TOC (wt.%)	Bitumen (mg/g orig.TOC)	Expelled oil (mg/g orig.TOC)	Generated gas (mg/g orig.TOC)	Total (mg/g orig.TOC)
M 930923-8	15.23	157.24	-	-	-
M 930923-8, 330°C/72 hr	15.23	576.14	276.43	262.64	1115.20
M 930923-8, 360°C/72 hr	15.23	140.20	1186.93	466.19	1793.32
BS 930922-1	5.86	145.22	-	-	-
BS 930922-1, 330°C/72 hr	5.86	682.95	686.01	767.92	2136.87
BS 930922-1, 360°C/72 hr	5.86	276.43	2394.54	1177.47	3848.45

3.4.2.1 Re and Os abundances of hydrous pyrolysis products

Rhenium and Os abundance data from the hydrous pyrolysis experiments are reported as ng/g of original rock using the equation:

$$\{M_i\} = [(A_i * g_i)/1000]/G$$

where the subscript ‘i’ refers to the material, (original rock, recovered rock, extracted rock, bitumen, etc.) being analysed, A is abundance in ng/g, g is weight of material in grams and G is weight of starting rock in grams (Rooney et al., 2012). Presenting the data in this format allows mass balance calculations to evaluate Re and

Os abundances located in the various fractions and to more accurately interpret the transfer behaviour and mechanisms of Re and Os in the source rock and hydrocarbon system relative to each other. The abundance data are presented in Table 3.7 for all the experiments. The Re-Os isotopic compositions are reported in Table 3.8.

In both the Mahogany Zone and black shale facies, the Re and Os contents of original rock, recovered rock and extracted rock are similar (Table 3.7). Analysis of these sets of rock samples is conducted on an aliquot of powdered rock fragments (~50 g) that are randomly selected from a bag contain ~200 - 400 g of thumb sized rock chips. Over 20 g is powdered in order to obtain a homogenised representation of the Re-Os abundance and isotope composition of the rock sample (Kendall et al., 2009). The small variations in Re and Os abundances are attributed to minor differences of the randomly selected rock fragments used for each Re-Os analysis. The Re and Os abundances of the Mahogany Zone and black shale facies original rocks are 24.6 and 0.337 ng/g orig. rock, and 3.88 and 0.161 ng/g orig. rock respectively. For all the rock sample aliquots derived from the hydrous pyrolysis experiments the Re and Os abundances are within 10 – 15 % of the original rock value (Table 3.7).

The bitumen that has been extracted from the original rocks contain low Re and Os abundances of 0.284 and 0.003 ng/g orig. rock (Mahogany Zone), and 0.010 and 0.001 ng/g orig. rock (black shale facies), respectively. The 330°C experiment represents the peak bitumen generation. Extracted bitumen from the recovered Mahogany Zone rock contains 0.231 ng/g orig. rock Re and 0.018 ng/g orig. rock Os. In comparison the extracted bitumen from the black shale facies 330°C experiment contains less Re (0.138 ng/g orig. rock Re), and very small amounts of Os (0.008 ng/g orig. rock).

Table 3.7: Mahogany Zone and black shale facies Re and Os contents of original rock, recovered rock, extracted rock, bitumen, free oil and equipment rinse

	Mahogany 930923-8								Black Shale Facies 930922-1							
Fraction	Re (ng/g fraction)		Re	Re	Os (ng/g fraction)		Os	Os	Re (ng/g fraction)		Re	Re	Os (ng/g fraction)		Os	Os
	Mean	±	(ng/g orig rock)	D %*	Mean	±	(ng/g orig rock)	D %*	Mean	±	(ng/g orig rock)	D %*	Mean	±	(ng/g orig rock)	D %*
Original Rock																
Original Rock	24.61	0.09	24.609		0.337	0.002	0.337		3.88	0.02	3.876		0.161	0.002	0.161	
Extracted Rock	28.31	0.09	27.634		0.389	0.002	0.380		3.90	0.02	3.871		0.162	0.002	0.161	
Bitumen	11.86	0.05	0.284		0.119	0.001	0.003		1.12	0.03	0.010		0.107	0.001	0.001	
Total**			27.918	113.4			0.383	113.6			3.880	100.1			0.162	100.5
330°C for 72h																
Recovered Rock	24.30	0.08	22.442		0.387	0.002	0.357		3.17	0.02	3.071		0.152	0.002	0.147	
Free Oil	0.03	0.03	0.000		0.006	0.001	0.000		0.81	0.03	0.007		0.018	0.001	0.000	
Equipment Rinse	0.08	0.03	0.001		0.023	0.001	0.000		ND				ND			
Total***			22.443	91.2			0.357	106.1			3.078	79.4			0.147	91.3
Extracted Rock	26.55	0.09	22.191		0.394	0.002	0.330		3.14	0.02	2.912		0.147	0.002	0.136	
Bitumen	2.64	0.03	0.231		0.200	0.002	0.018		3.44	0.03	0.138		0.198	0.002	0.008	
Total**			22.423	99.9			0.347	97.2			3.050	99.3			0.144	98.1
360°C for 72h																
Recovered Rock	28.94	0.10	24.325		0.402	0.002	0.338		3.64	0.02	3.409		0.162	0.002	0.152	
Free Oil	0.05	0.03	0.004		0.002	0.001	0.000		0.11	0.03	0.002		0.003	0.001	0.000	
Equipment Rinse	0.03	0.03	0.000		0.011	0.001	0.000		0.02	0.03	0.000		0.007	0.001	0.000	
Total***			24.329	98.9			0.339	100.5			3.411	88.0			0.152	94.4
Extracted Rock	28.55	0.09	23.390		0.401	0.002	0.328		4.01	0.02	3.689		0.167	0.002	0.153	
Bitumen	0.03	0.03	0.001		0.003	0.001	0.000		0.03	0.03	0.000		0.009	0.001	0.000	
Total**			23.390	96.2			0.328	97.1			3.690	108.2			0.153	101.0

*DRe and DOs = Total metal (extracted rock + bitumen)/Revovered rock x 100 or Total metal (recov. rock + oil + equip. rinse)/original rock x 100

** Total = Extracted rock + Bitumen

*** Total = Recovered rock + Free Oil + Equipment Rinse

ND = Not Determined

During both 360°C experiments, which represent peak oil generation, most of the bitumen has been converted to oil. For both rock types the extracted bitumen contains only very minor Re and Os (<0.001 ng/g orig. rock). In both the Mahogany Zone and black shale facies experiments Re and Os increase by an order of magnitude from the original rock bitumen to the recovered rock bitumen (330°C experiment), although Re stays the same in the Mahogany Zone bitumen. However, in the bitumen extracted from the recovered rock in the 360°C experiments both decrease by two orders of magnitude from the 330°C experiment bitumen.

In all the experiments there is limited transfer of Re and Os to the free oil collected as well as the equipment rinse which incorporates the rest of the oil produced. Thus the change in Re and Os abundance for the bitumen from the original rock, the 330˚ and 360˚C experiments cannot be explained by transfer to the generated oil. The asphaltene extracted from the free oil of the 360°C experiments have also been analysed because this is the location of >90% of the Re and Os in oil and thus gives higher precision measurements. The asphaltenes contain 5.1 and 1.3 ng/g Re and 0.049 and 0.036 ng/g Os for the Mahogany Zone and black shale facies free oils, respectively. This suggests that there must at least be minor transfer to the free oil from the bitumen.

In the Mahogany Zone experiments the mass balance calculations show discrepancies within 10 %, suggesting only minor loss or addition of Re and Os during the experimental procedure. In the black shale facies experiments there are nearly 20% discrepancies in the mass balance for Re, particularly during the 330°C experiment. However, these discrepancies may only reflect variation in the aliquots used for analysis.

3.4.2.2 Re-Os isotopic data for the hydrous pyrolysis products

The $^{187}Re/^{188}Os$ and $^{187}Os/^{188}Os$ data are reported in Table 3.8 and Figure 3.3. Several of the bitumen Re-Os data have large uncertainties associated with them related to the small sample size and very low Re and Os abundances and the

associated propagation of blank uncertainties (Table 3.7). The free oil and equipment rinse ratios had almost 100% uncertainties due to the negligible contents and so are not reported. The $^{187}Re/^{188}Os$ and $^{187}Os/^{188}Os$ ratios in the original rock and extracted rock, and the recovered rock and extracted recovered rock from each experiment show no variation within uncertainty. The $^{187}Re/^{188}Os$ ratios, however, decrease from 427.4 (original) to 367.3 (330°C) and then increase again to 420.2 (360°C) in the Mahogany Zone (see Fig. 3.3). For the black shale facies a similar pattern occurs, decreasing from 138.8 (original) to 120.5 (330°C) and then increasing to 129.3 (360°C). The $^{187}Os/^{188}Os$ ratios remain similar throughout, at ~1.8 for the Mahogany Zone rocks and ~1.6 for the black shale facies.

Table 3.8: Mahogany Zone and black shale facies Re-Os isotopic compositions of original rock, recovered rock, extracted rock, bitumen, and asphaltene* fraction of the free oil

	Mahogany 930923-8				Black Shale Facies 930922-1			
Fraction	$^{187}Re/^{188}Os$		$^{187}Os/^{188}Os$		$^{187}Re/^{188}Os$		$^{187}Os/^{188}Os$	
	Mean	±	Mean	±	Mean	±	Mean	±
Original Rock	427.4	3.1	1.768	0.014	138.8	2.3	1.640	0.033
Extracted Rock	425.5	2.6	1.766	0.012	138.7	2.2	1.641	0.033
Bitumen	596.0	10.9	2.008	0.040	59.9	2.0	1.607	0.034
330°C for 72h								
Recovered Rock	367.3	2.1	1.761	0.011	120.5	2.1	1.631	0.033
Extracted Rock	393.7	2.4	1.761	0.012	123.3	2.1	1.630	0.034
Bitumen	77.2	1.3	1.765	0.026	99.8	1.5	1.615	0.024
360°C for 72h								
Recovered Rock	420.2	2.4	1.756	0.011	129.3	2.1	1.626	0.033
Extracted Rock	416.3	2.5	1.754	0.011	138.4	2.2	1.613	0.033
Bitumen	46.6	59.8	0.949	0.536	16.6	17.9	0.320	0.070
Asphaltene*	590.3	23.7	1.519	0.062	209.9	13.7	1.590	0.096

*asphaltenes contain 5.1 and 1.3 ng/g Re and 48.9 and 35.9 pg/g Os for the Mahogany Zone and black shale facies free oils, respectively

The bitumen from the original rock and 330 °C experiments show in all cases that the $^{187}Re/^{188}Os$ values decrease, apart from in the bitumen extracted from the original rock of the Mahogany Zone, where the values increase, from 427.4 to 596.0. For $^{187}Os/^{188}Os$ ratios of the bitumen, the values all stay the same at ~1.8 (Mahogany Zone) and ~1.6 (black shale facies), again apart from in the original rock of the Mahogany Zone, where the values are ~2.0. The Re-Os isotope compositions for bitumen for the 360°C experiments are not considered because the negligible

abundances in these fractions have led to large uncertainties. The asphaltenes derived from the free oil of the peak oil generation (360 °C) experiments, show an increase in $^{187}Re/^{188}Os$ values from the recovered rock and a minor decrease in the $^{187}Os/^{188}Os$ ratios in the Mahogany Zone to 1.5, but staying the same at ~1.6 for the black shale facies. Figure 3.3 illustrates that the hydrous pyrolysis experiments have a more significant effect on the Mahogany Zone with larger variations in $^{187}Re/^{188}Os$ values than the black shale facies and also some variation in $^{187}Os/^{188}Os$ ratios in the bitumen extracted from the original rock and the asphaltene extracted from the free oil of the peak oil 360°C experiment.

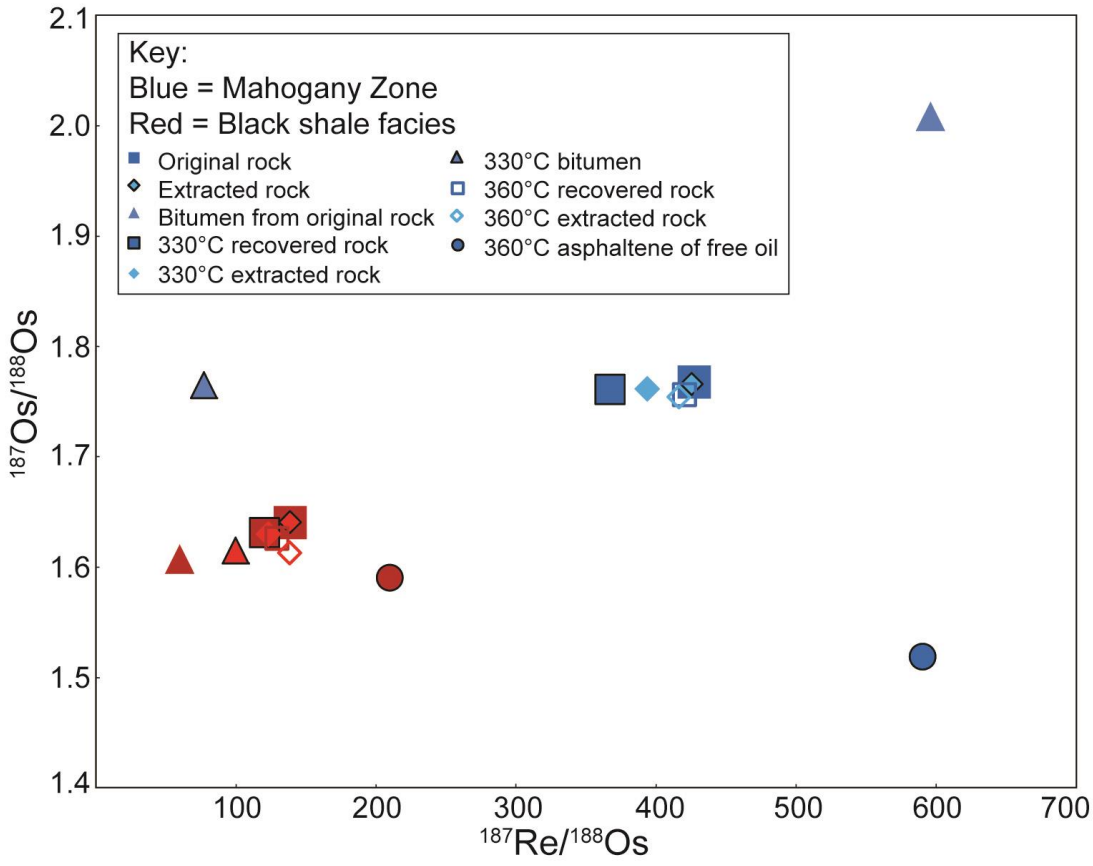

Figure 3.3: Re-Os isotopic data for the products derived from the hydrous pyrolysis experiments for both source units used. The Mahogany Zone (930923-8) is shown in blue and the black shale facies (930922-1) in red. Bitumen from the 360°C experiment is not plotted due to the large uncertainties derived from very low abundances of Re and Os in this bitumen.

3.5. Discussion

3.5.1 Dating hydrocarbon generation in the Green River petroleum system

Many petroleum systems, the Green River included, are complex and involve multi-stage/on-going generation from a number of source rock intervals, with resulting mixtures of oil of different ages or from different sources. If this is the case, care must be taken when interpreting Re-Os data for geochronology. In the Phosphoria petroleum system a complex charging history and events of mixing and re-migration are interpreted to cause scatter about the Re-Os isochron and uncertainty over what the age is recording (Lillis and Selby, in press). However, the UK Atlantic margin oils provide Re-Os geochronology in excellent agreement with oil generation models and Ar-Ar ages of feldspars containing oil inclusions (Finlay et al., 2011). In addition, Re-Os geochronology studies of the Western Canadian oil sands (Selby and Creaser, 2005a) and bitumen associated with the Polaris Mississippi Valley-type Zn-Pb deposit (Selby et al., 2005), have provided Re-Os geochronology in agreement with generation models, the latter also agreeing with an Rb-Sr sphalerite date of co-genetic mineralisation.

3.5.1.1 Previous generation models

The Uinta basin is currently an active petroleum system (Fouch et al., 1994; Ruble et al., 2001). Early oil generation models based on Rock-Eval pyrolysis kinetic parameters show oil generation beginning as early as 40 Ma in the lower Green River Formation, with the majority of generation in the Douglas Creek Member (containing the black shale facies) between 30 and 20 Ma, and then from 20 Ma to the present day the generation zone rises up section to the Mahogany Zone (Sweeney et al., 1987; Anders et al., 1992; Fouch et al., 1994). More recent hydrous pyrolysis kinetic models suggest oil generation began in the lower Green River Formation around 25 Ma, with generation moving up-section with time through the Douglas Creek Member, but unlikely to have allowed significant generation from the Mahogany Zone (middle Parachute Creek Member; Ruble et al., 2001). It is suggested that hydrous pyrolysis kinetic parameters for immiscible oil generation are generally consistent with

experimental and observed natural data (Ruble et al., 2001; Lewan and Ruble, 2002; Lewan and Roy, 2011). As the Green River petroleum system has on-going hydrocarbon generation (most reservoirs are overpressured), the reservoirs likely contain a mixture of oils from the Douglas Creek and Parachute Creek Members of the Green River Formation.

3.5.1.2 Re-Os hydrocarbon generation geochronology

Geochronology of all the hydrocarbon samples yields a Model 3 age of 19 ± 14 Ma (*n* = 38, MSWD = 30; Table 3.4, Isochron 4; Fig. 3.4A). This age broadly agrees with previous oil generation models, but most closely agrees with generation beginning at 25 Ma (Sweeney et al., 1987; Anders et al., 1992; Fouch et al., 1994; Ruble et al., 2001). Two samples (GRB-824A and VC03-10) have been excluded from all Re-Os geochronology calculations as they potentially represent contamination or a different source. This GRB-824A oil sample is derived from the Red Wash reservoir (Table 3.1), where the oil is thought to be derived from Paleocene to early Eocene source rocks dissimilar to the other Green River Formation source rocks (Picard, 1957; Anders et al., 1992). The VC03-10 tar sand sample has a drastically different $^{187}Re/^{188}Os$ ratio (4021.7) to the other samples and also a different Os_i of 0.20, which I suggest is due to contamination from another oil source. When each of the oils, tar sands and gilsonite are regressed separately they yield imprecise Model 3 ages with large MSWD's (Isochrons 1 to 3 - Table 3.4). A Model 3 age, large uncertainty and an MSWD much higher than 1 suggest scatter about the isochron is related to geological factors rather than purely analytical uncertainties (Ludwig, 2008). I suggest that this is due to the variation in Os_i of the oils and tar sand samples which could easily cause scatter as the isochron technique fundamentally requires samples to have the same Os_i but variable $^{187}Re/^{188}Os$ values (Cohen et al., 1999). It also requires samples to have been formed at the same time or generated at the same time and not to have undergone post-formational geochemical alteration (Lillis and Selby, in press). Thus the large uncertainty in the oil and tar sand ages may be caused by variation in the Os_i (1.44 – 1.78 and 1.31 – 1.82 at 25 Ma, for oils and tar sands respectively; Table 3.3) derived

from a mixture of oils from different sources and generated at different times. The variation in Os_i (1.61 - 1.76 at 25 Ma; Table 3.3) for the gilsonite is much lower than the tar sands or oils but the age is imprecise (93 % uncertainty). Considering the method and timing of emplacement is poorly constrained and the unusual nature of the gilsonite deposits, it is uncertain what may be the main control on the Re-Os system in gilsonite, however the large uncertainty could also be caused by the limited spread in $^{187}Re/^{188}Os$ ratios (~150 units). The tar sands are migrated deposits of the Green River oils (Fouch et al., 1994) and so they can be grouped together with the oils for Re-Os geochronology. Regression of all the samples without the gilsonite gives an age of 15 ± 17 Ma (*n* = 26, MSWD = 14; Table 3.4 - Isochron 5; Fig. 3.4B), however, the large range in Os_i still affects the precision of this age.

3.5.1.2.1 Re-Os geochronology based on Os_i composition

The variation in Os_i composition for all the samples can be plotted on a histogram showing the most common values (Fig. 3.5). When the Os_i values are calculated at 25 Ma to reflect the oil generation models distinct groups are evident. The histogram (Fig. 3.5) shows that the mode is at 1.6 and there are two smaller groups at 1.4 and 1.5. Calculation of the Os_i at 19 Ma reflecting the Re-Os age of all the hydrocarbons also yields groups, the mode at 1.6 and other groups at 1.5 and 1.7. Figure 3.5 demonstrates that the calculation at a younger age yields more radiogenic Os_i but similar groupings and so the age used for calculation of Os_i does not skew oil groupings. The different Os_i values are interpreted to reflect variation in Os composition of the Green River Formation source rock that is then transferred to the generated hydrocarbons. Plotting two groups for Re-Os geochronology would reflect geochronology of oils derived from different Green River Formation source units (see discussion section 3.5.2.2). Based on the Os_i calculated at 25 Ma, all the samples can be split into two distinct groups; the first with Os_i from 1.4 to 1.55 and the second from 1.55 to 1.70. The first group represents the two largest groups outside the mode and the second group incorporates the mode of the samples. All samples with Os_i from 1.40 to 1.55 yield an age of 33 ± 12 Ma (*n* = 12, MSWD = 6.6, Model 3; Table 3.4 -

Isochron 6; Fig. 3.4C) and samples with Os_i from 1.55 to 1.70 yield an age of 29.9 ± 9.5 Ma (*n* = 21, MSWD = 4.7, Model 3; Table 3.4 - Isochron 7). Separating the samples based on Os_i provides higher precision dates with lower MSWD's compared to the isochrons including samples with variable Os_i. Justification for this method comes from the fundamental aspect of Re-Os geochronology that requires samples to possess a common Os_i value to produce a precise isochron (York, 1969; Cohen et al., 1999; Kendall et al., 2009). Additionally, the variable Os_i suggests discrete source units produced the hydrocarbons (Selby et al., 2007; Finlay et al., 2011, 2012; Rooney et al., 2012; Lillis and Selby, in press). This approach can also be used for isochrons of all the samples without the gilsonite (Isochrons 8 and 9 - Table 3.4) as the gilsonite may have been generated by a different process at a different time (Tetting, 1984; Verbeek and Grout, 1992). This only significantly affects the 1.55 to 1.70 group as most of the gilsonite lies within this range. The Re-Os data give a Model 1 age of 22.6 ± 9.6 Ma (*n* = 11, MSWD = 0.53; Table 3.4 - Isochron 9; Fig. 3.4D) for the oils and tar sands. All the ages produced agree within uncertainty but this Model 1 age suggests any scatter is related to uncertainties in the analytical procedure rather than geological uncertainties. This age agrees well with the hydrous pyrolysis generation models of Ruble et al. (2001) and so suggests that the Re-Os geochronometer of petroleum records the timing of oil generation.

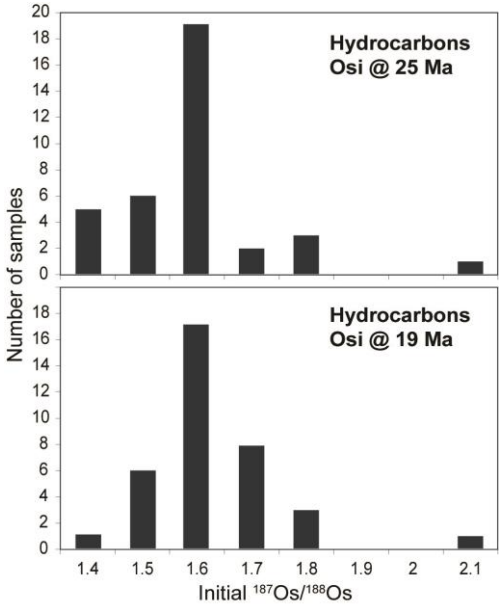

Figure 3.5: Histograms giving a visual impression of the distribution of Os_i data. Histograms for the hydrocarbons show Os_i calculated at 25 Ma and 19 Ma. Os_i calculation is based on the Re-Os isotopic data, the $\lambda^{187}Re$ of Smoliar et al. (1996) and age of hydrocarbon generation.

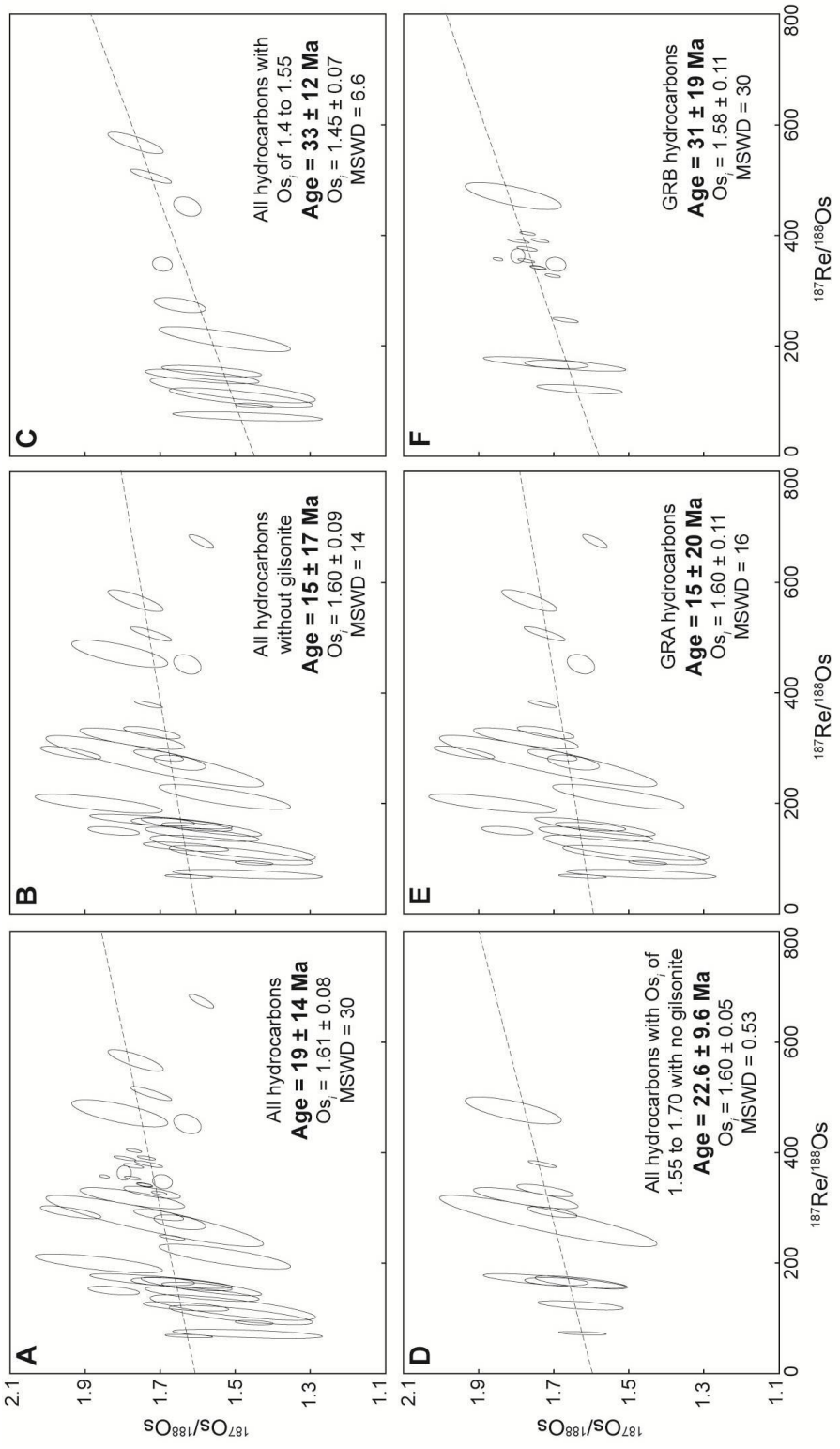

Figure 3.4: Re-Os isochrons for the Green River hydrocarbons, showing the age data derived. Uncertainty ellipses are 2σ. See Table 3.4 and text for further details. A = Isochron 4, B = Isochron 5, C = Isochron 6, D = Isochron 9, E = Isochron 13, F = Isochron 14 (Table 3.4).

3.5.1.2.2 Effects of biodegradation

The Os_i groupings can also be plotted for each of the oils and tar sands separately as this shows a distinction between biodegraded (tar sands; Isochron 12 - Table 3.4) and non-biodegraded (oils; Isochrons 10 and 11, Table 3.4) samples. Two oil samples, GRB-3885 and GRB-1602, show slight biodegradation (Table 3.1) and so are removed from the non-biodegraded oil isochrons. Isochrons 10, 11 and 12 (Table 3.4) give Model 1 ages, with low MSWD's that are within uncertainty of each other. The lack of precision on the oil isochrons is related to the uncertainty on the $^{187}Os/^{188}Os$ measurements that are challenging due to the low Os abundances, blank correction and propagation of all sources of uncertainty (Table 3.3). As the age for the tar sands (Isochron 12) that are all heavily biodegraded is similar to the Ruble et al. (2001) generation models (oil generation began in the lower Green River Formation at 25 Ma) and is within uncertainty of the other ages produced, it would suggest that biodegradation has not adversely affected the Re-Os systematics of Type I lacustrine kerogen derived hydrocarbons. This agrees with previous Re-Os studies that have proposed that the Re-Os isotope system is not adversely affected by biodegradation (Selby et al., 2005; Selby and Creaser, 2005a; Finlay et al., 2011; 2012).

3.5.1.2.3 Influence of the geochemical variability of the Green River hydrocarbons

Previous geochemical studies of the Green River oils have found distinct populations of oils based on geochemical heterogeneities (Lillis et al., 2003). The GRA oils have high wax content, a carbon preferential index less than 1.10, and low β-carotane content (Fig. 3.2; Lillis et al., 2003). The GRA oils are the most common type and make up most of the oil samples and all of the tar sand samples (n = 22; Table 3.1). This clarifies that the tar sands are migrated and biodegraded deposits of the Green River oils. The GRB oils, of which there are few samples (n = 5), are geochemically similar to gilsonite and generally have higher odd-carbon predominance (carbon preferential index greater than 1.2) and higher β-carotane content (Fig. 3.2; Lillis et al., 2003). Geochronology of these two subsets based on β-carotane content (Table 3.1)

provides ages in agreement with previous Re-Os geochronology (Isochrons 13 and 14 - Table 3.4; Fig. 3.4E,F), but does not provide distinct generation ages for these two subsets. This supports findings that suggest that the Green River hydrocarbons are geochemically more complex than two end-member hydrocarbon types which reflects complex spatial variation in the source rock (Ruble et al., 2001). This source rock variation is likely causing the large variation in Os_i and is the main reason for producing high uncertainties in the Re-Os geochronology as discussed in previous studies (Selby et al., 2005; Selby and Creaser, 2005a; Finlay et al., 2011).

Without considering Os_i the Re-Os geochronology derived from the Green River hydrocarbons broadly agrees with previous basin models (Fouch et al., 1994; Ruble et al., 2001). However, the geochronology is hampered by mixing of oils generated at different times and from different stratigraphic intervals of the Green River Formation and therefore containing variable Os_i as has been seen in previous studies (Lillis and Selby, in press). When taking the Os_i variation into account the precision of Re-Os geochronology improves. Regardless, this study suggests that Re-Os geochronology can be applied to Type I lacustrine kerogen derived hydrocarbons including oils and tar sands. Both oils and tar sands have previously been successfully dated using Re-Os in marine petroleum systems (Selby and Creaser, 2005a; Finlay et al., 2011). This study therefore widens the capabilities of Re-Os hydrocarbon geochronology beyond marine petroleum systems to lacustrine petroleum systems.

3.5.2 Os isotope oil to source rock correlation

3.5.2.1 Previous Green River petroleum system correlation studies

The source of the Green River petroleum system is known to be the Green River Formation. However this unit is over 3000 m thick in places and made up of several fluctuating-profundal organic rich-members interbedded with marginal fluvial sandstone deposits (Carroll and Bohacs, 2001; Keighley et al., 2003; Smith et al., 2008). Thus there is a large diversity of source rock facies available for hydrocarbon generation and the exact units within the Green River Formation that are generating

oil are ambiguous (Anders et al., 1992; Ruble et al., 2001). Oil-source rock correlation in these settings is complicated as multifaceted lacustrine facies can obscure maturity relationships usually distinguished by biomarkers (Ruble et al., 2001). However several correlation studies have been attempted (Tissot et al 1978; Anders et al., 1992; Hatcher et al., 1992; Ruble et al., 2001; Lillis et al., 2003). Source rock stratigraphy is said to control the composition of the oils and though the oil shales (e.g. the Mahogany Zone) are organic-rich, they are not considered the dominant source rock. A classic correlation study using biomarkers associated the oils with the basal Green River Formation (Tissot et al., 1978). Comparison of oils derived from hydrous pyrolysis experiments on units from the Uinta Basin with natural oils also found that the lower Green River Formation, namely the black shale facies (part of the Douglas Creek Member), to be the main source of oils generated in the Uinta Basin (Ruble et al., 2001). Most studies agree on the lower Green River Formation being the main source rock facies, but others do allude to the Mahogany Zone having generated oil based on Rock-Eval generation models (Fouch et al., 1994). While the oils and therefore the tar sands too, are sourced from predominantly the lower Green River Formation, gilsonite is sourced from the Mahogany Zone, this has been suggested based on infra-red spectra (Hunt et al., 1954), carbon isotopes (Schoell et al., 1994) and the observation that gilsonite veins are rooted in the Mahogany Zone beds (Verbeek and Grout, 1992). Other solid bitumen deposits are associated with different intervals of the Green River Formation and the depositional environment is thought to play a significant role in controlling what type of bitumen is produced (Hunt, 1963). Gilsonite is predominantly derived from an algal source consistent with high lake levels and organic production associated with the Mahogany Zone (Ruble et al., 1994; Schoell et al., 1994). Comparison of oil geochemical data with source rock geochemical data concluded that GRA hydrocarbons (most abundant oils and tar sands) are most likely derived from the black shale facies of the lower Douglas Creek Member whereas GRB hydrocarbons (some oils and all gilsonite) are derived from the Mahogany Zone (Lillis et al., 2003). However, even though these are still the main source units purported, it has also been

suggested that the Green River hydrocarbons reflect much more complex mixtures rather than two end-member types (Ruble et al., 2001).

3.5.2.2 Os isotope correlation

During hydrocarbon generation the Os isotopic composition of the source is transferred to the produced hydrocarbons (this study; Selby and Creaser, 2005a; Selby et al., 2005; Selby et al., 2007; Finlay et al., 2010, 2011, 2012; Rooney et al., 2012). This allows Os isotopes to be used as an oil source correlation tool. Oil-source fingerprinting using Os is based on the idea that the source $^{187}Os/^{188}Os$ composition at the time oil was generated (Os_g) will be transferred to the oil and hence the oils initial $^{187}Os/^{188}Os$ (Os_i) should have the same composition as the Os_g. Due to the lack of clarity in the Re-Os oil generation results, the age of oil generation is taken from most recent models which suggest it began at ~25 Ma, which is overlapped by the Re-Os ages produced in this study (Ruble et al., 2001). This age also represents an average age of generation from previous models (Fouch et al., 1994) and therefore is suggested to be the most accurate estimate of oil generation. The Os_g and Os_i are back calculated using the Re-Os isotopic compositions, the age of oil generation (25 Ma) and the ^{187}Re decay constant (Smoliar et al., 1996). The exact age of oil generation is not pertinent to oil-source correlation using Os as the Os_g and Os_i will generally co-vary when calculated with changing oil generation ages and so correlation will still be accurate (see Fig. 3.5). Comparison of the Os_i of the hydrocarbons to the Os_g of various source rocks gives the potential to fingerprint the source rock. For this study three Green River Formation source units from the Uinta Basin have been analysed as potential source rocks (Table 3.2; Cumming et al., 2012; Chapter 2). Two cores (CW1 and M16; Fig. 3.1) provide two sections of the lower Douglas Creek Member; one at the southwest edge of the basin and one in the central depocentre that has seen the most burial, and one section of the organic-rich oil shale the Mahogany Zone sampled from the central depocentre. The variation in the Os_g of the source is related to the Os_i of the sample originating from the composition of Os in the lake water column which is derived from weathering of the surrounding crust, the Re content of the sample and

the time since deposition (Cumming et al., 2012; Chapter 2). The large variation in Os_g of the source (1.43 to 2.13) highlights that varying Os isotopic compositions are passed onto the hydrocarbons and therefore make precise hydrocarbon geochronology challenging. Certainly with generation moving up-section, the hydrocarbons likely present a mixture of sources which would account for the large variation seen in Os_i, particularly in the oils (Os_i = 1.44 to 1.78) and tar sands (Os_i = 1.31 to 1.82). The lower variation in the gilsonite (Os_i = 1.61 to 1.76) compared to the oils and tar sands, may reflect one source rather than a potential mixture of oils/sources for the oils and tar sands. This supports the idea that gilsonite was generated quickly from one source (Hunt et al., 1963; Verbeek and Grout, 1992). Solid bitumen deposits such as gilsonite have not been assessed using Re-Os before and so the effects on Re-Os systematics of the process of solidification of the gilsonite are not known (Hunt et al., 1963; Tetting, 1984). Bitumen found in the Polaris Mississippi valley-type deposit was dated successfully using Re-Os (Selby et al., 2005), but this is interpreted to be a biodegraded residue of conventional crude oil (similar to the oil found in tar sands) rather than a solidified state (such as gilsonite).

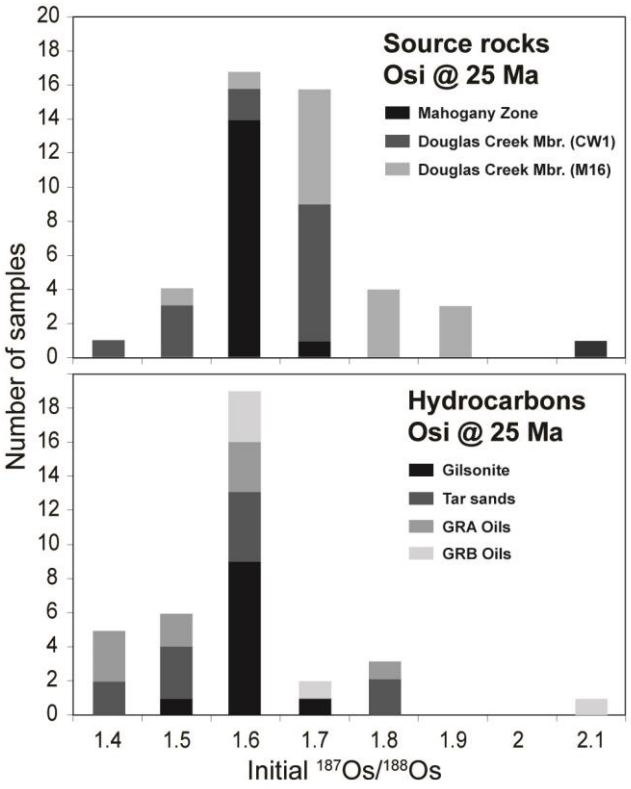

Figure 3.6: Os_i histograms for the hydrocarbons and source rocks calculated at 25 Ma. The different shades of grey (see key) show the different hydrocarbon types and different source rocks analysed. This gives an impression of which hydrocarbons were sourced from each unit sampled.

In order to analyse the Os_i and Os_g, histograms have been plotted of all the values for the source and for the hydrocarbons to deduce the modal values and link these to their respective sources, allowing the source rock to be identified. The spectrum seen on both the histograms illustrates the variation in the source rocks and hence the variation in the Os_i of the hydrocarbons that were generated. The source rocks show a majority of Os_g values around 1.6 and 1.7, with the hydrocarbon's mode at 1.6 (Fig. 3.6). However, there are smaller hydrocarbon groups at 1.4 and 1.5, with the group at ~1.4 not accounted for by the source rocks. This suggests that the three sampled units do not fully represent the Green River Formation units that are generating hydrocarbons in the Uinta Basin. When the hydrocarbons are analysed separately as oils, tar sands and gilsonite and the source rocks are separated into Douglas Creek Member (M16), Douglas Creek Member (CW1) and Mahogany Zone (CW1), a better appreciation of the Os composition of the sources and hydrocarbons is gained (Fig. 3.6). The gilsonite and the Mahogany Zone appear to dominate the 1.6 values in the two histograms, suggesting that Os fingerprinting supports the previously suggested notion that gilsonite is sourced from the Mahogany Zone (Hunt et al., 1954; Verbeek and Grout, 1992; Ruble et al., 1994; Schoell et al., 1994; Lillis et al., 2003). In addition, the GRB oils have an Os_i value of predominantly ~1.6, similar to the gilsonite and suggesting that they are both sourced from the Mahogany Zone as proposed by Lillis et al. (2003). This suggests that the Os correlation is supporting organic geochemical correlations using the biomarker β-carotane and odd-carbon predominance. The GRA oils and tar sands seem to dominate from 1.4 to 1.6. However, the other two source units dominate from 1.5 to 1.9, the Douglas Creek Member (M16), in particular, has values predominantly >1.7. This unit comes from the southwest corner of the basin where the units have not been buried sufficiently for oil generation, which is supported by the Os data suggesting that this unit has not generated any of the hydrocarbons sampled for this study. This suggests that lateral variation within source units can also affect the Os isotope composition. The other units are derived from the central depocentre where most of the hydrocarbon generation has occurred (Anders et al., 1992; Fouch et al., 1994). The exact source of

the GRA oils and tar sands is not conclusive from this study, but it would seem both the Douglas Creek Member (CW1) and the Mahogany Zone (CW1) are likely source units based on Os, or that the source may have originated in un-sampled strata between these two units. Based on previous studies, the GRA oils and tar sands should be sourced from the lower Green River Formation (Douglas Creek Member or black shale facies; Tissot et al., 1978; Fouch et al., 1994; Ruble et al., 2001; Lillis et al., 2003), however, they are geochemically complex rather than two end-member types and so the source rock may not be restricted to a specific interval. The Os data support this finding, therefore suggesting that Os isotopes provide a valuable means for oil-source correlation. The Os isotope fingerprinting tool may not be able to differentiate between complex lacustrine facies within the Green River Formation, but certainly the Os isotope composition is passed from source to hydrocarbons and can be used as a robust fingerprinting tool, despite biodegradation and unusual mechanisms of formation of solid bitumen (e.g. gilsonite).

3.5.3 Hydrous Pyrolysis insights into Re-Os systematics

3.5.3.1 Re-Os abundances and isotopic compositions of Hydrous Pyrolysis products

Hydrous pyrolysis has previously been used to assess Re and Os transfer to oils in Type II-S and Type III marine kerogens (Rooney et al., 2012). The findings from their study demonstrated that >95% of Re and Os remain within the extracted rock implying that thermal maturation at oil generative levels does not result in significant transfer of Re and Os into liquid organic phases and that the majority of Re and Os are complexed within the kerogen fraction of an organic-rich rock. Additionally, they found only minor variations in $^{187}Re/^{188}Os$ and $^{187}Os/^{188}Os$ ratios in the original rock, recovered rock and extracted rock from each experiment, suggesting that thermal maturation does not affect Re-Os systematics in organic-rich sediments of different maturities as seen in natural systems (Creaser et al., 2002; Kendall et al., 2004; Selby and Creaser, 2005b; Rooney et al., 2010). This study further corroborates these findings; only minor discrepancies in Re and Os abundances are recorded in the

original rock, recovered rock and extracted rock (Table 3.7) which are most probably due to natural variations seen in the different aliquots being used for analysis. This study also only sees <5% transfer of Re and Os into liquid organic phases from the source rock. The analysis of the extracted rock effectively represents analysis of the kerogen as the soluble bitumen has been removed and so the extracted rock contains only insoluble organic matter. Since the Re-Os digestion method preferentially digests organic matter only the kerogen will be analysed (Selby and Creaser, 2003; Kendall et al., 2004; Rooney et al., 2011). The finding that $^{187}Re/^{188}Os$ and $^{187}Os/^{188}Os$ ratios in the original rock and extracted rock, and the recovered rock and extracted rock from each experiment (Table 3.8) show only variations that are within uncertainty of each other provides evidence that Re and Os reside in the kerogen of a Type I lacustrine organic-rich rock and that maturation does not affect the systematics and abundances of Re and Os in these source rock types. This allows us to conclude that Re-Os geochronology of Type I lacustrine kerogen is not adversely affected by hydrocarbon maturation, just as is seen in marine kerogens (Creaser et al., 2002; Selby and Creaser, 2005a; Rooney et al., 2010, 2012; Cumming et al., 2012; Chapter 2).

The experimental conditions for the hydrous pyrolysis experiments undertaken in this study are based on a previous study on the same samples where a series of experiments allowed peak bitumen and peak oil generation to be deduced (Ruble et al., 2001). These temperatures of 330°C and 360°C, respectively, were employed in this study to enable assessment of Re and Os transfer and systematics at peak bitumen and peak oil generation for the two different Green River source rocks. In this study it is found that there is limited transfer of Re and Os to the free oil or bitumen during high temperature (360°C) hydrous pyrolysis experiments and also that there is limited transfer to the free oil during the 330°C experiment. This was also reported by Rooney et al. (2012) and it was suggested that the kinetic parameters fundamental for the transfer of Re and Os to oils are not achieved during hydrous pyrolysis experiments at the high temperatures and short durations employed. The peak bitumen 330°C experiments, however, do see transfer of Re and Os to the bitumen fraction. They

contain ~2 orders of magnitude less Re and Os than the source rock, but roughly two orders of magnitude more than the bitumen in the 360°C experiments and the free oils from both experiments (Table 3.7). Rooney et al. (2012) found that both Re and Os concentrations in bitumen increase with rising bitumen generation, until substantial oil generation occurs (>300°C) when the bitumen is thermally decomposing to oil and/or pyrobitumen. This study mimics these findings as in the peak oil generation experiments (360°C) there is limited Re and Os in the extracted bitumen. This suggests that the Re and Os in the bitumen could be assimilated into pyrobitumen by cross-linking reactions rather than transferring into the expelled oil during thermal cracking (Lewan, 1997; Rooney et al., 2012). This finding is also observed in V and Ni studies of hydrous pyrolysis products which found significant transfer to the bitumen but only minor amounts to the oils. The proportions of V to Ni stay the same indicating no preferential transfer of one element to another, suggesting they are bound in similar compounds (Lewan, 1980).

Assessment of $^{187}Re/^{188}Os$ and $^{187}Os/^{188}Os$ ratios in the rocks and extracted bitumens allow the relative systematics of Re and Os transfer to be assessed (Table 3.8; Fig. 3.3). Because of negligible abundances in the free oil these samples had large uncertainties (up to 100%) due to blank corrections and so are not reported. The $^{187}Re/^{188}Os$ ratios show slight variation from original rock to recovered rock in the 330°C experiment, but the $^{187}Os/^{188}Os$ ratios remain similar throughout, around 1.8 for the Mahogany Zone rocks and 1.6 for the black shale facies rocks. This suggests no appreciable disturbance to Os isotopic compositions in the rocks. In the naturally occurring bitumen extracted from the Mahogany Zone original rock both $^{187}Re/^{188}Os$ and $^{187}Os/^{188}Os$ ratios are higher than the original rock (427.4 to 596.0 and 1.768 to 2.008, respectively), which is not observed in the black shale facies experiment. Rooney et al. (2012) saw a large increase in the bitumen $^{187}Re/^{188}Os$ ratios (more than doubling) from the original rock and a slight increase in the $^{187}Os/^{188}Os$ ratios in hydrous pyrolysis experiments on the Phosphoria Formation. This was interpreted to be due to preferential transfer of Re over Os into the bitumen giving high $^{187}Re/^{188}Os$

ratios (Selby et al., 2005) which then allowed radiogenic ingrowth of Os over time. Due to the hydrous pyrolysis experiments being instantaneous on geological timescales, there is no radiogenic ingrowth of Os. As the Green River Formation is ~49 Ma (Smith et al., 2008; Cumming et al., 2012) there is also less time for ingrowth of radiogenic Os. The $^{187}Re/^{188}Os$ and $^{187}Os/^{188}Os$ for the Mahogany Zone natural bitumens follow this pattern, however in all other cases in the bitumen extracted from the original rock (black shale facies) and recovered rock (all 330 °C experiments), the $^{187}Re/^{188}Os$ values decrease and $^{187}Os/^{188}Os$ ratios all stay approximately the same at 1.8 (Mahogany Zone) and 1.6 (black shale facies). This may suggest that the natural bitumen extracted from the black shale facies has been generated very recently and so behaves similarly to an 'instantaneous' hydrous pyrolysis experiment giving minimal $^{187}Re/^{188}Os$ fractionation. As the Green River Formation sees on-going hydrocarbon generation it is certainly possible that the natural bitumens extracted from the original rocks have been generated relatively recently (Fouch et al., 1994; Ruble et al., 2001). Both samples have the same T_{max} values (438°C: Ruble et al., 2001), which is a measure of maturity and would suggest the samples are only moderately mature. The Mahogany Zone however has much higher TOC of 15.23 wt.% as opposed to 5.86 wt.% for the black shale facies (Table 3.6). It may be that variation in organic matter or levels of organic matter allowed the Mahogany Zone to have generated minor amounts of bitumen prior to the black shale facies. The black shale facies original rock contains much lower abundances of Re and Os in the bitumen than the Mahogany Zone original rock bitumen. This may suggest more recent bitumen generation has not allowed transfer of Re and Os to the bitumen. The bitumens from the 360 °C experiments have much lower $^{187}Re/^{188}Os$ and $^{187}Os/^{188}Os$ values than the other experiments (Table 3.8). The uncertainties are very large on very low abundances and so any interpretation must be made with caution, but the nominal values may suggest Re-Os fractionation during bitumen to oil cracking that hasn't gone to completion. The asphaltenes derived from the free oil of the peak oil generation (360 °C) experiments, show an increase in $^{187}Re/^{188}Os$ values from the recovered rock and a minor decrease in the $^{187}Os/^{188}Os$ ratios in the Mahogany Zone to 1.5, but staying the same at 1.6 for the black shale

facies. Overall, $^{187}Re/^{188}Os$ ratios tend to be decreasing in the bitumen relative to the original rock and then increasing slightly in the asphaltene of the expelled oil, which suggests some variation in the relative transfer of Re. The reason for the decrease in $^{187}Re/^{188}Os$ ratios may be that Re is more tightly bound in a Type I kerogen (compared to Type II-S and Type III; Rooney et al., 2012) and less is transferred to the bitumen during thermal cracking as evidenced by the low values in the $^{187}Re/^{188}Os$ bitumen. However, when the free oil is generated, there is enough temperature/pressure for Re to be transferred, hence the higher $^{187}Re/^{188}Os$ ratios in the asphaltene. On the other hand, $^{187}Os/^{188}Os$ ratios are very stable throughout thermal maturation, with the only exception of the asphaltene of Mahogany Zone free oil that reduces to 1.52 from 1.76. This may relate to the asphaltene extraction as incomplete extractions have previously been suggested to affect the Re-Os systematics in asphaltenes derived from artificial experiments (Reisberg et al., 2008). The similarity of Os compositions throughout thermal maturation is also found in Type II-S and Type III kerogens (Rooney et al., 2012) and confirms that Os can be a very useful correlation tool from oil to source as suggested in previous studies (Selby and Creaser, 2005a; Selby et al., 2007; Finlay et al., 2011, 2012; Rooney et al., 2012). The slight variation in both the $^{187}Re/^{188}Os$ and $^{187}Os/^{188}Os$ in the Mahogany Zone (Fig. 3.3) may suggest that the two source rocks contain different organic compounds where Re and Os are held, yielding different systematics, exemplified by their greatly different abundances of Re (24.61 and 3.88 ng/g for the Mahogany Zone and black shale facies, respectively) and Os (0.337 and 0.161 ng/g for the Mahogany Zone and black shale facies, respectively). The Mahogany Zone and black shale facies are known to be contain variation in their kerogen and were deposited under different conditions (Castle, 1990; Tuttle and Goldhaber, 1993; Ruble et al., 2001; Smith et al., 2008). The concentration of the precursors of the compounds responsible for chelating Re and Os may be different as a result of different depositional settings. Metal enrichment in sediments is a complex process where many variables are concerned, including sedimentation rate, type of organic matter and depth of the oxic-anoxic transition (Lewan and Maynard 1982; Selby et al., 2009; Rooney et al., 2012). The enigmatic chelating precursors of Re and Os may be

responsible for the different Re-Os systematics seen in the two source rock samples and exemplifies the need to identify the compounds containing Re-Os in order to better interpret both source rock and oil geochronology. Variation in $^{187}Re/^{188}Os$ could potentially suggest transfer of Re and Os at different rates and so they may not be held in the same compounds as V and Ni, which transfer proportionally (Lewan, 1980).

3.5.3.2 Comparison with the natural Green River petroleum system

Comparison of Re and Os abundances of the natural Green River petroleum system with the products derived from the hydrous pyrolysis experiments is illustrated in Figure 3.7. All of the samples from both natural and hydrous pyrolysis experiments plot along one trend. In the natural Green River petroleum system, there is a similar amount of variability in the Re and Os of the source as is seen in each of the derived hydrocarbons. The gilsonite contains an order of magnitude less Re and Os than the source rocks, with the tar sands and asphaltenes extracted from the oils containing another order of magnitude less. The whole oil abundances (based on asphaltene content) are approximately 4 orders of magnitude less than the source rock. The whole oil abundances are low because the asphaltene contents of these oils are generally very low (Table 3.1), perhaps because the majority of them show no biodegradation, which would normally enrich the asphaltene or because they are higher thermal maturity oils which decreases asphaltene contents (Milner et al., 1977). Thermal maturity of hydrocarbons in the Uinta Basin has been assessed in terms of vitrinite reflectance equivalent, with gilsonite having values of 0.5% R_m, tar sands <0.8% R_m and oils generally from 0.7 to 1.3 % R_m (Ander et al., 1992; Fouch et al., 1994). This shows that the oils are the most mature hydrocarbons produced and is reflected in their low asphaltene contents (Evans et al., 1971; Milner et al., 1977). Higher maturity oils would also have lower levels of NSO's and porphyrins, which may explain the low Re and Os abundances as Re and Os have been suggested to be held in these compounds (Miller, 2004; Selby et al., 2007; Rooney et al., 2012). The hydrocarbons with higher Re and Os abundances correlate with the higher asphaltene contents in the gilsonite and tar sands (Table 3.1), and also the GRB oils have higher Re and Os abundances and

asphaltene than the GRA oils. The GRB oils are thought to have been sourced from the Mahogany Zone, which would explain the lower maturity of the oils as the Mahogany Zone is higher in the section and so the GRB oils must have been generated more recently than the GRA oils (Fouch et al., 1994; Ruble et al., 2001; Lillis et al., 2003). The Mahogany Zone is also the most enriched source unit and so this suggests that Re and Os contents of the source directly affects how much is transferred to the hydrocarbons. Because Re and Os are predominantly held within the asphaltene fraction of hydrocarbons (Selby et al., 2007), the gilsonite and tar sands have higher Re and Os contents than the oils, most likely relative to their much higher asphaltene contents (Table 3.1). The gilsonite, like the GRB oils is said to be sourced from the Mahogany Zone and so the Re and Os contents that are up to an order of magnitude higher than the tar sands may be related to the higher Re and Os contents of the source, again showing proportionality in transfer from source to hydrocarbons.

There is limited transfer of Re and Os to expelled oils during experimental pyrolysis, a finding that has been noted in previous studies (Reisberg et al., 2008; Rooney et al., 2012). This study coupled with these previous studies, suggest that this is the case for Type I lacustrine, Type II, Type II-S and Type III kerogens. This is an unexpected experimental artefact in that natural crude oils derived from all these kerogen types contain Re and Os (Woodland et al., 2001; Selby and Creaser, 2005a; Selby et al., 2007; Finlay et al., 2010, 2011; Lillis and Selby, in press). However, when the Re and Os of the source rocks used for hydrous pyrolysis and the bitumen and free oil from the peak bitumen and peak oil experiments are plotted on Figure 3.7, there is a correlation with the natural Green River petroleum system. The pyrolyzed source rocks have similar abundance's to the range of source rocks sampled for analysis of the natural system, although are at the lower end of the scale. The peak bitumen generation Re and Os contents are similar to the lower abundance gilsonites and the higher abundance tar sands. This may suggest that the gilsonite is a similar hydrocarbon product to bitumen forming early at peak bitumen formation rather than during oil generation. Gilsonite has previously been suggested as an unusual early

expulsion product that is immature with thermal maturity equivalent to a vitrinite reflectance value of 0.5% R_m (Ander et al., 1992; Verbeek and Grout, 1992). The free oil from the peak oil experiments, interestingly, contains similar abundances to the lower abundance whole oils from the natural Green River petroleum system. This again reflects proportionality in transfer from the lower abundance sources to the free oil. These results suggest that the hydrous pyrolysis experiments are producing Re and Os abundances similar to the natural system and so may in fact be mimicking natural Re and Os transfer in a Type I lacustrine kerogen, unlike previous hydrous pyrolysis experiments (Rooney et al., 2012). This suggests that the kinetics achieved during hydrous pyrolysis of a Type I lacustrine kerogen allow Re and Os transfer and fractionation to occur in a similar fashion to natural Re and Os transfer.

In order to compare this with another system that has been assessed from a natural generation and hydrous pyrolysis generation perspective, data for the Phosphoria Formation petroleum system were plotted on Figure 3.7. The hydrous pyrolysis data are taken from Rooney et al. 2012 and the natural oil data are taken from Lillis and Selby (in press). The Phosphoria petroleum system shows a trend similar to the Green River petroleum system although with slightly more scatter. The Phosphoria source rock has Re and Os contents an order of magnitude higher than the Green River Formation. The natural oil asphaltenes are only an order of magnitude less than the Phosphoria source rock and the whole oils (based on asphaltene contents) are only again an order of magnitude less than the asphaltenes. This signifies that the Phosphoria whole oils are only two orders of magnitude less enriched in Re and Os than the source, compared to four orders of magnitude less for the Green River petroleum system. This suggests that the higher abundance source is delivering higher levels of Re and Os to the oils and the higher asphaltene contents of the oils (Lillis and Selby, in press) means that they are proportionally more enriched than the Green River natural oils, suggesting that source abundance and asphaltene content are controlling factors in Re and Os enrichment of hydrocarbons. The products from the Phosphoria hydrous pyrolysis experiments show that the peak bitumen Re and Os contents are

only slightly higher than the whole oils, compared to over an order of magnitude higher in the Green River Formation experiments. In stark contrast to the Green River Formation hydrous pyrolysis experiments, the Re and Os contents of the Phosphoria asphaltene from the free oil at peak oil generation has one to two orders of magnitude less Re and Os than most of the natural Phosphoria whole oils. The whole oil values for the free oil cannot be calculated as the asphaltene contents are not known and the whole free oil contained no measurable Re or Os. The hydrous pyrolysis asphaltene is almost three orders of magnitude lower than the natural oil asphaltenes in the Phosphoria system. This indicates completely different systematics in the Phosphoria system compared to the Green River petroleum system and suggests that kerogen type may play an important role in Re and Os transfer to hydrocarbons. It certainly indicates that the transfer seen in the Green River Formation hydrous pyrolysis experiments may be mimicking the kinetics achieved in the natural system, whereas the kinetics in the Phosphoria Formation hydrous pyrolysis experiments do not (Rooney et al., 2012). Although kerogen cracking may be different between the two types and certainly affects Re and Os transfer during hydrous pyrolysis experiments, the Re-Os isotopic compositions remain similar throughout both sets of experiments.

The similarity in $^{187}Os/^{188}Os$ compositions of the source rock and produced organic phases in the hydrous pyrolysis experiments provides strong support for $^{187}Os/^{188}Os$ compositions as an oil-source correlation tool as has been employed in the natural Green River petroleum system for this study. In the hydrous pyrolysis experiments the Mahogany Zone source rock has an $^{187}Os/^{188}Os$ composition of ~1.8 as does the produced bitumen (Fig. 3.3). In the black shale facies the $^{187}Os/^{188}Os$ composition is ~1.6, the same as the produced bitumen and asphaltene from the free oil (Fig. 3.3). The majority of Os compositions of the natural oils and sources is ~1.6, which is comparable to the hydrous pyrolysis experimental products. The similarity in compositions through the hydrous pyrolysis experiments shows that there is direct transfer of these isotopic compositions during oil generation and so the assumption that generated hydrocarbons will have the same Os isotopic composition as the source

at the time the hydrocarbons were generated is a correct assumption. This is strong evidence that the Os fingerprinting tool is robust and suggests that this tool can be successfully applied to multiple petroleum system types and with different hydrocarbons phases.

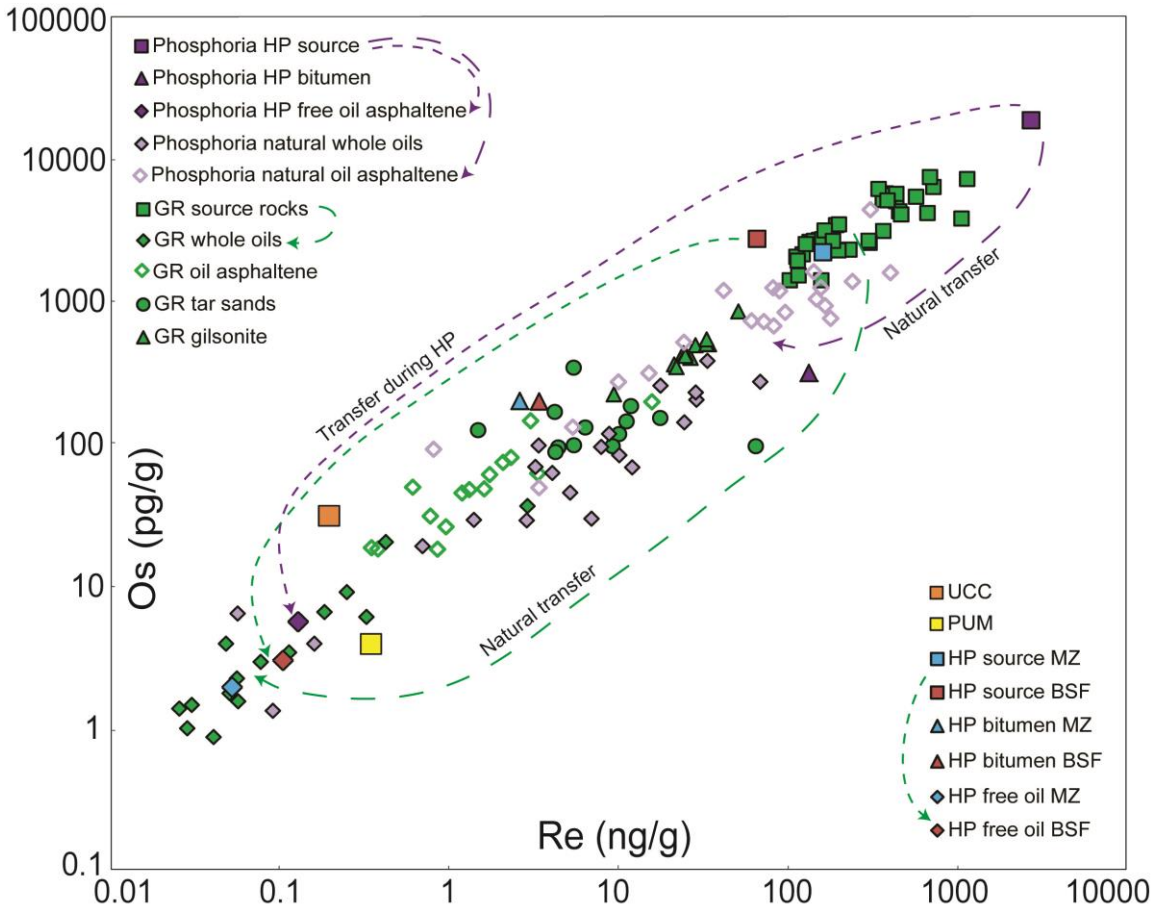

Figure 3.7: Log-log Re and Os abundance graph for the Green River and Phosphoria natural and hydrous pyrolysis systems. The Phosphoria natural data is taken from Lillis and Selby (in press) and the hydrous pyrolysis data is taken from Rooney et al. (2012). The Re and Os abundances of the source rocks are calculated on a TOC basis so as to see relative transfer from kerogen to hydrocarbons. The green arrows show approximate transfer from the source to the natural oils and the hydrous pyrolysis free oil for the Green River Formation. The purple arrows show approximate transfer from the source to the natural oil asphaltene and the hydrous pyrolysis free oil asphaltene for the Phosphoria Formation. Asphaltene is compared for the Phosphoria system as there are no

values for the free oil derived from hydrous pyrolysis experiments as the abundances were too low to measure (Rooney et al., 2012). The figure shows that the Green River hydrous pyrolysis experiments mimic the natural system much better than the Phosphoria system, which would be even more exaggerated if data for the Phosphoria free oil was able to be compared. See key for sample details. GR = Green River; HP = hydrous pyrolysis; MZ = Mahogany Zone; BSF = black shale facies; UCC = upper continental crust (Peucker-Ehrenbrink and Jahn, 2001); PUM = primitive upper mantle (Becker et al., 2006).

3.6. Conclusions

This study presents Re-Os geochronology of hydrocarbons derived from the Green River petroleum system that broadly agrees with previous petroleum generation basin models (Ruble et al., 2001). This suggests that Re-Os hydrocarbon generation geochronology can be applied to variable hydrocarbon phases (oils, tar sands and gilsonite) derived from lacustrine Type I kerogen just as successfully as when it is used in marine petroleum systems (Selby et al., 2005; Selby and Creaser, 2005a; Selby et al., 2007; Finlay et al., 2011). However, in this case of the Green River petroleum system, the young age and long-term oil generation possibilities make interpretation of Re-Os geochronology challenging. The large uncertainties (Table 3.4) produced for the hydrocarbon Re-Os geochronology are derived from variation in the Os_i of the Green River source rocks, which is transferred to the hydrocarbons during generation. This variation is due to it being a petroleum system with multiple generation events and multiple sources (within the ~3000 m thick Green River Formation; Fouch et al., 1994; Ruble et al., 2001) and therefore creating a mixture of Os isotope compositions in the produced hydrocarbons hampering Re-Os geochronology. When separating the samples based on Os_i, the precision of the geochronology increases as well as when separating them based on organic geochemical properties. The Green River oils also have very low Re and Os abundances which hampers precise determinations of isotope compositions, and reduces the

precision of Re-Os geochronology. A fundamental aspect of precise Re-Os hydrocarbon geochronology therefore requires samples with abundances at least above average upper continental crust (Fig. 3.7) in order to allow accurate analyses and also for samples to be sourced from a discrete source unit which would transfer similar Os isotopic compositions.

Oil to source fingerprinting using Os isotopes is also effective in lacustrine systems as exemplified by this study. The Os_i values of ~1.6 for the gilsonite and GRB oils deduces their source as the Mahogany Zone which has an Os_g value of ~1.6. The Os_i also suggests the lower Douglas Creek Member (CW1) as the most probable source of the GRA oils and tar sands. These Os isotope fingerprinting results are consistent with previous correlation studies in the Green River petroleum system. The Douglas Creek Member from the M16 core has Os_i higher than all the hydrocarbons (>1.7) and as it is from an area that is not buried sufficiently for oil generation, it is likely that this this unit has not generated oil. This illustrates the ability of Os isotopes to elucidate the spatial variations within a petroleum system.

Hydrous pyrolysis experiments on the Green River Formation source rocks show that Re and Os transfer are mimicking the natural system unlike a previous study on the Phosphoria (Type II-S) and Staffin (Type III) Formations (Rooney et al., 2012). This transfer from source to bitumen to oil does not affect source rock systematics or Os isotopic compositions. This confirms that Os isotope compositions are transferred intact from source to hydrocarbon during hydrocarbon generation and so can be used as a powerful correlation tool. In addition these experiments further confirm that Re-Os systematics in source rocks are not adversely affected by hydrocarbon maturation. Overall this study illustrates that the Re-Os hydrocarbon geochronometer and Os isotope fingerprinting tools can be used on a wide range of hydrocarbon phases sourced from variable kerogen types. Furthermore, hydrous pyrolysis experiments corroborate the findings from the natural system giving much stronger support for these tools.

3.7 References

Anders, D.E., Palacas, J.G., Johnson, R.C., 1992. Thermal maturity of rocks and hydrocarbon deposits, Uinta Basin, Utah. *In* Fouch, T.D., Nuccio, V.F., Chidsey, T.C., eds. Hydrocarbon and mineral resources of the Uinta basin, Utah and Colorado. Utah Geological Association Guidebook 20, 53-76.

Becker, H., Horan, M.F., Walker, R.J., Gao, S., Lorand, J.P., Rudnick, R.L., 2006. Highly siderophile element composition of the Earth's primitive upper mantle: Constraints from new data on peridotite massifs and xenoliths. Geochimica et Cosmochimica Acta 70, 4528-4550.

Bohacs, K.M., Carroll, A.R., Neal, J.E., Mankiewicz, P.J., 2000. Lake-basin type, source potential, and hydrocarbon character: an integrated sequence-stratigraphic-geochemical framework. Lake Basins through Space and Time: American Association of Petroleum Geologists, Studies in Geology 46, 3-34.

Bradley, W.H., 1931. Origin and microfossils of the oil shale of the Green River formation of Colorado and Utah. U.S. Geological Survey, Prof. Pap. 168, 58.

Bredehoeft, J., Wesley, J., Fouch, T., 1994. Simulations of the origin of fluid pressure, fracture generation, and the movement of fluids in the Uinta Basin, Utah. AAPG Bulletin 78, 1729-1747.

Carroll, A.R., Bohacs, K.M., 1999. Stratigraphic classification of ancient lakes: Balancing tectonic and climatic controls. Geology 27, 99-102.

Carroll, A.R., Bohacs, K.M., 2001. Lake-Type Controls on Petroleum Source Rock Potential in Nonmarine Basins. AAPG Bulletin 85, 1033-1053.

Cashion, W.B., 1967. Geology and fuel resources of the Green River Formation, southeastern Uinta basin, Utah and Colorado. US, Geological Survey, Prof. Pap. 548.

Castle, J.W., 1990. Sedimentation in Eocene Lake Uinta (Lower Green River Formation), Northeastern Uinta Basin, Utah. AAPG Tulsa.

Cohen, A.S., Coe, A.L., Bartlett, J.M., Hawkesworth, C.J., 1999. Precise Re-Os ages of organic-rich mudrocks and the Os isotope composition of Jurassic seawater. Earth and Planetary Science Letters 167, 159-173.

Creaser, R.A., Papanastassiou, D.A., Wasserburg, G.J., 1991. Negative thermal ion mass spectrometry of osmium, rhenium and iridium. Geochimica et Cosmochimica et Acta 55, 397-401.

Creaser, R.A., Sannigrahi, P., Chacko, T., Selby, D., 2002. Further evaluation of the Re-Os geochronometer in organic-rich sedimentary rocks: A test of hydrocarbon maturation effects in the Exshaw Formation, Western Canada Sedimentary Basin. Geochimica et Cosmochimica Acta 66, 3441-3452.

Cumming, V.M., Selby, D., Lillis, P.G., 2012. Re–Os geochronology of the lacustrine Green River Formation: Insights into direct depositional dating of lacustrine successions, Re–Os systematics and paleocontinental weathering. Earth and Planetary Science Letters 359–360, 194-205.

Dyni, J.R., 2006. Geology and Resources of Some World Oil-Shale Deposits. U.S. Geological Survey Scientific Investigations Report 2005–5294.

Evans, C.R., Rogers, M.A., Bailey, N.J.L., 1971. Evolution and alteration of petroleum in western Canada. Chemical Geology 8, 147-170.

Finlay, A.J., Selby, D., Osborne, M.J., 2011. Re-Os geochronology and fingerprinting of United Kingdom Atlantic margin oil: Temporal implications for regional petroleum systems. Geology 39, 475-478.

Finlay, A.J., Selby, D., Osborne, M.J., 2012. Petroleum source rock identification of United Kingdom Atlantic Margin oil fields and the Western Canadian Oil Sands using Platinum, Palladium, Osmium and Rhenium: Implications for global petroleum systems. Earth and Planetary Science Letters 313–314, 95-104.

Finlay, A.J., Selby, D., Osborne, M.J., Finucane, D., 2010. Fault-charged mantle-fluid contamination of United Kingdom North Sea oils: Insights from Re-Os isotopes. Geology 38, 979-982.

Fouch, T.D., Nuccio, V., Anders, D., Rice, D., Pitman, J., Mast, R., 1994. Green River (!) petroleum system, Uinta Basin, Utah, USA. AAPG Memoir 60, 399.

Gramlich, J.W., Murphy, T.J., Garner, E.L., Shields, W.R., 1973. Absolute isotopic abundance ratio and atomic weight of a reference sample of rhenium. Journal of research of the National Bureau of Standards 77A, 691-698.

Hatcher, H.J., Meuzelaar, H.L.C., Urban, D.T., 1992. A comparison of biomarkers in gilsonite, oil shale, tar sand and petroleum from Threemile Canyon and adjacent areas in the Uinta Basin, Utah. *In* Fouch, T.D., Nuccio, V.F., Chidsey, T.C., eds. Hydrocarbon and mineral resources of the Uinta basin, Utah and Colorado. Utah Geological Association Guidebook 20, 271-287.

Hunt, J.M., 1963. Composition and origin of the Uinta Basin bitumens. *In* Crawford, A.L., ed. The oil and gas possibilities of Utah, re-evaluated. Utah Geological and Mineralogical Survey Bulletin 54, 249-276.

Hunt, J.M., Stewart, F., Dickey, P.A., 1954. Origin of hydrocarbons of Uinta basin, Utah. AAPG Bulletin 38, 1671-1698.

Johnson, S.Y., 1992. Phanerozoic evolution of sedimentary basins in the Uinta-Piceance Basin region, northwestern Colorado and northeastern Utah. U.S. Geological Survey Bulletin 1787-FF.

Katz, B.J., 1995. The Green River Shale: an Eocene Carbonate Lacustrine Source Rock. *In* Katz, B.J., ed. Petroleum Source Rocks. Springer-Verlag, 309-324.

Keighley, D., Flint, S., Howell, J., Moscariello, A., 2003. Sequence Stratigraphy in Lacustrine Basins: A Model for Part of the Green River Formation (Eocene), Southwest Uinta Basin, Utah, U.S.A. Journal of Sedimentary Research 73, 987-1006.

Kendall, B., Creaser, R.A., Selby, D., 2009. ^{187}Re-^{187}Os geochronology of Precambrian organic-rich sedimentary rocks. Geological Society, London, Special Publications 326, 85-107.

Kendall, B.S., Creaser, R.A., Ross, G.M., Selby, D., 2004. Constraints on the timing of Marinoan "Snowball Earth" glaciation by Re-187-Os-187 dating of a Neoproterozoic, post-glacial black shale in Western Canada. Earth and Planetary Science Letters 222, 729-740.

Klemme, H., Ulmishek, G.F., 1991. Effective petroleum source rocks of the world: stratigraphic distribution and controlling depositional factors (1). AAPG Bulletin 75, 1809-1851.

Lewan, M., 1985. Evaluation of petroleum generation by hydrous pyrolysis experimentation. Philosophical Transactions of the Royal Society of London. Series A 315, 123-134.

Lewan, M.D., 1980. Geochemistry of vanadium and nickel in organic matter of sedimentary rocks. PhD Thesis, University of Cincinnati.

Lewan, M.D., 1997. Experiments on the role of water in petroleum formation. Geochimica et Cosmochimica Acta 61, 3691-3723.

Lewan, M.D., Maynard, J.B., 1982. Factors controlling enrichment of vanadium and nickel in the bitumen of organic sedimentary rocks. Geochimica et Cosmochimica Acta 46, 2547-2560.

Lewan, M.D., Roy, S., 2011. Role of water in hydrocarbon generation from Type-I kerogen in Mahogany oil shale of the Green River Formation. Organic Geochemistry 42, 31-41.

Lewan, M.D., Ruble, T.E., 2002. Comparison of petroleum generation kinetics by isothermal hydrous and nonisothermal open-system pyrolysis. Organic Geochemistry 33, 1457-1475.

Lillis, P.G., Selby, D., Evaluation of the rhenium-osmium geochronometer in the Phosphoria petroleum system, Bighorn Basin of Wyoming and Montana, USA. Geochimica et Cosmochimica. In press.

Lillis, P.G., Warden, A., King, J.D., Nuccio, V.F., Roberts, L.N.R., Dubiel, R., 2003. Petroleum Systems and Geologic Assessment of Oil and Gas in the Uinta-Piceance Province, Utah and Colorado. US Department of the Interior, US Geological Survey.

Ludwig, K., 2008. Isoplot version 4.15: a geochronological toolkit for microsoft Excel. Berkeley Geochronology Center, Special Publication No. 4.

Ludwig, K.R., 1980. Calculation of uncertainties of U-Pb isotope data. Earth and Planetary Science Letters 46, 212-220.

Miller, C.A., 2004. Re-Os dating of algal laminites: reduction-enrichment of metals in the sedimentary environment and evidence for new geoprphyrins. PhD Thesis, University of Saskatchewan.

Milner, C.W.D., Rogers, M.A., Evans, C.R., 1977. Petroleum transformations in reservoirs. Journal of Geochemical Exploration 7, 101-153.

Nowell, G.M., Luguet, A., Pearson, D.G., Horstwood, M.S.A., 2008. Precise and accurate $^{186}Os/^{188}Os$ and $^{187}Os/^{188}Os$ measurements by multi-collector plasma ionisation mass spectrometry (MC-ICP-MS) part I: Solution analyses. Chemical Geology 248, 363-393.

Peters, K.E., Walters, C., Moldowan, J., 2005. The Biomarker Guide: Volume 2, Biomarkers and Isotopes in Petroleum Systems and Earth History. Cambridge University Press, UK.

Peucker-Ehrenbrink, B., Jahn, B., 2001. Rhenium-osmium isotope systematics and platinum group element concentrations: Loess and the upper continental crust. Geochem. Geophys. Geosyst. 2, 22.

Picard, M.D., 1957. Red Wash-Walker Hollow Field, Stratigraphic Trap, Eastern Uinta Basin, Utah. AAPG Bulletin 41, 923-936.

Pietras, J.T., Carroll, A.R., 2006. High-Resolution Stratigraphy of an Underfilled Lake Basin: Wilkins Peak Member, Eocene Green River Formation, Wyoming, U.S.A. Journal of Sedimentary Research 76, 1197-1214.

Reisberg, L., Michels, R., Hautevelle, Y., 2008. Re/Os fractionation during generation and evolution of hydrocarbons. Geochimica et Cosmochimica Acta Supplement 72, 786.

Remy, R.R., 1992. Stratigraphy of the Eocene Part of the Green River Formation in the South-Central Part of the Uinta Basin, Utah. U.S. Geological Survey Bulletin 1787-BB.

Rooney, A.D., Chew, D.M., Selby, D., 2011. Re-Os geochronology of the Neoproterozoic-Cambrian Dalradian Supergroup of Scotland and Ireland: Implications for Neoproterozoic stratigraphy, glaciations and Re-Os systematics. Precambrian Research 185, 202-214.

Rooney, A.D., Selby, D., Houzay, J.-P., Renne, P.R., 2010. Re-Os geochronology of a Mesoproterozoic sedimentary succession, Taoudeni basin, Mauritania: Implications for basin-wide correlations and Re-Os organic-rich sediments systematics. Earth and Planetary Science Letters 289, 486-496.

Rooney, A.D., Selby, D., Lewan, M.D., Lillis, P.G., Houzay, J.-P., 2012. Evaluating Re–Os systematics in organic-rich sedimentary rocks in response to petroleum generation using hydrous pyrolysis experiments. Geochimica et Cosmochimica Acta 77, 275-291.

Ruble, T., Philp, R., 1991. Organic geochemical characterization of native bitumens from the Uinta Basin, Utah, USA. Organic Geochemistry: Advances and Applications in the Natural Environment, 97.

Ruble, T.E., Bakel, A.J., Philp, R.P., 1994. Compound-specific isotopic variability in Uinta Basin native bitumens - paleoenvironmental implications Organic Geochemistry 21, 661-671.

Ruble, T.E., Lewan, M.D., Philp, R.P., 2001. New Insights on the Green River Petroleum System in the Uinta Basin from Hydrous Pyrolysis Experiments. AAPG Bulletin 85, 1333-1371.

Schoell, M., Hwang, R.J., Carlson, R.M.K., Welton, J.E., 1994. Carbon isotopic composition of individual biomarkers in gilsonites (Utah). Organic Geochemistry 21, 673-683.

Selby, D., Creaser, R.A., 2003. Re-Os geochronology of organic rich sediments: an evaluation of organic matter analysis methods. Chemical Geology 200, 225-240.

Selby, D., Creaser, R.A., 2005a. Direct radiometric dating of hydrocarbon deposits using rhenium-osmium isotopes. Science 308, 1293-1295.

Selby, D., Creaser, R.A., 2005b. Direct radiometric dating of the Devonian-Mississippian time-scale boundary using the Re-Os black shale geochronometer. Geology 33, 545-548.

Selby, D., Creaser, R.A., Dewing, K., Fowler, M., 2005. Evaluation of bitumen as a Re-187-Os-187 geochronometer for hydrocarbon maturation and migration: A test

case from the Polaris MVT deposit, Canada. Earth and Planetary Science Letters 235, 1-15.

Selby, D., Creaser, R.A., Fowler, M.G., 2007. Re-Os elemental and isotopic systematics in crude oils. Geochimica et Cosmochimica Acta 71, 378-386.

Selby, D., Mutterlose, J., Condon, D.J., 2009. U-Pb and Re-Os geochronology of the Aptian/Albian and Cenomanian/Turonian stage boundaries: Implications for timescale calibration, osmium isotope seawater composition and Re-Os systematics in organic-rich sediments. Chemical Geology 265, 394-409.

Smith, M.E., Carroll, A.R., Singer, B.S., 2008. Synoptic reconstruction of a major ancient lake system: Eocene Green River Formation, western United States. Geological Society of America Bulletin 120, 54-84.

Smith, M.E., Chamberlain, K.R., Singer, B.S., Carroll, A.R., 2010. Eocene clocks agree: Coeval $^{40}Ar/^{39}Ar$, U-Pb, and astronomical ages from the Green River Formation. Geology 38, 527-530.

Smoliar, M.I., Walker, R.J., Morgan, J.W., 1996. Re-Os isotope constraints on the age of Group IIA, IIIA, IVA, and IVB iron meteorites. Science 271, 1099-1102.

Sweeney, J., Burnham, A., Braun, R., 1987. A Model of Hydrocarbon generation from type I kerogen: application to Uinta basin, Utah. AAPG Bulletin 71, 967-985.

Tetting, T.N., 1984. Origin of gilsonite fractures in the Uinta Basin, Utah. AAPG Bulletin 68, 951-952.

Tissot, B., Deroo, G., Hood, A., 1978. Geochemical study of the Uinta Basin: formation of petroleum from the Green River formation. Geochimica et Cosmochimica Acta 42, 1469-1485.

Tuttle, M.L., Goldhaber, M.B., 1993. Sedimentary sulfur geochemistry of the Paleogene Green River Formation, western USA: Implications for interpreting depositional and diagenetic processes in saline alkaline lakes. Geochimica et Cosmochimica Acta 57, 3023-3039.

Vandenbroucke, M., Largeau, C., 2007. Kerogen origin, evolution and structure. Organic Geochemistry 38, 719-833.

Verbeek, E.R., Grout, M.A., 1992. Structural evolution of gilsonite dikes, eastern Uinta Basin, Utah. U.S. Geological Survey Bulletin 1787-HH.

Völkening, J., Walczyk, T., G. Heumann, K., 1991. Osmium isotope ratio determinations by negative thermal ionization mass spectrometry. International Journal of Mass Spectrometry and Ion Processes 105, 147-159.

Walczyk, T., Hebeda, E., Heumann, K., 1991. Osmium isotope ratio measurements by negative thermal ionization mass spectrometry (NTI-MS). Fresenius J. Anal. Chem. 341, 537-541.

Woodland, S., Ottley, C., Pearson, D., Swarbrick, R., 2001. Microwave digestion of oils for analysis of platinum group and rare earth elements by ICP-MS. Special Publications of the Royal Society of Chemistry 267, 17-24.

Xu, G.P., Hannah, J.L., Stein, H.J., Bingen, B., Yang, G., Zimmerman, A., Weitschat, W., Mork, A., Weiss, H.M., 2009. Re-Os geochronology of Arctic black shales to evaluate the Anisian-Ladinian boundary and global faunal correlations. Earth and Planetary Science Letters 288, 581-587.

York, D., 1969. Least-squares fitting of a straight line with correlated arrors. Earth and Planetary Science Letters 5, 320-324.

Chapter 4

Re-Os geochronology of the lacustrine Nonesuch Formation

Anoxia in the terrestrial environment during the late Mesoproterozoic

A version of this chapter is in press at *Geology* (accepted 11-12-12); co-authored by Simon W. Poulton of Leeds University, Alan D. Rooney of Harvard University and David Selby of Durham University. See Appendix B.

4.1 Introduction

Recent reconstructions suggest that the global ocean remained anoxic between Earth's two major periods of rising atmospheric oxygen at either end of the Proterozoic Eon (2500 – 542 Ma). In detail, sulphidic water column conditions were prevalent along productive continental margins, overlying ferruginous deeper waters that contained dissolved Fe (Canfield et al., 2008; Poulton et al., 2010; Poulton and Canfield, 2011; Planavsky et al., 2011). However, in contrast to these advances in our understanding of the evolution of mid-Proterozoic ocean chemistry, much less is known about oxygenation of terrestrial aquatic environments during this period.

Recently, the determination of sulphur isotope fractionations between sulphate and sulphide ($\delta^{34}S$) of >50‰ in lacustrine sediments from the Mesoproterozoic Torridon and Stoer Groups of NW Scotland, were interpreted to suggest that oxygenation of terrestrial aquatic environments preceded oxygenation of the oceans (Parnell et al., 2010). Such fractionations are generally considered to require an active oxidative sulphur cycle driven by disproportionation reactions involving sulphide-oxidising bacteria, and are interpreted to reflect a major rise in oxygen in the late Neoproterozoic (Canfield and Teske, 1996). If correct, this suggests that, unlike the marine realm, late Mesoproterozoic terrestrial aquatic environments were sufficiently oxidized to support a complex biota adapted to an oxygen-rich atmosphere (Parnell et al., 2010). However, $\delta^{34}S$ fractionations of 60 – 70‰ have recently been measured in an anoxic, low sulphate lake in the absence of oxidative sulphur cycling (Canfield et al., 2010). This builds upon theoretical calculations of the magnitude of fractionation possible by bacterial sulphate reduction alone (Brunner and Bernasconi, 2005), and is supported by direct measurements of fractionations obtained during growth of a pure culture of bacterial sulphate reducers (Sim et al., 2011).

Considering the evolutionary significance of possible early oxygenation of terrestrial environments, coupled with these recent developments in our

understanding of sulphur isotope fractionation, a more direct assessment of the redox state of the terrestrial realm during the late Mesoproterozoic is clearly warranted. This study focusses on the Nonesuch Formation, deposited within the ~1100 Ma intracratonic Mid-Continent Rift System of central North America (Ojakangas et al., 2001). Like the Torridon Group of NW Scotland, the Nonesuch Formation contains a rich record of eukaryotic life (Pratt et al., 1991; Strother and Wellman, 2010) and thus represents an ideal locality to assess possible links to early terrestrial oxygenation. To evaluate this system, Fe-S-C systematics are utilised to assess water column redox conditions, coupled with Re-Os geochronology to provide a depositional age for the Nonesuch Formation, and Os isotope systematics to yield insight into the nature of the depositional setting.

4.2 Geological setting

4.2.1 Stratigraphy and sedimentology

The Mesoproterozoic Nonesuch Formation was deposited in the intracratonic Mid-Continent Rift System of central North America which reached >2000 km in length, with extension of <100 km due to rift failure as a result of the onset of the Grenvillian Orogeny to the east (Ojakangas et al., 2001). In the Lake Superior region, ~30 km of volcanic and sedimentary rift-fill sequences make up the Keweenawan Supergroup, which comprises 20 km of predominantly flood basalts overlain by post-rift fluvial and alluvial red beds of the Oronto and Bayfield Groups (Ojakangas et al., 2001; Fig. 4.1). The Oronto Group consists of fluvial and alluvial volcaniclastics, with the exception of the Nonesuch Formation, a 40 to 200 m thick succession of organic-rich grey to black siltstones and shales. Overlying the Oronto Group, the Bayfield Group is predominantly made up of fluvial and alluvial sandstones. Lacustrine and marginal lacustrine facies assemblages have been documented in the Nonesuch Formation (Elmore et al., 1989). The lacustrine assemblage consists of laminated dark shales, siltstones and minor carbonate laminites, and suggests deposition in a progressively shallowing perennial lake (Elmore et al., 1989). Bacterial and algal

organic matter accumulated in the lacustrine facies with seasonal carbonate laminites that are a product of precipitation of calcite through intense planktonic blooms (Elmore et al., 1989; Imbus et al., 1992). These carbonate laminations are interbedded with siltstone, mudstone and shale facies. The marginal lacustrine facies contains interbedded lithic sandstones, siltstones and mudstones and also sandstone-shale couplets interpreted to have been deposited on a sandflat-mudflat (Elmore et al., 1989).

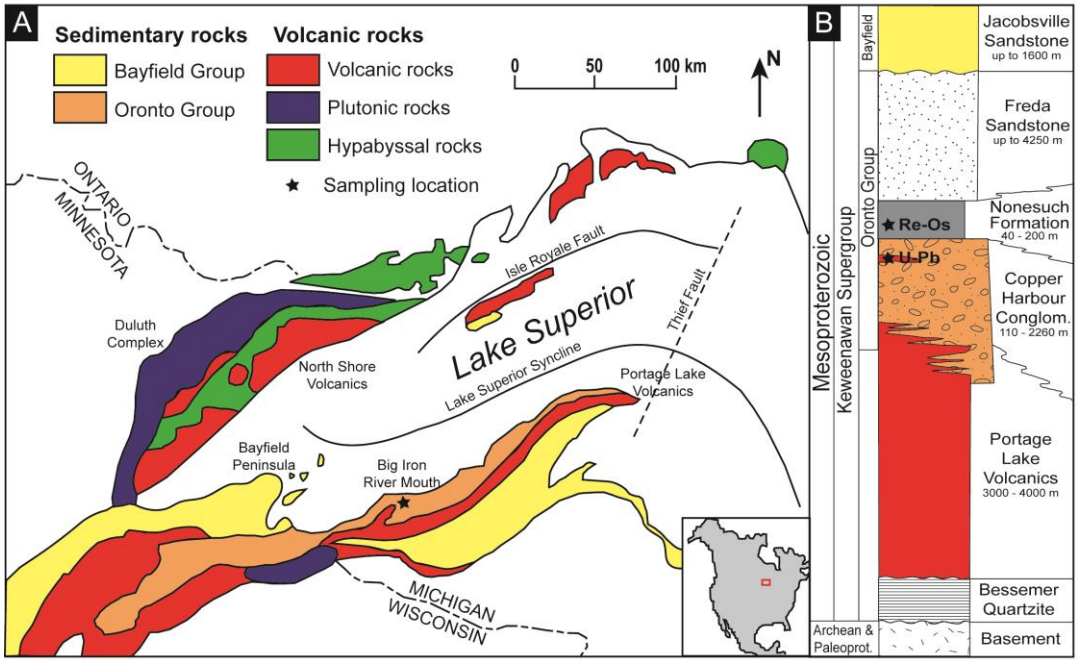

Figure 4.1: A. Geological map of the Lake Superior region showing the location of the main Keweenawan Supergroup units. The Nonesuch Formation is situated between continental red-beds of the Copper Harbour Conglomerate and the Freda Sandstone and now outcrops on the southern shores of Lake Superior. B. Schematic stratigraphy of the Keweenawan Supergroup, showing depth variations for each unit. Locations of the Re-Os (1078 ± 24 Ma; this study) and U-Pb (1087.2 ± 1.6 Ma; Davis and Paces, 1990) ages are labelled. Figures adapted from Elmore et al. (1989) and Ojakangas et al. (2001).

4.2.2 Current geochronology

Geochronological constraints of the Keweenawan Supergroup are derived from U-Pb zircon ages of rift-related volcanics (Davis and Paces, 1990). An existing LA-ICP-

MS U-Pb age of 1087.2 ± 1.6 Ma (2σ, including decay constant uncertainty) from zircons in one of the final andesite flows within the Copper Harbour Conglomerate (underlying the Nonesuch Formation; Fig. 4.1) provides a maximum age for the Nonesuch Formation. However, this old U-Pb geochronology does not provide any constraints for the post-rift sedimentary units. The Re-Os geochronometer is a widely used tool for dating marine organic-rich sedimentary rocks and has recently been successfully applied to lacustrine organic-rich sedimentary rocks (Cumming et al., 2012; Chapter 2), making it an ideal tool to attempt to further constrain the age of the Nonesuch Formation.

4.2.3 Lacustrine versus marine depositional setting

Sedimentological characteristics of the Nonesuch Formation (section 4.2.1) and proximity to continental red-beds, coupled with paleogeographic reconstructions suggesting that the nearest coastline was ~800 km away, indicate that the Nonesuch Formation was likely deposited in a lacustrine environment (Elmore et al., 1989; Imbus et al., 1992; Ojakangas et al., 2001). However, a marine embayment or estuarine environment has also been suggested based on the presence of specific biomarkers and S/C ratios (Pratt et al., 1991; Hieshima and Pratt, 1991). Biomarkers extracted from the Nonesuch Formation include low levels of 24-*n*-propylcholestane (Pratt et al., 1991), which is commonly, but not uniquely, found in rocks of Phanerozoic marine origin (Moldowan et al., 1990) and may in fact relate to the presence of eukaryotic organisms in the Nonesuch Formation. Thus, the presence of 24-*n*-propylcholestane at low concentration does not unambiguously denote a marine depositional setting for the Nonesuch Formation.

Enrichments in S/C ratios have previously been interpreted to reflect deposition of the Nonesuch Formation under sulphate-rich marine conditions (Fig. 4.2; Hieshima and Pratt, 1991; Imbus et al., 1992). However, enhanced fixation of sulphide as a result of the absence of bioturbation in the Precambrian and (potentially) non-Fe limited conditions during ferruginous deposition, combined with differences in the

metabolisability of Precambrian organic matter, could readily lead to the observed enrichments in sulphur and decoupling between sulphur and carbon under lacustrine conditions (e.g., Raiswell and Canfield, 2012).

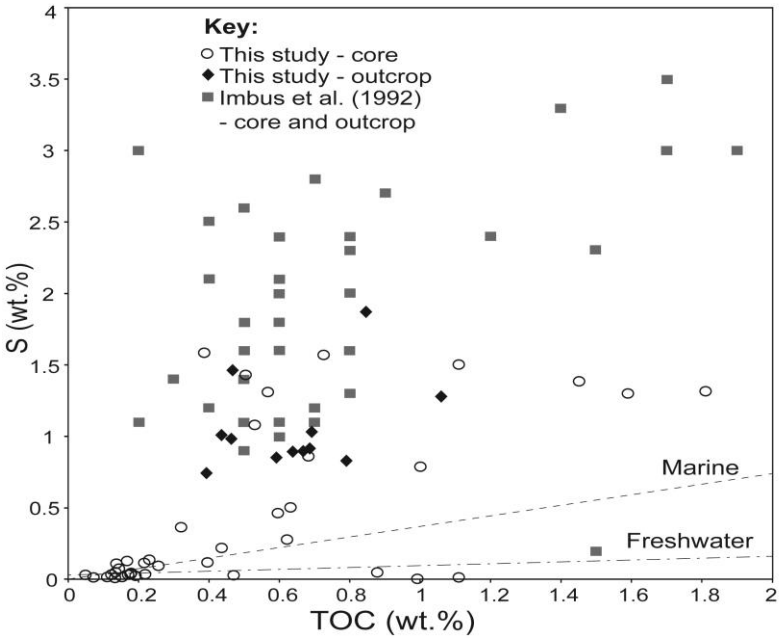

Figure 4.2: Compilation of new and old S/C data for core and outcrop samples. The marine and freshwater lines denote typical trends for sediments deposited in modern depositional settings (Berner and Raiswell, 1983).

4.3 Sampling and analytical methodology

4.3.1 Sampling

The sampled units consist of the lacustrine facies assemblages that have been documented in the Nonesuch Formation (Elmore et al., 1989). These assemblages consist of laminated dark shales, siltstones and minor seasonal carbonate laminites, and suggest deposition in a progressively shallowing perennial lake (Elmore et al., 1989; Imbus et al., 1992).

Samples for Re-Os geochronology were collected from outcrop of the Nonesuch Formation at Bonanza Falls (46°49’15.74 N, 89°34’21.69 W) along the Big Iron River near White Pine, Michigan. The Nonesuch Formation is exposed here almost

continuously in a low angle southeast-dipping section along the river for ~200 m (Suszek, 1997). Upper and lower contacts are not directly exposed. There is a predominance of fine-grained siltstones and fine sandstones in coarsening upward sequences. The lower section of the Nonesuch Formation contains finely-laminated organic-rich siltstones and shales that were sampled ~30-40 m above the Copper Harbour Conglomerate. Samples of ~100 g were taken at 1 m intervals for 12 m along a horizontal bed ~20 cm thick trending NE-SW (NS1 begins in the SW). Further sampling at 50 cm intervals between the NS1 samples provided an NS2 sample set. Outcrop samples in excess of 100 g were cut to remove any weathered material from the surface and polished to remove any metal contamination from the rock saw. Several samples were large enough (>150 g) to sub-divide into multiple parts which are regarded as individual samples e.g., A, B and C and do not refer to repeats. All samples were air-dried at 60 °C for 24 h before crushing to a powder (~30 µm) using a zirconium dish in a shatterbox which avoids metal contact. More than 30 g of sample was powdered to homogenize any Re and Os heterogeneity within the sample (Kendall et al., 2009a).

Samples for Fe speciation and S isotopes were collected from drill core PI-1 (drilled by the Bear Creek Mining Company) located in western Michigan near the shores of Lake Superior, west of the Big Iron River. Core PI-1 has a nearly complete section of the Nonesuch Formation including upper and lower contacts (Pratt et al., 1991). Sampling encompasses the entire Nonesuch Formation starting at the contact with the Copper Harbour Conglomerate at 109.42 m, and including seasonal carbonate laminites in some samples. Samples of ~20 g were taken every ~2 to 3 m until a depth 51.21 m.

The Nonesuch Formation contains copper mineralisation at its base in the White Pine mine area, associated with faults (Mauk and Hieshima, 1992). In order to avoid sampling any mineralised zones, the White Pine mine area and heavily faulted beds were avoided. The Cu contents of the samples were also analysed (Table 4.2) in order to rule out any influence from the fluid flow driving Cu mineralisation.

Mineralised zones of the Nonesuch Formation can contain ~11 wt.% Cu (Mauk and Hieshima, 1992). The samples for this study all contain less than 200 ppm Cu apart from three samples near the base of the core (PI-1) that contain ~5000 ppm. These three samples were sampled from the transition between the Copper Harbour Conglomerate and the Nonesuch Formation and have not been used for interpretation purposes as they may have been affected by mineralisation.

4.3.2 Re-Os analytical methodology

The Re and Os isotopic abundances and compositions were determined at Durham University's TOTAL laboratory for source rock geochronology and geochemistry at the Northern Centre for Isotopic and Elemental Tracing (NCIET) following methodology outlined by Selby and Creaser (2003) and Selby (2007). Between 1 g and 1.2 g of sample was digested and equilibrated in 10 ml of Cr^{VI}-H_2SO_4 together with a mixed tracer (spike) solution of ^{190}Os and ^{185}Re in carius tubes at 220 °C for 48 hours. The Cr^{VI}-H_2SO_4 digestion method was employed as it has been shown to preferentially liberate hydrogenous Re and Os thus yielding more accurate and precise age determinations (Selby and Creaser, 2003; Kendall et al., 2004; Rooney et al., 2011). Rhenium was purified using anion column chromatography and Os using solvent extraction ($CHCl_3$) and micro-distillation techniques. Purified Re and Os were loaded onto Ni and Pt filaments, respectively and analysed using negative thermal ionisation mass spectrometry (NTIMS; Selby and Creaser, 2003 and references therein). During this study adjustments were made to the Re purification methodology, whereby reduction of Cr^{6+} to Cr^{3+} through the SO_2 gas procedure was replaced by reduction in 5 N NaOH and transfer to Acetone prior to column chromatography. This also removed the requirement of a single bead clean-up step (c.f., Selby and Creaser, 2003). Isotopic measurements were performed using a ThermoElectron TRITON mass spectrometer with static Faraday collection for Re and ion-counting using a secondary electron multiplier in peak-hopping mode for Os. In-house Re and Os solutions were continuously analysed during the course of this study at NCIET to ensure and monitor long-term mass spectrometry reproducibility (Table 4.1) and both are identical, within

uncertainty, to those reported by Rooney et al. (2010). The measured difference in $^{185}Re/^{187}Re$ values for the Re standard solution and the accepted $^{185}Re/^{187}Re$ value (0.5974; Gramlich et al., 1973) is used to correct the Re sample data. Results and blanks are presented in Table 4.1.

Table 4.1: Re-Os isotope data for the Nonesuch Formation outcrop samples

Sample	Re (ng/g)	±	Os (pg/g)	±	$^{187}Re/^{188}Os$	±	$^{187}Os/^{188}Os$	±	rho*	Os_i †
NS1-11	1.74	0.01	54.12	0.59	256.7	3.0	5.137	0.071	0.746	0.65
NS1-6A	2.40	0.01	65.32	0.64	317.5	2.6	6.213	0.065	0.647	0.66
NS1-4A	1.53	0.01	42.67	0.51	305.0	4.3	6.000	0.093	0.801	0.67
NS1-1A	2.80	0.01	72.42	0.78	346.9	3.2	6.739	0.079	0.682	0.68
NS1-9A	1.79	0.01	49.53	0.58	309.0	4.0	6.075	0.089	0.783	0.67
NS1-8B	3.22	0.01	76.91	0.96	401.2	4.3	7.718	0.111	0.673	0.71
NS2-9B	4.48	0.01	109.07	1.19	389.4	3.5	7.534	0.087	0.669	0.73
NS1-2B	2.77	0.01	71.36	0.77	352.3	3.2	6.882	0.081	0.682	0.72
NS1-7C	1.90	0.01	53.89	0.61	297.6	3.6	5.923	0.083	0.764	0.72
NS2-9A	3.59	0.01	87.30	0.96	390.9	3.6	7.595	0.089	0.676	0.76
NS1-8A	2.66	0.01	67.29	0.78	363.7	4.2	7.124	0.096	0.754	0.77
NS1-3B	2.30	0.01	63.97	0.73	314.7	3.6	6.366	0.087	0.746	0.87
NS1-7A	1.81	0.01	54.07	0.73	281.3	5.3	5.803	0.114	0.845	0.89
NS1-2A	2.79	0.01	74.60	0.97	335.9	5.2	6.766	0.115	0.826	0.90
NS1-5B	1.49	0.00	44.75	0.62	279.1	3.8	5.773	0.109	0.687	0.89
NS2-5A	4.14	0.01	105.39	1.18	367.5	3.7	7.334	0.091	0.709	0.91

* Rho is the associated error correlation at 2σ (Ludwig, 1980)

† Os_i is the initial $^{187}Os/^{188}Os$ isotope ratio calculated at 1040 Ma

Total procedural blanks = 4.1 ± 0.03 pg Re and 0.18 ± 0.07 pg Os (1 S.D., n = 2), with an average $^{187}Os/^{188}Os$ value = 0.59 ± 0.58

Re standard solution yields an average $^{185}Re/^{187}Re$ value of 0.5982 ± 0.00148 (1 SD, n = 257)

Os isotope reference material (DROsS) yields a $^{187}Os/^{188}Os$ ratio of 0.106095 ± 0.00048 (1 SD, n = 178)

4.3.3 Iron Speciation, C, Al, Cu and S analytical methodology

Iron speciation was determined via the sequential extraction technique of Poulton and Canfield (2005). This method extracts different operationally-defined Fe pools, including Fe carbonates such as siderite (Fe_{carb}), ferric oxides such as goethite and hematite (Fe_{ox}), and magnetite (Fe_{mag}). These minerals define an Fe pool which is

considered 'highly reactive' (Fe_{HR}) during sedimentation and diagenesis (Raiswell and Canfield, 1998). Elevated Fe_{HR}/Fe_T (total Fe) in anoxic settings arises from additional water column formation of either pyrite in euxinic basins, or non-sulphidised Fe minerals in ferruginous basins (Poulton and Canfield, 2011). The Nonesuch Formation shows no visible evidence of post-depositional oxidation resulting from exposure of reduced minerals to oxygen. Hence, the only post-early diagenetic alteration of primary Fe minerals likely to have occurred relates to low grade metamorphic or diagenetic alteration of some unsulphidised highly reactive Fe minerals to sheet silicate Fe. Pyrite (Fe_{py}) was determined via the chromous chloride distillation technique of Canfield et al. (1986). A boiling HCl extraction was also performed to determine an Fe pool (consisting largely of sheet silicate Fe) that is considered to be poorly reactive during diagenesis (Fe_{PRS}; Raiswell and Canfield, 1998; Poulton and Canfield, 2005).

Total Fe and Al were determined via a HF-$HClO_4$-HNO_3 extraction. All Fe solutions were measured via AAS, and Al and Cu were determined via ICP-OES. All extractions gave RSD's of <5%, based on replicate extractions. Organic C (C_{org}) was measured on a LECO C/S Analyzer, following pre-treatment with 10% HCl to remove carbonate phases. Pyrite S isotope compositions were determined (via EA-IRMS) on Ag_2S precipitates from the chromous chloride extractions by Iso-analytical Ltd, UK, with a RSD of 1.2% based on repeat analyses of an in-house standard. All results are presented in table 4.2.

Due to the seasonal carbonate laminites deposited within the Nonesuch Formation (Imbus et al., 1992), sample NS31 was split into light and dark sections for redox analysis. Both the organic-rich and carbonate-rich laminae show evidence of anoxia (Table 4.2), suggesting that anoxia was persistent and not seasonal.

Table 4.2: Fe speciation, C, Al, Cu and S isotope data for the Nonesuch Formation core and outcrop samples, ND = not determined

Sample i.d.	Height (m)	C_{org} (wt.%)	Al (wt.%)	Cu (ppm)	Fe_T (wt.%)	Fe_{carb} (wt.%)	Fe_{ox} (wt.%)	Fe_{mag} (wt.%)	Fe_{py} (wt.%)	Fe_{HR} (wt.%)	Fe_{PRS} (wt.%)	$\delta^{34}S$ (‰)
Core PI-1 samples												
NS29	51.21	1.81	7.33	53.08	4.66	0.526	0.106	0.530	1.146	2.31	2.024	10.05
NS30	55.17	0.39	7.91	61.06	5.33	0.518	0.126	0.557	1.383	2.58	2.525	9.56
NS23	58.22	0.73	8.07	67.87	5.74	0.436	0.108	0.495	1.369	2.41	2.682	2.41
NS24	59.13	0.57	7.91	118.33	5.59	0.494	0.136	0.555	1.139	2.32	2.384	5.28
NS25	60.05	1.11	7.83	51.44	4.65	0.318	0.081	0.347	1.307	2.05	1.572	0.97
NS26	60.96	0.50	7.81	65.99	5.82	0.604	0.129	0.428	1.238	2.40	2.388	4.07
NS27	61.87	1.59	8.05	81.49	4.84	0.313	0.086	0.301	1.136	1.84	2.286	7.02
NS28	62.79	0.40	8.14	59.11	4.95	0.552	0.129	0.656	0.103	1.44	3.055	14.30
NS17	63.40	0.63	7.82	56.34	4.32	0.326	0.088	0.406	0.442	1.26	2.281	10.06
NS18	64.62	0.60	7.84	60.38	4.45	0.517	0.123	0.575	0.401	1.62	1.916	10.33
NS19	65.23	0.68	7.62	285.20	4.94	0.433	0.108	0.451	0.761	1.75	3.063	9.82
NS20	65.53	0.62	8.00	83.18	5.57	0.784	0.185	0.871	0.249	2.09	3.008	8.89
NS11	65.84	0.16	8.20	75.25	6.05	0.556	0.153	0.869	0.024	1.60	3.089	ND
NS21	66.14	1.45	7.34	82.02	4.46	0.432	0.100	0.417	1.210	2.16	1.551	-1.55
NS22	66.45	0.22	8.33	73.48	6.70	0.569	0.151	0.896	0.029	1.64	5.124	13.28
NS12	66.60	0.25	8.05	58.17	5.48	0.712	0.181	0.955	0.082	1.93	2.309	10.08
NS13	67.36	0.13	8.27	77.80	6.01	0.766	0.241	1.091	0.006	2.10	4.541	ND
NS14	68.12	0.11	7.54	80.83	5.27	0.644	0.262	0.908	0.012	1.83	2.741	ND
NS15	68.88	0.13	8.27	128.55	6.49	0.551	0.320	0.810	0.038	1.72	3.523	4.63
NS16	69.19	0.15	8.46	66.91	6.75	0.434	0.411	1.149	0.011	2.00	3.342	7.67
NS6	69.49	0.19	8.13	47.70	5.79	0.479	0.323	0.954	0.020	1.78	3.506	ND
NS7	70.41	0.14	8.40	220.97	7.85	0.967	0.246	1.296	0.019	2.53	5.670	6.41
NS8	71.32	0.44	7.56	14.84	3.95	0.284	0.085	0.421	0.190	0.98	1.906	-12.52
NS9	72.24	0.18	8.10	119.93	6.70	0.595	0.362	0.942	0.038	1.94	4.595	10.88
NS10	73.76	0.13	7.36	96.52	5.97	0.401	0.321	0.938	0.016	1.68	4.042	ND
NS1	75.59	0.47	8.04	111.11	7.84	1.116	0.514	1.598	0.009	3.24	1.336	6.55
NS2	75.90	0.17	8.44	110.43	7.76	0.771	0.422	1.494	0.038	2.72	4.743	8.01
NS3	76.50	0.13	7.89	125.79	7.07	0.634	0.325	0.937	0.022	1.92	4.832	ND
NS4	77.11	0.17	7.88	129.87	6.00	0.732	0.457	1.270	0.022	2.48	3.510	8.86
NS5	77.72	1.11	8.36	104.69	7.29	0.692	0.426	1.817	0.015	2.95	3.997	10.39
NS31	79.25	0.14	7.90	101.64	7.99	0.588	0.267	1.058	0.084	2.00	4.076	9.94
NS32	81.08	0.14	7.97	79.87	6.55	0.541	0.311	0.905	0.058	1.81	2.791	7.68
NS33	81.38	0.13	8.14	166.05	7.36	0.552	0.283	1.030	0.042	1.91	5.043	7.23
NS34	87.17	0.32	7.02	51.79	5.19	0.486	0.124	0.627	0.319	1.56	2.162	9.54
NS35	87.48	0.53	5.42	88.40	4.02	0.452	0.099	0.332	0.942	1.83	1.289	9.99
NS36	89.92	1.00	7.29	56.94	5.22	0.652	0.142	0.505	0.684	1.98	2.885	10.30
NS37	90.53	0.22	7.55	81.46	5.24	0.459	0.129	0.495	0.094	1.18	3.712	ND
NS38	95.10	0.05	5.35	816.88	6.66	0.704	0.572	1.210	0.016	2.50	4.689	6.36
NS39	97.54	0.88	7.94	1996.29	7.56	0.607	0.391	0.950	0.044	1.99	4.641	16.06
NS40	99.36	0.22	7.84	5208.63	5.74	0.431	0.232	0.865	0.109	1.64	3.751	-2.29
NS41	103.63	0.17	6.80	5393.00	5.15	0.333	0.344	0.518	0.110	1.30	2.697	28.70
NS42	105.46	0.07	7.79	182.71	7.35	0.195	1.261	0.854	0.001	2.31	3.549	ND
NS43	106.68	0.99	7.41	76.78	7.37	0.062	3.301	0.579	0.001	3.94	2.319	ND
NS44	109.42	0.13	7.66	59.75	7.57	0.033	2.926	0.745	0.001	3.70	3.144	ND
Outcrop samples												
NS1-4A		0.40	3.84	72.18	2.29	0.276	0.044	0.162	0.648	1.13	ND	14.70
NS1-8A		0.69	4.86	118.22	3.00	0.271	0.064	0.219	0.902	1.46	ND	14.81
NS2-5A		1.06	5.34	80.54	3.47	0.428	0.069	0.295	1.115	1.91	ND	ND
NS1-8B		0.79	4.93	72.76	2.99	0.307	0.071	0.155	0.727	1.26	ND	ND
NS1-5B		0.44	4.38	73.45	2.58	0.273	0.047	0.191	0.883	1.39	ND	ND
NS1-6A		0.59	4.53	134.00	2.82	0.227	0.046	0.201	0.747	1.22	ND	14.60
NS1-9A		0.46	4.73	62.50	2.79	0.276	0.044	0.192	0.864	1.38	ND	ND
NS1-2A		0.67	4.65	78.40	2.92	0.265	0.070	0.215	0.776	1.32	ND	ND
NS1-1A		0.68	4.61	79.04	2.88	0.257	0.049	0.211	0.809	1.33	ND	13.50
NS1-3B		0.64	4.73	189.53	2.91	0.303	0.062	0.234	0.783	1.38	ND	ND
NS2-9B		0.86	7.10	73.23	5.98	0.394	0.100	0.283	1.329	2.11	ND	ND
NS1-11		0.62	8.00	45.01	5.57	0.784	0.185	0.871	0.249	2.09	ND	ND
NS2-9A		0.83	7.15	72.99	5.91	0.509	0.106	0.338	1.255	2.21	ND	ND
NS1-7A		0.75	4.52	39.20	3.80	0.380	0.071	0.231	0.953	1.63	ND	ND
NS1-7C		0.88	4.85	42.32	3.81	0.403	0.077	0.257	0.947	1.68	ND	ND
NS1-2B		0.71	3.77	34.35	3.43	0.287	0.089	0.215	0.765	1.36	ND	ND
Sample split into light (L) and dark (D) sections												
NS31 L	79.25	ND	ND	ND	5.280	1.053	0.558	0.890	0.020	2.521	2.364	ND
NS31 D	79.25	ND	ND	ND	9.180	1.151	0.754	1.355	0.030	3.289	5.283	ND

4.4 Results and discussion

4.4.1 Re-Os geochronology

The Re and Os abundances for the Nonesuch Formation are 1.49 - 4.48 ng/g and 42.67 - 109.07 pg/g, respectively. Linear regression of all the Nonesuch Formation Re-Os isotope data using the program Isoplot V.4.15 (with 2σ uncertainties for $^{187}Re/^{188}Os$ and $^{187}Os/^{188}Os$, the error correlation function (rho) and the $\lambda^{187}Re$ of 1.666 x 10^{-11} a^{-1}) yields a Model 3 age of 1040 ± 75 (78) Ma (2σ, *n* = 16, Mean Squared of Weighted Deviation [MSWD] = 10.6, Os_i = 0.76 ± 0.42, bracketed uncertainty includes the uncertainty in the decay constant; Figure 4.3; Table 4.1). The Model 3 age and the large MSWD strongly suggest that any scatter in the data is controlled by geological factors, rather than purely analytical uncertainties.

Variation in initial $^{187}Os/^{188}Os$ (Os_i) has previously been demonstrated to cause larger MSWD's in Re-Os geochronology (e.g. Cohen et al., 1999; Azmy et al., 2008; Kendall et al., 2009b; Xu et al., 2009; Rooney et al., 2010). In order to assess the variation, the Os_i is calculated using the $\lambda^{187}Re$ constant at 1040 Ma for all samples and is found to vary from 0.65 to 0.91 (Table 4.1). The age of 1040 Ma is used for this calculation as it represents the age when all the samples are regressed and is used to identify any groupings within the samples. The variations present in Os_i are visible on the composite isochron with two clear linear sets of samples representative of different groups of Os_i (Fig. 4.3A). Variation in Os_i can suggest that the $^{187}Os/^{188}Os$ influx into the basin was heterogeneous or that there could have been post-depositional disturbance to the Re-Os isotope system. I would suggest that post-depositional disturbance is unlikely given the relative precision and lack of scatter in the composite isochron. Several recent studies have evaluated the effect of post-depositional fluid-flow on Re-Os systematics, highlighting the extremely imprecise and often nonsensical data generated (e.g., ages >100 Myrs younger than the known age of a unit and/or negative initial Os isotope compositions; Kendall et al., 2009a,b; Rooney et al., 2011). In these cases there is extreme scatter about the isochron and very large

MSWD's of 86 and 338 (Kendall et al., 2009b; Rooney et al., 2011, respectively). An MSWD of 10.6 for the Nonesuch Formation isochron implies that samples started with different Os_i. Several previous studies have presented accurate Re-Os age data (agreeing with interpolated or biostratigraphy ages) with MSWD's similar to 10.6 (e.g. Cohen et al., 1999; Azmy et al., 2008; Kendall et al., 2009a,b; Xu et al., 2009; Yang et al., 2009; Rooney et al., 2010). The composite Nonesuch Formation Re-Os age is within uncertainty of the stratigraphic age (i.e. younger than 1086 Ma) and suggests that the imprecision is an artefact of the sample Os_i heterogeneity as opposed to a resetting of the Re-Os systematics, and thus post-depositional fluid flow can be discounted. This is further supported by the low levels of Cu in the samples (<150 ppm; Table 4.2), which would be expected to be higher if there had been post-depositional fluid flow, as local hydrothermal mineralisation has resulted in high Cu contents in some areas.

The $^{187}Os/^{188}Os$ composition of seawater today records a balance of radiogenic (~1.4; from continental weathering) and unradiogenic (~0.13; from hydrothermal inputs, alteration of oceanic crust or cosmic dust flux) inputs (Peucker-Ehrenbrink and Ravizza, 2000). In a terrestrial water body the $^{187}Os/^{188}Os$ composition records a balance of inputs from continental weathering surrounding the water body. For the Nonesuch Formation, the Os_i variation will reflect a balance between weathering of radiogenic Archean-Proterozoic cratonic lithosphere (~1.01; upper continental crust calculated at 1100 Ma; Esser and Turekian, 1993) and unradiogenic rift-related flood basalts (~0.13; Allegre et al., 1999). The sedimentology of the Nonesuch Formation is controlled by interactions between rates of subsidence, climatic changes and differences in tectonic setting, which produce variable facies associations and sedimentation rates (Elmore et al., 1989; Imbus et al., 1992). Therefore, the heterogeneity of the surrounding continental crust and the changes in sedimentation and weathering rates provided a mixed Os signal that may have varied considerably with prevailing climate regimes. A fundamental assumption of the isochron technique is that the samples all started with similar initial Os isotope compositions (Cohen et al., 1999; Kendall et al., 2009a). It is apparent in Figure 4.3A that there are two isochrons,

an upper and a lower one each defined by a range of Os_i values. In order to improve the accuracy of the ages, isochrons with similar Os_i values are plotted. Separate regressions of the Re-Os data based on the Os_i values (0.65 – 0.77 and 0.87 – 0.91), yield Model 1 ages of 1078 ± 23 (24) Ma (2σ, *n* = 11, MSWD = 1.05, Os_i = 0.49 ± 0.13; Fig. 4.3B) and 1054 ± 51 (52) Ma (2σ, *n* = 5, MSWD = 0.29, Os_i = 0.81 ± 0.28; Fig. 4.3C), respectively. Both of these ages are identical within uncertainty and are in agreement with the stratigraphic position of the 1087.2 ± 1.6 Ma U-Pb age of the underlying Copper Harbour Conglomerate. The large age uncertainties can be explained by the small range in $^{187}Re/^{188}Os$, particularly in the 1054 ± 51 Ma isochron. These restricted ranges in $^{187}Re/^{188}Os$ have been reported from both marine and lacustrine sediments (Cumming et al., 2012; Turgeon et al., 2007; Selby et al., 2009) and, although the causes of such small ranges have not been fully resolved, they are likely related to organic matter type and depositional conditions rather than redox (Cumming et al., 2012; Chapter 2; Selby et al., 2009).

The Os_i provides a useful constraint on the depositional setting of the Nonesuch Formation as the Os_i of organic-rich sedimentary rocks has been shown to be useful in deriving the depositional setting of sediments (Poirier and Hillaire-Marcel, 2011; Cumming et al., 2012; Chapter 2). If traditional geochemical and geobiological techniques fail to discern between lacustrine or marine deposition and the $^{187}Os/^{188}Os$ composition of seawater at the time is known, the Os_i of the system in question can allude to the nature of deposition. The Os_i derived from the two Re-Os isochrons are 0.81 ± 0.28 and 0.49 ± 0.13 (Fig. 4.3), a At 1100 Ma, seawater $^{187}Os/^{188}Os$ was relatively unradiogenic at ~0.3 (a value derived from two separate margins; Rooney et al., 2010; Azmy et al., 2008), and therefore the more radiogenic values measured for the Nonesuch Formation (0.81 and 0.49) suggest that minimal Os was sourced from the marine realm. Thus, the Os isotope data support sedimentological and paleogeographic evidence for lacustrine depositional conditions.

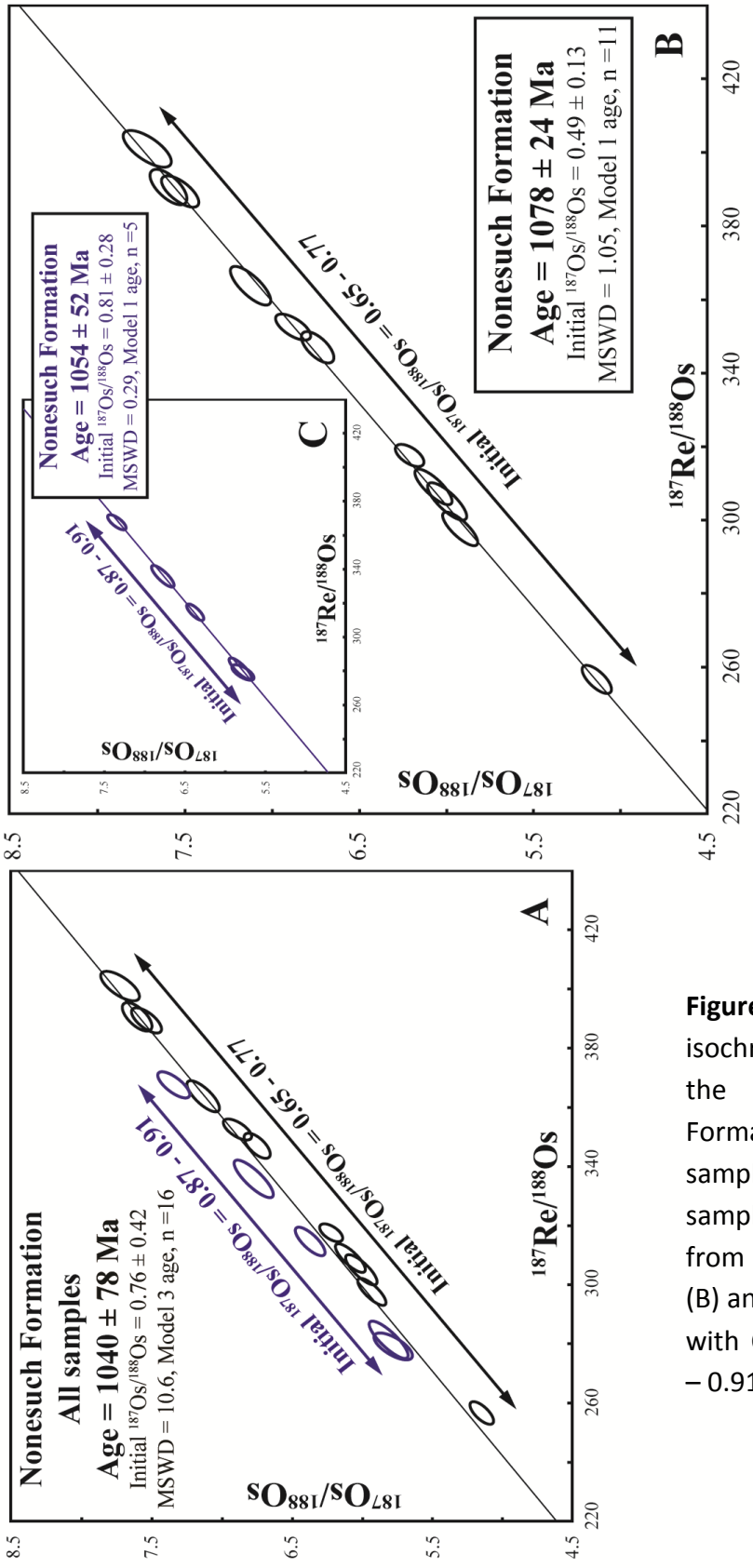

Figure 4.3: Re-Os isochrons for all of the Nonesuch Formation outcrop samples (A), for samples with Os_i from 0.65 – 0.77 (B) and for samples with Os_i from 0.87 – 0.91 (C).

4.4.2 Redox conditions

4.4.2.1 Fe speciation

Water column redox conditions during deposition of the Nonesuch Formation were evaluated using Fe speciation. Modern and ancient sediments deposited under anoxic conditions commonly have Fe_{HR}/Fe_T ratios >0.38, in contrast to oxic depositional conditions, where ratios are consistently below 0.22 (Poulton and Canfield, 2011). About 40% of drill core samples (Fig. 4.4), and all outcrop samples (Table 4.2), were clearly deposited from an anoxic water column with Fe_{HR}/Fe_T >0.38, while others fall within the equivocal range (Fe_{HR}/Fe_T = 0.22 - 0.38). These equivocal samples may reflect the masking of water column Fe_{HR} enrichments due to rapid sedimentation or transformation of non-sulfidized Fe_{HR} to clay minerals during burial diagenesis or metamorphism (Poulton and Raiswell, 2002; Poulton et al., 2010). The latter possibility can be evaluated by considering Fe/Al ratios (Fig. 4.4), whereby significant enrichments in Fe relative to both average shale (Lyons and Severmann, 2006) and typical oxic lacustrine sediments (e.g., Kemp and Thomas, 1976; Fagel et al., 2005) throughout the Nonesuch Formation provide strong evidence for anoxic depositional conditions. Post-depositional loss of Fe_{HR} can also be assessed through an extraction that targets Fe associated with clay minerals (termed poorly reactive silicate Fe; Fe_{PRS}) (Poulton et al., 2010). Extreme enrichment in Fe_{PRS} in the Nonesuch Formation (Fe_{PRS}/Fe_T values are well above the modern and Phanerozoic averages; Fig. 4.4; Poulton and Raiswell, 2002) suggests that significant loss of Fe_{HR} through authigenic clay mineral formation was responsible for reducing original depositional Fe_{HR}/Fe_T ratios (Poulton et al., 2010), supporting anoxic deposition for all Nonesuch Formation samples. For samples showing evidence of anoxic deposition, the extent to which the Fe_{HR} pool has been pyritized (Fe_{py}/Fe_{HR}) can then distinguish euxinic (Fe_{py}/Fe_{HR} >0.7 - 0.8) from ferruginous (Fe_{py}/Fe_{HR} <0.7 - 0.8) depositional conditions (Poulton and Canfield, 2011). All of the Nonesuch Formation samples have Fe_{Py}/Fe_{HR} ratios well below the euxinic threshold (Fig. 4.4), indicating anoxic ferruginous depositional conditions throughout and thus refuting the suggestion of a possible euxinic depositional setting (Imbus et al., 1992).

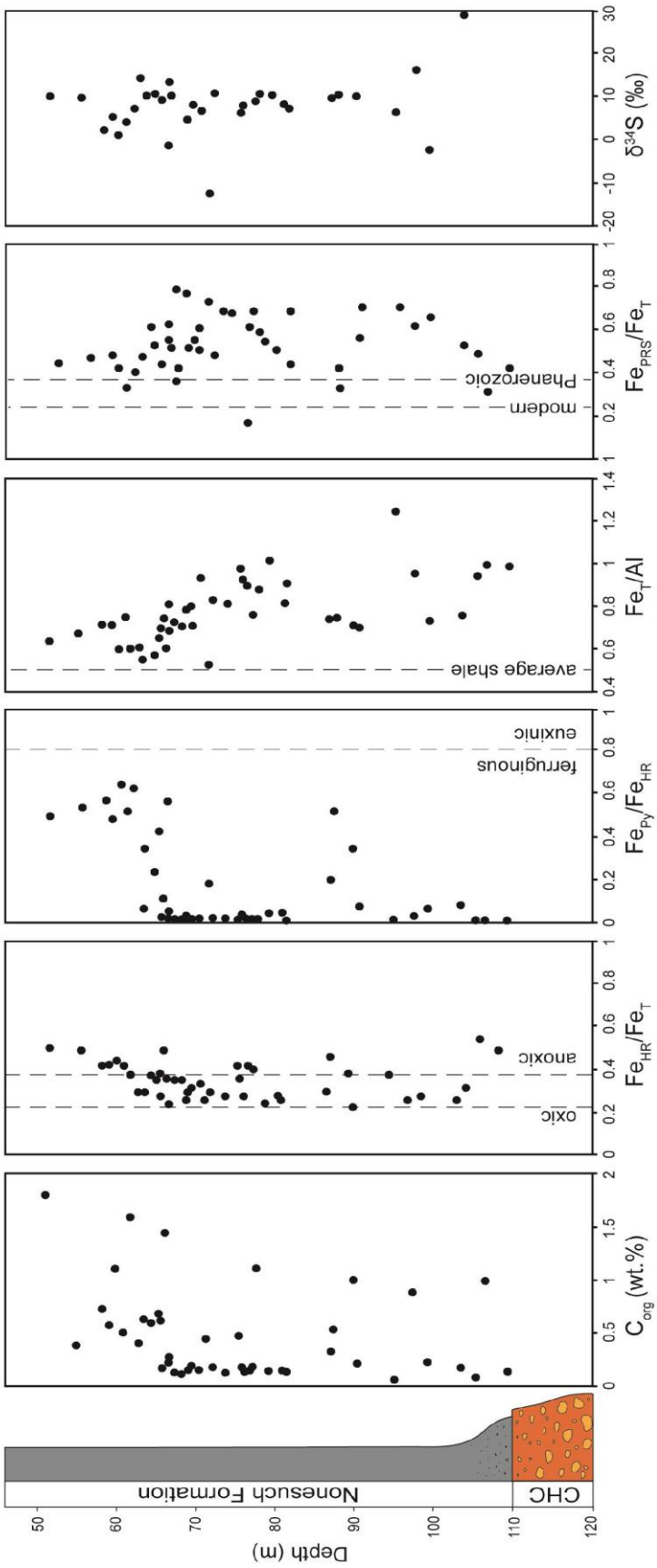

Figure 4.4: Geochemical profiles for the Nonesuch Formation core samples. For the Fe_{HR}/Fe_T and Fe_{Py}/Fe_{HR} graphs the dashed lines show the fields for oxic or anoxic deposition and ferruginous or euxinic deposition, respectively (Poulton and Canfield, 2011). On the Fe_T/Al graph the dashed line represents average anoxic shale (Lyons and Severmann, 2006). On the Fe_{PRS}/Fe_T graph the dashed lines represent modern (Raiswell and Canfield, 1998) and Phanerozoic (Poulton and Raiswell, 2002) averages. CHC stands for Copper Harbour Conglomerate.

4.4.2.2 Implications for terrestrial biospheric oxygenation

The upper Nonesuch Formation comprises fining and coarsening upward packages interpreted to be the transition between lacustrine deposition and fluvial conditions of the conformably overlying Freda Sandstone (Elmore et al., 1989). This suggests that the Nonesuch Formation was likely deposited under progressively more oxic conditions as water depth decreased towards the top of the succession (Elmore et al., 1989). Oxygenated surface waters in ~1.1 Ga terrestrial aquatic environments would be expected, particularly since shallow marine waters were apparently oxygenated much earlier in Earth history (~2.7 Ga; Kendall et al., 2010; Zerkle et al., 2012). However, there is no evidence for oxic deposition in core PI-1, suggesting that anoxia was a persistent feature throughout the depositional period, and any oxygenation was likely restricted to surface waters.

The observation of persistent ferruginous water column conditions suggests that the flux of Fe_{HR} to the lake overwhelmed the flux of sulphate (Poulton and Canfield, 2011). I note here that the Os_i values suggest that any hydrothermal fluid contribution to the lake from rifting or extensive weathering of rift-related basalts would have been negligible, as Os_i values closer to ~0.13 (Allegre et al., 1999; Miesel et al., 2001) would otherwise be expected. In consequence, there is no evidence to support a particularly enhanced influx of Fe due to rifting. Instead, the prevalence of ferruginous water column conditions is consistent with low rates of oxidative pyrite weathering driven by only modest levels of atmospheric oxygen (Canfield and Raiswell, 1999). Although it is not possible to directly determine water column sulphate concentrations, it is noted that pyrite sulphur isotope compositions are relatively heavy (8.5 ± 6.3‰) throughout most of the Nonesuch Formation (Fig. 4.4). A compilation of pyrite sulphur isotope data for the Nonesuch Formation show a similar distribution (possibly skewed towards slightly heavier values) to 1.5 - 1.0 Ga marine sediments (Fig. 4.5). This is entirely consistent with a relatively low sulphate environment (e.g., Canfield and Raiswell, 1999), and further supports efficient trapping of sulphide (and hence high S/C ratios; Fig. 4.2) driven by a lack of bioturbation, and

deposition from a ferruginous system which was sulphur (rather than reactive Fe) limited (e.g., Raiswell and Canfield, 2012).

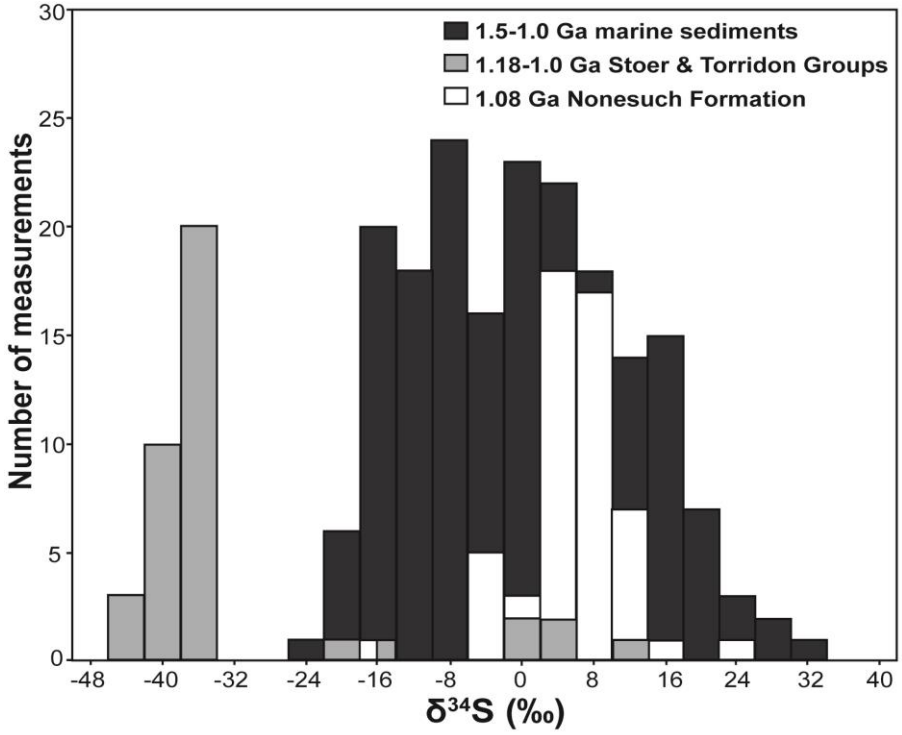

Figure 4.5: Probability density plot of pyrite sulphur isotope data for the Nonesuch Formation (this study; Imbus et al., 1992), the Torridon and Stoer Groups (Parnell et al., 2010) and 1.5 – 1.0 Ga marine sediments (Canfield and Raiswell, 1999).

The distribution of the Nonesuch Formation sulphur isotope data is very different to that observed for 1.18-1.0 Ga lacustrine sediments from NW Scotland (Fig. 4.5), with no indication of large-scale fractionations that would indicate significant oxidative sulphur cycling through microbial disproportionation. This is likely a consequence of the restriction of oxic conditions to surface waters, and the limitation of sulphate reduction to sediment porewaters beneath the ferruginous water column of the Nonesuch basin. Together, this would limit formation of the oxidized sulphur species required for disproportionation (Thamdrup et al., 1993). In addition, the low sulphate concentrations inferred for the Nonesuch basin would limit the maximum expression

of sulphur isotope fractionation even if oxidative sulphur cycling and disproportionation reactions were prevalent (Canfield and Raiswell, 1999). This is consistent with multiple ($^{32/33/34}$S) sulphur isotope systematics in marine sediments, which suggest that microbial sulphur disproportionation was prevalent by at least 1.3 Ga (Johnston et al., 2005), but was only manifest in the major ($^{32/34}$S) sulphur isotope record after a later Neoproterozoic rise in atmospheric oxygen led to a significant increase in seawater sulphate concentrations (Canfield and Teske, 1996). Thus, rather than reflecting high sulphate concentrations (Hieshima and Pratt, 1991) potentially attributable to extensive oxygenation of the continents under high atmospheric oxygen, Fe-S-C systematics in the Nonesuch Formation suggest low sulphate concentrations, ferruginous conditions and only modest atmospheric oxygenation.

In light of this, the sulphur isotope data for the Stoer and Torridon Groups may reflect either an unusually sulphate-rich environment that allowed maximum expression of sulphur isotope fractionations (Parnell et al., 2010), or the preservation of large sulphur isotope fractionations through bacterial sulphate reduction alone (Canfield et al., 2010; Sim et al., 2011). Thus, while it remains possible that sulphur isotope systematics in the Torridon and Stoer Groups may be providing an early record of terrestrial oxygenation; the redox and sulphur isotope data for the Nonesuch Formation suggest that early terrestrial oxygenation was not a pervasive feature of the localities that preserve evidence for diverse eukaryotic life. Instead, the redox characteristics display strong similarities to the marine realm (Poulton and Canfield, 2011), implying that in terms of water column and atmospheric oxygenation, terrestrial environmental conditions were likely no more pre-disposed towards eukaryote evolution than shallow marine environments. It is suggested that the identification and detailed redox evaluation of other late Mesoproterozoic terrestrial sediments should be a priority in order to more precisely evaluate potential links between the redox evolution of aquatic systems and the rich terrestrial biological record.

4.5 Conclusions

This study provides a geochemical and isotopic assessment of sediments from the late Mesoproterozoic Nonesuch Formation of central North America. The Re-Os geochronology data show variation in Os_i, but when regressed based on Os_i, the data yield a most precise depositional age of 1078 ± 24 Ma. The Re-Os dates agree with underlying U-Pb age constraints and crucially provide the Os isotopic composition of the lake water at the time of deposition. Comparison of the Os isotope data with seawater during this time period supports existing evidence for a lacustrine depositional setting for the Nonesuch Formation and suggests the Os signal is predominantly derived from weathering of surrounding Precambrian crust, ruling out any hydrothermal influence from rifting.

Redox conditions are assessed using Fe-S-C systematics that suggest the Nonesuch Formation was deposited from an anoxic ferruginous water column. Thus, similar to the marine realm, anoxia persisted in terrestrial aquatic environments in the mid-late Proterozoic, but sulphidic water column conditions were not ubiquitous. The data herein suggest that oxygenation of the terrestrial realm was not pervasive at this time and may not have preceded oxygenation of the marine environment, signifying a major requirement for further investigation of links between the oxygenation state of terrestrial aquatic environments and eukaryote evolution.

4.6 References

Allègre, C. L. and Luck, J. M., 1980. Osmium isotopes as petrogenetic and geological tracers. Earth and Planetary Sciences Letters 48, 148-154.

Azmy, K., Kendall, B., Creaser, R.A., Heaman, L., de Oliveira, T.F., 2008. Global correlation of the Vazante Group, Sao Francisco Basin, Brazil: Re-Os and U-Pb radiometric age constraints. Precambrian Research 164, 160-172.

Berner, R.A., Raiswell, R., 1983. Burial of organic-carbon and pyrite sulfur in sediments over Phanerozoic time – a new theory. Geochimica et Cosmochimica Acta 47, 855-862.

Berner, R.A., Raiswell, R., 1984. C/S method for distinguishing fresh-water from marine sedimentary rocks. Geology 12, 365-368.

Brunner, B., Bernasconi, S.M., 2005. A revised isotope fractionation model for dissimilatory sulfate reduction in sulfate reducing bacteria. Geochimica et Cosmochimica Acta 69, 4759-4771.

Canfield, D.E., Farquhar, J., Zerkle, A.L., 2010. High isotope fractionations during sulfate reduction in a low-sulfate euxinic ocean analog. Geology 38, 415-418.

Canfield, D.E., Poulton, S.W., Knoll, A.H., Narbonne, G.M., Ross, G., Goldberg, T., Strauss, H., 2008. Ferruginous Conditions Dominated Later Neoproterozoic Deep-Water Chemistry. Science 321, 949-952.

Canfield, D.E., Raiswell, R., 1999. The evolution of the sulfur cycle. Am. J. Sci. 299, 697-723.

Canfield, D.E., Raiswell, R., Westrich, J.T., Reaves, C.M., Berner, R.A., 1986. The use of chromium reduction in the analysis of reduced inorganic sulfur in sediments and shales. Chemical Geology 54, 149-155.

Canfield, D.E., Teske, A., 1996. Late Proterozoic rise in atmospheric oxygen concentration inferred from phylogenetic and sulphur-isotope studies. Nature 382, 127-132.

Cumming, V.M., Selby, D., Lillis, P.G., 2012. Re–Os geochronology of the lacustrine Green River Formation: Insights into direct depositional dating of lacustrine successions, Re–Os systematics and paleocontinental weathering. Earth and Planetary Science Letters 359–360, 194-205.

Davis, D.W., Paces, J.B., 1990. Time resolution of geologic events on the Keweenaw Peninsula and implications for development of the Midcontinent Rift system. Earth and Planetary Science Letters 97, 54-64.

Elmore, D.R., Milavec, G.J., Imbus, S.W., Engel, M.H., 1989. The Precambrian nonesuch formation of the North American mid-continent rift, sedimentology and organic geochemical aspects of lacustrine deposition. Precambrian Research 43, 191-213.

Esser, B.K., Turekian, K.K., 1993. The osmium isotopic composition of the continental-crust. Geochimica et Cosmochimica Acta 57, 3093-3104.

Fagel, N., Alleman, L.Y., Granina, L., Hatert, F., Thamo-Bozso, E., Cloots, R., André, L., 2005. Vivianite formation and distribution in Lake Baikal sediments. Global and Planetary Change 46, 315-336.

Gramlich, J.W., Murphy, T.J., Garner, E.L., Shields, W.R., 1973. Absolute isotopic abundance ratio and atomic weight of a reference sample of rhenium. Journal of research of the National Bureau of Standards 77A, 691-698.

Hieshima, G.B., Pratt, L.M., 1991. Sulfur/carbon ratios and extractable organic matter of the middle Proterozoic nonesuch formation, north American midcontinent rift. Precambrian Research 54, 65-79.

Imbus, S.W., Macko, S.A., Elmore, R.D., Engel, M.H., 1992. Stable isotope (C, S, N) and molecular studies on the Precambrian Nonesuch shale (Wisconsin-Michigan, USA) – evidence for differential preservation rates, depositional environment and hydrothermal influence. Chemical Geology 101, 255-281.

Johnston, D.T., Wing, B.A., Farquhar, J., Kaufman, A.J., Strauss, H., Lyons, T.W., Kah, L.C., Canfield, D.E., 2005. Active Microbial Sulfur Disproportionation in the Mesoproterozoic. Science 310, 1477-1479.

Kemp, A.L., Thomas, R.L., 1976. Cultural impact on geochemistry of sediments of Lake Ontario, Erie and Huron. Geosci. Can. 3, 191-207.

Kendall, B., Creaser, R.A., Selby, D., 2009a. ^{187}Re-^{187}Os geochronology of Precambrian organic-rich sedimentary rocks. Geological Society, London, Special Publications 326, 85-107.

Kendall, B., Creaser, R.A., Gordon, G.W., Anbar, A.D., 2009b. Re-Os and Mo isotope systematics of black shales from the Middle Proterozoic Velkerri and Wollogorang Formations, McArthur Basin, northern Australia. Geochimica Et Cosmochimica Acta 73, 2534-2558.

Kendall, B., Reinhard, C.T., Lyons, T.W., Kaufman, A.J., Poulton, S.W., Anbar, A.D., 2010. Pervasive oxygenation along late Archaean ocean margins. Nature Geoscience 3, 647-652.

Kendall, B.S., Creaser, R.A., Ross, G.M., Selby, D., 2004. Constraints on the timing of Marinoan "Snowball Earth" glaciation by Re-187-Os-187 dating of a Neoproterozoic, post-glacial black shale in Western Canada. Earth and Planetary Science Letters 222, 729-740.

Ludwig, K.R., 1980. Calculation of uncertainties of U-Pb isotope data. Earth and Planetary Science Letters 46, 212-220.

Lyons, T.W., Severmann, S., 2006. A critical look at iron paleoredox proxies: New insights from modern euxinic marine basins. Geochimica et Cosmochimica Acta 70, 5698-5722.

Mauk, J.L., Hieshima, G.B., 1992. Organic matter and copper mineralization at White Pine, Michigan, U.S.A. Chemical Geology 99, 189-211.

Meisel, T., Walker, R.J., Irving, A.J., Lorand, J.-P., 2001. Osmium isotopic compositions of mantle xenoliths: a global perspective. Geochimica et Cosmochimica Acta 65, 1311-1323.

Moldowan, J.M., Fago, F.J., Lee, C.Y., Jacobson, S.R., Watt, D.S., Slougui, N.-E., Jeganathan, A., Young, D.C., 1990. Sedimentary 12-*n*-Propylcholestanes, Molecular Fossils Diagnostic of Marine Algae. Science 247, 309-312.

Ojakangas, R.W., Morey, G.B., Green, J.C., 2001. The Mesoproterozoic Midcontinent Rift System, Lake Superior Region, USA. Sedimentary Geology 141-142, 421-442.

Parnell, J., Boyce, A.J., Mark, D., Bowden, S., Spinks, S., 2010. Early oxygenation of the terrestrial environment during the Mesoproterozoic. Nature 468, 290-293.

Peucker-Ehrenbrink, B., Ravizza, G., 2000. The marine osmium isotope record. Terra Nova 12, 205-219.

Planavsky, N.J., McGoldrick, P., Scott, C.T., Li, C., Reinhard, C.T., Kelly, A.E., Chu, X., Bekker, A., Love, G.D., Lyons, T.W., 2011. Widespread iron-rich conditions in the mid-Proterozoic ocean. Nature 477, 448-451.

Poirier, A., Hillaire-Marcel, C., 2011. Improved Os-isotope stratigraphy of the Arctic Ocean. Geophys. Res. Lett. 38.

Poulton, S.W., Canfield, D.E., 2005. Development of a sequential extraction procedure for iron: implications for iron partitioning in continentally derived particulates. Chemical Geology 214, 209-221.

Poulton, S.W., Canfield, D.E., 2011. Ferruginous Conditions: A Dominant Feature of the Ocean through Earth's History. Elements 7, 107-112.

Poulton, S.W., Fralick, P.W., Canfield, D.E., 2010. Spatial variability in oceanic redox structure 1.8 billion years ago. Nature Geoscience 3, 486-490.

Poulton, S.W., Raiswell, R., 2002. The low-temperature geochemical cycle of iron: From continental fluxes to marine sediment deposition. Am. J. Sci. 302, 774-805.

Pratt, L.M., Summons, R.E., Hieshima, G.B., 1991. Sterane and triterpane biomarkers in the Precambrian Nonesuch Formation, North American Midcontinent Rift. Geochimica et Cosmochimica Acta 55, 911-916.

Raiswell, R., Canfield, D.E., 1998. Sources of iron for pyrite formation in marine sediments. Am. J. Sci. 298, 219-245.

Raiswell, R., Canfield, D.E., 2012. The Iron Biogeochemical Cycle Past and Present. Geochemical Perspectives 1, 232.

Rooney, A.D., Chew, D.M., Selby, D., 2011. Re-Os geochronology of the Neoproterozoic-Cambrian Dalradian Supergroup of Scotland and Ireland: Implications for Neoproterozoic stratigraphy, glaciations and Re-Os systematics. Precambrian Research 185, 202-214.

Rooney, A.D., Selby, D., Houzay, J.-P., Renne, P.R., 2010. Re-Os geochronology of a Mesoproterozoic sedimentary succession, Taoudeni basin, Mauritania: Implications for basin-wide correlations and Re-Os organic-rich sediments systematics. Earth and Planetary Science Letters 289, 486-496.

Selby, D., 2007. Direct Rhenium-Osmium age of the Oxfordian-Kimmeridgian boundary, Staffin bay, Isle of Skye, U.K., and the Late Jurassic time scale. Norwegian Journal of Geology 87, 9.

Selby, D., Creaser, R.A., 2003. Re-Os geochronology of organic rich sediments: an evaluation of organic matter analysis methods. Chemical Geology 200, 225-240.

Selby, D., Mutterlose, J., Condon, D.J., 2009. U-Pb and Re-Os geochronology of the Aptian/Albian and Cenomanian/Turonian stage boundaries: Implications for timescale calibration, osmium isotope seawater composition and Re-Os systematics in organic-rich sediments. Chemical Geology 265, 394-409.

Sim, M.S., Bosak, T., Ono, S., 2011. Large Sulfur Isotope Fractionation Does Not Require Disproportionation. Science 333, 74-77.

Strother, P.K., Wellman, C.H., 2010. Paleobiology of a Nonmarine Precambrian Shale: Well-Preserved Eukaryotes from the 1.1 Ga Nonesuch Formation, The Palaeontological Association 54th Annual Meeting. The Palaeontological Association, Ghent University.

Suszek, T., 1997. Petrography and sedimentation of the middle Proterozoic (Keweenawan) Nonesuch Formation, western Lake Superior region, Midcontinent Rift System. Geological Society of America Special Papers 312, 195-210.

Thamdrup, B., Finster, K., Hansen, J.W., Bak, F., 1993. Bacterial Disproportionation of Elemental Sulfur Coupled to Chemical Reduction of Iron or Manganese. Applied and Environmental Microbiology 59, 101-108.

Turgeon, S.C., Creaser, R.A., Algeo, T.J., 2007. Re-Os depositional ages and seawater Os estimates for the Frasnian-Famennian boundary: Implications for weathering

rates, land plant evolution, and extinction mechanisms. Earth and Planetary Science Letters 261, 649-661.

Xu, G.P., Hannah, J.L., Stein, H.J., Bingen, B., Yang, G., Zimmerman, A., Weitschat, W., Mork, A., Weiss, H.M., 2009. Re-Os geochronology of Arctic black shales to evaluate the Anisian-Ladinian boundary and global faunal correlations. Earth and Planetary Science Letters 288, 581-587.

Yang, G., Hannah, J.L., Zimmerman, A., Stein, H.J., Bekker, A., 2009. Re-Os depositional age for Archean carbonaceous slates from the southwestern Superior Province: Challenges and insights. Earth and Planetary Science Letters 280, 83-92.

Zerkle, A.L., Claire, M.W., Domagal-Goldman, S.D., Farquhar, J., Poulton, S.W., 2012. A bistable organic-rich atmosphere on the Neoarchaean Earth. Nature Geoscience 5, 359-363.

Chapter 5

Conclusions and future research

Chapter 5: Conclusions and future research

This thesis presents the first in-depth research into Re-Os geochronology and systematics of ancient lacustrine sedimentary and petroleum systems. Accurate Re-Os geochronology of the Green River Formation highlights the ability of this geochronometer to be used to date lacustrine organic-rich rocks and for Os isotopes to provide information about continental weathering. This is augmented by organic geochemical analysis of the samples giving new insights into Re-Os systematics in sedimentary systems. The Green River petroleum system in the Uinta Basin is then used to provide new data on Re-Os hydrocarbon generation geochronology and Os isotope fingerprinting of variable hydrocarbon phases sourced from a lacustrine Type I kerogen. This study is enhanced by hydrous pyrolysis supporting the Os isotope correlation in particular and strengthening the hypothesis that these tools can be applied to multiple petroleum system types with variable hydrocarbon phases. The final study evaluates the Re-Os lacustrine organic-rich sedimentary rock geochronometer in a more 'elusive' lacustrine system, the late Mesoproterozoic Nonesuch Formation. This provides further agreement that the Re-Os geochronometer can be used in lacustrine systems but alludes to some of the problems that can be met when using this tool. Osmium isotopes as well as Fe-S-C systematics are used to help refine the previously ambiguous depositional settings of this unit.

This thesis is written as a series of papers and as such, each chapter has its own specific conclusions. Below, I will highlight the main conclusions from each of the chapters. As with any research, the more you do the more questions you come across, so for each chapter I have highlighted some areas of potential future research

5.1 Re-Os geochronology of the Green River Formation

The results from this chapter demonstrate that the Re-Os geochronometer can be successfully applied to lacustrine organic-rich sedimentary rocks bringing the tool beyond only marine systems. The Re-Os geochronology data of three intervals of the Green River Formation yield dates that are in agreement, within uncertainty, of

interbedded U-Pb and Ar-Ar tuff geochronology. The Re-Os dates for the two Douglas Creek Member sections provide the most precise dates (49.2 ± 1.0 Ma and 48.7 ± 0.6 Ma) although the precision of the ages are controlled by the degree of variability of the initial $^{187}Os/^{188}Os$ composition within the sampled intervals. The Mahogany Zone gives the most imprecise age (47.8 ± 9.9 Ma) related to a small spread in $^{187}Re/^{188}Os$ values, which are comparable to those seen in some marine systems (e.g. Turgeon et al., 2007). Because the same problem of limited spread in $^{187}Re/^{188}Os$ values is found in marine systems (Turgeon et al., 2007; Selby et al., 2009), it is suggested that there is a fundamental aspect of Re-Os geochronology (specifically Re-Os fractionation between the water column and the host organic matter) that is not fully understood in both lacustrine and marine systems.

Assessment of Re-Os systematics by comparison to organic geochemical parameters derived from Rock-Eval pyrolysis suggests that the controls on Re and Os fractionation within organic-rich sedimentary rocks are complex. In this case controls are related to depositional environment (proximal lake shore versus distal lake centre) and organic matter type (terrestrial versus algal). However, the relationship of Re and Os to oxygen index (measure of oxygen content of kerogen) suggests there appears to be a threshold below which enrichment and fractionation are optimal. This data highlights the importance of understanding the chelating precursors of Re and Os in organic matter. We currently do not have strong constraints on where Re and Os are held within organic matter. Most studies suggest them to be held in porphyrins similar to Ni and V (Lewan and Maynard, 1982; Miller, 2004; Selby et al., 2007; Rooney et al., 2012), but this is still an area of research that needs to be more fully addressed as Re and Os do not always behave in the same manner as Ni and V. Oxygen index is a proxy for the atomic O/C ratio, so in order to investigate this link further, studies comparing Re-Os and atomic O/C could be a starting point. However, most crucial is the ability to separate organic matter into its components and assess Re and Os abundances and fractionation in each one and hence define the chelating precursors of Re and Os. However, there currently does not exist a method to do this without disturbing Re-Os systematics, so this is an urgent area of research.

It is clear from this study that the main controls on Re and Os uptake and fractionation will require more studies to pin down, but I think it is important to highlight one other aspect. That is the relationship of Re and Os with organic matter, particularly prior to sequestration within an organic-rich unit. We currently have limited knowledge of how Re and Os relate to the biological cycle and whether this has any impact on where and why it is held in kerogen. Both elements are generally thought to be unrelated to the biological cycle (Crusius et al., 1996). However, this study suggests that the type of organic matter (algal versus terrestrial) has a bearing on Re-Os fractionation, and so it is essential that these areas are investigated further in order to further our knowledge of the Re-Os organic-rich sedimentary rock geochronometer.

In addition to geochronology, this study highlights the initial $^{187}Os/^{188}Os$ composition (1.41 - 1.54) of lake water at the time of deposition derived from Re-Os data of these lacustrine organic-rich sedimentary rocks. This can be used to determine the geochemical signature of continental runoff into lake basins, derived from weathering of the geological hinterland of the Green River Formation. Firstly, this is a potential tool to distinguish between marine and lacustrine sediments when seawater $^{187}Os/^{188}Os$ is well characterised (Chapter 2; Poirier and Hillaire-Marcel, 2011). However, in order for this method to be accurate throughout geological time, the seawater Os isotope curve needs a huge amount more work particularly pre-Cenozoic, where most constraints are limited by individual geochronological studies. The critical difference between Os isotope stratigraphy and other chemostratigraphic tools is that the Re-Os geochronometer can provide direct age constraints giving much higher confidence in global correlations. Secondly, Os isotope stratigraphy of lacustrine successions can be applied to understanding fluctuations in continental climatic, tectonic and magmatic regimes through its record of runoff. An area of research that would be very interesting would be to make further assessments of the Os composition of runoff into lake basins through geological time. Currently we have no means of assessing the Os composition of runoff throughout history and so it can be difficult to make inferences on the causes of variations in the Os isotope composition

of seawater. A more complete picture of runoff Os composition would aid this research, but would need to be cautious to take into account individual catchments and their relation to global scale dynamics.

This study has demonstrated that the Re-Os geochronometer can be successfully applied to lacustrine organic-rich sedimentary rocks, providing a valuable tool for determining the direct depositional history of lacustrine systems and furthermore, for understanding and correlating continental geological processes. Lacustrine sedimentary successions provide exceptionally high-resolution records of continental geological processes, responding to tectonic, climatic and magmatic influences. These successions are therefore essential for correlating geological and climatic phenomena across continents and furthermore the globe.

5.2 Re-Os geochronology, Os isotope fingerprinting and hydrous pyrolysis of the Green River petroleum system

This chapter details Re-Os systematics and geochronology for the Green River petroleum system hydrocarbons in the Uinta Basin, including oils, tars sands and gilsonite. The Re-Os geochronology derived from all the hydrocarbons of the Green River petroleum system (19 ± 14 Ma) broadly agrees with the most recent petroleum generation basin models (25 Ma; Ruble et al., 2001). However, a long and variable generation history and a very thick source unit (>3000 m) has made Re-Os geochronology challenging. Previous studies have suggested that a fundamental aspect of precise Re-Os hydrocarbon geochronology requires samples to be sourced from a discrete source unit that will transfer similar Os isotopic compositions to the hydrocarbons (Lillis and Selby, in press). This then allows deduction of precise isochrons as they will have started with similar initial Os isotopic compositions (Os_i). This study corroborates these findings. The large uncertainties produced for the Green River hydrocarbon Re-Os geochronology are clearly derived from variation in the Os_i of the Green River source rocks, which is transferred to the hydrocarbons during generation. The Green River Formation has experienced multiple generation stages

and is potentially still generating petroleum. This results in the hydrocarbons containing a mix of Os_i. When separating the samples based on Os_i, the precision of the geochronology increases as well as when separating them based on organic geochemical properties (levels of β-carotane). The Green River oils also have very low Re and Os abundances which hampers analysis and so larger uncertainties are derived, again reducing the precision of geochronology. This suggests that low abundance samples are not ideal for Re-Os geochronology. Nevertheless this study illustrates that the Re-Os hydrocarbon generation geochronology can be applied to variable hydrocarbon phases (oils, tar sands and gilsonite) derived from lacustrine Type I kerogen just as successfully as when it is used in marine petroleum systems (Selby et al., 2005; Selby and Creaser, 2005; Selby et al., 2007; Finlay et al., 2011). This study broadens the range of systems that could be used for Re-Os geochronology, but further studies should seek to establish this as a tool in all hydrocarbons sourced from all kerogen types. In order to more fully comprehend Re-Os fractionation during hydrocarbon generation, a better appreciation of the location of Re and Os in kerogen is needed (as described in section 5.1) and this cannot be fully understood until all kerogen types have been analysed. In addition, further studies tying organic geochemical parameters to Re-Os may elucidate how these elements relate to variable organic matter.

This study also analyses osmium isotopes as a fingerprinting tool able to trace the hydrocarbons to their source, the Green River Formation. The most satisfying results find that the Os_i values of the gilsonite and GRB oils (~1.6) deduces their source as the Mahogany Zone agreeing with previous gilsonite correlation studies. The data for the GRA oils and tar sands is more ambiguous. The Os_i suggests the lower Douglas Creek Member (CW1 core) as the most probable source of the GRA oils and tar sands. The Douglas Creek Member (M16 core) has Os_i higher than all the hydrocarbons (>1.7) and as it is from an area that is not buried sufficiently for oil generation, it is likely that this this unit has not generated oil. The Douglas Creek Member (CW1 core) may be the most likely source sampled and this is consistent with previous correlation studies in the Green River petroleum system, but it may be that the exact source has not been

sampled, or is from multiple depths as generation moves up section. This study illustrates the ability of Os isotopes to elucidate the spatial variations within a petroleum system. In future work it would be useful to sample more source units within the Green River Formation in order to more comprehensively fingerprint the hydrocarbons to their specific source, which may also aid in geochronology. This would also elucidate lateral as well as vertical variations within the petroleum system, and may help define the location of the source 'kitchen', a key problem in petroleum geoscience.

Hydrous pyrolysis experiments are also carried out on the Green River Formation source rocks. This technique involves artificial maturation of a source rock and provides oil and bitumen samples through maturation stages, which are then analysed for their Re and Os abundances and isotopic compositions. This allows the transfer and fractionation behaviour of Re and Os to be assessed. The hydrous pyrolysis experiments on the Green River Formation source rocks show that Re and Os transfer are mimicking the natural system in contrast to a previous hydrous pyrolysis study on the Phosphoria and Staffin Formations (Rooney et al., 2012). The transfer of Re and Os from source to bitumen to oil does not affect source rock systematics or isotopic compositions. Thus these experiments further confirm that Re-Os systematics in source rocks are not adversely affected by hydrocarbon maturation. In addition, these experiments confirm that Os isotope compositions are transferred intact from source to hydrocarbon during hydrocarbon generation and so can be used as a powerful correlation tool, exemplified in this natural and experimental study on the Green River Formation. This study illustrates that the Os isotope fingerprinting tool can be used on a wide range of hydrocarbon phases sourced from variable kerogen types and so could be very useful in the petroleum industry where oil-source correlation can often be challenging. Future work in this area could employ hydrous pyrolysis experiments to a wider variety of source rocks and kerogen types in order to more fully comprehend Re-Os systematics. In particular this may explain why the Phosphoria Formation (Type II-S) shows such different systematics in comparison to the Green

River Formation (Type I) and whether kerogen type is a major controlling factor in Re-Os geochemistry.

This study has successfully demonstrated that Re-Os hydrocarbon geochronology and Os isotope fingerprinting can be applied to variable petroleum systems and hydrocarbon types, whether they are biodegraded or not. This is particularly important to the petroleum industry where smaller and more unusual plays are being explored much more frequently and so inorganic tools for elucidating the nature of these systems are of utmost importance.

5.3 Re-Os geochronology and Fe speciation of the Nonesuch Formation

This chapter involves dating the late Mesoproterozoic lacustrine Nonesuch Formation in order to assess Re-Os geochronology in more complex lacustrine systems. This North American rift succession only contains geochronology in the volcanics associated with rifting; the overlying post-rift sediments contain no age constraints. The most precise Re-Os depositional date is 1078 ± 24 Ma for samples with similar Os_i, which agrees with the underlying U-Pb ages. There is a large variation in Os_i in the Nonesuch Formation as well as a low range in $^{187}Re/^{188}Os$ ratios, which hamper geochronology. This is similar to geochronology of some of the Green River Formation units (Chapter 2) and may suggest that lacustrine depositional systems have an effect on Re-Os fractionation. Certainly in these systems it may be possible that the residence time of Os is lower than the ocean and so changes in the inputs of Os are more easily recorded in the sediments. However this would require further research of several different lake systems in order to try to quantify the variation in residence time of Os that occurs in a lake. In order to explain the homogeneity in $^{187}Re/^{188}Os$ ratios, an increased understanding of the influences on Re-Os fractionation is required as highlighted in section 5.1.

In this study I also use Os isotopes to gain a better understanding of the depositional setting providing an appraisal for this technique defined in chapter 2. The arguments against a lacustrine environment of deposition for the Nonesuch Formation

are weak, but here we assess the depositional setting using Os. The Os composition is compared to two studies of marine systems at this time that have Os_i of ~0.3 (Azmy et al., 2008; Rooney et al., 2010). As these are the only studies from this time period, we extrapolate that the marine Os value is not likely to have deviated much from this value. Because the Nonesuch Formation has consistently more radiogenic Os_i values (0.65 to 0.91), we suggest that it is a lacustrine signal derived from input from the surrounding continental crust, making it more radiogenic than seawater and so arguing against an influx of seawater that would likely overcome this value. These conclusions would greatly benefit from better constraints on the seawater Os isotope curve as well as the residence time of Os in lakes (as discussed in section 5.1).

The Fe speciation technique is also employed during this study to assess the water column redox conditions of the lake during deposition of the Nonesuch Formation. A significant body of evidence suggests that the marine environment remained largely anoxic throughout most of the Precambrian. In contrast, the oxygenation history of terrestrial aquatic environments has received little attention, despite the significance of such settings for early eukaryote evolution. The Fe speciation technique allows distinction between euxinic (H_2S-bearing) and ferruginous conditions (Fe-rich). The Fe-S-C systematics for the Nonesuch Formation suggest that it was deposited from an anoxic ferruginous water column. Thus, similar to Mid-Late Proterozoic oceans, anoxia persisted in terrestrial aquatic environments, and euxinic water column conditions were apparently not widespread. This new data refutes suggestions that oxygenation of the terrestrial realm was pervasive based on S isotopes alone (Parnell et al., 2010). Therefore, oxygenation of the terrestrial realm may not have preceded that of the marine environment, signifying a major requirement for further investigation of links between the oxygenation state of terrestrial aquatic environments and eukaryote evolution. This area of research requires further redox studies of these environments to establish how and when they became oxygenated.

This study provides evidence that Precambrian lacustrine organic-rich sedimentary rocks can be dated using Re-Os geochronology and that Os isotopes can help to deduce depositional environments. However, it highlights the need for more research in areas such as: the seawater Os isotope curve, residence time of Os in lakes and redox conditions of lakes early in Earth's history.

5.4 References

Azmy, K., Kendall, B., Creaser, R. A., Heaman, L., and de Oliveira, T. F., 2008. Global correlation of the Vazante Group, Sao Francisco Basin, Brazil: Re-Os and U-Pb radiometric age constraints. Precambrian Research 164, 160-172.

Crusius, J., Calvert, S., Pedersen, T., Sage, D., 1996. Rhenium and molybdenum enrichments in sediments as indicators of oxic, suboxic and sulfidic conditions of deposition. Earth and Planetary Science Letters 145, 65-78.

Finlay, A. J., Selby, D., Osborne, M.J., 2011. Re-Os geochronology and fingerprinting of United Kingdom Atlantic margin oil: Temporal implications for regional petroleum systems. Geology 39, 475-478.

Lewan, M. D. and Maynard, J. B., 1982. Factors controlling enrichment of vanadium and nickel in the bitumen of organic sedimentary rocks. Geochimica et Cosmochimica Acta 46, 2547-2560.

Lillis, P.G., Selby, D., Evaluation of the rhenium-osmium geochronometer in the Phosphoria petroleum system, Bighorn Basin of Wyoming and Montana, USA. Geochimica et Cosmochimica. In press.

Miller, C.A., 2004. Re-Os dating of algal laminites: reduction-enrichment of metals in the sedimentary environment and evidence for new geoprphyrins. PhD Thesis, University of Saskatchewan.

Parnell, J., Boyce, A. J., Mark, D., Bowden, S., and Spinks, S., 2010, Early oxygenation of the terrestrial environment during the Mesoproterozoic: Nature 468, 290-293.

Poirier, A., Hillaire-Marcel, C., 2011. Improved Os-isotope stratigraphy of the Arctic Ocean. Geophysical Research Letters 38. L14607.

Rooney, A.D., Selby, D., Houzay, J.-P., Renne, P.R., 2010. Re-Os geochronology of a Mesoproterozoic sedimentary succession, Taoudeni basin, Mauritania: implications for basin-wide correlations and Re-Os organic-rich sediments systematics. Earth and Planetary Science Letters 289, 486-496.

Rooney, A.D., Selby, D., Lewan, M.D., Lillis, P.G., Houzay, J.-P., 2012. Evaluating Re–Os systematics in organic-rich sedimentary rocks in response to petroleum generation using hydrous pyrolysis experiments. Geochimica et Cosmochimica Acta 77, 275-291.

Ruble, T.E., Lewan, M.D., Philp, R.P., 2001. New insights on the Green River Petroleum System in the Uinta Basin from hydrous pyrolysis experiments. AAPG Bulletin 85, 1333-1371.

Selby, D. and Creaser, R. A., 2005. Direct radiometric dating of hydrocarbon deposits using rhenium-osmium isotopes. Science 308, 1293-1295.

Selby, D., Creaser, R. A., Dewing, K., and Fowler, M., 2005. Evaluation of bitumen as a Re-187-Os-187 geochronometer for hydrocarbon maturation and migration: A test case from the Polaris MVT deposit, Canada. Earth and Planetary Science Letters 235, 1-15.

Selby, D., Creaser, R. A., and Fowler, M. G., 2007. Re-Os elemental and isotope systematics in crude oils. Geochimica et Cosmochimica Acta 71, 378-386.

Selby, D., Mutterlose, J., and Condon, D.J., 2009. U-Pb and Re-Os geochronology of the Aptian/Albian and Cenomanian/Turonian stage boundaries: Implications for timescale calibration, osmium isotope seawater composition and Re-Os systematics in organic-rich sediments. Chemical Geology 265, 394-409.

Turgeon, S. C., Creaser, R. A., and Algeo, T. J., 2007. Re-Os depositional ages and seawater Os estimates for the Frasnian-Famennian boundary: Implications for weathering rates, land plant evolution, and extinction mechanisms. Earth and Planetary Science Letters 261, 649-661.

Appendix A

Earth and Planetary Science Letters 359-360 (2012) 194–205

Contents lists available at SciVerse ScienceDirect

Earth and Planetary Science Letters

journal homepage: www.elsevier.com/locate/epsl

Re–Os geochronology of the lacustrine Green River Formation: Insights into direct depositional dating of lacustrine successions, Re–Os systematics and paleocontinental weathering

Vivien M. Cumming [a,*], David Selby [a], Paul G. Lillis [b]

[a] Department of Earth Sciences, Durham University, Durham, DH1 3LE, UK
[b] US Geological Survey, Box 25046, MS977, Denver Federal Centre, Denver, CO 80225, USA

ARTICLE INFO

Article history:
Received 16 May 2012
Received in revised form
26 September 2012
Accepted 11 October 2012
Editor: T. Elliot
Available online 16 November 2012

Keywords:
Re–Os geochronology
lacustrine
Green River Formation
Uinta basin
osmium

ABSTRACT

Lacustrine sedimentary successions provide exceptionally high-resolution records of continental geological processes, responding to tectonic, climatic and magmatic influences. These successions are therefore essential for correlating geological and climatic phenomena across continents and furthermore the globe. Producing accurate geochronological frameworks within lacustrine strata is challenging because the stratigraphy is often bereft of biostratigraphy and directly dateable tuff horizons. The rhenium–osmium (Re–Os) geochronometer is a well-established tool for determining precise and accurate depositional ages of marine organic-rich rocks. Lake systems with stratified water columns are predisposed to the preservation of organic-rich rocks and thus should permit direct Re–Os geochronology of lacustrine strata. We present Re–Os systematics from one of the world's best documented lacustrine systems, the Eocene Green River Formation, providing accurate Re–Os depositional dates that are supported by Ar–Ar and U–Pb ages of intercalated tuff horizons. Precision of the Green River Formation Re–Os dates is controlled by the variation in initial $^{187}Os/^{188}Os$ and the range of $^{187}Re/^{188}Os$ ratios, as also documented in marine systems. Controls on uptake and fractionation of Re and Os are considered to relate mainly to depositional setting and the type of organic matter deposited, with the need to further understand the chelating precursors of Re and Os in organic matter highlighted. In addition to geochronology, the Re–Os data records the $^{187}Os/^{188}Os$ composition of lake water (1.41–1.54) at the time of deposition, giving an insight into continental runoff derived from weathering of the geological hinterland of the Green River Formation. Such insights enable us to evaluate fluctuations in continental climatic, tectonic and magmatic processes and provide the ability for chemostratigraphic correlation combined with direct depositional dates. Furthermore, initial $^{187}Os/^{188}Os$ values can be used as a diagnostic tool to distinguish between lacustrine and marine depositional settings when compared to known oceanic $^{187}Os/^{188}Os$ values.

1. Introduction

Lake systems are common to the continental landscape throughout the world and frequently record deposition over millions of years (e.g., Carroll et al., 1992; Olsen, 1997). Lacustrine sediments provide a valuable archive of continental geological processes, at a much higher resolution than globally averaged marine records (Pietras and Carroll, 2006). The importance of lacustrine deposits is exemplified by the numerous studies providing vital insights into processes such as continental tectonics and magmatism, paleoclimatic fluctuations, geomagnetic timescales, Milankovitch cycles, terrestrial biotic evolution and economic resources (e.g., Carroll and Bohacs, 1999; Hao et al., 2011; Katz, 2001; Lambiase, 1990; Machlus et al., 2004; Meyers, 2008). Sedimentation in lake settings can range from fluvial to highly organic-rich profundal deposits documenting a complex amalgamation of continental and atmospheric processes. A more complete understanding of the relationship of lacustrine sediments to global geological systems requires accurate and precise geochronological frameworks. Age control in lacustrine settings is often hampered by the lack of biostratigraphic constraints common to the marine record. In the absence of tuff horizons for U–Pb and Ar–Ar geochronology, or sufficient and documented mammalian biostratigraphy, direct dating of lacustrine sedimentary stratigraphy is challenging.

The Re–Os geochronometer is a widely-used tool for determining precise and accurate depositional ages of marine organic-rich rocks (e.g., Cohen et al., 1999; Georgiev et al., 2011;

* Corresponding author. Tel.: +44 191 3342300; fax: +44 191 3342301.
E-mail address: v.m.cumming@durham.ac.uk (V.M. Cumming).

0012-821X/$ - see front matter © 2012 Elsevier B.V. All rights reserved.
http://dx.doi.org/10.1016/j.epsl.2012.10.012

Kendall et al., 2009a; Selby and Creaser, 2005; Xu et al., 2009). These and additional studies have demonstrated that Re–Os systematics are not adversely affected by processes such as hydrocarbon maturation and greenschist-grade metamorphism (e.g., Creaser et al., 2002; Kendall et al., 2004; Rooney et al., 2012, 2010; Yang et al., 2009). However, application of the Re–Os geochronometer to lacustrine strata has only been partially evaluated (Creaser et al., 2008; Poirier and Hillaire-Marcel, 2011). Here we present a comprehensive study of one of the world's best documented lacustrine systems, the Green River Formation (GRF), to assess whether Re–Os geochronology can be used as a tool to directly date the deposition of lacustrine organic-rich rocks.

Previous studies suggest the uptake of Re and Os in marine organic-rich rocks relies on the capture of hydrogenous Re and Os at or below the sediment/water interface under oxygen limited conditions (Cohen et al., 1999; Colodner et al., 1993; Crusius et al., 1996; Ravizza and Turekian, 1992; Ravizza et al., 1991), with the majority of Re and Os bound in organic matter (Cohen et al., 1999; Georgiev et al., 2011; Rooney et al., 2012; Selby and Creaser, 2003). This implies that organic-rich rocks deposited in reducing bottom waters of a stratified lake should be predisposed to Re and Os uptake, and thus viable for Re–Os geochronology, provided there is sufficient runoff containing dissolved Re and Os. As interpreted for the marine realm, the initial $^{187}Os/^{188}Os$ (Os_i) composition of lacustrine organic-rich rocks should reflect the $^{187}Os/^{188}Os$ composition of lake water at the time of deposition (Cohen et al., 1999; Ravizza and Turekian, 1992, 1989). The $^{187}Os/^{188}Os$ composition of seawater records a balance of radiogenic ($\sim$1.40) continental inputs derived chiefly from runoff with minor contributions from aeolian dust, and unradiogenic ($\sim$0.12) inputs derived from cosmic dust and hydrothermal alteration of oceanic crust (Peucker-Ehrenbrink and Ravizza, 2000). Assuming that runoff from the surrounding continental crust is the predominant source of Os into a lake, the $^{187}Os/^{188}Os$ composition of lake water will reflect the composition of regional continental runoff at the time of deposition. Os isotopes therefore provide an insight into regional geological processes and allow chemostratigraphic correlation making Re–Os geochronology beneficial beyond direct depositional age dating.

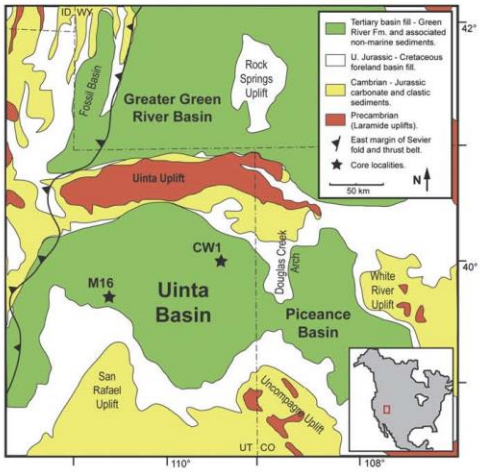

Fig. 1. Location map displaying the main basins containing the Green River Formation, the surrounding geology and the location of the sampled Marsing 16 (M16; 39°57′ 1.4904″N, 111°1′37.527″W) and Coyote Wash 1 (CW1; 40°1′22.224″N, 109°18′38.4834″W) cores in the Uinta Basin (adapted from Smith et al., 2008a). The GRF basins formed east of the thin-skinned Sevier orogenic belt, and are separated by Laramide basement-cored uplifts, the geometry of which is controlled by Precambrian and late Palaeozoic structures (Johnson, 1992). These structures were occupied by two large lakes covering an area of 65,000 km^2 during the early to middle Eocene. The CW1 core is located in the central depocentre of an asymmetric basin structure (See Fig. 2, inset A), while the M16 core is proximal to the lake margin. Inset map of North America shows the study area.

Here we evaluate and discuss lacustrine Re–Os geochronology and Os isotope compositions of the GRF in the Uinta Basin, Utah, USA. The GRF succession represents a classic model of lacustrine sediment deposition and is primarily comprised of organic-rich carbonaceous siltstones, mudstones and marly oil shales (Keighley et al., 2003; Smith et al., 2008a; Tuttle and Goldhaber, 1993). Interbedded tuff horizon Ar–Ar and U–Pb dates provide an extensive geochronological framework, which has been tied to mammalian biostratigraphy, paleomagnetic and astronomical ages (Smith et al., 2010, 2008a, 2006, 2003). This temporal framework makes the GRF an ideal natural laboratory for testing the applicability of the Re–Os geochronometer to lacustrine deposits.

2. Geological setting

2.1. Geology of the Green River Formation basins

The GRF was deposited in three main continental basins (Fig. 1: Uinta, Piceance and Greater Green River), in Colorado, Wyoming and Utah (Dyni, 2006). The extensive Green River lake system was associated with temperate to subtropical climate of the early to middle Eocene (Smith et al., 2008a), which resulted in exceptionally high continental denudation rates (175 ± 30 m/Myr; Smith et al., 2008b). Sedimentary facies within the GRF can be divided into fluvio-lacustrine, fluctuating profundal and evaporative facies (Carroll and Bohacs, 1999, 2001; Fig. 2). Deposition occurred in freshwater to hypersaline lakes with lake-level fluctuations resulting in thick packages of organic-rich carbonaceous shales interbedded with fluvial clastic deposits (Keighley et al., 2003; Pietras and Carroll, 2006). The final stages of GRF deposition occurred at the end of the Laramide orogeny when the basins were infilled from the north by volcanics from the Absaroka volcanic field (Johnson, 1992). The Uinta Basin was the final basin to be infilled and therefore had the longest-lived lake containing the thickest section of GRF (>3 km). Organic-rich units from the Uinta basin were sampled for this study as they record the complete history of the GRF.

2.2. Uinta Basin stratigraphy

Lacustrine deposition in the Uinta Basin began in the early Eocene following eastward retreat of the Late Cretaceous seaway (Ryder et al., 1976). Initial deposition began with the Colton Formation (coarse grained clastic beds and red mudstones), which was deposited in a fluvial setting. As lake-levels rose the depositional setting evolved into fluvio-lacustrine deposition of sandstones interbedded with the base of the GRF and at the lake edges (Fig. 2). Stratigraphically above the Colton Formation, the Douglas Creek Member of the GRF was deposited in response to rising lake-levels (Bradley, 1931; Tuttle and Goldhaber, 1993). The Douglas Creek Member is a siliciclastic-dominated interval with fluvial sandstones and siltstones deposited at the edges of the basin and oil shales deposited in the central depocentres, considered correlative to the green shale and black shale facies of the GRF in other parts of the basin (Remy, 1992; Ruble et al., 2001). This depositional model has been attributed to fluctuating profundal facies deposition (Carroll and Bohacs, 2001). Following deposition of this interval an increase in salinity is

attributed to the development of a more arid climate between 49 and 50 Ma (Ryder et al., 1976; Tuttle and Goldhaber, 1993). Increased aridity resulted in evaporitic deposition of saline minerals interbedded with dolomitic marlstones, mudstones, sandstones and oil shales of the carbonate dominated Parachute Creek Member, stratigraphically above the Douglas Creek Member (Fig. 2). The basal section of the Parachute Creek Member (~49 Ma) records a rise in lake-levels to their maximum extent that resulted in the deposition of oil shales interbedded with mudstones, marlstones and siltstones. This section, the Mahogany Zone, is the most organic-rich horizon of the GRF (total organic carbon [TOC] up to 30 wt%; Bradley, 1931; Smith et al., 2008a; Tuttle and Goldhaber, 1993). Deposition in the Uinta Basin continued until ~44 Ma with conditions becoming progressively more evaporitic (Smith et al., 2008a). Above the Parachute Creek Member red-brown shale and fluvial coarse-grained clastics make up interbeds of the Uinta Formation of the GRF (Keighley et al., 2003).

2.3. Previous geochronology

The current geochronological framework for the GRF is based on Ar–Ar ages of interbedded tuffs concentrated in the Greater Green River and Uinta Basins (Smith et al., 2008a; 2006; 2003). More recently, the Ar–Ar ages have been recalibrated to Fish Canyon Sanidine (KO_8) and accurately correlated to U–Pb zircon ages from the tuff beds and astronomical ages preserved within cyclical sediments (Kuiper et al., 2008; Smith et al., 2010). Uinta Basin deposition began ~52 Ma, but the oldest dated tuff is the Curly tuff at 49.32 ± 0.30 Ma lying just below the Mahogany Zone (Fig. 2). This makes correlation of the older stratigraphy in the Uinta Basin more difficult, especially as there is a lack of surface exposure (Smith et al., 2008a). Lacustrine deposition ended just after deposition of the Strawberry tuff dated at 44.27 ± 0.93 Ma. Geochronology in the Uinta Basin allows cross-correlation of Re–Os and Ar–Ar ages in order to assess the accuracy of Re–Os lacustrine organic-rich rock geochronology.

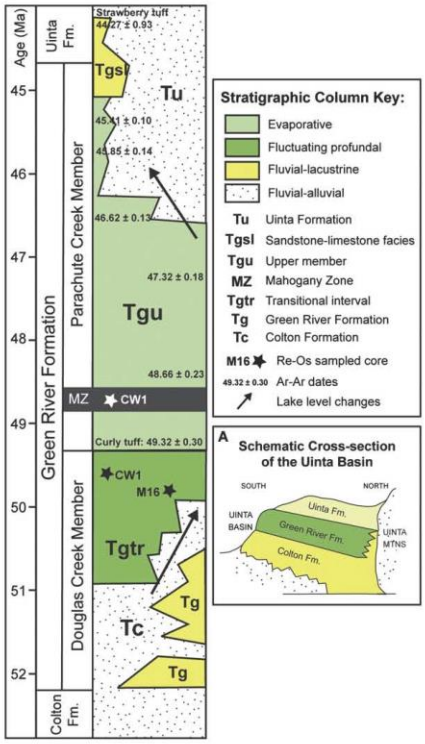

Fig. 2. Generalised chronostratigraphy displaying the main members of the GRF and the location of sampled units. Age constraints labelled on the stratigraphic column are based on Ar–Ar dates of interbedded tuffs. Lacustrine facies associations of each unit are illustrated in the right hand panel of the stratigraphic column; these are adapted from lithostratigraphy of Smith et al. (2008a). This lithostratigraphy illustrates the complex nature of spatial and temporal variation of units within the Uinta basin. Nomenclature of Smith et al. (2008a) is included in the key in order to aid comparison with Ar–Ar ages. Inset A is a simplified cross-section of the Uinta Basin at the present day that illustrates the asymmetric nature of the basin and that the erosional remnant now outcrops within the southern limb of a gentle syncline, dipping <5° to the North. The southern margin of the basin has mostly been eroded, with the most continuous exposure in the northeast corner of the basin where up to ~4 km of sediment was deposited. With a lack of surface exposure this asymmetric nature makes correlation of units challenging.

3. Sampling and methodology

Uinta Basin GRF samples were collected from two exploration drill-cores (Coyote Wash 1 [CW1] and Marsing 16 [M16]; Fig. 1). The Mahogany Zone and the Douglas Creek Member were sampled as these are the most organic-rich intervals of GRF in the Uinta Basin (3.5–28.1 wt% TOC: Table 1). The sampled stratigraphy comprises grey–black carbonaceous mudstones and oil shales of the profundal dominated intervals. All sampled core sections are absent of alteration and veining. Re–Os isotope analysis was performed at Durham University's TOTAL laboratory for source rock geochronology and geochemistry following published methods used for Re–Os dating of marine organic-rich rocks (Selby, 2007; Selby and Creaser, 2003). TOC analysis and Rock-Eval pyrolysis was performed at Weatherford labs, Houston. A detailed description of the samples and methods used for this study is provided in the Supplementary Material.

4. Results

4.1. TOC and Rock-Eval

The TOC and Rock-Eval pyrolysis results for all samples are presented in Table 1. The Douglas Creek Member (M16) has the lowest TOC of the 3 sections (3.5 to 9.7 wt%), with the Douglas Creek Member (CW1) possessing highly variable TOC (2.6 to 24.7 wt%), with 9 of the 12 samples yielding TOC < 10 wt%. In comparison, the Mahogany Zone (CW1) possesses TOC values between 9.3 and 28.1 wt%, with 9 of 11 samples analysed yielding TOC > 10 wt%. Rock-Eval pyrolysis is used to assess the type and maturity of organic matter in the samples. The T_{max} (assessment of maturity using the temperature at maximum generation of remaining hydrocarbons after free oil is removed) values for all the samples are similar and range between 432 and 448 °C signifying moderate maturity. The type of organic matter in our samples is assessed using the hydrogen and oxygen indexes (HI versus OI), as screening proxies to the van Krevelen atomic H/C versus O/C diagram (Espitalie et al., 1977; Peters, 1986; Fig. 3). The HI and OI data illustrate that all samples are Type I kerogen, consistent with previous GRF studies (Katz, 1995; Tissot et al., 1978).

4.2. Re–Os geochronology

The Re and Os abundances for the Douglas Creek Member (M16) are 21.0–62.4 ppb and 178–490 ppt, respectively (Table 1). This is a substantial enrichment in comparison to estimates for average continental crust (0.2–1 ppb Re and 30–50 ppt Os; Esser and Turekian, 1993; Hattori et al., 2003; Peucker-Ehrenbrink and Jahn, 2001; Sun et al., 2003). These abundances generally co-vary and are comparable to abundances in marine organic-rich rocks (e.g., Cohen et al., 1999; Kendall et al., 2009a; Selby and Creaser, 2005; Xu et al., 2009). The $^{187}Re/^{188}Os$ and $^{187}Os/^{188}Os$ ratios range from 328.6 to 1015.2 and 1.82 to 2.35, respectively. Linear regression of the Re–Os data yields a Model 3 age of 48.4 ± 2.7 Ma (2σ, n=13, Mean Squared of Weighted Deviation [MSWD]=6.8, Os_i=1.54 ± 0.03; Fig. 4A; all ages include ^{187}Re decay constant uncertainty). Douglas Creek Member samples (CW1) are also enriched in Re and Os with abundances of 10.5–83.5 ppb and 114–412 ppt, respectively (Table 1). The $^{187}Re/^{188}Os$ ratios range from 326.9 to 1830.5, with $^{187}Os/^{188}Os$ ratios between 1.57 and 2.89. Linear regression of the Re–Os data yields a Model 3 age of 49.8 ± 4.8 Ma (2σ, n=13, MSWD=39, Os_i=1.41 ± 0.06; Fig. 4D). Samples from the Mahogany Zone (CW1) also display enriched Re and Os abundances ranging from 11.8 to 39.5 ppb and 198 to 815 ppt, respectively (Table 1). The $^{187}Re/^{188}Os$ values have a limited range from 296 to 451 but exhibit a positive correlation to the $^{187}Os/^{188}Os$ values ranging from 1.72 to 1.83. Regression of this Re-Os data yields a Model 1 age of 47.8 ± 9.9 Ma (2σ, n=13, MSWD=0.43, Os_i of 1.48 ± 0.06; Fig. 4F).

Table 1
Re–Os isotope data, total organic carbon (TOC) content and Rock-Eval data for the Green River Formation samples.

Sample	Depth (m)	Re (ppb)	±	Os (ppt)	±	^{192}Os (ppt)	±	$^{187}Re/^{188}Os$	±	$^{187}Os/^{188}Os$	±	rho [a]	Os_i [b]	TOC (wt%)	T_{max} [c] (°C)	S1[d]	S2[e]	S3[f]	HI[g]	OI[h]
Douglas Creek Member, Marsing 16 core (39°57′1.4904″N, 111°1′37.527″W)																				
M16-27[i]	323.8	22.6	0.1	341.3	2.3	115.3	0.9	390.2	3.3	1.831	0.018	0.722	1.52	5.96	435	2.33	59.28	0.81	994	13.6
M16-26[i]	323.9	23.6	0.1	333.5	2.6	112.3	1.0	418.3	4.1	1.861	0.022	0.718	1.52	6.47	437	2.17	51.46	0.74	796	11.4
M16-25[i]	324.0	42.6	0.1	490.0	2.8	163.4	0.9	518.6	3.3	1.950	0.013	0.680	1.53	9.71	437	2.89	68.68	0.86	707	8.9
M16-24[j]	324.0	27.8	0.1	393.8	3.0	132.7	1.2	417.4	4.0	1.854	0.022	0.704	1.52	7.09	440	2.85	54.60	0.78	770	11.0
M16-23[i]	324.5	54.9	0.2	341.6	1.9	109.5	0.6	997.4	6.5	2.336	0.014	0.819	1.53	8.20	435	1.99	61.77	0.93	753	11.3
M16-22[i]	324.6	56.0	0.2	343.1	2.1	109.8	0.7	1015.2	7.1	2.352	0.016	0.790	1.53	–	–	–	–	–	–	–
M16-21[i]	324.6	62.4	0.2	392.8	2.5	126.0	0.8	984.8	6.9	2.326	0.017	0.735	1.53	5.42	438	1.91	44.93	0.69	829	12.7
M16-20[i]	324.7	40.1	0.1	351.6	1.5	115.7	0.4	690.2	3.2	2.079	0.008	0.599	1.52	5.53	441	2.10	49.53	0.73	896	13.2
M16-19[i]	324.7	24.5	0.1	263.1	1.4	87.5	0.4	556.4	3.4	1.982	0.013	0.665	1.53	3.53	437	1.64	33.23	0.78	942	22.1
M16-18[j]	324.9	29.2	0.1	273.4	1.5	90.0	0.4	645.0	3.8	2.078	0.013	0.651	1.56	6.39	448	2.23	68.53	0.89	1073	13.9
M16-16[j]	325.1	21.0	0.1	178.2	1.2	58.2	0.4	716.3	5.5	2.145	0.019	0.725	1.57	5.71	443	13.44	51.69	0.81	906	14.2
M16-15[j]	325.3	22.9	0.1	297.1	1.6	99.4	0.5	458.1	2.7	1.923	0.012	0.648	1.55	5.23	442	1.56	42.36	0.73	811	14.0
M16-14[j]	325.4	16.8	0.1	300.2	1.8	101.5	0.6	328.6	2.2	1.819	0.014	0.654	1.55	4.87	445	1.23	42.67	0.75	877	15.4
Douglas Creek Member, Coyote Wash 1 core (40°1′22.224″N, 109°18′38.4834″W)																				
CW1-40[k]	1026.0	23.4	0.1	307.8	1.7	104.6	0.6	445.0	2.9	1.774	0.012	0.682	1.40	6.01	441	2.13	52.15	1.59	867	26.4
CW1-41[k]	1026.1	14.6	0.1	258.5	1.9	89.0	0.8	326.9	3.2	1.654	0.020	0.699	1.38	7.55	444	1.72	63.99	1.90	848	25.2
CW1-42[k]	1026.2	10.5	0.0	184.0	1.5	63.3	0.7	330.0	3.6	1.657	0.022	0.732	1.38	6.83	442	2.35	57.89	1.95	847	28.5
CW1-44	1026.5	14.2	0.1	245.4	1.8	85.2	0.8	331.7	3.3	1.573	0.020	0.702	1.30	7.07	442	1.50	73.03	1.24	1032	17.5
CW1-45	1026.6	30.3	0.1	256.7	1.5	84.9	0.5	711.0	4.7	2.028	0.014	0.728	1.44	9.98	439	5.24	106.70	1.28	1069	12.8
CW1-46	1026.8	34.9	0.1	303.2	1.6	100.2	0.5	692.4	4.2	2.036	0.013	0.695	1.46	7.44	438	3.06	76.44	1.06	1027	14.2
CW1-48[k]	1027.0	15.3	0.1	145.4	1.3	48.6	0.6	627.6	7.4	1.921	0.027	0.756	1.40	2.67	434	2.62	22.24	1.03	832	38.5
CW1-49[k]	1027.2	83.5	0.3	298.9	1.8	90.7	0.5	1830.5	11.1	2.889	0.018	0.712	1.37	7.85	441	2.74	83.74	0.92	1066	11.7
CW1-50[k]	1027.4	46.6	0.2	412.1	3.8	137.3	1.5	675.1	7.6	1.963	0.032	0.635	1.40	15.46	440	4.48	146.19	1.20	946	7.8
CW1-51	1027.5	11.5	0.0	114.3	1.1	38.2	0.5	600.3	8.2	1.936	0.030	0.807	1.44	4.97	436	1.22	42.69	0.86	859	17.3
CW1-53	1027.7	17.7	0.1	180.5	1.4	60.2	0.6	584.4	5.9	1.960	0.023	0.751	1.47	–	–	–	–	–	–	–
CW1-54[k]	1027.8	39.1	0.1	346.0	1.9	115.3	0.6	674.9	4.1	1.956	0.013	0.645	1.40	24.70	438	8.12	222.95	1.51	903	6.1
CW1-55	1028.0	33.8	0.1	385.3	2.1	129.5	0.7	519.5	3.1	1.879	0.012	0.635	1.45	16.92	437	5.05	163.78	1.30	968	7.7
Mahogany Zone, Coyote Wash 1 core (40°1′22.224″N, 109°18′38.4834″W)																				
CW1-05	682.5	15.2	0.1	294.0	2.3	100.5	1.0	301.1	3.2	1.716	0.022	0.719	1.48	11.28	439	6.45	117.31	2.13	1040	18.9
CW1-06	682.7	28.0	0.1	486.0	2.9	165.7	1.0	336.0	2.4	1.746	0.014	0.673	1.48	22.78	443	11.69	237.11	1.92	1041	8.4
CW1-07	682.8	25.5	0.1	464.1	2.8	158.5	1.0	320.2	2.3	1.730	0.014	0.673	1.48	22.59	445	9.55	248.16	2.10	1099	9.3
CW1-09	683.2	26.7	0.1	362.6	4.5	122.6	2.2	433.0	7.8	1.822	0.048	0.668	1.48	25.82	436	11.95	272.55	1.81	1055	7.0
CW1-10	683.4	20.8	0.1	383.2	3.0	130.8	1.2	316.4	3.2	1.735	0.022	0.698	1.48	14.47	437	7.47	149.11	2.04	1031	14.1
CW1-12	683.6	15.5	0.1	264.2	2.8	89.9	1.4	344.1	5.3	1.765	0.036	0.721	1.49	9.69	434	6.65	95.36	2.48	985	25.6
CW1-13	683.7	15.6	0.1	295.3	2.4	100.8	1.0	307.1	3.4	1.737	0.023	0.717	1.49	9.39	434	6.84	96.77	2.01	1031	21.4
CW1-14	683.9	16.7	0.1	326.8	3.3	111.8	1.6	297.9	4.5	1.717	0.034	0.710	1.48	–	–	–	–	–	–	–
CW1-15	684.3	11.8	0.0	198.4	2.2	67.5	1.1	349.0	5.8	1.768	0.037	0.742	1.49	10.30	439	6.29	108.94	2.20	1058	21.4
CW1-16	684.5	14.6	0.1	286.2	2.3	97.7	1.0	296.6	3.3	1.730	0.024	0.717	1.49	11.35	441	5.70	119.94	1.68	1057	14.8
CW1-20	684.9	32.7	0.1	426.9	5.3	144.1	2.7	451.2	8.5	1.837	0.048	0.684	1.48	28.15	436	13.85	265.66	1.80	944	6.4
CW1-22	685.2	39.2	0.1	559.9	4.4	189.4	1.6	411.3	3.8	1.816	0.023	0.612	1.49	21.14	432	10.45	223.98	2.01	1060	9.5
CW1-23	685.4	20.1	0.1	366.4	3.2	125.0	1.4	320.1	3.7	1.737	0.026	0.704	1.48	–	–	–	–	–	–	–

All uncertainties are stated at 2σ.

[a] Rho is the associated error correlation at 2σ (Ludwig, 1980).
[b] Os_i is the initial $^{187}Os/^{188}Os$ isotope ratio calculated at 48.4, 49.8 and 47.8 Ma for each unit, respectively.
[c] T_{max}=temperature at maximum evolution of S2 hydrocarbons.
[d] S1=free oil content (mg hydrocarbons/g of rock).
[e] S2=remaining hydrocarbon potential (mg hydrocarbons/g of rock).
[f] S3=organic carbon dioxide (mg CO_2/g of rock).
[g] HI=Hydrogen Index (mg hydrocarbon/g C_{org}).
[h] OI=Oxygen Index (mg CO_2/g C_{org}).
[i] Re–Os Age=49.2 ± 1.0 Ma.
[j] Re–Os Age=50.1 ± 2.6 Ma.
[k] Re–Os Age=48.7 ± 0.6 Ma.

5. Discussion

5.1. Re–Os lacustrine organic-rich rock geochronology

Regression of all Re–Os data from the individually sampled sections of the CW1 and M16 cores yield ages that agree, within uncertainty, with the GRF Ar–Ar and U–Pb dates (see Section 5.2). However, Model 3 ages and large MSWD values strongly suggest that any scatter about the isochron is controlled by geological factors, rather than purely analytical uncertainties (Ludwig, 2008). Precise Re–Os geochronology requires samples with similar Os_i, and a spread in $^{187}Re/^{188}Os$ ratios of at least a few hundred units (Kendall et al., 2009a; Selby and Creaser, 2005). To assess whether samples have similar Os_i, the isotopic compositions of each sample are back-calculated using the ^{187}Re decay constant (1.666×10^{-11} a^{-1}; Smoliar et al., 1996) and the age determined from the respective isochron (Table 1).

Regression of the Douglas Creek Member (M16) yields a Model 3 age of 48.4 ± 2.7 Ma, (MSWD=6.8; Fig. 4A). The calculated Os_i at 48.4 Ma for all the samples varies from 1.52 to 1.57, with stratigraphically lower samples having higher Os_i values of 1.55–1.57 (n=4) and the remaining stratigraphically higher samples possessing Os_i values of 1.52–1.53 (n=9). Separate regression of the Re–Os data based on the Os_i values (1.55–1.57 and 1.52–1.53; Table 1), yield Model 1 ages of 50.1 ± 2.6 Ma (2σ, n=4, MSWD=0.43, $Os_i = 1.54 \pm 0.02$; Fig. 4C) and 49.2 ± 1.0 Ma (2σ, n=9, MSWD=0.99, $Os_i = 1.52 \pm 0.01$; Fig. 4B), respectively. Both of these ages are identical within uncertainty, with the 49.2 ± 1.0 Ma date providing the most precise depositional age for the Douglas Creek Member. The Model 1 ages and lower MSWD values suggest that stratigraphic changes in Os_i values is the principal control on the degree of scatter associated with the isochron of all M16 samples. The precise and accurate ages for these subsets strongly discounts any post-depositional disturbance to the Re–Os system. The stratigraphic variation in Os_i suggests a change in Os inputs or alteration of the balance and/or flux of Os inputs into the lake over time. In the case of the M16 samples, the 1 m of stratigraphy sampled could represent approximately 2.5–10 Ka (Smith et al., 2008a).

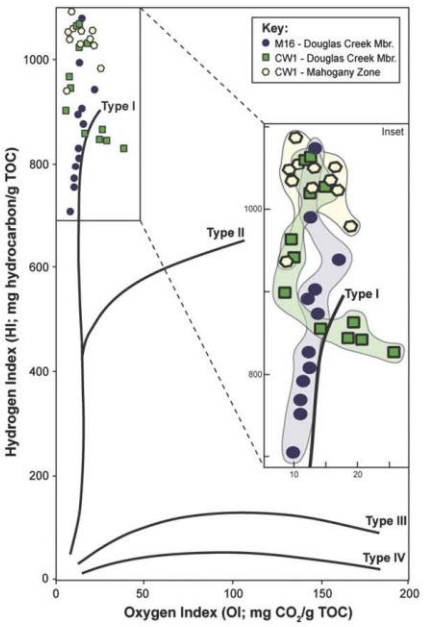

Fig. 3. Graph of hydrogen index versus oxygen index (HI/OI) as a proxy to an atomic H/C versus atomic O/C van Krevelen diagram (Espitalie et al., 1977; Peters, 1986). Lines for kerogen Types I to IV are annotated on the graph (taken from Hunt, 1996). All the samples are plotted illustrating that they are all Type I kerogen. The enlarged inset shows the area where samples are plotted with each of the sampled units outlined in order to demonstrate the variation in each horizon. See text for further discussion.

The Douglas Creek Member (CW1) yields a Model 3 age of 49.8 ± 4.8 Ma with an MSWD of 39 (Fig. 4D). The Os_i values calculated at 49.8 Ma vary substantially (1.30–1.47; Table 1). Unlike the Douglas Creek Member (M16), there is no stratigraphic relationship to Os_i in this core, suggesting that Os influx into the basin was very heterogeneous or that the Re–Os isotopic system has been disturbed during post-depositional processes. The isochronous nature of the samples and good agreement between the Re–Os data and Ar–Ar geochronology of the GRF suggest limited or no disturbance to the Re–Os system. We suggest that the scatter about the linear regression relates to variations in the Os_i of these samples (Fig. 4D inset). Interestingly seven of the samples have similar Os_i (1.37–1.40) and regression of this Re–Os data yields a precise Model 1 age of 48.7 ± 0.6 Ma (2σ, n=7, MSWD=1.8, $Os_i = 1.41 \pm 0.01$; Table 1; Fig. 4E).

The Mahogany Zone (CW1) Re–Os data yield a Model 1 age of 47.8 ± 9.9 Ma, MSWD 0.43 (Fig. 4F). The Os_i values calculated at 47.8 Ma are very similar (1.48 to 1.49; Table 1) and $^{187}Re/^{188}Os$ and $^{187}Os/^{188}Os$ values display limited spread through this core (150 and 0.1 units, respectively). These ranges are much smaller than the Douglas Creek Member (M16 and CW1) sections which have ranges in $^{187}Re/^{188}Os$ values >650 and >1500 units, respectively and ranges in $^{187}Os/^{188}Os$ values >0.5 and >1.3 units, respectively. The lower MSWD is due to the very small range in $^{187}Os/^{188}Os$, which exaggerates the measured uncertainty thereby permitting an isochron fit. The larger uncertainty in the age for the Mahogany Zone CW1 can be attributed to the small ranges in $^{187}Os/^{188}Os$ and $^{187}Re/^{188}Os$. In an attempt to increase the variation in $^{187}Re/^{188}Os$ values, the sampled interval was increased from 2 m to 3 m (see Fig. 4), however $^{187}Re/^{188}Os$ and $^{187}Os/^{188}Os$ values remained extremely similar. The small spread cannot be attributed to sampling or analytical problems as the same protocols were used for all units and previous studies on marine sequences (e.g. Kendall et al., 2009a, Rooney et al., 2012; Selby and Creaser, 2005).

A limited spread in $^{187}Re/^{188}Os$ of organic-rich rocks has also been seen for marine units. For example, over the Frasnian–Famennian (F–F) boundary $^{187}Re/^{188}Os$ values range only ~20 units, with the Re–Os data yielding an imprecise date of 476 ± 140 Ma (Turgeon et al., 2007). Three other units surrounding the F–F boundary produced more precise ages with $^{187}Re/^{188}Os$ values spanning 200–400 units. The low spread in $^{187}Re/^{188}Os$ was interpreted to be the result of Re drawdown due to increasing anoxia (Turgeon et al., 2007), with the dated interval at the F–F boundary recording the highest sea-level and most anoxic stage compared to the other dated intervals (Johnson et al., 1985; Ver Straeten et al., 2011). Likewise, it has also been suggested that in restricted basins organic matter sedimentation draws down dissolved Re and Os from the water column thus shortening residence time and causing rapid variations in Os_i values due to higher sensitivity to changes in Os inputs (McArthur et al., 2008). This may be the case for the Douglas Creek Member (CW1) unit where we see the largest variation in Os_i values which is causing scatter about the isochron (Fig. 4D). However, large

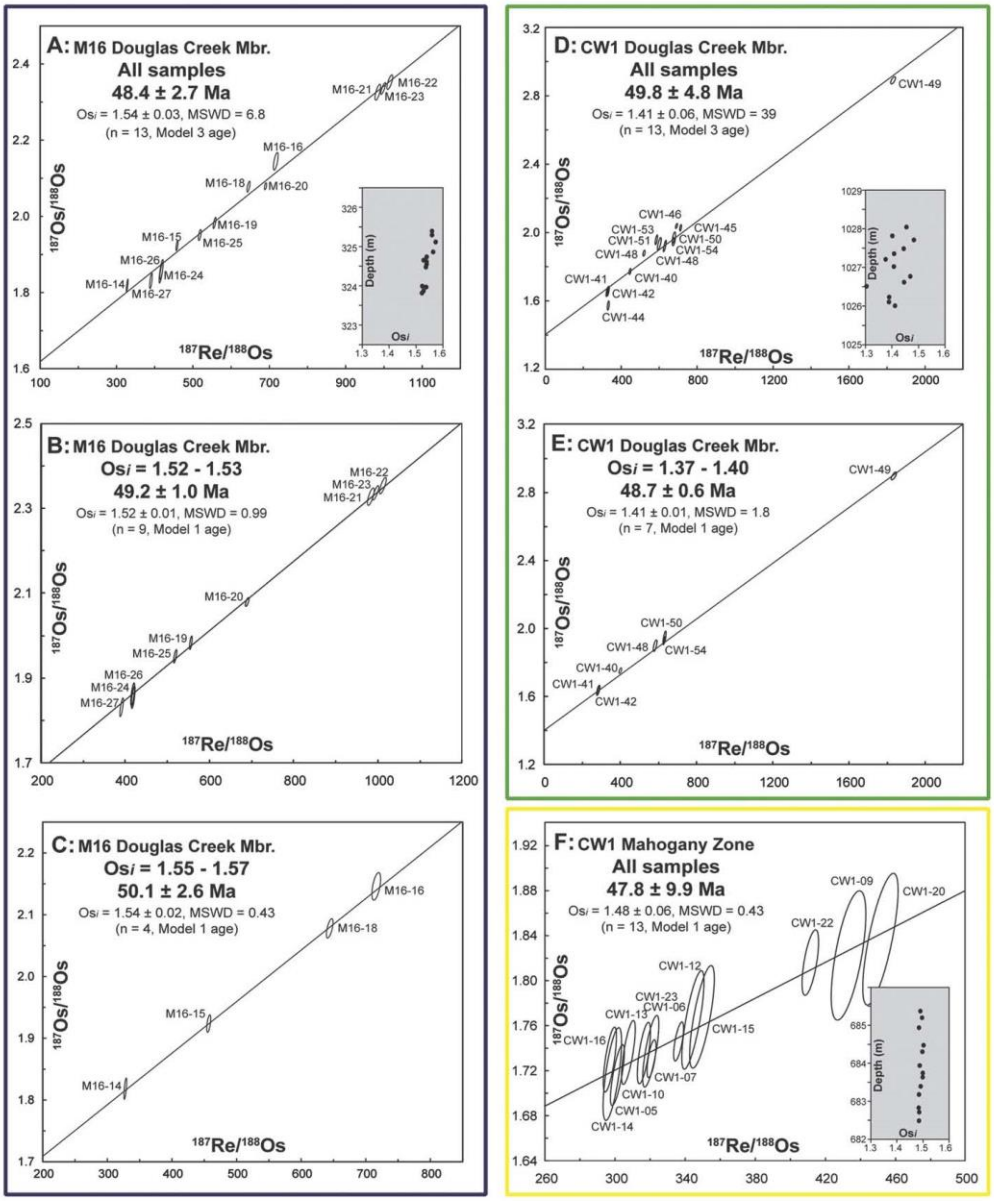

Fig. 4. Re–Os isochron diagrams for the Douglas Creek Member in the Marsing 16 core (A, B and C) and the Coyote Wash 1 core (D and E), and for the Mahogany Zone (F). The Re–Os isotopic data including the 2σ calculated uncertainties for $^{187}Re/^{188}Os$ and $^{187}Os/^{188}Os$ and the associated error correlation function (rho) are regressed to yield a Re–Os date using *Isoplot V.* 4.0 and the λ ^{187}Re constant of 1.666×10^{-11} a^{-1} (Ludwig, 2008, 1980; Smoliar et al., 1996). The age uncertainty including the uncertainty of 0.35% in the ^{187}Re decay constant (Selby et al., 2007; Smoliar et al., 1996) only affects the third decimal place. A Model 1 isochron is accomplished by assuming that scatter along the regression line is derived only from the input of 2σ uncertainties for $^{187}Re/^{188}Os$ and $^{187}Os/^{188}Os$, and ρ (rho). MSWD = Mean Squared of Weighted Deviation. Data point ellipses are 2σ uncertainties. Isochrons A, D and F represent regression of all the samples for each horizon and isochrons B, C and E represent regression of samples with similar initial $^{187}Os/^{188}Os$ (see text for discussion). Isochron E provides a precise depositional age for the Douglas Creek Member (CW1); however, although it agrees within uncertainty of the other ages, it has questionable validity due to the nature of the Os_i variation (see text for discussion). It can also be suggested that isochron E is pinned by sample CW1-49, but when the other 6 points are regressed they produce a Model 1 age of 51.0 ± 2.7 Ma (2σ, $n = 6$, MSWD = 1.5, $Os_i = 1.39 \pm 0.02$) which is within uncertainty of the seven point Re–Os seen in isochron E. The inset graphs show the Os_i versus depth of the samples for each horizon. The scales are the same for each graph so the variation in sampling depth and Os_i is visible. The sampled horizon for the Douglas Creek Member in the M16 core is 1.6 m, in the CW1 core it is 2 m and in the Mahogany Zone in the CW1 core it is 2.9 m.

gradients in Os_i values are not observed in the GRF and there is no significant change in Re and Os abundance through the sampled intervals suggesting that Re and Os drawdown does not occur. In similarity to the F–F boundary interval, the Mahogany Zone was deposited during the highest lake-levels and most anoxic period (Bradley, 1931; Tuttle and Goldhaber, 1993). We suggest that, rather than having intense Re or Os drawdown, the Mahogany Zone depositional environment (high lake-level, steady sedimentation and stable water column stratification; Smith et al., 2008a; Tuttle and Goldhaber, 1993) allowed for homogenous Re and Os uptake and thus minimal fractionation throughout the sampled interval, which hampers the utility of the strata for precise Re–Os geochronology.

In addition, it has been suggested that organic-rich rocks deposited in terrestrial basins will possess low $^{187}Re/^{188}Os$ values (<200; Baioumy et al., 2011). However, the $^{187}Re/^{188}Os$ data for all GRF sections is >200, with two of the sections (Douglas Creek Member) that represent more restricted deposition yielding significant variation in $^{187}Re/^{188}Os$ ratios (328–1831), similar to marine organic-rich rocks (Kendall et al., 2009a and references therein). As such, our findings contradict previous studies that suggest restricted and terrestrial deposits may not be viable for Re–Os geochronology (Baioumy et al., 2011; McArthur et al., 2008). We suggest that lacustrine deposits, like marine systems, vary enormously and basins should be assessed individually for Re–Os geochronology.

5.2. Comparison of Re–Os dates with Ar–Ar geochronology in the Uinta Basin

Although the Uinta Basin is an intensively studied lacustrine succession, correlation of the stratigraphy is hampered by informal and overlapping terminology, mainly due to a lack of surface exposure (Remy, 1992; Smith et al., 2008a). In this case Ar–Ar geochronology provides the ability to assess the accuracy of the Re–Os dates of the GRF lacustrine organic-rich rocks, although the Ar–Ar dates are more precise. The Curly tuff (Ar–Ar: 49.32 ± 0.30 Ma) is the oldest tuff dated in the Uinta Basin, lying ~50 m below the Mahogany Zone at the top of the Transitional interval (Smith et al., 2008a). This interval forms part of the lower Parachute Creek Member and the upper Douglas Creek Member (Fig. 2), defined as a time of fluctuating profundal deposition (Smith et al., 2008a). The Douglas Creek Member intervals sampled are ~300 m (CW1 core) and ~400 m (M16 core) below the Curly tuff (Tuttle and Goldhaber, 1993). With estimated sedimentation rates ranging from 100 to 400 mm/Kyr in the Green River basins (Smith et al., 2008a), 400 m of sediment could have been deposited in 1 to 4 Myr. This suggests that the Re–Os dates for the Douglas Creek Member and the Mahogany Zone (Fig. 4) are in agreement with the Ar–Ar date for the Curly tuff (Fig. 2). A larger sequence stratigraphic study of the Uinta Basin would be needed to clarify this further. The oldest dated tuff in the adjacent Piceance Creek Basin is the Yellow tuff dated at 51.55 ± 0.52 Ma, which is stratigraphically equivalent to the lowest Douglas Creek Member and therefore should be and is older than the Re–Os dated sections. This agreement between the Ar–Ar and Re–Os geochronology demonstrates that the Re–Os system can be successfully applied to lacustrine organic-rich rocks to provide much-needed direct depositional age constraints in lacustrine basins, especially in the absence of Ar–Ar and U–Pb tuff geochronology. The concordance between direct and indirect depositional age determinations emphasises the expediency of geochronological methods for correlating global phenomena.

5.3. Re-Os uptake and fractionation

Our current understanding of the definitive controls of Re and Os uptake and fractionation in organic-rich rocks is incomplete. Here we briefly summarise previous findings and reveal how this study contributes to solving the dilemma emphasising the complex nature of Re and Os systematics in organic-rich rocks. Early studies suggested that sub-oxic to anoxic or euxinic conditions must exist for Re and Os uptake into organic-rich rocks, which occurs at or below the sediment–water interface (Cohen et al., 1999; Colodner et al., 1993; Crusius et al., 1996; Koide et al., 1991; Morford and Emerson, 1999). These studies and further experimental works provided evidence that Re and Os behave differently in the water column, with distinct uptake mechanisms and unknown controls on fractionation (Levasseur et al., 1998; Morford et al., 2009; Selby et al., 2009; Sundby et al., 2004; Yamashita et al., 2007). Recent work has also questioned the notion that Re and Os are directly linked to TOC values, with correlations occasionally but not always apparent despite the majority of these metals being held within the kerogen (Cohen et al., 1999; Rooney et al., 2012; Selby et al., 2009). High TOC requires high primary productivity with preservation potential reliant on a calm, oxygen-poor water body, without scavenging benthic life (Demaison and Moore, 1980; Sageman et al., 2003), however, these factors may not solely regulate Re and Os uptake and fractionation. Slow sedimentation has been proposed as one of the key factors in enhanced Re and Os uptake as seen for Ni and *V* enrichment in organic-rich rocks (Crusius and Thomson, 2000; Lewan and Maynard, 1982; Rooney et al., 2012; Selby et al., 2009). However, slow sedimentation may adversely affect TOC preservation due to the longer residence time for oxidation (Ibach, 1982). Aside from the principal condition requiring Re and Os in the water column, other influences that have been proposed to control Re and Os enrichment and fractionation are salinity (Martin et al., 2001), post-deposition mobility of the elements (Crusius and Thomson, 2000; Kendall et al., 2009a), pH and temperature (Georgiev et al., 2011). Since Re and Os are bound within the kerogen of an organic-rich rock (Rooney et al., 2012), but enrichment is affected by numerous processes beyond TOC preservation, a better appreciation of the organic matter chelating precursors of Re and Os is needed. In V and Ni studies it has been shown that the chelating precursor is not always preserved proportionally to organic matter (Lewan and Maynard, 1982) thus understanding the chelating precursor systematics of Re and Os will significantly advance our understanding of the Re–Os system.

Our data have shown that Re–Os geochronology can be successfully applied to lacustrine organic-rich rocks, and that element fractionation and abundances are similar to marine systems. However, the results are mixed with an accurate and precise isochron for the Douglas Creek Member (M16), but larger age uncertainties for the Mahogany Zone and Douglas Creek Member (CW1). We suggest that homogenous Re–Os fractionation is the cause of the larger uncertainty in the Mahogany Zone geochronology, although the reasons for this are currently ambiguous. In order to explain why these units behave differently in terms of Re–Os fractionation, TOC and Rock-Eval data are evaluated. These data yield insights into the GRF organic matter and hence Re–Os uptake and fractionation in lacustrine settings.

5.3.1. Insights from TOC and depositional conditions

In the three GRF units a positive but weak linear correlation of Re and common Os (^{192}Os) to TOC exists (Fig. 5A and B), with the Mahogany Zone displaying the best correlation. Rhenium versus TOC in the Mahogany Zone displays a positive trend (R^2 of 0.73)

yet the Douglas Creek Member shows no correlation (R^2 of 0.12 [CW1] and 0.17 [M16]). In terms of ^{192}Os versus TOC there is no strong correlation in any of the sections and they all have similar R^2 values (Mahogany Zone=0.56; Douglas Creek Member CW1=0.52; Douglas Creek Member M16=0.41). Despite weak correlations, the sampled horizons display variable relationships to TOC. The Douglas Creek Member (M16) has negligible correlation of both Re and Os to TOC, but much higher slopes than the other two units. These findings suggest an uptake mechanism possibly unrelated to TOC dominated in this region of the lake/water column, in contrast to Re and Os uptake in the Mahogany Zone which has the best correlation with TOC. The Douglas Creek Member represents a proximal lake margin setting during a time of fluctuating lake-levels producing variation in the sedimentation rate and terrigenous input; possibly allowing variable Re–Os uptake and fractionation. In contrast, the Mahogany Zone was deposited in the distal lake centre when lake-levels were at their maximum and enhanced primary productivity and slow and steady sedimentation rates in a stratified water column produced an extremely organic-rich and homogenous section (Boyer, 1982; Bradley, 1931; Smith et al., 2008a; Tuttle and Goldhaber, 1993). The homogenous depositional system of the Mahogany Zone may have allowed greater association of Re and Os with organic matter allowing less ^{187}Re/^{188}Os fractionation making precise Re–Os geochronology challenging. The relationship to depositional conditions suggests that, contrary to the Mahogany Zone, in the Douglas Creek Member sections the organic chelating components responsible for Re and Os uptake are not being preserved uniformly or that there are variable chelating surfaces derived from different organic matter types.

Additional GRF depositional factors to take into account are salinity, carbonate content and redox conditions. The Mahogany Zone is more saline and carbonate-rich than the Douglas Creek Member (Keighley et al., 2003; Tuttle and Goldhaber, 1993), with increased salinity creating greater water column stability and higher pH (Tuttle and Goldhaber, 1993). Improved water column stability may have been a contributing factor to the uniform preservation and Re–Os fractionation of the Mahogany Zone, however, these parameters cannot be fully assessed as there is no study of our samples quantifying salinity or carbonate content. Redox conditions of the GRF have not been directly studied although it has been suggested to be euxinic based on sulphur geochemistry (Tuttle and Goldhaber, 1993). During the late lake stage when the Mahogany Zone was deposited, δ^{34}S of sulphides (30–40‰) were higher than during deposition of the early stage Douglas Creek Member (δ^{34}S: 5–15‰). In particular the Mahogany Zone values are unusual as they are much higher than those in marine, freshwater or modern saline lake systems, reflecting complex sulphur geochemistry (Tuttle and Goldhaber, 1993). Fundamentally, the δ^{34}S values are due to a constant supply of sulphate to the lake being progressively reduced by sulphate reducing bacteria causing a gradual enrichment of ^{34}S. Euxinic systems have been previously dated using Re–Os geochronology with success (e.g., Kendall et al., 2009b), however the influence on Re–Os fractionation of extensive sulphate reduction and an abundance of H_2S are unknown. We suspect that the resulting stable water column stratification, particularly evident during Mahogany Zone deposition, is likely to have contributed to the homogenous Re–Os fractionation observed in the Mahogany Zone. This gives further indication of the complex nature of the controls on Re and Os uptake and fractionation and suggests that the depositional system plays a large role in the Re–Os organic system.

5.3.2. Effects of organic matter type

The relationship of Re and Os to TOC and depositional setting highlights that organic matter type may play a key role in Re and Os uptake and fractionation and so hydrogen index (HI) and oxygen index (OI) values from Rock-Eval pyrolysis are used to assess organic matter type of the GRF. A plot of HI/OI values indicates that all samples contain Type I kerogen, consistent with a lacustrine algal source of organic matter, with minimal terrestrial organic matter input (Fig. 3). The variation in HI and OI values cannot easily be explained by changing maturity as all the samples have similar T_{max} values (Peters, 1986; Table 1). Generally both the Douglas Creek Member horizons display more variability in both HI and OI than the Mahogany Zone (See inset Fig. 3). This is consistent with previous observations that strata from the central lake (e.g. Mahogany Zone) contain predominantly alganite organic matter, whereas samples deposited nearer the lake margins or during fluctuating lake-levels (e.g. Douglas Creek Member) contain alganite but also some vitrinite (Castle, 1990). The predominance of alganite in the Mahogany Zone coupled with the lack of Re-Os fractionation may suggest that organic matter type is a controlling factor in Re-Os fractionation. It has previously been postulated that Re and Os are bound by different organic ligands causing variable ^{187}Re/^{188}Os in different organic fractions (Miller, 2004), and also that an unknown method of biological uptake of Re over Os may occur (Georgiev et al., 2011). Our findings suggest that variation in organic matter type (e.g. from terrestrial and algal sources) may enable variable ^{187}Re/^{188}Os (as is seen in the Douglas Creek Member sections), whereas homogenous algal organic matter may lead to homogenous ^{187}Re/^{188}Os (as is seen in the Mahogany Zone) through providing uniform chelating sites for both elements. These findings have strong implications for any future Re-Os geochronological study, however, further studies are required to fully quantify and assess the relationship of Re and Os with organic matter.

Oxygen index is a proxy measurement of oxygen content in kerogen, which can be derived from terrestrial organic matter or oxidation of organic matter (Peters, 1986). We see no correlation between OI and Re and Os abundance (Fig. 5C and D) but below an OI value of ~15 mg CO_2/g TOC, abundances of both Re and Os increase. This may suggest that Re and Os enrichment requires lower oxygen-bearing kerogen or lower oxygen conditions in which the kerogen was deposited. Vanadium and Ni have been found to be bound in tetrapyrroles, of which chlorophyll is the main precursor (Lewan and Maynard, 1982). Chlorophyll is sensitive to oxygen as it opens up the ring structure making it incapable of hosting metals and so sediments settling in an oxygenated water column will have less chance to bind *V* and Ni in tetrapyrroles (Lewan and Maynard, 1982). The binding sites of Re and Os are unknown, but the relationship with OI illustrates the importance of deducing where these metals are held. If Re and Os are more enriched at low OI, this suggests that oxygen has a significant effect on the chelating precursors of Re and Os during deposition and also that the chelating precursors of Re and Os cannot be related to carboxyl complexes. The OI also seems to exert a minor control on ^{187}Re/^{188}Os fractionation below 15 mg CO_2/g TOC (Fig. 5E). This would support the findings of Yamashita et al. (2007) who note that Re is more readily incorporated into organic-rich rocks under highly reducing conditions leading to high ^{187}Re/^{188}Os. However, this study and previous studies concluded that specific controls on fractionation are poorly constrained. For organic matter of lacustrine sedimentary rocks, the non-linear relationship between OI and Re and Os potentially suggests that oxygen content in kerogen and/or organic matter type have a significant effect on chelation of Re and Os and hence Re-Os fractionation. If this proves to be the case in other studied sections, OI may provide a means of assessing whether a section

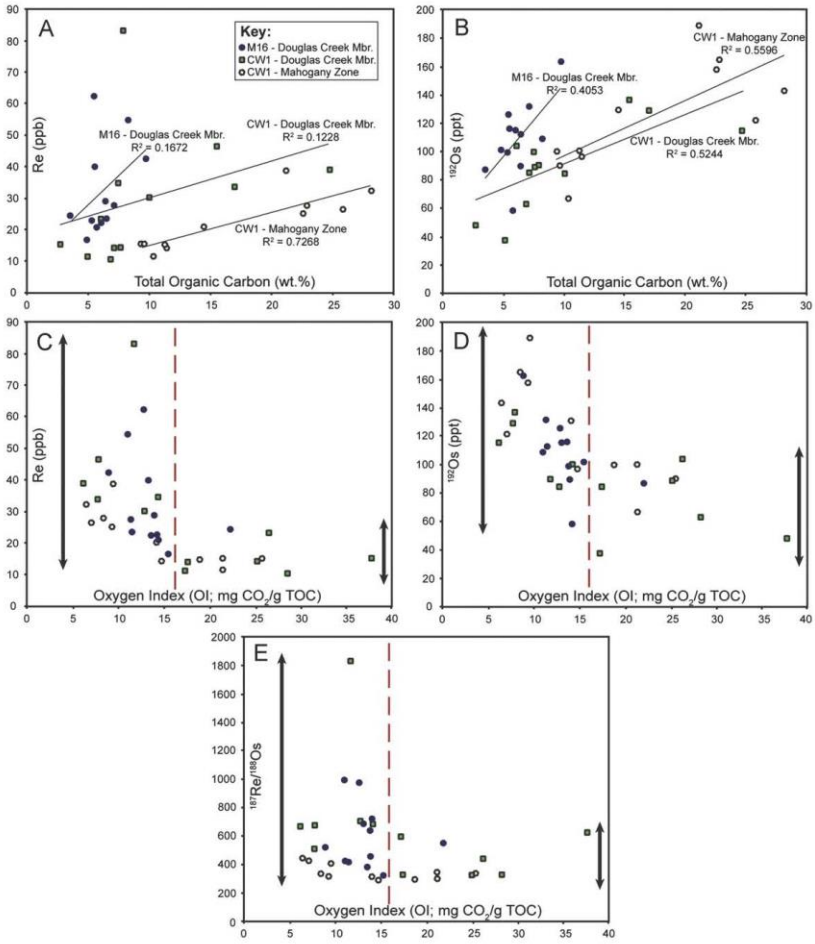

Fig. 5. Graphs of total organic carbon (TOC) versus Re (A) and ^{192}Os (B) of all the studied Green River Formation units showing linear correlations. Common Os (^{192}Os) is plotted to remove the effect of radiogenic in-growth. R^2 for each unit is annotated on the graphs. Oxygen index (OI) versus Re (C), ^{192}Os (D) and $^{187}Re/^{188}Os$ (E) of all the units are also plotted. The dashed line represents the threshold OI below which Re and Os concentrations are increased, and $^{187}Re/^{188}Os$ values are more variable (see text for discussion). The black bars represent the amount of variation in Re, Os and $^{187}Re/^{188}Os$ on each side of the dashed threshold line.

may be viable for precise Re-Os geochronology providing an understanding of maturity and organic matter variation exists as these can affect OI values. However, as OI is a proxy for the atomic O/C ratio, future studies of atomic O/C versus Re–Os may shed further light on these findings and on the chelating precursors of Re and Os. Previous work has utilised OI as a proxy for weathering in order to assess Re–Os isochroneity, with non-isochronous samples possessing higher OI suggested to be caused by weathering (Georgiev et al., 2012). Disparity in OI can be caused by organic facies and maturity variations and therefore can only be a proxy for weathering in a weathering profile of identical strata. As such, ranges in OI should not be employed as a tool for estimating weathering intensity of differing strata.

5.4. Os isotope systematics

The Re-Os isotope data yield Os_i values of 1.54 ± 0.03, 1.41 ± 0.06 and 1.48 ± 0.06 (Fig. 4) for the M16 Douglas Creek Member, CW1 Douglas Creek Member, and CW1 Mahogany Zone, respectively, suggesting a radiogenic terrestrial source of Os in the Uinta lake water column, derived primarily from continental runoff. The variation in Os_i between the three units may be explained by the proximity to different Os sources (e.g., radiogenic Precambrian crust or unradiogenic volcanic units) and the temporal variation in weathering into the Uinta Lake water column. Spatial and temporal variations related to drainage variation are also observed in Sr isotope studies from the Uinta and Greater Green River Basins (Davis et al., 2008;

Rhodes et al., 2002). In the Uinta Basin Sr resolution through the GRF is low, but $^{87}Sr/^{86}Sr$ is radiogenic (mean: 0.71183) and fluctuates (Davis et al., 2008) similarly to the Os_i from this study. In the Greater Green River Basin Sr exhibits fluctuations with more radiogenic $^{87}Sr/^{86}Sr$ (up to 0.71331) during lowstands due to more exposure of radiogenic crust leading to increased riverine input of radiogenic Sr (Rhodes et al., 2002). Although Sr and Os records are decoupled, we suggest that this may also be a contributing factor to the change in Os_i seen in the separate samples used for Re-Os geochronology (see Fig. 4 insets and Table 1), although higher resolution Os isotope stratigraphy through the GRF would be needed to confirm this. In light of the results from this study it is clear that the Os_i of lacustrine sediments, like Sr, can be a useful tool for deducing continental geological processes as it responds to changes in drainage from the surrounding geology, in turn controlled by regional climate, tectonics and magmatism. Oceanic Os has a shorter residence time ($\leq$10,000 years) than Sr (1–4 Myrs), thus yielding much higher resolution perturbations in the geochemical record (Peucker-Ehrenbrink and Ravizza, 2000). However, the variable geological history of lakes means that each lake would need to be assessed individually to deduce Os and Sr residence time.

In addition to providing information about the regional geology and climate, the Os_i can also provide high-resolution data are able to distinguish between marine and lacustrine deposition where other methods fail. The depositional setting of sedimentary basins is often ambiguous and can transition from lacustrine to marine to restricted marine with few clues to the precise nature and timing of these events. An Os isotope stratigraphic study of Lomonosov Ridge sediments from the Arctic Ocean revealed a change from 'lake stage' deposition to oceanic conditions (Poirier and Hillaire-Marcel, 2011). In this case the Os_i is radiogenic (up to 1.3) during the 'lake stage' and with a change to oceanic conditions, the Os_i ($\sim$0.4) then matches the Cenozoic seawater $^{187}Os/^{188}Os$ curve. This allows for the exact transition in the stratigraphy to be determined. Poirier and Hillaire-Marcel's (2011) study coupled with data from this study suggest that if the $^{187}Os/^{188}Os$ of seawater at the time of sediment deposition is known (e.g., seawater during GRF deposition=$\sim$0.56; Kato et al., 2011), large deviations from this value would suggest that the sediments are not marine. Therefore Os_i stratigraphy could be especially helpful in basins where the depositional origin is uncertain or in marine basins that have undergone periods of restriction for unknown lengths of time.

Reconstructing the global ocean Os isotope record and understanding its fluctuations is a major challenge for our understanding of ocean chemistry (Peucker-Ehrenbrink and Ravizza, 2012, 2000). During the Cenozoic, the global ocean Os isotope composition became progressively more radiogenic (0.56 at 50 Ma to a modern day ratio of 1.06; Kato et al., 2011; Peucker-Ehrenbrink and Ravizza, 2000). The specific causes behind this change in Os isotope composition are unknown although similar changes in the Sr record have been related to increases in continental weathering due, principally, to the uplift of the Himalayas (Raymo and Ruddiman, 1992; Richter et al., 1992). However, these two records are decoupled as they vary in their influences and respective residence times and it has also been suggested that the Himalayas are not the dominant source of Os to the oceans during the Cenozoic (Sharma et al., 1999). An underlying problem is that, while we can reconstruct the past global ocean Os curve, we cannot accurately deduce the nature and changes in the sources of Os to the ocean and therefore cannot make accurate inferences as to what is causing the perturbations. Gaining further understanding of the sources of Os to the ocean in the past is vital to further elucidate these problems. The only reliable records of the geochemical composition of past continental runoff are lacustrine sediments as they are minimally affected by other potential inputs into the oceans (e.g. cosmic dust, mid-ocean ridge hydrothermal alteration). In this study the Os_i of the GRF (1.41–1.54) provides the $^{187}Os/^{188}Os$ composition of regional continental runoff into the Green River lakes, similar to estimates for present day $^{187}Os/^{188}Os$ composition of upper continental crust (1.40; Peucker-Ehrenbrink and Ravizza, 2000) and continental runoff (1.54; Levasseur et al., 1999). This similarity may suggest that the composition of continental runoff in the Eocene may have been comparable to the present day. While the GRF Os_i cannot be used as a sole representation of continental runoff into the ocean, it can be noted that lacustrine basins do give an insight into past continental runoff regimes. Though this study cannot rule out radiogenic flux of Os from weathering as the cause of the increase in seawater $^{187}Os/^{188}Os$ over the last 50 Ma, it highlights that continental runoff may not have been the driving force for these changes. Variations in the unradiogenic input to the oceans between 50 Ma and the present day should be more closely examined as a potential cause for seawater $^{187}Os/^{188}Os$ changes. Poirier and Hillaire-Marcel (2011) also find radiogenic $^{187}Os/^{188}Os$ (up to 1.3 at $\sim$36 Ma) during the Arctic Ocean's 'lake stage' before it became fully connected with the global ocean. They suggest that the opening of the Fram Strait may have swamped the global ocean with radiogenic Os contributing to the Cenozoic seawater increase in $^{187}Os/^{188}Os$. These Os isotope studies of lacustrine systems provide valuable insights into continental Os inputs to the oceans and with further research could be used to reconstruct a picture of past global continental runoff and its influence on climate change.

6. Conclusions

The Re–Os systematics of three core intervals of the GRF yield dates that are in agreement, within uncertainty, of U–Pb and Ar–Ar tuff geochronology. This demonstrates that the Re–Os geochronometer can be successfully applied to lacustrine carbonaceous organic-rich rocks, providing a valuable tool for determining the direct depositional history of lacustrine systems and furthermore, for understanding and correlating continental geological processes. Coupled with previous Re–Os studies, our data suggest that, in general, any rock type deposited in conditions where organic matter is preserved is viable for Re–Os geochronology and the tool is not restricted to marine black shales, making this a far-reaching tool for lacustrine and marine depositional settings alike.

This study brings further to light the complexity of Re–Os systematics in organic-rich rocks. The Re–Os dates for the Douglas Creek Member are controlled by the degree of variability of the initial $^{187}Os/^{188}Os$ composition within the sampled 2 m interval. For the Mahogany Zone the imprecise age relates to a small spread in $^{187}Re/^{188}Os$ values comparable to those seen in some marine systems (Turgeon et al., 2007). We suggest that the controls on Re and Os fractionation within organic-rich rocks are complex but in this case are related to depositional environment (proximal lake shore versus distal lake centre) and organic matter type (terrestrial versus algal). The relationship of Re and Os to OI highlights the importance of understanding the chelating precursors of Re and Os in organic matter, in order to further our knowledge of the Re–Os organic-rich sediment geochronometer.

In addition to geochronology, the initial $^{187}Os/^{188}Os$ composition of lacustrine organic-rich rocks can be used to determine the geochemical signature of continental runoff into lake basins. This yields a potential tool to distinguish between marine and lacustrine sediments when seawater $^{187}Os/^{188}Os$ is well

characterised (this study; Poirier and Hillaire-Marcel, 2011). Furthermore, Os isotope stratigraphy of lacustrine successions can be applied to understanding regional climatic, tectonic and magmatic regimes and allows for chemostratigraphic correlations that combine direct depositional ages, giving much higher confidence in global correlations.

Acknowledgements

This research was funded by a Lundin Petroleum CeREES PhD scholarship and the Rocky Mountain Association of Geologists Norman H. Foster scholarship awarded to VMC. The USGS Core Research Centre is thanked for provision of samples and help with sample collection. Michelle Tuttle is thanked for help with core logs and sample information. Mark Allen, Dick Keefer, Greg Ravizza, Mike Lewan and Brian Marshall are thanked for valuable contributions to previous versions of this manuscript. Katz Suzuki and an anonymous reviewer are thanked for helpful reviews of the manuscript. Any use of trade, firm, or product names is for descriptive purposes only and does not imply endorsement by the U.S. Government.

Appendix A. Supporting information

Supplementary data associated with this article can be found in the online version at http://dx.doi.org/10.1016/j.epsl.2012.10.012.

References

Baioumy, H.M., Eglinton, L.B., Peucker-Ehrenbrink, B., 2011. Rhenium–osmium isotope and platinum group element systematics of marine vs. non-marine organic-rich sediments and coals from Egypt. Chem. Geol. 285, 70–81.
Boyer, B.W., 1982. Green River laminites: does the playa-lake model really invalidate the stratified-lake model? Geology 10, 321–324.
Bradley, W.H., 1931. Origin and microfossils of the oil shale of the Green River Formation of Colorado and Utah. US Geological Survey, Professional paper 168.
Carroll, A.R., Bohacs, K.M., 2001. Lake-type controls on petroleum source rock potential in nonmarine basins. AAPG Bull. 85, 1033–1053.
Carroll, A.R., Bohacs, K.M., 1999. Stratigraphic classification of ancient lakes: balancing tectonic and climatic controls. Geology 27, 99–102.
Carroll, A.R., Brassell, S.C., Graham, S.A., 1992. Upper Permian lacustrine oil shales, southern Junggar Basin, Northwest China. AAPG Bull. 76, 1874–1902.
Castle, J.W., 1990. Sedimentation in Eocene lake Uinta (Lower Green River Formation), northeastern Uinta basin, Utah. in: Katz, B.J. (Ed.), Lacustrine Basin Exploration: Case Studies and Modern Analogs, AAPG Memoir 50, AAPG Tulsa, pp. 243–263.
Cohen, A.S., Coe, A.L., Bartlett, J.M., Hawkesworth, C.J., 1999. Precise Re–Os ages of organic-rich mudrocks and the Os isotope composition of Jurassic seawater. Earth Planet. Sci. Lett. 167, 159–173.
Colodner, D., Sachs, J., Ravizza, G., Turekian, K., Edmond, J., Boyle, E., 1993. The geochemical cycles of rhenium: a reconnaissance. Earth Planet. Sci. Lett. 117, 205–221.
Creaser, R., Szatmari, P., Milani, E.J., 2008. Extending Re–Os shale geochronology to lacustrine depositional systems: a case study from the major hydrocarbon source rocks of the Brazilian Mesozoic marginal basins. In: Proceedings of the 33rd International Geological Congress, Oslo (abstract).
Creaser, R.A., Sannigrahi, P., Chacko, T., Selby, D., 2002. Further evaluation of the Re–Os geochronometer in organic-rich sedimentary rocks: a test of hydrocarbon maturation effects in the Exshaw Formation, Western Canada Sedimentary Basin. Geochim. Cosmochim. Acta 66, 3441–3452.
Crusius, J., Calvert, S., Pedersen, T., Sage, D., 1996. Rhenium and molybdenum enrichments in sediments as indicators of oxic, suboxic and sulfidic conditions of deposition. Earth Planet. Sci. Lett. 145, 65–78.
Crusius, J., Thomson, J., 2000. Comparative behavior of authigenic Re, U, and Mo during reoxidation and subsequent long-term burial in marine sediments. Geochim. Cosmochim. Acta 64, 2233–2242.
Davis, S.J., Wiegand, B.A., Carroll, A.R., Chamberlain, C.P., 2008. The effect of drainage reorganization on paleoaltimetry studies: an example from the Paleogene Laramide foreland. Earth Planet. Sci. Lett. 275, 258–268.
Demaison, G.J., Moore, G.T., 1980. Anoxic environments and oil source bed genesis. Org. Geochem. 2, 9–31.
Dyni, J.R., 2006. Geology and resources of some world oil-shale deposits. US Geological Survey Scientific Investigations Report 2005, 5294.
Espitalie, J., Laporte, J.L., Madec, M., Marquis, F., Leplat, P., Paulet, J., Boutefeu, A., 1977. Rapid method for source rocks characterization and for determination of petroleum potential and degree of evolution. Rev. Inst. Fr. Pet. Ann. 32, 23–42.
Esser, B.K., Turekian, K.K., 1993. The osmium isotopic composition of the continental-crust. Geochim. Cosmochim. Acta 57, 3093–3104.
Georgiev, S., Stein, H.J., Hannah, J.L., Bingen, B., Weiss, H.M., Piasecki, S., 2011. Hot acidic late Permian seas stifle life in record time. Earth Planet. Sci. Lett. 310, 389–400.
Georgiev, S., Stein, H.J., Hannah, J.L., Weiss, H.M., Bingen, B., Xu, G., Rein, E., Hatlø, V., Løseth, H., Nali, M., Piasecki, S., 2012. Chemical signals for oxidative weathering predict Re–Os isochroneity in black shales, East Greenland. Chem. Geol. 324–325, 108–121.
Hao, F., Zhou, X., Zhu, Y., Yang, Y., 2011. Lacustrine source rock deposition in response to co-evolution of environments and organisms controlled by tectonic subsidence and climate, Bohai Bay Basin, China. Org. Geochem. 42, 323–339.
Hattori, Y., Suzuki, K., Honda, M., Shimizu, H., 2003. Re–Os isotope systematics of the Taklimakan Desert sands, moraines and river sediments around the Taklimakan Desert, and of Tibetan soils. Geochim. Cosmochim. Acta 67, 1203–1213.
Hunt, J.M., 1996. Petroleum Geochemistry and Geology, 2nd ed. W.H. Freeman and Company, New York.
Ibach, L.E.J., 1982. Relationship between sedimentation-rate and total organic carbon content in ancient marine-sediments. AAPG Bull. Am. Assoc. Pet. Geol. 66, 170–188.
Johnson, J.G., Klapper, G., Sandberg, C.A., 1985. Devonian eustatic fluctuations in Euramerica. Geol. Soc. Am. Bull. 96, 567–587.
Johnson, S.Y., 1992. Phanerozoic evolution of sedimentary basins in the Uinta–Piceance Basin region, northwestern Colorado and northeastern Utah. US Geological Survey Bulletin 1787-FF.
Kato, Y., Fujinaga, K., Suzuki, K., 2011. Marine Os isotopic fluctuations in the early Eocene greenhouse interval as recorded by metalliferous umbers from a Tertiary ophiolite in Japan. Gondwana Res. 20, 594–607.
Katz, B.J., 2001. Lacustrine basin hydrocarbon exploration – current thoughts. J. Paleolimnol. 26, 161–179.
Katz, B.J., 1995. The Green River Shale: an Eocene Carbonate Lacustrine Source Rock. in: Katz, B.J. (Ed.), Petroleum Source Rocks. Springer-Verlag, Berlin, Heidelberg, pp. 309–324.
Keighley, D., Flint, S., Howell, J., Moscariello, A., 2003. Sequence stratigraphy in lacustrine basins: a model for part of the Green River Formation (Eocene), Southwest Uinta Basin, Utah, USA. J. Sediment. Res. 73, 987–1006.
Kendall, B., Creaser, R.A., Selby, D., 2009a. ^{187}Re–^{187}Os geochronology of Precambrian organic-rich sedimentary rocks. Geological Society, 326. Special Publications, London, pp. 85–107.
Kendall, B., Creaser, R.A., Gordon, G.W., Anbar, A.D., 2009b. Re–Os and Mo isotope systematics of black shales from the Middle Proterozoic Velkerri and Wollogorang formations, McArthur Basin, northern Australia. Geochim. Cosmochim. Acta 73, 2534–2558.
Kendall, B.S., Creaser, R.A., Ross, G.M., Selby, D., 2004. Constraints on the timing of Marinoan "Snowball Earth" glaciation by ^{187}Re–^{187}Os dating of a Neoproterozoic, post-glacial black shale in Western Canada. Earth Planet. Sci. Lett. 222, 729–740.
Koide, M., Goldberg, E.D., Niemeyer, S., Gerlach, D., Hodge, V., Bertine, K.K., Padova, A., 1991. Osmium in marine sediments. Geochim. Cosmochim. Acta 55, 1641–1648.
Kuiper, K.F., Deino, A., Hilgen, F.J., Krijgsman, W., Renne, P.R., Wijbrans, J.R., 2008. Synchronizing rock clocks of Earth history. Science 320, 500–504.
Lambiase, J.J., 1990. A model for tectonic control of lacustrine stratigraphic sequences in continental rift basins. in: Katz, B.J. (Ed.), Lacustrine Basin Exploration: Case Studies and Modern Analogs. AAPG Memoir 50, AAPG Tulsa, pp. 265–276.
Levasseur, S., Birck, J., Allegre, C.J., 1998. Direct measurement of femtomoles of osmium and the $^{187}Os/^{186}Os$ ratio in seawater. Science 282, 272–274.
Levasseur, S., Birck, J.L., Allègre, C.J., 1999. The osmium riverine flux and the oceanic mass balance of osmium. Earth Planet. Sci. Lett. 174, 7–23.
Lewan, M.D., Maynard, J.B., 1982. Factors controlling enrichment of vanadium and nickel in the bitumen of organic sedimentary rocks. Geochim. Cosmochim. Acta 46, 2547–2560.
Ludwig, K., 2008. Isoplot, version 4.0: a geochronological toolkit for microsoft Excel. Berkeley Geochronology Centre Special Publication no. 4.
Ludwig, K.R., 1980. Calculation of uncertainties of U-Pb isotope data. Earth Planet. Sci. Lett. 46, 212–220.
Machlus, M., Hemming, S.R., Olsen, P.E., Christie-Blick, N., 2004. Eocene calibration of geomagnetic polarity time scale reevaluated: evidence from the Green River Formation of Wyoming. Geology 32 (137–140).
Martin, C.E., Peucker-Ehrenbrink, B., Brunskill, G., Szymczak, R., 2001. Osmium isotope geochemistry of a tropical estuary. Geochim. Cosmochim. Acta 65, 3193–3200.
McArthur, J.M., Algeo, T.J., van de Schootbrugge, B., Li, Q., Howarth, R.J., 2008. Basinal restriction, black shales, Re–Os dating, and the Early Toarcian (Jurassic) oceanic anoxic event. Paleoceanography 23 (4), PA4217.
Meyers, S.R., 2008. Resolving Milankovitchian controversies: the Triassic Latemar Limestone and the Eocene Green River Formation. Geology 36, 319–322.

Miller, C.A., 2004. Re–Os dating of algal laminites: reduction-enrichment of metals in the sedimentary environment and evidence for new geoporphyrins. Masters Thesis, University of Saskatchewan, pp. 124–128.
Morford, J.L., Emerson, S., 1999. The geochemistry of redox sensitive trace metals in sediments. Geochim. Cosmochim. Acta 63, 1735–1750.
Morford, J.L., Martin, W.R., Francois, R., Carney, C.M., 2009. A model for uranium, rhenium, and molybdenum diagenesis in marine sediments based on results from coastal locations. Geochim. Cosmochim. Acta 73, 2938–2960.
Olsen, P.E., 1997. Stratigraphic record of the early Mesozoic breakup of Pangea in the Laurasia–Gondwana rift system. Annu. Rev. Earth Planet. Sci. 25, 337–401.
Peters, K.E., 1986. Guidelines for evaluating petroleum source rock using programmed pyrolysis. AAPG Bull. 70, 318–329.
Peucker-Ehrenbrink, B., Jahn, B.-m., 2001. Rhenium–osmium isotope systematics and platinum group element concentrations: Loess and the upper continental crust. Geochem. Geophys. Geosyst. 2 (10), 1061–1083.
Peucker-Ehrenbrink, B., Ravizza, G., 2012. Osmium isotope stratigraphy. in: Gradstein, F.M., Ogg, J.G., Schmitz, M., Ogg, G. (Eds.), The Geological Timescale, 1. Elsevier, Oxford, pp. 145–166.
Peucker-Ehrenbrink, B., Ravizza, G., 2000. The marine osmium isotope record. Terr. Nova 12, 205–219.
Pietras, J.T., Carroll, A.R., 2006. High-resolution stratigraphy of an underfilled lake Basin: Wilkins Peak Member, Eocene Green River Formation, Wyoming, USA. J. Sediment. Res. 76, 1197–1214.
Poirier, A., Hillaire-Marcel, C., 2011. Improved Os-isotope stratigraphy of the Arctic Ocean. Geophys. Res. Lett. 38, L14607.
Ravizza, G., Turekian, K.K., 1992. The osmium isotopic composition of organic-rich marine sediments. Earth Planet. Sci. Lett. 110, 1–6.
Ravizza, G., Turekian, G.G., Hay, B.J., 1991. The geochemistry of rhenium and osmium in recent sediments from the Black Sea. Geochim. Cosmochim. Acta 55, 3741–3752.
Ravizza, G., Turekian, K.K., 1989. Application of the ^{187}Re-^{187}Os system to black shale geochronometry. Geochim. Cosmochim. Acta 53, 3257–3262.
Raymo, M.E., Ruddiman, W.F., 1992. Tectonic forcing of late Cenozoic climate. Nature 359, 117–122.
Remy, R.R., 1992. Stratigraphy of the Eocene part of the Green River Formation in the South-Central Part of the Uinta Basin, Utah. US Geological Survey Bulletin 1787-BB.
Rhodes, M.K., Carroll, A.R., Pietras, J.T., Beard, B.L., Johnson, C.M., 2002. Strontium isotope record of paleohydrology and continental weathering, Eocene Green River Formation, Wyoming. Geology 30, 167–170.
Richter, F.M., Rowley, D.B., Depaolo, D.J., 1992. Sr isotope evolution of seawater – the role of tectonics. Earth Planet. Sci. Lett. 109, 11–23.
Rooney, A.D., Selby, D., Houzay, J.-P., Renne, P.R., 2010. Re–Os geochronology of a Mesoproterozoic sedimentary succession, Taoudeni basin, Mauritania: implications for basin-wide correlations and Re–Os organic-rich sediments systematics. Earth Planet. Sci. Lett. 289, 486–496.
Rooney, A.D., Selby, D., Lewan, M.D., Lillis, P.G., Houzay, J.-P., 2012. Evaluating Re–Os systematics in organic-rich sedimentary rocks in response to petroleum generation using hydrous pyrolysis experiments. Geochim. Cosmochim. Acta 77, 275–291.
Ruble, T.E., Lewan, M.D., Philp, R.P., 2001. New insights on the Green River Petroleum System in the Uinta Basin from hydrous pyrolysis experiments. AAPG Bull. 85, 1333–1371.
Ryder, R.T., Fouch, T.D., Elison, J.H., 1976. Early Tertiary sedimentation in the Western Unita Basin, Utah. Geol. Soc. Am. Bull. 87, 496–512.
Sageman, B.B., Murphy, A.E., Werne, J.P., Ver Straeten, C.A., Hollander, D.J., Lyons, T.W., 2003. A tale of shales: the relative roles of production, decomposition, and dilution in the accumulation of organic-rich strata, middle–upper Devonian, Appalachian basin. Chem. Geol. 195, 229–273.
Selby, D., 2007. Direct rhenium–osmium age of the Oxfordian–Kimmeridgian boundary, Staffin bay, Isle of Skye, UK, and the late Jurassic time scale. Norw. J. Geol. 87, 291–300.
Selby, D., Creaser, R.A., 2003. Re–Os geochronology of organic rich sediments: an evaluation of organic matter analysis methods. Chem. Geol. 200, 225–240.
Selby, D., Creaser, R.A., 2005. Direct radiometric dating of the Devonian–Mississippian time-scale boundary using the Re–Os black shale geochronometer. Geology 33, 545–548.
Selby, D., Creaser, R.A., Stein, H.J., Markey, R.J., Hannah, J.L., 2007. Assessment of the Re-187 decay constant by cross calibration of Re–Os molybdenite and U–Pb zircon chronometers in magmatic ore systems. Geochim. Cosmochim. Acta 71, 1999–2013.
Selby, D., Mutterlose, J., Condon, D.J., 2009. U–Pb and Re–Os geochronology of the Aptian/Albian and Cenomanian/Turonian stage boundaries: implications for timescale calibration, osmium isotope seawater composition and Re–Os systematics in organic-rich sediments. Chem. Geol. 265, 394–409.
Sharma, M., Wasserburg, G.J., Hofmann, A.W., Chakrapani, G.J., 1999. Himalayan uplift and osmium isotopes in oceans and rivers – its relation to global tectonics and climate. Geochim. Cosmochim. Acta 63, 4005–4012.
Smith, M.E., Carroll, A.R., Singer, B.S., 2008a. Synoptic reconstruction of a major ancient lake system: Eocene Green River Formation, western United States. Geol. Soc. Am. Bull. 120, 54–84.
Smith, M.E., Carroll, A.R., Mueller, E.R., 2008b. Elevated weathering rates in the rocky mountains during the early Eocene climatic optimum. Nat. Geosci. 1, 370–374.
Smith, M.E., Chamberlain, K.R., Singer, B.S., Carroll, A.R., 2010. Eocene clocks agree: Coeval $^{40}Ar/^{39}Ar$, U–Pb, and astronomical ages from the Green River Formation. Geology 38, 527–530.
Smith, M.E., Singer, B., Carroll, A., 2003. $^{40}Ar/^{39}Ar$ geochronology of the Eocene Green River Formation, Wyoming. Geol. Soc. Am. Bull. 115, 549–565.
Smith, M.E., Singer, B.S., Carroll, A.R., Fournelle, J.H., 2006. High-resolution calibration of Eocene strata: $^{40}Ar/^{39}Ar$ geochronology of biotite in the Green River Formation. Geology 34, 393–396.
Smoliar, M.I., Walker, R.J., Morgan, J.W., 1996. Re–Os isotope constraints on the age of Group IIA, IIIA, IVA, and IVB iron meteorites. Science 271, 1099–1102.
Sun, W.D., Bennett, V.C., Eggins, S.M., Kamenetsky, V.S., Arculus, R.J., 2003. Enhanced mantle-to-crust rhenium transfer in undegassed arc magmas. Nature 422, 294–297.
Sundby, B., Martinez, P., Gobeil, C., 2004. Comparative geochemistry of cadmium, rhenium, uranium, and molybdenum in continental margin sediments. Geochim. Cosmochim. Acta 68, 2485–2493.
Tissot, B., Deroo, G., Hood, A., 1978. Geochemical study of the Uinta basin: formation of petroleum from the Green River Formation. Geochim. Cosmochim. Acta 42, 1469–1485.
Turgeon, S.C., Creaser, R.A., Algeo, T.J., 2007. Re–Os depositional ages and seawater Os estimates for the Frasnian–Famennian boundary: implications for weathering rates, land plant evolution, and extinction mechanisms. Earth Planet. Sci. Lett. 261, 649–661.
Tuttle, M.L., Goldhaber, M.B., 1993. Sedimentary sulfur geochemistry of the Paleogene Green River Formation, western USA: implications for interpreting depositional and diagenetic processes in saline alkaline lakes. Geochim. Cosmochim. Acta 57, 3023–3039.
Ver Straeten, C.A., Brett, C.E., Sageman, B.B., 2011. Mudrock sequence stratigraphy: a multi-proxy (sedimentological, paleobiological and geochemical) approach, Devonian Appalachian Basin. Palaeogeog. Palaeoclim. Palaeoecol. 304, 54–73.
Xu, G.P., Hannah, J.L., Stein, H.J., Bingen, B., Yang, G., Zimmerman, A., Weitschat, W., Mork, A., Weiss, H.M., 2009. Re–Os geochronology of Arctic black shales to evaluate the Anisian–Ladinian boundary and global faunal correlations. Earth Planet. Sci. Lett. 288, 581–587.
Yamashita, Y., Takahashi, Y., Haba, H., Enomoto, S., Shimizu, H., 2007. Comparison of reductive accumulation of Re and Os in seawater–sediment systems. Geochim. Cosmochim. Acta 71, 3458–3475.
Yang, G., Hannah, J.L., Zimmerman, A., Stein, H.J., Bekker, A., 2009. Re–Os depositional age for Archean carbonaceous slates from the southwestern superior province: challenges and insights. Earth Planet. Sci. Lett. 280, 83–92.

Appendix B

Anoxia in the terrestrial environment during the late Mesoproterozoic

Vivien M. Cumming[1]*, Simon W. Poulton[2], Alan D. Rooney[3], and David Selby[1]
[1]Department of Earth Sciences, Durham University, South Road, Durham DH1 3LE, UK
[2]School of Earth and Environment, University of Leeds, Leeds LS2 9JT, UK
[3]Department of Earth and Planetary Sciences, Harvard University, Cambridge, Massachusetts 02138, USA

ABSTRACT

A significant body of evidence suggests that the marine environment remained largely anoxic throughout most of the Precambrian. In contrast, the oxygenation history of terrestrial aquatic environments has received little attention, despite the significance of such settings for early eukaryote evolution. To address this, we provide here a geochemical and isotopic assessment of sediments from the late Mesoproterozoic Nonesuch Formation of central North America. We utilize rhenium-osmium (Re-Os) geochronology to yield a depositional age of 1078 ± 24 Ma, while Os isotope compositions support existing evidence for a lacustrine setting. Fe-S-C systematics suggest that the Nonesuch Formation was deposited from an anoxic Fe-rich (ferruginous) water column. Thus, similar to the marine realm, anoxia persisted in terrestrial aquatic environments in the Middle to Late Proterozoic, but sulfidic water column conditions were not ubiquitous. Our data suggest that oxygenation of the terrestrial realm was not pervasive at this time and may not have preceded oxygenation of the marine environment, signifying a major requirement for further investigation of links between the oxygenation state of terrestrial aquatic environments and eukaryote evolution.

INTRODUCTION

Recent reconstructions suggest that the global ocean remained anoxic between Earth's two major periods of rising atmospheric oxygen at either end of the Proterozoic eon (2500–542 Ma). In detail, sulfidic water column conditions were prevalent along productive continental margins, overlying deeper waters that contained dissolved Fe (ferruginous) (Canfield et al., 2008; Poulton et al., 2010; Poulton and Canfield, 2011; Planavsky et al., 2011). However, in contrast to these advances in our understanding of the evolution of Middle Proterozoic ocean chemistry, much less is known about oxygenation of terrestrial aquatic environments during this period.

Recently, sulfur isotope fractionations between sulfate and sulfide ($\delta^{34}S$) of >50‰ in lacustrine sediments from the Mesoproterozoic Torridon and Stoer Groups of northwest Scotland were interpreted to suggest that oxygenation of terrestrial aquatic environments preceded oxygenation of the oceans (Parnell et al., 2010). Such fractionations are generally considered to require an active oxidative sulfur cycle driven by disproportionation reactions involving sulfide-oxidizing bacteria, and are interpreted to reflect a major rise in oxygen in the late Neoproterozoic (Canfield and Teske, 1996). If correct, this suggests that, unlike the marine realm, late Mesoproterozoic terrestrial aquatic environments were sufficiently oxidized to support a complex biota adapted to an oxygen-rich atmosphere (Parnell et al., 2010). However, $\delta^{34}S$ fractionations of 60‰–70‰ have recently been measured in an anoxic, low-sulfate lake in the absence of oxidative sulfur cycling (Canfield et al., 2010). This builds upon theoretical calculations of the magnitude of fractionation possible by bacterial sulfate reduction alone (Brunner and Bernasconi, 2005), and is supported by direct measurements of fractionations obtained during growth of a pure culture of bacterial sulfate reducers (Sim et al., 2011).

Considering the evolutionary significance of possible early oxygenation of terrestrial environments, coupled with these recent developments in our understanding of sulfur isotope fractionation, a more direct assessment of the redox state of the terrestrial realm during the late Mesoproterozoic is clearly warranted. Our focus is on the Nonesuch Formation, deposited within the ca. 1100 Ma intracratonic Midcontinent Rift System of central North America (Ojakangas et al., 2001). Like the Torridon Group of northwest Scotland, the Nonesuch Formation contains a rich record of eukaryotic life (Pratt et al., 1991; Strother and Wellman, 2010) and thus represents an ideal locality to assess possible links to early terrestrial oxygenation. We utilize Fe-S-C systematics to assess water column redox conditions, coupled with Re-Os geochronology to provide a depositional age for the Nonesuch Formation, and Os isotope systematics to yield an insight into the nature of the depositional setting.

GEOLOGICAL SETTING

The Midcontinent Rift System of central North America was one of the world's largest continental rifts (Ojakangas et al., 2001). In the Lake Superior region, up to 30 km of volcanic and sedimentary rift-fill sequences make up the Keweenawan Supergroup (Ojakangas et al., 2001) (Fig. 1). The Oronto Group consists of fluvial and alluvial volcaniclastics, with the exception of the Nonesuch Formation, a 40–200 m thick succession of organic-rich siliciclastics. Geochronology of the Keweenawan Supergroup is based upon U-Pb zircon ages of rift-related volcanics, with the overlying postrift sediments poorly constrained temporally. An existing U-Pb zircon age of 1087.2 ± 1.6 Ma from the final andesite flow in the Copper Harbor Conglomerate (Davis and Paces, 1990) (Fig. 1) provides a maximum age for the Nonesuch Formation.

To allow redox assessment using Fe-S-C systematics, we sampled well-preserved drill core (PI-1) across a 60 m interval that covers the entire Nonesuch Formation (Pratt et al., 1991). These samples are augmented by Re-Os geochronology and Os isotope analyses of outcrop samples collected ~30 m above the Copper Harbor Conglomerate (Fig. 1; full details of the sampling and analytical protocols are provided in the GSA Data Repository[1]). The Re-Os age for all of the outcrop samples is 1040 ± 78 Ma (2σ, n = 16, mean square of weighted deviates [MSWD] = 10.6; Fig. DR1 and Table DR1 in the Data Repository). The large MSWD and uncertainty on this Re-Os date is due to variation in the initial $^{187}Os/^{188}Os$ (Os_i) values rather than disturbance to the isotope system, as suggested by the isochronous nature of the samples and agreement with the underlying U-Pb date (see the Data Repository). In fact, the Os_i values form two distinct groups, with 11 of the 16 samples yielding the most precise depositional age of 1078 ± 24 Ma (2σ, n = 11, MSWD = 1.05; Fig. DR1).

DEPOSITIONAL ENVIRONMENT

Sedimentological characteristics of the Nonesuch Formation and proximity to continental red beds (Fig. 1), coupled with paleogeographic reconstructions suggesting that the nearest coastline was ~800 km away, indicate that the Nonesuch Formation was likely deposited in a lacustrine environment (Elmore et al., 1989; Imbus et al., 1992; Ojakangas et al., 2001). However, a marine embayment or estuarine environment has also been suggested based on the presence of specific biomarkers and S/C ratios (Pratt et al., 1991; Hieshima and Pratt, 1991). Biomarkers extracted from the Nonesuch Formation include low levels of 24-*n*-propylcholestane (Pratt et al., 1991), which is commonly, but not uniquely,

*E-mail: v.m.cumming@durham.ac.uk.

[1]GSA Data Repository item 2013160, detailed sampling and methodology and detailed Re-Os geochronology results, is available online at www.geosociety.org/pubs/ft2013.htm, or on request from editing@geosociety.org or Documents Secretary, GSA, P.O. Box 9140, Boulder, CO 80301, USA.

GEOLOGY Data Repository item 2013160 | doi:10.1130/G34299.1

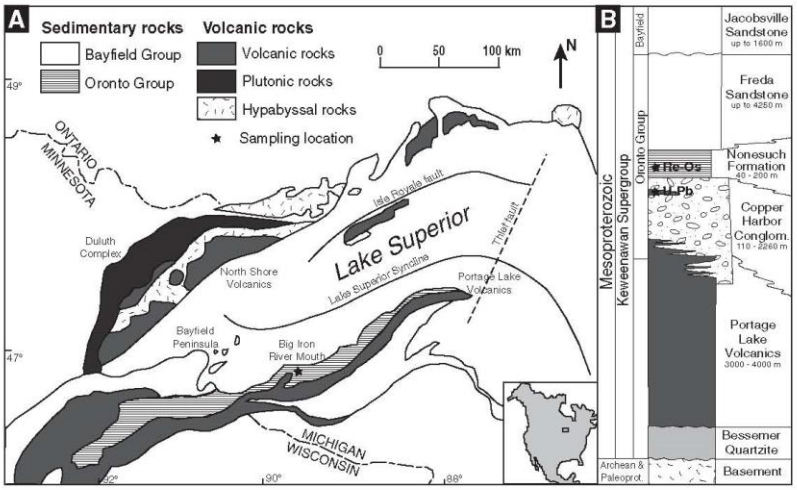

Figure 1. A: Geological map of the Lake Superior (North America) region showing the locations of the main Keweenawan Supergroup units. The Nonesuch Formation is part of the Oronto Group situated between continental red beds of the Copper Harbor Conglomerate and the Freda Sandstone, and outcrops on the southern shores of Lake Superior. B: Schematic stratigraphy of the Keweenawan Supergroup, focusing on postrift sediments. The right-hand panel illustrates depth variations for each unit. Locations of the Re-Os ages (1078 ± 24 Ma; this study) and U-Pb ages (1087.2 ± 1.6 Ma; Davis and Paces, 1990) are labeled. Figures adapted from Elmore et al. (1989) and Ojakangas et al. (2001).

found in rocks of marine origin (Moldowan et al., 1990) and may in fact relate to the presence of eukaryotic organisms in the Nonesuch Formation. Thus, the presence of 24-*n*-propylcholestane at low concentration does not unambiguously denote a marine depositional setting for the Nonesuch Formation.

Enrichments in S/C ratios have previously been interpreted to reflect deposition of the Nonesuch Formation under sulfate-rich marine conditions (Fig. DR2) (Hieshima and Pratt, 1991; Imbus et al., 1992). However, enhanced fixation of sulfide as a result of the absence of bioturbation in the Precambrian and (potentially) non-Fe-limited conditions during ferruginous deposition, combined with differences in the metabolizability of Precambrian organic matter, could readily lead to the observed enrichments in sulfur and decoupling between sulfur and carbon under lacustrine conditions (e.g., Raiswell and Canfield, 2012).

Application of Re-Os geochronology provides an additional, novel constraint on the nature of the depositional environment by yielding the Os_i composition of the water column at the time of deposition, which can be used to distinguish between lacustrine and marine settings (Poirier and Hillaire-Marcel, 2011; Cumming et al., 2012). The Os_i values derived from the Re-Os isochrons are 0.81 ± 0.28 and 0.49 ± 0.13 (Fig. DR1), a variation reflecting a balance between weathering of radiogenic Archean–Proterozoic cratonic lithosphere (~1.01; upper continental crust calculated at 1100 Ma; Esser and Turekian, 1993) and unradiogenic rift-related flood basalts (~0.13; Allegre et al., 1999). At 1100 Ma, seawater Os_i was relatively unradiogenic at ~0.3 (a value derived from two separate margins; Rooney et al., 2010; Azmy et al., 2008), and therefore the more radiogenic values measured for the Nonesuch Formation (0.81 and 0.49) suggest that minimal Os was sourced from the marine realm. Thus, the Os isotope data support sedimentological and paleogeographic evidence for lacustrine depositional conditions.

REDOX CONDITIONS

Water column redox conditions during deposition of the Nonesuch Formation were evaluated using Fe speciation. A biogeochemically "highly reactive" Fe (Fe_{HR}) pool is analyzed through a series of extractions (Poulton and Canfield, 2005). Modern and ancient sediments deposited under anoxic conditions commonly have Fe_{HR} to total Fe ratios (Fe_{HR}/Fe_T) of >0.38, in contrast to oxic depositional conditions, where ratios are consistently below 0.22 (Poulton and Canfield, 2011). Roughly 40% of drill core samples (Fig. 2), and all outcrop samples (Table DR2), were clearly deposited from an anoxic water column with Fe_{HR}/Fe_T > 0.38, while others fall within the equivocal range (Fe_{HR}/Fe_T = 0.22–0.38). These equivocal samples may reflect the masking of water column Fe_{HR} enrichments due to rapid sedimentation or transformation of nonsulfidized Fe_{HR} to clay minerals during burial diagenesis or metamorphism (Poulton and Raiswell, 2002; Poulton et al., 2010). The latter possibility can be evaluated by considering Fe/Al ratios (Fig. 2), whereby significant enrichments in Fe relative to both average shale (Lyons and Severmann, 2006) and typical oxic lacustrine sediments (e.g., Kemp and Thomas, 1976; Fagel et al., 2005) throughout the Nonesuch Formation provide strong evidence for anoxic depositional conditions. Post-depositional loss of Fe_{HR} can also be assessed through an extraction that targets Fe associated with clay minerals (termed poorly reactive silicate Fe, or Fe_{PRS}) (Poulton et al., 2010). Extreme enrichment in Fe_{PRS} in the Nonesuch Formation (Fe_{PRS}/Fe_T values are well above the modern and Phanerozoic averages; Fig. 2) (Poulton and Raiswell, 2002) suggests that significant loss of Fe_{HR} through authigenic clay mineral formation was responsible for reducing original depositional Fe_{HR}/Fe_T ratios (Poulton et al., 2010), supporting anoxic deposition for all Nonesuch Formation samples.

For samples showing evidence of anoxic deposition, the extent to which the Fe_{HR} pool has been pyritized (Fe_{Py}/Fe_{HR}) can then distinguish euxinic (Fe_{Py}/Fe_{HR} > 0.7–0.8) from ferruginous (Fe_{Py}/Fe_{HR} < 0.7–0.8) depositional conditions (Poulton and Canfield, 2011). All of the Nonesuch Formation samples have Fe_{Py}/Fe_{HR} ratios well below the euxinic threshold (Fig. 2), indicating anoxic ferruginous depositional conditions throughout and thus refuting suggestions of a possible euxinic depositional setting (cf. Imbus et al., 1992).

IMPLICATIONS FOR TERRESTRIAL BIOSPHERIC OXYGENATION

The upper Nonesuch Formation comprises fining- and coarsening-upward packages interpreted to be the transition between lacustrine deposition and fluvial conditions of the conformably overlying Freda Sandstone (Elmore et al., 1989). This suggests that the Nonesuch Formation was likely deposited under progressively more oxic conditions as water depth decreased

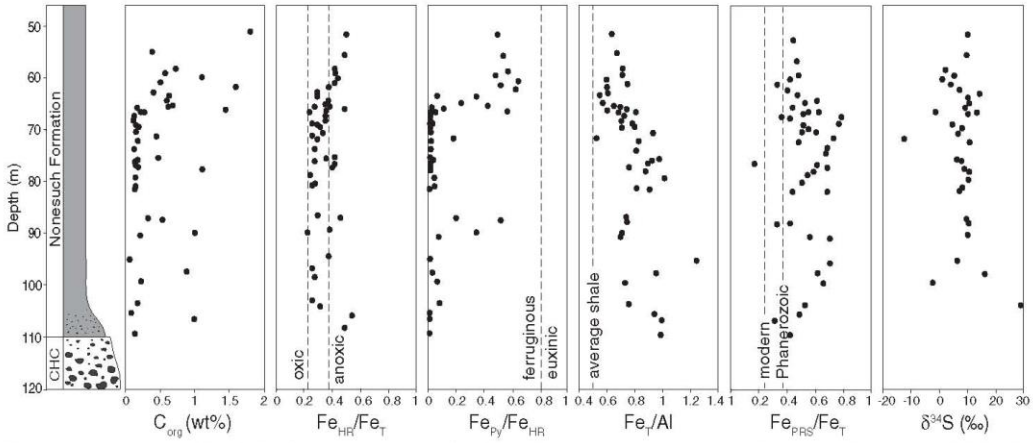

Figure 2. Geochemical profiles for the Nonesuch Formation (North America) core samples. For the Fe_{HR}/Fe_T and Fe_{Py}/Fe_{HR} graphs (HR—highly reactive; T—total; Py—pyritized), the dashed lines show the fields for oxic or anoxic deposition and ferruginous or euxinic deposition, respectively (Poulton and Canfield, 2011). On the Fe_T/Al graph, the dashed line represents average anoxic shale (Lyons and Severmann, 2006). On the Fe_{PRS}/Fe_T graph (PRS—poorly reactive silicate), the dashed lines represent modern (Raiswell and Canfield, 1998) and Phanerozoic (Poulton and Raiswell, 2002) averages. CHC—Copper Harbor Conglomerate.

toward the top of the succession (Elmore et al., 1989). Oxygenated surface waters in ca. 1.1 Ga terrestrial aquatic environments would be expected, particularly since shallow marine waters were apparently oxygenated much earlier in Earth history (ca. 2.7 Ga; Kendall et al., 2010; Zerkle et al., 2012). However, we find no evidence for oxic deposition in core PI-1, suggesting that anoxia was a persistent feature throughout the depositional period, and any oxygenation was likely restricted to surface waters.

The observation of persistent ferruginous water column conditions suggests that the flux of Fe_{HR} to the lake overwhelmed the flux of sulfate (Poulton and Canfield, 2011). We note here that our Os_i values suggest that any hydrothermal fluid contribution to the lake from rifting or extensive weathering of rift-related basalts would have been negligible, because Os_i values closer to ~0.13 (Allegre et al., 1999; Meisel et al., 2001) would otherwise be expected. In consequence, there is no evidence to support a particularly enhanced influx of Fe due to rifting. Instead, the prevalence of ferruginous water column conditions is consistent with low rates of oxidative pyrite weathering driven by only modest levels of atmospheric oxygen (Canfield and Raiswell, 1999). Although it is not possible to directly determine water column sulfate concentrations, we note that pyrite sulfur isotope compositions are relatively heavy (8.5‰ ± 6.3‰) throughout most of the Nonesuch Formation (Fig. 2) and show a distribution similar to 1.5–1.0 Ga marine sediments, possibly skewed toward slightly heavier values (Fig. 3). This is entirely consistent with a relatively

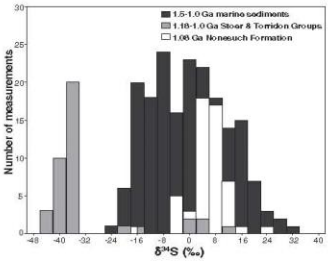

Figure 3. Probability density plot of pyrite sulfur isotope data for the Nonesuch Formation (North America; this study; Imbus et al., 1992), the Torridon and Stoer Groups (Scotland; Parnell et al., 2010), and 1.5–1.0 Ga marine sediments (Canfield and Raiswell, 1999).

low-sulfate environment (e.g., Canfield and Raiswell, 1999), and further supports efficient trapping of sulfide (and hence high S/C ratios; Fig. DR2) driven by a lack of bioturbation, and deposition from a ferruginous system that was sulfur (rather than reactive Fe) limited (e.g., Raiswell and Canfield, 2012).

The distribution of the Nonesuch Formation sulfur isotope data is very different from that observed for 1.18–1.0 Ga lacustrine sediments from northwest Scotland (Fig. 3), with no indication of large-scale fractionations that would indicate significant oxidative sulfur cycling through microbial disproportionation. This is likely a consequence of the restriction of oxic conditions to surface waters, and limitation of sulfate reduction to sediment porewaters beneath the ferruginous water column of the Nonesuch basin. Together, this would limit formation of the oxidized sulfur species required for disproportionation (Thamdrup et al., 1993). In addition, the low sulfate concentrations inferred for the Nonesuch basin would limit the maximum expression of sulfur isotope fractionation even if oxidative sulfur cycling and disproportionation reactions were prevalent (Canfield and Raiswell, 1999). This is consistent with multiple ($^{32/33/34}S$) sulfur isotope systematics in marine sediments, which suggest that microbial sulfur disproportionation was prevalent by at least 1.3 Ga (Johnston et al., 2005), but was only manifest in the major ($^{32/34}S$) sulfur isotope record after a later Neoproterozoic rise in atmospheric oxygen led to a significant increase in seawater sulfate concentrations (Canfield and Teske, 1996). Thus, rather than reflecting high sulfate concentrations (Hieshima and Pratt, 1991) potentially attributable to extensive oxygenation of the continents under high atmospheric oxygen, Fe-S-C systematics in the Nonesuch Formation suggest low sulfate concentrations, ferruginous conditions, and only modest atmospheric oxygenation.

In light of this, the sulfur isotope data for the Stoer and Torridon Groups may reflect either an unusually sulfate-rich environment that allowed maximum expression of sulfur isotope fractionations (Parnell et al., 2010), or the preservation of large sulfur isotope fractionations through bacterial sulfate reduction alone (Canfield et al., 2010; Sim et al., 2011). Thus, while it remains possible that sulfur isotope systematics in the Stoer and Torridon Groups may be providing

an early record of terrestrial oxygenation, our redox and sulfur isotope data for the Nonesuch Formation suggest that early terrestrial oxygenation was not a pervasive feature of localities that preserve evidence for diverse eukaryotic life. Instead, the redox characteristics display strong similarities to the marine realm (Poulton and Canfield, 2011), implying that in terms of water column and atmospheric oxygenation, terrestrial environmental conditions were likely no more predisposed toward eukaryote evolution than shallow marine environments. We suggest that the identification and detailed redox evaluation of other late Mesoproterozoic terrestrial sediments should be a priority in order to more precisely evaluate potential links between the redox evolution of aquatic systems and the rich terrestrial biological record.

ACKNOWLEDGMENTS

This research was funded by a Lundin Petroleum CeREES Ph.D. scholarship awarded to Cumming, and by the Natural Environment Research Council (Life and the Planet Scheme). Three anonymous reviewers are thanked for helpful comments that have much improved the manuscript.

REFERENCES CITED

Allegre, C.J., Birck, J.L., Capmas, F., and Courtillot, V., 1999, Age of the Deccan Traps using ^{187}Re-^{187}Os systematics: Earth and Planetary Science Letters, v. 170, p. 197–204, doi:10.1016/S0012-821X(99)00110-7.

Azmy, K., Kendall, B., Creaser, R.A., Heaman, L., and de Oliveira, T.F., 2008, Global correlation of the Vazante Group, Sao Francisco Basin, Brazil: Re-Os and U-Pb radiometric age constraints: Precambrian Research, v. 164, p. 160–172, doi:10.1016/j.precamres.2008.05.001.

Brunner, B., and Bernasconi, S.M., 2005, A revised isotope fractionation model for dissimilatory sulfate reduction in sulfate reducing bacteria: Geochimica et Cosmochimica Acta, v. 69, p. 4759–4771, doi:10.1016/j.gca.2005.04.015.

Canfield, D.E., and Raiswell, R., 1999, The evolution of the sulfur cycle: American Journal of Science, v. 299, p. 697–723, doi:10.2475/ajs.299.7-9.697.

Canfield, D.E., and Teske, A., 1996, Late Proterozoic rise in atmospheric oxygen concentration inferred from phylogenetic and sulphur-isotope studies: Nature, v. 382, p. 127–132, doi:10.1038/382127a0.

Canfield, D.E., Poulton, S.W., Knoll, A.H., Narbonne, G.M., Ross, G., Goldberg, T., and Strauss, H., 2008, Ferruginous conditions dominated later Neoproterozoic deep-water chemistry: Science, v. 321, p. 949–952, doi:10.1126/science.1154499.

Canfield, D.E., Farquhar, J., and Zerkle, A.L., 2010, High isotope fractionations during sulfate reduction in a low-sulfate euxinic ocean analog: Geology, v. 38, p. 415–418, doi:10.1130/G30723.1.

Cumming, V.M., Selby, D., and Lillis, P.G., 2012, Re-Os geochronology of the lacustrine Green River Formation: Insights into direct depositional dating of lacustrine successions, Re-Os systematics and paleocontinental weathering: Earth and Planetary Science Letters, v. 359–360, p. 194–205, doi:10.1016/j.epsl.2012.10.012.

Davis, D.W., and Paces, J.B., 1990, Time resolution of geologic events on the Keweenaw Peninsula and implications for development of the Mid-continent Rift system: Earth and Planetary Science Letters, v. 97, p. 54–64, doi:10.1016/0012-821X(90)90098-I.

Elmore, D.R., Milavec, G.J., Imbus, S.W., and Engel, M.H., 1989, The Precambrian Nonesuch Formation of the North American mid-continent rift, sedimentology and organic geochemical aspects of lacustrine deposition: Precambrian Research, v. 43, p. 191–213, doi:10.1016/0301-9268(89)90056-9.

Esser, B.K., and Turekian, K.K., 1993, The osmium isotopic composition of the continental crust: Geochimica et Cosmochimica Acta, v. 57, p. 3093–3104, doi:10.1016/0016-7037(93)90296-9.

Fagel, N., Alleman, L.Y., Granina, L., Hatert, F., Thamo-Bozso, E., Cloots, R., and André, L., 2005, Vivianite formation and distribution in Lake Baikal sediments: Global and Planetary Change, v. 46, p. 315–336, doi:10.1016/j.gloplacha.2004.09.022.

Hieshima, G.B., and Pratt, L.M., 1991, Sulfur/carbon ratios and extractable organic matter of the Middle Proterozoic Nonesuch Formation, North American midcontinent rift: Precambrian Research, v. 54, p. 65–79, doi:10.1016/0301-9268(91)90069-M.

Imbus, S.W., Macko, S.A., Elmore, R.D., and Engel, M.H., 1992, Stable isotope (C, S, N) and molecular studies on the Precambrian Nonesuch Shale (Wisconsin-Michigan, USA): Evidence for differential preservation rates, depositional environment and hydrothermal influence: Chemical Geology, v. 101, p. 255–281, doi:10.1016/0009-2541(92)90007-R.

Johnston, D.T., Wing, B.A., Farquhar, J., Kaufman, A.J., Strauss, H., Lyons, T.W., Kah, L.C., and Canfield, D.E., 2005, Active microbial sulfur disproportionation in the Mesoproterozoic: Science, v. 310, p. 1477–1479, doi:10.1126/science.1117824.

Kemp, A.L., and Thomas, R.L., 1976, Cultural impact on geochemistry of sediments of lakes Ontario, Erie and Huron: Geoscience Canada, v. 3, p. 191–207.

Kendall, B., Reinhard, C.T., Lyons, T.W., Kaufman, A.J., Poulton, S.W., and Anbar, A.D., 2010, Pervasive oxygenation along late Archaean ocean margins: Nature Geoscience, v. 3, p. 647–652, doi:10.1038/ngeo942.

Lyons, T.W., and Severmann, S., 2006, A critical look at iron paleoredox proxies: New insights from modern euxinic marine basins: Geochimica et Cosmochimica Acta, v. 70, p. 5698–5722, doi:10.1016/j.gca.2006.08.021.

Meisel, T., Walker, R.J., Irving, A.J., and Lorand, J.-P., 2001, Osmium isotopic compositions of mantle xenoliths: A global perspective: Geochimica et Cosmochimica Acta, v. 65, p. 1311–1323, doi:10.1016/S0016-7037(00)00566-4.

Moldowan, J.M., Fago, F.J., Lee, C.Y., Jacobson, S.R., Watt, D.S., Slougui, N.-E., Jeganathan, A., and Young, D.C., 1990, Sedimentary 12-*n*-propylcholestanes: Molecular fossils diagnostic of marine algae: Science, v. 247, p. 309–312, doi:10.1126/science.247.4940.309.

Ojakangas, R.W., Morey, G.B., and Green, J.C., 2001, The Mesoproterozoic Midcontinent Rift System, Lake Superior region, USA: Sedimentary Geology, v. 141–142, p. 421–442, doi:10.1016/S0037-0738(01)00085-9.

Parnell, J., Boyce, A.J., Mark, D., Bowden, S., and Spinks, S., 2010, Early oxygenation of the terrestrial environment during the Mesoproterozoic: Nature, v. 468, p. 290–293, doi:10.1038/nature09538.

Planavsky, N.J., McGoldrick, P., Scott, C.T., Li, C., Reinhard, C.T., Kelly, A.E., Chu, X., Bekker, A., Love, G.D., and Lyons, T.W., 2011, Widespread iron-rich conditions in the mid-Proterozoic ocean: Nature, v. 477, p. 448–451, doi:10.1038/nature10327.

Poirier, A., and Hillaire-Marcel, C., 2011, Improved Os-isotope stratigraphy of the Arctic Ocean: Geophysical Research Letters, v. 38, L14607, doi:10.1029/2011GL047953.

Poulton, S.W., and Canfield, D.E., 2005, Development of a sequential extraction procedure for iron: Implications for iron partitioning in continentally derived particulates: Chemical Geology, v. 214, p. 209–221, doi:10.1016/j.chemgeo.2004.09.003.

Poulton, S.W., and Canfield, D.E., 2011, Ferruginous conditions: A dominant feature of the ocean through Earth's history: Elements, v. 7, p. 107–112, doi:10.2113/gselements.7.2.107.

Poulton, S.W., and Raiswell, R., 2002, The low-temperature geochemical cycle of iron: From continental fluxes to marine sediment deposition: American Journal of Science, v. 302, p. 774–805, doi:10.2475/ajs.302.9.774.

Poulton, S.W., Fralick, P.W., and Canfield, D.E., 2010, Spatial variability in oceanic redox structure 1.8 billion years ago: Nature Geoscience, v. 3, p. 486–490, doi:10.1038/ngeo889.

Pratt, L.M., Summons, R.E., and Hieshima, G.B., 1991, Sterane and triterpane biomarkers in the Precambrian Nonesuch Formation, North American Midcontinent Rift: Geochimica et Cosmochimica Acta, v. 55, p. 911–916, doi:10.1016/0016-7037(91)90351-5.

Raiswell, R., and Canfield, D.E., 1998, Sources of iron for pyrite formation in marine sediments: American Journal of Science, v. 298, p. 219–245, doi:10.2475/ajs.298.3.219.

Raiswell, R., and Canfield, D.E., 2012, The iron biogeochemical cycle past and present: Geochemical Perspectives, v. 1, p. 1–220.

Rooney, A.D., Selby, D., Houzay, J.-P., and Renne, P.R., 2010, Re-Os geochronology of a Mesoproterozoic sedimentary succession, Taoudeni basin, Mauritania: Implications for basin-wide correlations and Re-Os organic-rich sediments systematics: Earth and Planetary Science Letters, v. 289, p. 486–496, doi:10.1016/j.epsl.2009.11.039.

Sim, M.S., Bosak, T., and Ono, S., 2011, Large sulfur isotope fractionation does not require disproportionation: Science, v. 333, p. 74–77, doi:10.1126/science.1205103.

Strother, P.K., and Wellman, C.H., 2010, Paleobiology of a nonmarine Precambrian shale: Well-preserved eukaryotes from the 1.1 Ga Nonesuch Formation: Proceedings of the Palaeontological Association, 54th Annual Meeting, 17–20 December, 2010, Ghent University, Belgium, p. 34.

Thamdrup, B., Finster, K., Hansen, J.W., and Bak, F., 1993, Bacterial disproportionation of elemental sulfur coupled to chemical reduction of iron or manganese: Applied and Environmental Microbiology, v. 59, p. 101–108.

Zerkle, A.L., Claire, M.W., Domagal-Goldman, S.D., Farquhar, J., and Poulton, S.W., 2012, A bistable organic-rich atmosphere on the Neoarchaean Earth: Nature Geoscience, v. 5, p. 359–363, doi:10.1038/ngeo1425.

Manuscript received 9 October 2012
Revised manuscript received 10 December 2012
Manuscript accepted 11 December 2012

Printed in USA